Received: 3 July 2018 | Revised: 1 October 2018 | Accepted: 5 October 2018

DOI: 10.1002/ajpa.23750

WILEY Yearbook of PHYSICAL ANTHROPOLOGY

YEARBOOK OF PHYSICAL ANTHROPOLOGY ARTICLE

One small step: A review of Plio-Pleistocene hominin foot evolution

Jeremy DeSilva[1,2] | Ellison McNutt[1] | Julien Benoit[2] | Bernhard Zipfel[2]

[1]Department of Anthropology, Dartmouth College, Hanover, New Hampshire

[2]Evolutionary Studies Institute and School of Geosciences, University of the Witwatersrand, Johannesburg, South Africa

Correspondence
Jeremy M. DeSilva, Department of Anthropology, Dartmouth College, Hanover, NH 03755, USA.
Email: jeremy.m.desilva@dartmouth.edu

Funding information
African Origins Platform; Dartmouth College; Leakey Foundation; National Research Foundation

Abstract

Bipedalism is a hallmark of being human and the human foot is modified to reflect this unique form of locomotion. Leonardo da Vinci is credited with calling the human foot "a masterpiece of engineering and a work of art." However, a scientific approach to human origins has revealed that our feet are products of a long, evolutionary history in which a mobile, grasping organ has been converted into a propulsive structure adapted for the rigors of bipedal locomotion. Reconstructing the evolutionary history of foot anatomy benefits from a fossil record; yet, prior to 1960, the only hominin foot bones recovered were from Neandertals. Even into the 1990s, the human foot fossil record consisted mostly of fragmentary remains. However, in the last two decades, the human foot fossil record has quadrupled, and these new discoveries have fostered fresh new perspectives on how our feet evolved. In this review, we document anatomical differences between extant ape and human foot bones, and comprehensively examine the hominin foot fossil record. Additionally, we take a novel approach and conduct a cladistics analysis on foot fossils (n = 19 taxa; n = 80 characters), and find strong evidence for mosaic evolution of the foot, and a variety of anatomically and functionally distinct foot forms as bipedal locomotion evolved.

KEYWORDS

Ardipithecus, *Australopithecus*, bipedalism, hominin, *Homo*

1 | INTRODUCTION

A mere four years after Charles Darwin promised that "light will be thrown on the origin of man and his history" (Darwin, 1859), Huxley (1863) got to work providing, at the time, the most comprehensive postcranial comparison between humans and other primates through an evolutionary lens. Among other observations, Huxley (1863) remarked on the striking resemblances between the musculoskeletal anatomy of a gorilla foot, and the foot of a human. Surely, fossils would be found that would indeed throw light on the manner by which the human foot evolved.

However, for the next 100 years, the only foot fossils recovered were from European Neandertals. Boule (1911, 1912, 1913) mistakenly endowed Neandertals with an ape-like[1] foot, complete with a divergent hallux, but Morton (1926a) challenged some of these initial claims and most now regard the Neandertal foot as essentially modern human-like (e.g., Trinkaus, 1983a). Still, many early 20th century scholars hypothesized that Pleistocene hominins were equipped with ape-like feet. Even a sculpture of *Pithecanthropus* (*Homo*) *erectus* made by Eugene Dubois for the 1900 Paris World's Fair stood on an ape-like foot, complete with an abducent big toe (Shipman, 2002).

Without fossils to test these inferences about early hominin foot form, researchers instead turned to comparative anatomy of living primates to create models of foot evolution (Midlo, 1934; Schultz, 1930). Weidenreich (1923) presented evidence from which he inferred that the chimpanzee foot is anatomically most similar to a human foot. Keith (1928) countered that the chimpanzee foot was the most generalized of the apes and likely the one from which all apes evolved; but that the gorilla foot was the most human-like. Elftman and Manter (1935) compromised and regarded it as equally likely that the human foot could have evolved from a chimpanzee or gorilla one, an idea that appeared to be endorsed by Schultz (1930) as well. Gregory (1928) drew attention to similarities between gibbons and humans. Straus Jr (1949) found the human foot to most resemble that of monkeys, rather than apes.

[1]Throughout this review, we use the word "hominoid" as a term to describe all extant apes, including humans. The term "ape" is used as a shorthand paraphyletic term that includes chimpanzees (and bonobos), gorillas, orangutans, and gibbons, but not humans.

 © 2018 American Association of Physical Anthropologists

Wood Jones (1916) went even deeper into the primate tree and drew comparisons between the often-upright tarsier and humans.

Using these modern models, early 20th century scholars of the foot hypothesized what changes were critical for the evolution of the human foot. Morton (1935) most notably argued that a "Dryopithecine" foot, which combined the elongated midtarsus of gibbons with proportions found in the chimpanzee foot, evolved into a gorilla-like "prehuman foot". Morton (1924, 1935) drew attention to changes in metatarsal torsion that would convert an inverted ape foot into an everted human one. Elftman and Manter (1935) focused on the transverse tarsal joint and suggested that skeletal modifications that promote midtarsal plantarflexion and adduction were central to the evolution of the human foot, and its unique longitudinal arch. A decade earlier, Weidenreich (1923) proposed that expansion of the calcaneal tuber and changes to the ankle joint that positioned the foot in an everted set, rather than an inverted one, were central to the evolution of the human foot. Again, these efforts were made despite the almost complete absence of a foot fossil record.

However, that all changed in 1960 with the discovery of the remarkably complete OH 8 foot (Day & Napier, 1964; Leakey, 1960). The following decades would witness the discovery of Lucy, the Laetoli footprints, and the remains from the 333 site at Hadar, which provided a window into the geologically older foot of *Australopithecus afarensis* (Latimer, Lovejoy, Johanson, & Coppens, 1982). With new fossil data points, one could connect these evolutionary dots and begin to hypothesize how an ape foot could evolve into a human one via these fossil intermediates (Susman, 1983). With these fossil remains, new models for foot evolution emerged. Instead of the abducted hallux becoming adducted in humans, Lewis (1980a, 1980b, 1980c, 1989) envisioned a realignment of the subtalar axis of the foot, so that the forefoot became medially shifted toward a stable hallux. Years earlier, Keith (1928) similarly proposed that the lateral forefoot was redirected toward the hallux during human evolution. Kidd (1999) and Kidd, O'Higgins, and Oxnard (1996) proposed that evolutionary changes to the lateral forefoot occurred early in human evolution and that the medial forefoot remained ape-like well into the Pleistocene. Though this hypothesis was based on interpretations of the OH 8 foot that have been questioned (e.g., Harcourt-Smith, 2002; Harcourt-Smith & Aiello, 2004; this study), more recent discoveries and analyses support this general framework of human foot evolution in which the lateral forefoot was the target of natural selection in the earliest known bipedal hominins (Fernández et al., 2018; Fernández, Holowka, Demes, & Jungers, 2016; Lovejoy, Latimer, Suwa, Asfaw, & White, 2009; McNutt, Zipfel, & DeSilva, 2018).

During the last 20 years, however, the human foot fossil record has more than quadrupled (Table 1), including a large number of foot skeletons associated with craniodental remains (e.g., *Ardipithecus ramidus*, *A. afarensis*, *A. sediba*, *H. naledi*, and *H. floresiensis*). Simple linear models for foot evolution are no longer tenable (Haile-Selassie et al., 2012), and some suggest that extant ape feet are too derived to serve as placeholders for the last common ancestor (Lovejoy et al., 2009). Some of the taxonomic allocations of important fossil specimens presented in this article are likely to provoke debate. For instance, we recognize we are in a minority position in placing OH 8 into *P. boisei* rather than its more conventional allocation to *H. habilis*. To facilitate this discussion, we outline our preferred hypodigms for the taxa discussed in this article in Table 1. Justifications for these allocations are presented throughout the text.

In this review, we proceed bone-by-bone through the foot skeleton,[2] noting anatomical differences between the human foot and those from apes and how those differences are hypothesized to be functionally relevant. While joint-based studies (e.g., Inman, 1976; Prang, 2016a) may be functionally more informative than bone-based ones, paleoanthropology remains a science of skeletal fragments and we can maximize sample size by grouping fossils by skeletal element. We are well aware that many of the form: function assumptions presented in this article have yet to be rigorously evaluated, and we envision decades of research ahead that test these hypotheses (see Holowka & Lieberman, 2018). Work examining the relationship between intraspecific skeletal variation and foot function (e.g., DeSilva et al., 2015), combined with more sophisticated X-ray Reconstruction of Moving Morphology (XROMM) studies examining in real-time precisely how bony anatomy correlates with joint motion in primates (e.g., Granatosky, Laird, Kuo, Alemseged, & Ross, 2018) will be needed to more accurately assess foot function in early hominins. Furthermore, even if the form: function hypotheses are upheld, it remains unclear in many cases whether these differences actually matter from a performance standpoint. More studies are needed which test how variation in skeletal form (and resulting function) impact locomotor energetics and/or injury risk (e.g., Raichlen, Armstrong, & Lieberman, 2011; Rolian, Lieberman, Hamill, Scott, & Werbel, 2009). Finally, even if there are performance differences, it remains unclear whether these anatomical regions have actually been the target of selection and future work should examine what regions of the foot have been under selection during human evolution, as scholars have done for other regions of the body (e.g., Ackermann & Cheverud, 2004; Grabowski & Roseman, 2015).

This review is composed of three sections. The first takes a bone-by-bone tour through the foot comparing human skeletal anatomy to that of our primate relatives. Fossils are included in this section knowing that students interested in a single element (e.g., talus) would benefit from a review of both modern comparative anatomy, and contributions made by paleoanthropology. The second section describes foot functional anatomy in known hominin taxa, starting with the earliest hominin foot fossils (e.g., *Ardipithecus*) and proceeding through fossil *H. sapiens*. Whereas we discuss the foot of Miocene apes in places, this review focuses specifically on Plio-Pleistocene hominins; Langdon (1986) is a good starting point for those interested in Miocene foot evolution. Finally, the third section of the article presents the first cladistic analysis of the human foot fossil record. Here, we present additional evidence for mosaic evolution of the foot and taxonomic diversity in foot forms throughout human evolution (e.g., Haile-Selassie et al., 2012; Harcourt-Smith & Aiello, 2004).

[2]For reviews examining the function of the foot as a whole, see Aiello and Dean (1990), Martin (2011), Kelikian and Sarrafian (2011), and Holowka and Lieberman (2018). Also see Sobczak et al. (2008) and Vereecke et al. (2008) for detailed comparisons of human and ape foot bones. For reviews that broaden the taxonomic lens and take a "from fins to feet" approach, see Klenerman and Wood (2006) and D'Août and Aerts (2008).

TABLE 1 Hominin foot fossils

Accession number	Taxon	Age (Ma)	Elements preserved
ARA-VP-6/500	*Ardipithecus ramidus*	4.4	Left: Cuboid, all cuneiforms, all Mts, PP2-5, IP5 Right: Partial calcaneus, talus, int. cun., cuboid, Mt 1–2, PP2-5, IP 4–5, DP Unsided: PP1, IP 3, DP (x3), hallucal sesamoid, os peroneum
GWM67/P2	*Ardipithecus ramidus*	4.3–4.6	Talus, partial calcaneus, lat. cun., distal Mt1, proximal Mt3-4, pedal phalanges
StW 573	*Australopithecus prometheus*?	3.67?	Talus, navicular, all 3 cuneiforms, Mt1, Mt2
BRT-VP-2/73	Hominin sp.	3.4	Mt 1,2,4; Mt 3 head; PP 1,2,4; IP 2
DIK-1-1f	*Australopithecus afarensis*	3.3	All tarsals and bases of all Mts
A.L. 333-115	*Australopithecus afarensis*	3.2	Forefoot: all Mt heads, all PPs, IP4, IP5, DP5
A.L. 288-1	*Australopithecus afarensis*	3.18	Talus, PP, IP
StW 595	*Australopithecus africanus*?	2.0–2.6	Mt 1–3; PP1 assumed to be associated based on shared accession number
MH 1 (U.W. 88-16, 22, 113)	*Australopithecus sediba*	1.98	Mt 4 and 5, calcaneal apophysis
MH 2 (U.W. 88-98, 99; 33)	*Australopithecus sediba*	1.98	Talus, calcaneus, Mt 5 base
OH 8	*Paranthropus boisei?*	1.85	All tarsals and bases & shafts of all Mts
KNM-ER 64062	*Homo* sp.	1.84	All tarsals but medial cuneiform; Mt1-Mt3; Mt4 head; Mt5 head and base; PP1
Dmanisi	*Homo erectus*	1.77	Talus; Mt3-5
KNM-ER 803	*Homo erectus*	1.53	Partial talus; Mt3,5, PP1, IP (x2), DP
Atapuerca	Middle Pleistocene *Homo*	0.43	Associations not yet published; many partial (or complete) feet likely present.
Dinaledi foot 1	*Homo naledi*	0.24–0.34	All tarsals but medial cuneiform; all Mts; PP1. Four additional partial feet from Dinaledi.
Jinniushan	Middle Pleistocene *Homo*	0.26	Left: all tarsals except navicular and int. cun. Mt1-2; PP(x4); IP(x3); DP(x2) Right: all tarsals except med. & int. cun., PP(x2); IP; DP1
Omo-Kibish	*Homo sapiens*	0.195	Talus, navicular, med. cun., cuboid, Mt1, fragmentary Mt2-5; PP1, DP1
Many	Neandertal	0.2–0.03	Amud, La Chapelle, La Ferrassie, Kiik-Koba, Krapina, Regourdou, Shanidar, Tabun partial feet
LB1	*Homo floresiensis*	0.06	Left: all tarsals except calcaneus. Mt 1–5 (some fragmentary); PPs, IPs, DPs Right: talus, navicular, cuboid, lat. cun., Mt1-5 (some fragmentary)

Foot defined as having 3 or more associated pedal elements. Mt, metatarsal; PP, proximal phalanx; IP, intermediate phalanx; DP, distal phalanx.

2 | COMPARATIVE ANATOMY OF THE FOOT

Below, the general anatomy of each foot element is described, including salient differences between the human and ape foot, and our general understanding of this element in the human fossil record. On the whole, human feet have proportionately short metatarsals and phalanges, and a long midtarsus (Figure 1). Ape feet are characterized by their long and internally facing lateral metatarsals and phalanges, and abducent hallux.

2.1 | Calcaneus

The calcaneus is the largest tarsal. It articulates dorsally with the talus and distally with the cuboid. Proximally, the tuberosity is the insertion for the Achilles tendon of the *M. triceps surae*. Several intrinsic foot muscles, including the *M. abductor hallucis* and the *M. flexor digitorum brevis*, originate on the calcaneus. The medial head of *M. quadratus plantae* (also called flexor accessorius) is unique to the human foot (Oishi et al., 2018; Schroeder, Rosser, & Kim, 2014; Susman, 1983) and helps balance the oblique pull of the tendons of *M. flexor digitorum longus*. Deriving from the calcaneus as well are the fibers of the long and short plantar ligaments. The short plantar ligament is found in all apes and stabilizes the lateral calcaneocuboid joint (Gomberg, 1981; Lewis, 1980a, 1980b, 1980c). The long plantar ligament, which inserts onto the cuboid and bases of the lateral metatarsals and stabilizes the tarsometatarsal joint, is unique to humans (Langdon, 1985). A palpable tubercle on the plantar calcaneus demonstrates that this ligament was present in *Australopithecus*. Superficially, the plantar aponeurosis originates from the medial plantar process of the calcaneus.

The proximal surface of the calcaneus is composed of three distinct regions—a dorsal facet that contacts the subcalcaneal bursa, a middle facet that terminates inferiorly in Sharpey fibers for insertion of the Achilles tendon, and a plantar region (Kachlik et al., 2008). The relative size of the dorsal facet corresponds with Achilles tendon length across primates and the relative size of this facet in *Australopithecus* calcanei suggests that they too had an elongated tendon, though one slightly shorter than in modern humans (McNutt & DeSilva, 2016). Modern apes, in contrast, possess a short tendon and larger muscle belly (Kuo, DeSilva, Devlin, McDonald, & Morgan, 2013), which permits greater ankle joint excursion (Myatt, Schilling, & Thorpe, 2011).

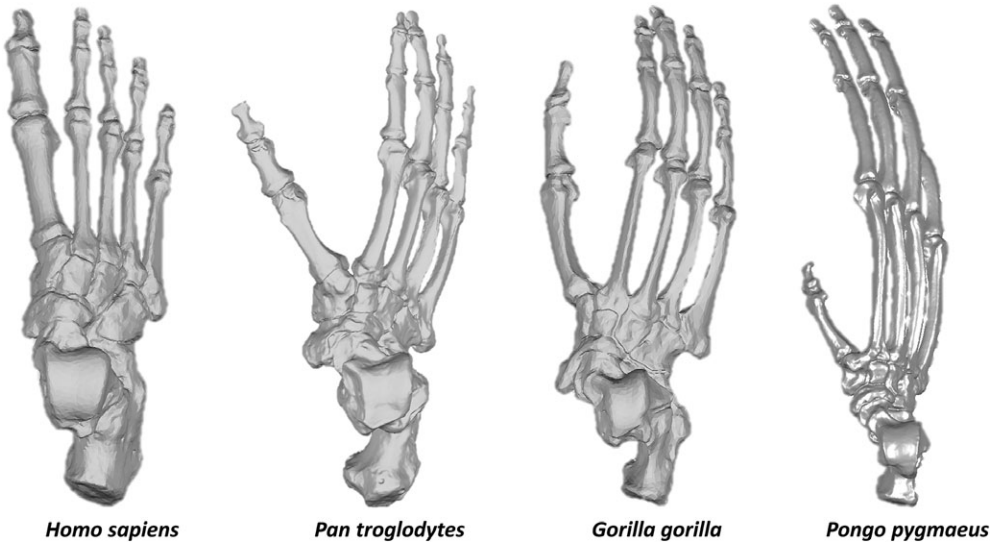

FIGURE 1 Dorsal view of articulated feet from *H. sapiens*, *P. troglodytes*, *G. gorilla*, and *P. pygmaeus*. They are all from the right side and scaled so that they are the same length. The human foot has a robust calcaneus, proximodistally elongated midtarsal region, and short phalanges (especially intermediate phalanges). Notice on the ape feet: the divergent hallux, the foreshortened midtarsus, long metatarsals, and phalanges (especially in *Pongo*). Notice too that the human forefoot is in an everted position, whereas the ape lateral forefoot is inverted putting the lateral digits in opposition to the hallux, which is large in the African apes, but reduced in *Pongo*

Plantigrade apes have a relatively larger calcaneal tuber than other primates (Gebo, 1992); in humans, the tuber is even more voluminous (Latimer & Lovejoy, 1989). While variable across populations (Hatala, Dingwall, Wunderlich, & Richmond, 2013a, 2013b; Lieberman et al., 2015; Pontzer et al., 2014), unshod humans tend to contact the midfoot or forefoot on the substrate during running bouts (Lieberman et al., 2010). While walking, however, humans consistently heel-strike, which functionally helps increase the effective limb length and thus reduce energetic costs (Webber & Raichlen, 2016). However, heel-striking also increases the impact force on the calcaneus and thus it has been proposed that the proximal tuber is enlarged in humans to dissipate these high forces (Latimer & Lovejoy, 1989), though this hypothesis has never been experimentally demonstrated (Holowka & Lieberman, 2018). This relatively enlarged tuber is also present in the Hadar calcanei (A.L. 333–8, –37, –55) from *A. afarensis* (Latimer & Lovejoy, 1989; Zipfel et al., 2011; Prang, 2015a; Table 2). Interestingly, though, the juvenile *A. afarensis* from Dikika has an ape-like gracile calcaneus (DeSilva, Gill, et al., 2018). These data imply that the enlargement of the calcaneal tuber in *A. afarensis* happened developmentally. In contrast, modern human infants are already born with enlarged proximal tubers—an anatomy adaptive for heel-striking bipedalism that has become developmentally canalized. Not all australopiths had robust tubers, however. The proximal tuber is more gracile in those from South African australopiths (StW 352—*A. africanus*?; U.W. 88-99—*A. sediba*; Zipfel et al., 2011; Prang, 2015a). Furthermore, the general geometry of the proximal calcaneus differs between humans and apes (Latimer & Lovejoy, 1989). In humans, a unique structure called the lateral plantar process (LPP) is plantarly positioned (Weidenreich, 1923) and is hypothesized to broaden the area of bony support as the heel contacts the substrate. It may also serve to increase the volume of the calcaneus, though this remains to be tested. In contrast, apes have a dorsally positioned homologous structure to the human LPP, palpable in adults and detectable as an apophyseal flange in juveniles. A plantarly positioned LPP is present in the Hadar calcanei from *A. afarensis* (Latimer & Lovejoy, 1989) and is already present in a human-like position in the juvenile *A. afarensis* from Dikika (DeSilva, Gill, et al., 2018). However, the LPP is more dorsally located in both the adult and juvenile *A. sediba* calcanei from Malapa, South Africa (Boyle et al., 2018; Zipfel et al., 2011). Whether these differences represent normal variation in australopiths, or functionally (and even phylogenetically) relevant differences in different bipedal lineages remains unclear.

Laterally, the ape calcaneus possesses a large projection called the peroneal tubercle (or trochlea); the corresponding structure in humans is considerably smaller and more distally positioned. The peroneal trochlea remains large and ape-like in all known *Australopithecus* calcanei (Gebo & Schwartz, 2006; Stern & Susman, 1983). It is small and human-like in *Homo naledi* (Harcourt-Smith et al., 2015); its relative size remains unknown in earlier *Homo* fossils. Along the lateral body of the calcaneus, apes possess a pit for the insertion of the calcaneofibular ligament. In humans, the insertion is generally a small rugosity. A pit insertion for this ligament is present in the Hadar calcanei and in the Dikika juvenile.

Plantarly, the human calcaneus is broad and the two plantar tubercles (lateral plantar and medial plantar) are roughly subequal. In apes, the plantar surface is dominated by a large, beak-like medial plantar tubercle. This anatomy has been suggested to improve the mechanical advantage of the superficial head of *M. flexor digitorum brevis* during pedal grasping bouts in apes (Sarmiento, 1983). The Hadar calcanei are human-like and lack this ape-like anatomy. However, some hominin calcanei (e.g., *A. sediba*) retain prominent plantar beaks (Zipfel et al., 2011; Figure 2).

Dorsally, humans have a relatively flat proximal talar facet, reflecting substantially less motion at the subtalar joint than in apes. The radius of curvature of this joint is low and human-like in the Hadar calcanei of *A. afarensis* (Latimer & Lovejoy, 1989) and in the taxonomically unassigned Omo calcaneus (Gebo & Schwartz, 2006; Prang,

TABLE 2 Comparative measurements of the calcaneus in fossil hominins

Specimen	Taxon	Age (Ma)	Length of calcaneus (mm) (M1)	Posterior calcaneal length (mm) (M5)	Maximum dorsoplantar height of calcaneal tuberosity (mm) (M7)	Maximum mediolateral breadth of calcaneal tuberosity (mm)	Maximum mediolateral breadth of posterior talar facet (mm) (M10)	Maximum proximodistal length of posterior talar facet (mm) (M9)	Subtended angle of posterior talar facet (°)	Volume of posterior calcaneus (cm^3)
A.L. 333-8	*A. afarensis*	3.2	64.5[a]	46.8	38.1	22.7[a]	24.4[a]	29.8[a]	82°	28.7
A.L. 333-37	*A. afarensis*	3.2	–	–	33.5[a]	24.6	–	–	–	–
A.L. 333-55	*A. afarensis*	3.2	–	46.4	38.8	23.6	24.5[a]	–	–	29.8
StW 352	*A. africanus*	2.0–2.6	–	–	–	–	14.5	22	120°	–
Omo-33-74-896	*Paranthropus?*	2.36	69.4	51.9	–	–	19.4	28.4	87°	–
U.W. 88-99	*A. sediba*	1.98	56.9	43.7	33	21.8	17.3	19.8	118°	13.4
OH 8	*P. boisei?*	1.85	–	–	–	–	–	–	–	–
Sima de los Huesos (Pablos et al., 2012)	*Homo*	0.43	78.5 ± 5.1 (n = 13)	58.3 ± 4.3 (n = 13)	44.5 ± 2.1 (n = 12)	34.2 ± 3.1 (n = 12)	21.9 ± 1.9 (n = 15)	31.7 ± 2.0 (n = 14)	–	–
U.W. 101-724	*H. naledi*	0.24–0.34	–	–	–	–	15.4[a]	–	–	–
U.W. 101-1322	*H. naledi*	0.24–0.34	57.0	40.7	–	–	14.4	20.8	89°	15.4
Jinniushan (Lu, Meldrum, Huang, He, & Sarmiento, 2011)	*Homo*	0.26	75.6	–	42.4	33.0	23.7	30	–	–
Neandertals	*Homo*	0.2–0.03	79.7 ± 6.5 (n = 16)	60.2 ± 5.7 (n = 15)	46.2 ± 4.9 (n = 13)	31.7 ± 3.8 (n = 9)	24.6 ± 1.9 (n = 15)	30.8 ± 3.8 (n = 18)	–	–

Note. KNM-ER 1500t and KB 3297 were tentatively identified as hominin 4 calcanei, but are not. The hominin foot StW 573 possesses a fragmentary calcaneus, but it is probably from a cercopithecoid. Only adult calcanei are shown in this table. Juvenile specimens DIK-1-1f (*A. afarensis*) and U.W. 88-113 (*A. sediba*) are described elsewhere (see DeSilva et al., 2018, b). Juvenile fossils from *H. naledi* (U.W. 101–907 and U.W. 101-1662) are described in Harcourt-Smith et al., (2015). ATD6-117 is a piece of the posterior talar facet from Gran Dolina (Pablos et al., 2012). It is too fragmentary to yield any of the measurements reported in this table. Calcanei from *Ardipithecus* (ARA-VP-6/500–096; White et al., 2009) and Gona (Simpson, Levin, Quade, Rogers, & Semaw, 2018), along with StW 643 (Clarke, 2013) and KNM-ER 64062 (Jungers et al., 2015) have been mentioned in print but are not yet formally described.

[a] Estimate that approximates the actual value.

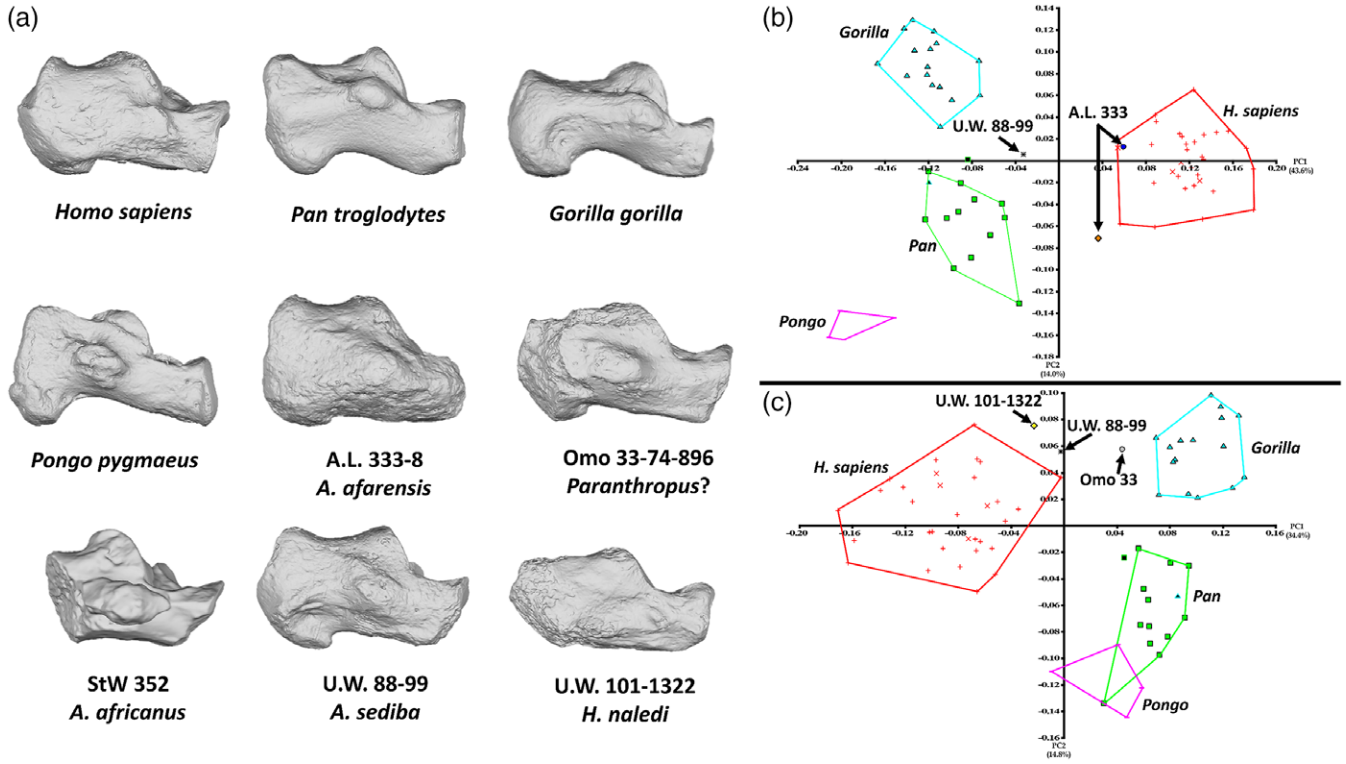

FIGURE 2 (a) Calcanei from extant apes, modern human, and fossil hominins in lateral view. Each bone is from the right side (mirrored if necessary) and has been scaled so that the proximodistal length of the calcaneus is roughly the same. Notice the gracile tuber, projecting medial plantar process, and large peroneal trochlea in the ape calcanei. (b) PCA of a geometric morphometrics analysis performed on the most complete hominin calcanei (A.L. 333-8, A.L. 333-55, and U.W. 88-99). PC1 explains 43.6% of the variation; PC2 14%. Notice that the *A. afarensis* calcanei plot either within or just outside the human distribution, whereas *A. sediba* falls between the human and ape scatter. (c) PCA of a geometric morphometrics analysis performed using a smaller set of landmarks allows inclusion of the Omo 33-74-896 calcaneus and *H. naledi*. PC1 explains 34.4% of the variation; PC2 14.8%. Notice that the Omo calcaneus nears the *Gorilla* distribution, whereas both *A. sediba* and *H. naledi* fall outside the modern human range. Details of landmarks and PCA analysis in McNutt, Zipfel, and DeSilva (2018) and DeSilva, Carlson, et al. (2018)

2016b), but is high and ape-like in calcanei assigned to *A. africanus* (StW 352) and *A. sediba* (U.W. 88-99; Zipfel et al., 2011; Prang, 2016b). Furthermore, in dorsal view, the human calcaneus lies on a relatively continuous proximodistal (PD) axis (Figure 3). In contrast, the African ape calcaneus possesses a medial deflection of the distal body relative to the proximal, with the deflection point positioned at the peroneal trochlea (Deloison, 1985; Gebo, 1992). Given that the calcaneus forms developmentally from two distinct regions (Čihák, 1972), we hypothesize that the ape calcaneus forms such that the distal portion is medially deflected relative to the proximal. This has the effect of adducting the forefoot relative to the hindfoot. In humans, the proximal calcaneus has reoriented laterally (relative to the distal calcaneus), which corresponds to a final change in the evolution of the foot according to Lewis (1981), and aligns the long axis of the foot with the axis of the subtalar joint. Interestingly and importantly, the Hadar calcanei, while human-like in many respects, retain the ape-like medial deflection of the distal calcaneus. In contrast, chronologically later calcanei from Omo, OH 8, and even *A. sediba* have the human-like geometry in which the body of the calcaneus is aligned in the sagittal plane (Figure 3).

Distally, the calcaneocuboid joint is shaped quite differently in humans and apes. In humans, the joint is flat and spills onto the medial side of the bone for articulation with the cuboid beak (Bojsen-Møller, 1979). Dorsally, there is a bony overhang (anterolateral process) that restricts rotation at the calcaneocuboid joint (Elftman & Manter, 1935). In contrast, the African ape cuboid is more concave with a medially positioned pit around which the beak of the cuboid can pivot (Lewis, 1980b). In orangutans, the cuboid facet is convex and abruptly spills medially into a groove for the cuboid beak. The Hadar calcanei are damaged distally; however, A.L. 333-8 has a preserved pit, suggesting more calcaneocuboid mobility than in modern humans. The joint is more human-like in the Omo calcaneus and in OH 8. Damage precludes assessment of this joint in the South African australopiths. In lateral view, the cuboid facet is vertically oriented in the apes, but is diagonally positioned dorsodistally to plantoproximally in humans. This tilt to the calcaneocuboid joint in humans is correlated with the medial and lateral longitudinal arching of the foot (Berillon, 2003; Heard-Booth, 2017; Morton, 1935; Weidenreich, 1923). This angulation is present in the Omo calcaneus and OH 8, but also in the preserved portion of the *A. africanus* and *A. sediba* calcanei suggesting the presence of at least an incipient arch in these early hominins.

A geometric morphometrics analysis of hominin fossil calcanei (McNutt, Zipfel, & DeSilva, 2018; McNutt & DeSilva, 2018; Figure 2) found the *A. afarensis* calcanei to cluster within, or just outside, the modern human range. In contrast, calcanei from *A. sediba*, and the Omo calcaneus are positioned between the human and ape (mostly gorilla) shape-space.

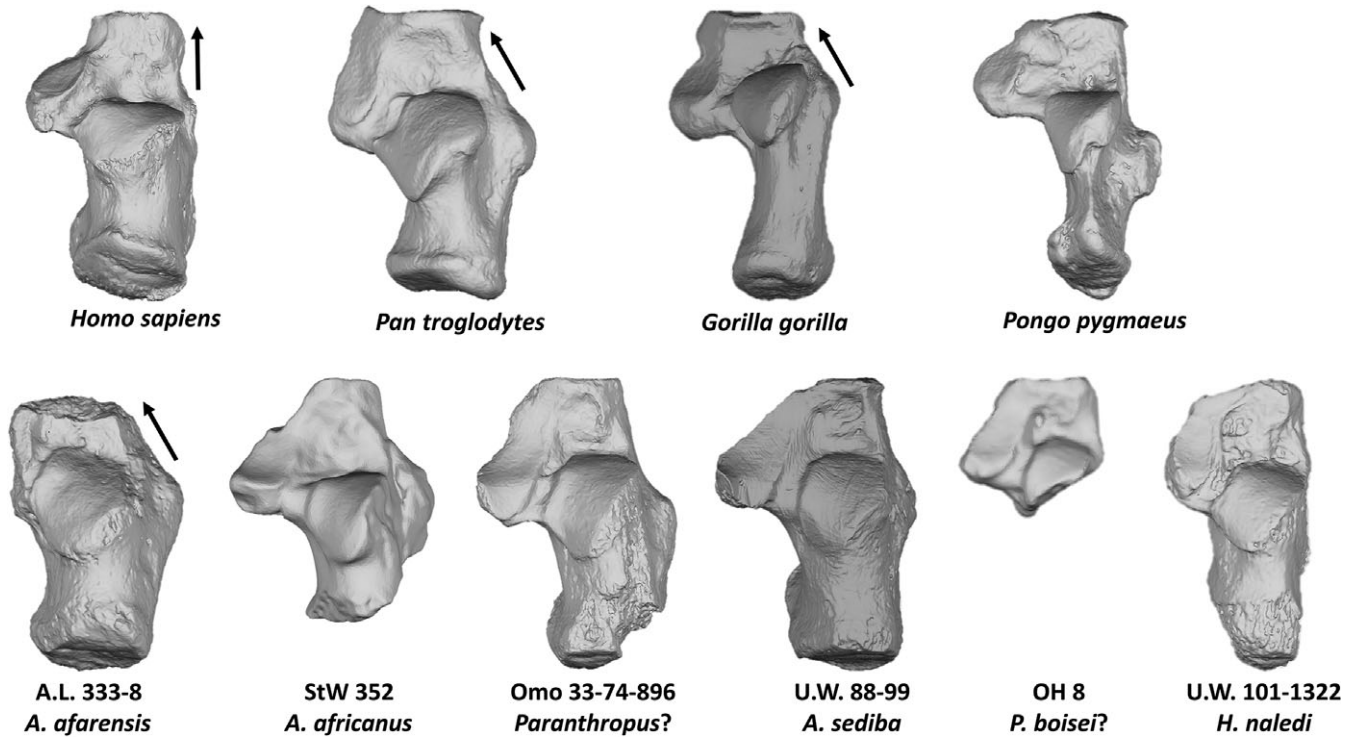

FIGURE 3 Calcanei from extant apes, modern human, and fossil hominins in dorsal view. Each bone is from the right side (mirrored if necessary) and has been scaled so that the proximodistal length of the calcaneus is roughly the same. Notice that in chimpanzees and gorillas, the distal portion of the calcaneus deflects medially relative to the proximal portion of the bone, whereas in humans the distal and proximal portions of the bone are aligned in the sagittal plane. *A. afarensis* is African ape-like for this anatomy (see arrow)

2.2 | Talus

The talus is the bony junction between the foot and the leg and is thus of critical functional importance. Additionally, and fortunately, the talus is a robust bone without any muscular attachments and these are probably contributing factors resulting in so many hominin and hominoid fossil tali (Table 3). The talus articulates dorsally and medially with the tibia; laterally with the fibula; plantarly with the calcaneus; and distally with the navicular. The anterior talofibular ligament, one of the most often sprained ligaments in the human body (Butler & Walsh, 2004), is typically absent in ape feet (Gomberg, 1981), though it can occasionally be found in gibbons (Inman, 1976).

In dorsal view, the talar trochlea is wedge shaped (distally wide). This wedging is much more pronounced in apes (Figure 4), and particularly in African apes (Sewell, 1904) and is hypothesized to be related to loading in dorsiflexion, as happens during bouts of vertical climbing (DeSilva, 2009). A study comparing tali from captive and zoo settings revealed that wild-shot apes (*Pan*, *Gorilla*, *Pongo*) have significantly more wedged talar trochlea than their zoo counterparts, suggesting that this is indeed an arboreal signal (Venkataraman, Kraft, DeSilva, & Dominy, 2013). The absence of strong wedging in cercopithecoid tali, or tali from many Miocene hominoids, but its presence in atelines and hylobatids would suggest that beyond just an arboreal signal, this is more specifically an orthograde, flexed-ankle vertical climbing one (DeSilva, 2008). The strongly wedged talus of the Aramis *Ardipithecus ramidus* foot skeleton would indicate that this hominin moved from the ground to the canopy using ape-like flexed ankle vertical climbing. No other hominin talus exhibits strong wedging, suggesting that australopiths either did not climb on a highly-flexed ankle or alternatively, given that some humans can climb this way today (Venkataraman, Kraft, & Dominy, 2013), they did not do so frequently or rapidly enough to leave a bony signal.

The talus has been referred to as a "badly mounted wheel" (Rasmussen, Kromann-Anderson, & Boe, 1983; see also Inman, 1976) in part because the lateral trochlear surface is extended compared with the medial. This difference would produce foot abduction during dorsiflexion (Lewis, 1980a), which is beneficial for proper positioning of the foot during climbing. In humans, the medial and lateral rims are subequal in length. The "apical angle" of the talar body, formed dorsally between the lateral and medial trochlear rims, is low in humans and higher in the apes (DeSilva, 2008). Fossil *Australopithecus* and early *Homo* tali fall within the human range, while OH 8 (*P. boisei*) appears to have unique foot adduction during dorsiflexion (Day & Wood, 1968).

Viewed proximally, the ape talus possesses a high lateral trochlear rim and a relatively low medial trochlear rim. In contrast, humans possess subequal trochlear rims (Weidenreich, 1923). This morphological difference has important functional consequences. In apes, this talar geometry, combined with an oblique angulation to the distal tibia results in an inverted set to the foot, conducive for tree climbing and general arboreal behaviors (DeSilva, 2009; Latimer, Ohman, & Lovejoy, 1987). The connection between this talar morphology and arboreality is reinforced by the presence of a higher lateral trochlear rim in western lowland gorillas than in the more terrestrial eastern mountain gorillas (Dunn, Tocheri, Orr, & Jungers, 2014; Knigge, Tocheri, Orr, &

TABLE 3 Comparative measurements of the talus in fossil hominins

Fossil talus	Taxon	Age (Ma)	Trochlear body width (mm) (M5)	Head ML width (mm) (M9)	Head DP height (mm) (M10)	Torsion angle (°)	Declination angle (°)	Horizontal angle (°)
StW 573	*A. prometheus*?	3.67?	–	24.4	17.1	26.1		31.3
A.L. 288-1as	*A. afarensis*	3.2	18.0	20.7	14.5	29	10.9	33.4
A.L. 333-75	*A. afarensis*	3.2	–	25.0	16.1	–	–	–
A.L. 333–147	*A. afarensis*	3.2	24.1	–	–	–	12[a]	–
StW 88	*A. africanus*	2.0–2.6	19.1	24.7	17.9	17	9.3	32.0
StW 102	*A. africanus*	2.0–2.6	19.4	–	–	–	–	–
StW 347	*A. africanus*	2.0–2.6	–	21.1	17.1	41	–	–
StW 363	*A. africanus*	2.0–2.6	19.0	–	–	–	12[a]	32[a]
StW 486	*A. africanus*	2.0–2.6	21.0	24.6	–	–	10[a]	27[a]
Omo 323-76-898	*Homo*?	2.2	23.2	27.5	18.1	31	20.1	
U.W. 88-98	*A. sediba*	1.98	18.1	23.5	19.5	22	28	31.3
TM 1517	*P. robustus*	1.9	18.9	27.7	–	24	–	32
SKX 42695	*Homo*?	1.5–2.0	23.1	–	–	–	–	–
KNM-ER 1476	*P. boisei*?	1.88	20.4	25.9	–	31	17.6	30
KNM-ER 813	*Homo*?	1.85	24.7	27.8[a]	–	47	23.9	14
OH 8	*P. boisei*?	1.85	19.5	24.4	17.5	26	17.0	33.5
D4110	*H. erectus*	1.77	–	27.0	–	–	–	26.0
KNM-ER 1464	*P. boisei*?	1.7	25.3	28.4	20.1	24	22	20
KNM-ER 5428	*H. erectus*	1.6	33.9	36.6	24.0	39	41	20
ATD6-95	*H. antecessor*	0.77–0.95	30.7	–	–	–	–	–
Sima de los Huesos	*Homo*	0.43	29.1 ± 2.3 (n = 20)	30.4 ± 2.2 (n = 18)	21.8 ± 1.9 (n = 18)	–	–	–
U.W. 101-148	*H. naledi*	0.24–0.34	20.6	23.9[a]	18.4	45	14	25
U.W. 101-520	*H. naledi*	0.24–0.34	18.3[a]	21.3[a]	–	35[a]	18[a]	20[a]
U.W. 101-1417	*H. naledi*	0.24–0.34	18.4	20.7[a]	14.3	37	10	26
Jinniushan	*Homo*	0.26	30.3	31.3	21.5	46	–	30
Neandertals	*Homo*	0.03–0.2	28.6 ± 2.1 (n = 22)	34.7 ± 3.4 (n = 23)	22.5 ± 2.2 (n = 24)	38.7 ± 5.2 (n = 14)	–	25.5 ± 4.2 (n = 14)
KHS 1–59	*H. sapiens*	0.195	25.3[a]	30.1[a]	19.8[a]	30[a]	20[a]	17[a]
LB1/15	*H. floresiensis*	0.06	19.5	22.6	16.2	26		23

Note. Data in this table from original fossils and measurements reported in Day & Wood, 1968; Leakey & Wood, 1973; Day, Leakey, Walker, & Wood, 1976; Trinkaus, 1983; DeSilva, 2008; Jungers et al., 2009; Lu et al., 2011; Zipfel et al., 2011; Pablos et al., 2012; Boyle & DeSilva, 2015; Prang, 2016b. Only adult tali are shown in this table. Juvenile talus DIK-1-1f (*A. afarensis*) is described elsewhere (DeSilva, Gill, et al., 2018) as are juvenile fossils from *H. naledi* (U.W. 101-080, U.W. 101-910, U.W. 101-1623; Harcourt-Smith et al., 2015). Fossils too fragmentary to yield any of the measurements reported in this table include KNM-ER 803, U.W. 101-1031, U.W. 101-1215, and LB1/54. Tali from *Ardipithecus* (ARA-VP-6/500-023; White et al., 2009; Lovejoy et al., 2009) and Gona (Simpson et al., 2018), along with BOU-VP-2/95 (Asfaw and Gilbert, 2008) and KNM-ER 64062 (Jungers et al., 2015) have been discussed in print but are not yet formally described.

[a] Estimate that approximates the actual value.

McNulty, 2015). Humans have an everted foot upon which an orthogonal tibia is positioned (Latimer et al., 1987). This geometry orients the foot directly under the knee and is one feature that minimizes mediolateral sway during bipedal locomotion (Saunders, Inman, & Eberhart, 1953). The talar axis angle is a measure of this inverted or everted "set" to the foot. *Ardipithecus ramidus* from the Aramis locality possesses a high, ape-like talar axis angle (Lovejoy et al., 2009), indicating an inverted set to this foot. In contast, the *Ardipithecus* talus from Gona, Ethiopia has a lower, more human-like talar axis angle, in part because of a higher medial trochlear rim (Simpson et al., 2018). Bearing in mind the small sample sizes currently available, these differences could indicate that the Gona *Ardipithecus* possessed a more everted, human-like foot better adapted for bipedal locomotion than the Aramis *Ardipithecus*. All chronologically subsequent hominin tali from *Australopithecus* and fossil *Homo* have low human-like talar axis angles (DeSilva, 2009). In fact, the angles tend to be lower than typically found in modern humans because only recently have modern humans dorsoplantarly expanded the body of the talar trochlea (which would have the effect of raising the talar axis angle; Boyle & DeSilva, 2015). Related to this morphology is the orientation of the groove between the medial and lateral tubercles for the tendon of *M. flexor hallucis longus*, which is vertically oriented in human and hominin tali, and obliquely oriented in ape tali (Latimer et al., 1987).

These data together allow one to construct a general evolutionary history of the trochlear body. Based on tali from Miocene apes and *Ardipithecus*, the talus of the human–chimpanzee last common ancestor (LCA) and that of the earliest hominins had a high lateral trochlear body, a high talar axis angle (in the coronal plane), and an inverted set

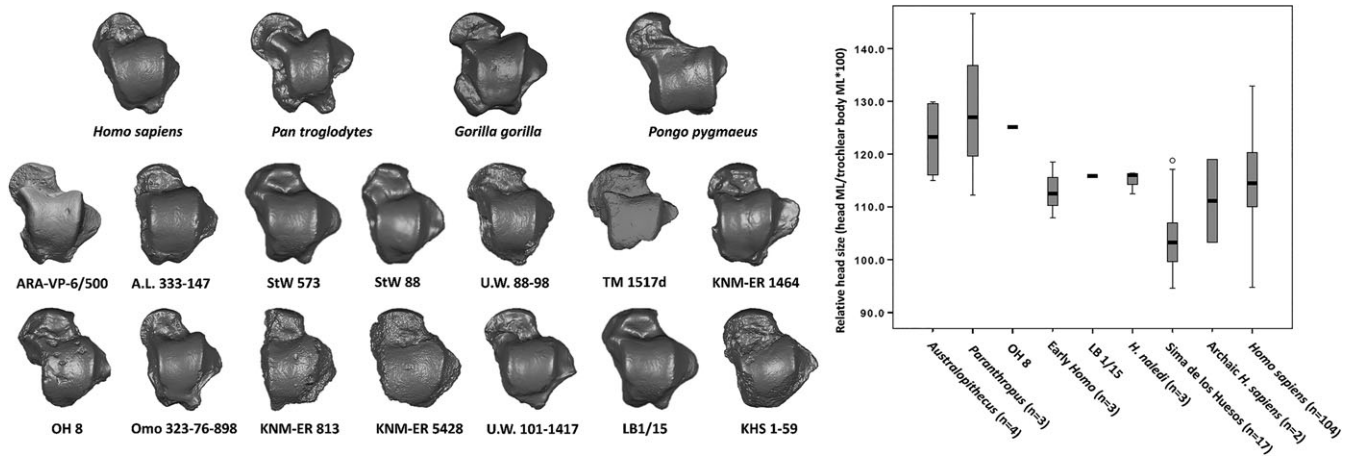

FIGURE 4 Tali from a modern human, extant apes, and fossil hominins in dorsal view. Each bone is from the right side (mirrored if necessary) and has been scaled so that the proximodistal length of the talus is roughly the same. Notice that the distal aspect of the talar trochlea is mediolaterally expanded (wedged) in apes (especially in African apes) and *Ardipithecus* (ARA-VP-6/500), compared with humans and most fossil hominins. Right: Boxplot displaying mediolateral width of talar head to the width of the trochlear body. Boxes span the interquartile ranges, with the horizontal center lines indicating median values. Whiskers indicate sample range, excluding outliers (dots). Relative to the width of the trochlear body, fossils from *Australopithecus* and *Paranthropus* (including OH 8) have a mediolaterally broad head (data in Table 3). The head is ML shorter (or the body is ML wider) in fossils attributed to *Homo*, especially in the Sima de los Huesos fossils, which have a uniquely small talar head. Image of *Ardipithecus ramidus* talus courtesy of Tim White and Gen Suwa

to the ankle joint, functionally consistent with frequent arboreality. Boyle and DeSilva (2015) hypothesized that the first change to the talus was a lowering of the lateral trochlear body. However, the Gona *Ardipithecus* talus suggests that we were in error and instead the evening of the trochlear rims was not solely a product of a lowering of the lateral rim, but an elevation of the medial rim as proposed long ago (Elftman & Manter, 1935). Additionally, in Boyle and DeSilva (2015), we missed a key change in which the mediolateral width of the talar trochlea must have increased to accommodate the functional demands of bipedality. This had not yet happened in the Gona *Ardipithecus* and instead is first seen in fossil *Australopithecus* from Hadar (A.L. 333-147 and A.L. 288-1) and Sterkfontein Member 2 (StW 573; McNutt, Zipfel, & DeSilva, 2018). Stasis in this morphology can be seen through the human fossil record and even into early members of our own species. The Omo-Kibish talus from the 195 ka *H. sapiens* skeleton is dorsoplantarly short, similar to the 1.6 Ma *H. erectus* talus KNM-ER 5428 (McNutt, Zipfel, & DeSilva, 2018). Only recently did the dorsoplantar height of the human talus increase, for reasons that remain unclear (Boyle & DeSilva, 2015).

One final observation on the talar trochlea is warranted: the human talar trochlea, in proximal or distal view, is relatively flat, with only a weak groove dividing the medial and lateral aspects of the trochlea. Apes, in contrast, have a deeper keel, accentuated by the raised lateral rim of the trochlea and low medial rim (Figure 5). The Aramis *Ardipithecus* talus is ape-like in this morphology (Lovejoy et al., 2009; Supporting Information Figure S1). However, with the elevation of the medial rim in hominins, a deep groove is produced. This is evident in the Gona *Ardipithecus* and may have helped to stabilize the ankle joint. However, in some hominins, the talar trochlea became remarkably flat, perhaps to more effectively dissipate high forces across a broad surface, though this remains to be tested. This flat morphology of the trochlear surface is present in tali assigned to *A. afarensis* (A.L. 288-1, A.L. 333-147), *A. sediba* (U.W. 88-98), early *Homo* (Dmanisi), *H. erectus* (KNM-ER 5428), *H. floresiensis*, and *H. naledi*. The deeply keeled talar trochlea is variably retained in fossils assigned to *A. africanus* and the robust australopiths. It is most strongly expressed in OH 8, considered here to be from *P. boisei* and not, as is standard in our field, *H. habilis* (e.g., Leakey, Tobias, & Napier, 1964).

Human tali differ from ape tali in three angular measures reflecting how the head and neck are positioned relative to the talar trochlea. In the transverse plane, apes possess a larger horizontal angle in which the head and neck are medially deflected compared with the trochlear body (Figure 4). Some have suggested that this anatomy is related to a grasping hallux (e.g., Kidd et al., 1996), but others disagree (e.g., Barnett, 1955; Lovejoy, 1975, 1978) and an ape-like horizontal angle in a fossil foot known to have an adducted hallux (OH 8) effectively refutes this idea. Nevertheless, an ape-like horizontal angle is found in early *Australopithecus* tali and in OH 8. In the coronal plane, the head and neck exhibit strong torsion compared with the trochlear body in humans, but not in apes. Elftman and Manter (1935) suggest that the head and neck of human and ape tali are the same and that it is the talar trochlea that is oriented differently in humans. Nevertheless, *Australopithecus* tali generally possess the low, ape-like condition (but see StW 347; Prang, 2016b), whereas tali assigned to *Homo* (e.g., KNM-ER 813, KNM-ER 5428) have more human-like head/neck torsion. Manter (1941), Elftman (1960), and Langdon, Bruckner, and Baker (1991) proposed that head/neck torsion is related to "locking" and "unlocking" of the transverse tarsal (Chopart's) joint during foot pronation and supination. In apes, the low torsion would align the transverse tarsal joint and permit midfoot flexibility, whereas high torsion would prevent joint alignment and limit joint motion—what Kidd (1999) calls the "midtarsal restraining mechanism". However, it is worth noting that head/neck torsion is highly variable in human tali (Lovejoy, 1978). In sagittal view, the head/neck of the ape talus is roughly in the same plane as the body of the talus. However, in human

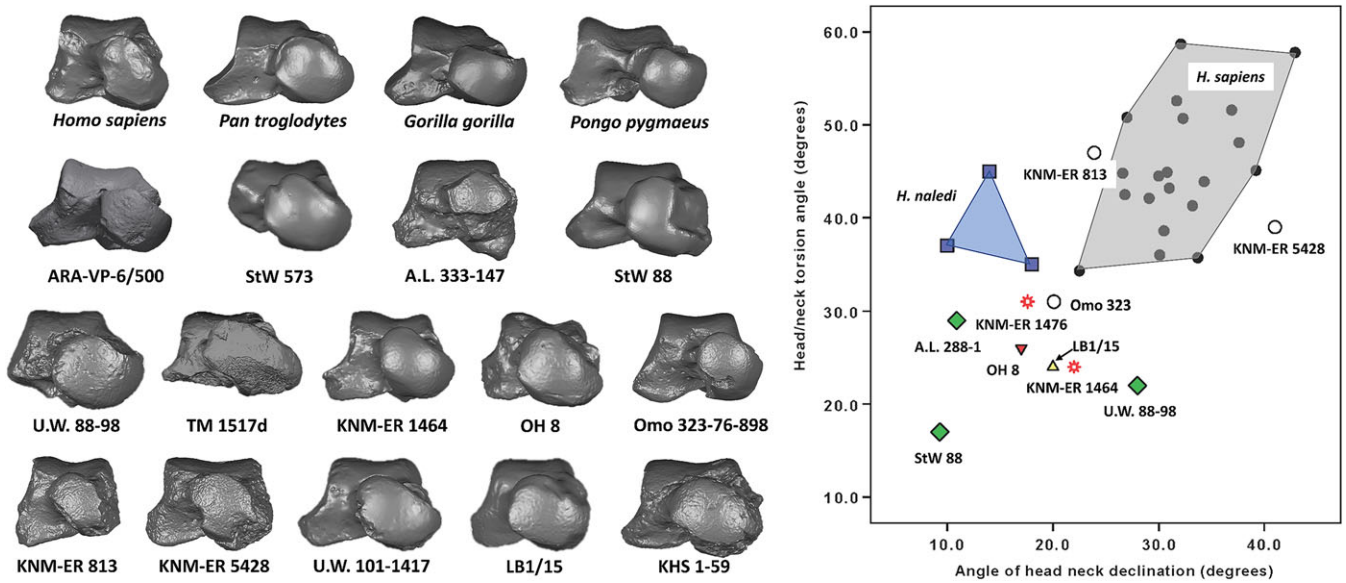

FIGURE 5 Tali from a modern human, extant apes, and fossil hominins in distal view. Each bone is from the right side (mirrored if necessary) and has been scaled so that the dorsoplantar height of the talus is roughly the same. Note that the talar trochlea in humans is flat whereas apes and *Ardipithecus* have a dorsolateral to plantomedial tilt to the talar trochlea, which helps positions the foot in an inverted set. Note as well that the grooved trochlear surface and large talar head in OH 8 is similar to that found in KNM-ER 1464 (*Paranthropus*) and quite distinct from fossil *Homo* (Omo 323, KNM-ER 813, KNM-ER 5428). The human talar head and neck are twisted relative to the trochlear body, whereas the ape head and neck are more horizontally positioned. To the right, this head/neck torsion is plotted against sagittal plane declination of the head and neck in humans (black dots; gray outline) and fossil hominins. Notice that early hominins tend to have lower (ape-like) head/neck torsion and declination, whereas fossil *Homo* tali are just outside the human range. *H. naledi* occupies a unique space with low, ape-like declination and high, human-like torsion. Image of *Ardipithecus ramidus* talus courtesy of Tim White and Gen Suwa

tali, the head and neck of the talus are plantarly directed relative to the plane of the ankle joint, giving the human talus a strong plantar declination [originally called inclination by Day & Wood, 1968]. A CT-based study of modern humans has shown this anatomy to vary with medial longitudinal arch height (Peeters et al., 2013). In australopiths, OH 8, *H. floresiensis* and *H. naledi* the head/neck declination angle is low and ape-like. It is slightly higher in the *A. sediba* talus (but see Prang, 2015b), and has human-like declination in *H. erectus* (KNM-ER 5428).

There are additional differences between the talus of humans and apes. Relative to human tali, African ape tali tend to possess a laterally flaring fibular facet (Gebo, 1992) and a concavely excavated medial cotylar fossa for contact with the medial malleolus. These anatomies vary considerably in hominin tali. Tali suggested to belong to robust australopiths (KNM-ER 1464, ER 1476, and TM 1517) and OH 8 have strongly flared fibular facets. Additionally, in proximal view the fibular and tibial facets are roughly parallel in humans and markedly angled in apes. Tali from South African localities (StW 88, U.W. 88-98, *H. naledi*) and OH 8 possess more chimpanzee-like, angled malleolar facets, whereas the Hadar and Koobi Fora tali have more human-like parallel facets (Harcourt-Smith et al., 2015).

The talar head is generally more curved both mediolaterally and dorsoplantarly in apes compared with the human talus (Prang, 2016a). In particular, the ape head extends more posterolaterally (Elftman & Manter, 1935), which may be a skeletal correlate of the elevated talo-navicular motion that occurs in the ape foot (Thompson, Holowka, O'Neill, & Larson, 2014). Tali assigned to early *Australopithecus* (A.L. 288-1 and StW 88) retain the ape-like mediolateral curvature of the talar head, though this may also be related to their small size. Fossil tali from *Australopithecus* and early *Homo* have human-like dorsoplantar (DP) curvature of the head, and in some cases (*A. sediba* and *H. floresiensis*) are even flatter than is common in modern humans (Prang, 2016a). Similarly, the calcaneal facets are flatter in human tali than in ape tali (Prang, 2016a). The South African australopiths (*A. africanus* and *A. sediba*) are more ape-like, suggesting elevated mobility at the subtalar joint (Prang, 2016b). Other hominins, including *A. afarensis*, are more human-like (Prang, 2016b). Plantarly, at the junction of the talar head and the anterior calcaneal facet, is a smooth triangular impression caused by the plantar calcaneonavicular (spring) ligament. This ligament is present in the African ape foot (Gebo, 1992; Gomberg, 1981), but does not leave a mark on the plantar talar head (Lamy, 1986). This impression can be found in tali of *A. afarensis* and other early hominins, suggesting the presence of at least an incipient medial longitudinal arch (Lamy, 1986).

2.3 | Navicular

The navicular articulates with the talus proximally and with the three cuneiforms distally. Laterally, the ape navicular contacts the cuboid, a condition that is variably present in humans. A significant portion of the tendon of *M. tibialis posterior* inserts on the navicular tuberosity. In humans, the cuneiform facets are in roughly the same coronal plane. In apes, the lateral cuneiform facet faces laterally and is more concave than the corresponding facet in humans. African ape naviculars possess a large, projecting tuberosity. The tuberosity is smaller in humans, and smaller still in *Pongo* (Figure 6). The human navicular, compared with extant apes, is proximodistally (PD) elongated

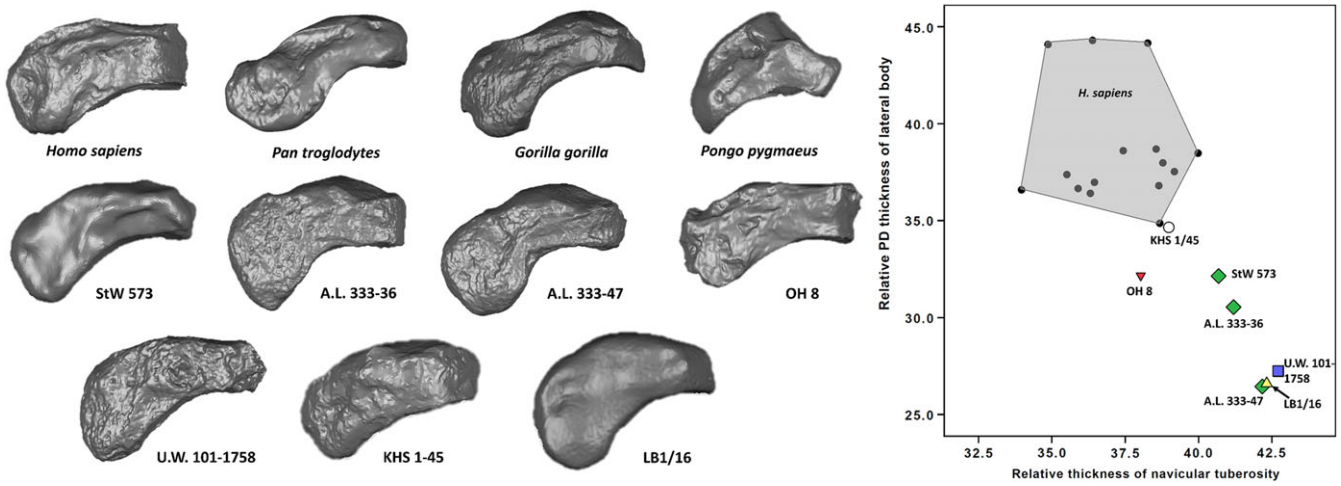

FIGURE 6 Naviculars from extant apes, modern human, and fossil hominins in dorsal view. Each bone is from the right side (mirrored if necessary) and has been scaled so that the mediolateral width of the navicular is roughly the same. Notice that relative to the ape naviculars, humans have a proximodistally elongated lateral body and relative to the African ape naviculars, a reduced, nonprojecting tuberosity. The tuberosity is essentially nonexistant in *Pongo*. The tuberosity remains large and the lateral body is pinched in fossil naviculars from *Australopithecus*, *H. naledi*, and *H. floresiensis*. Right: relative to the navicular width, the square root of the product of the dorsoplantar and proximodistal thickness of the tuberosity, and the proximodistal thickness of the lateral navicular body are plotted in humans (n = 15) and fossil hominins. Notice that the Omo-Kibish navicular is close to the modern human distribution whereas all other hominins, including *H. naledi* and *H. floresiensis*, possess larger tuberosities and laterally pinched navicular bodies

(Elftman & Manter, 1935), consistent with the generally PD expanded tarsal row in humans. In contrast, the ape navicular body is PD narrow and thins laterally. The human navicular also has rugose attachments for the plantar calcaneonavicular (spring) and cubonavicular ligaments.

Hominin fossils (Table 4) have been difficult to interpret and there are conflicting findings. Lovejoy et al. (2009) suggested that an elongated tarsal row is the primitive condition from which humans have further experienced tarsal elongation, including in the navicular body, and apes independently evolved a foreshortened navicular; a fragmentary navicular body from *Ardipithecus* appears to be PD thick. Lovejoy et al. (2009) further contended that the navicular tuberosity enlargement in African apes is illusory and that the PD enlargement of the navicular body in humans masks a still-large tuberosity. Harcourt-Smith (2002) results are in conflict with this interpretation; he used a geometric morphometrics analysis to show that African apes have both an enlarged tuberosity and a laterally tapered navicular body.

The Hadar naviculars (A.L. 333-36 and A.L. 333-47) from *A. afarensis* also possess a large navicular tuberosity and laterally narrow PD navicular body, and are thus African ape-like in certain respects (Berillon, 2003; Harcourt-Smith, 2002; Sarmiento & Marcus, 2000). Harcourt-Smith (2002) interprets the large navicular tuberosity as evidence for medial weight bearing in a foot that lacks a human-like longitudinal arch. Prang's (2016a, 2016b, 2016c) reanalysis of the Hadar naviculars finds them to be more human-like than African ape-like.

StW 573 was originally interpreted as being more primitive and ape-like (Clarke & Tobias, 1995; Deloison, 2003; Kidd & Oxnard, 2005). However, a reanalysis by Harcourt-Smith (2002) found instead that the shape of this bone is more human-like, with a relatively smaller navicular tuberosity and more PD elongated navicular body than the Hadar naviculars (Figure 6). Similarly, he found the OH 8 navicular to cluster with humans, in contrast to a study that found the OH 8 navicular to be more ape-like (Kidd et al., 1996). Prang's (2016a, 2016b, 2016c) reanalysis found the OH 8 navicular to be human-like, consistent with other studies on this foot (Stern & Susman, 1983). Surprisingly though, the new *Homo* foot from Ileret and the late Pleistocene foot of *H. floresiensis* are more primitive in possessing enlarged navicular tuberosities and laterally pinched navicular bodies (Jungers et al., 2009; Jungers et al., 2015; Figure 6). These data might suggest lower medial longitudinal arches in these hominins, and a less efficient medial weight transfer mechanism. Naviculars from *H. naledi* are fragmentary, though a preliminary look at a recently recovered complete bone (U.W. 101-1758) also finds a large navicular tuberosity and laterally tapering navicular body (Figure 6).

2.4 | Cuboid

The cuboid articulates proximally with the calcaneus and distally with the fourth and fifth metatarsals (Mt4 and Mt5). Medially, the cuboid articulates with the lateral cuneiform and in apes (but only occasionally in humans) proximomedially with the navicular. Laterally, a sesamoid (os peroneum) can be found in the cuboidal groove of monkey and gibbon cuboids, or proximolaterally positioned outside of the groove in human cuboids. The os peroneum is typically absent in great apes. Lovejoy et al. (2009) document an os peroneum facet in the cuboidal groove in *Ardipithecus ramidus* and proposed that this monkey-like anatomy was evidence for the independent loss of the os peroneum in *Pongo*, *Gorilla*, and *Pan*. They further suggested that the proximolateral repositioning of the os peroneum in humans (and OH 8) lifted the *M. peroneus longus* (PL) tendon out of the cuboidal groove and obliquely across the foot (Lovejoy et al., 2009). This reorientation of the PL tendon is hypothesized to help stiffen the midfoot and support the arch in a foot that had lost a grasping hallux. The importance of the os peroneum for foot evolution will require additional

TABLE 4 Comparative measurements of the navicular in fossil hominins

Accession number	Taxon	Age (Ma)	Maximum ML width	Maximum DP height (mm)	PD thickness of tuberosity (mm)	DP height of tuberosity (mm)	Maximum length of talar facet (mm)	Maximum height of talar facet (mm)	Lateral PD thickness of body (mm)
StW 573	*A. prometheus*?	3.67?	33.6	18.5	16.8	10.1	22.2	–	10.8
A.L. 333-36	*A. afarensis*	3.2	37.0	20.2	22.5	11.5	26.1	16.5	11.3
A.L. 333-47	*A. afarensis*	3.2	36.3	21.5	18.5	10.9	24.1	16.5	9.6
OH 8	*P. boisei*?	1.85	31.4	18.6	15.5	9.2	23.8	15.8	10.1
Sima de los Huesos	*Homo*	0.43	44.2 ± 4.0 (n = 9)	–	–	–	–	–	–
U.W. 101-623	*H. naledi*	0.24–0.34	–	–	–	–	–	–	8.5[a]
U.W. 101-811	*H. naledi*	0.24–0.34	–	–	–	–	–	–	7.9
U.W. 101-1030	*H. naledi*	0.24–0.34	–	–	–	–	–	13.5	8.9
U.W. 101-1562	*H. naledi*	0.24–0.34	–	14.7[a]	–	–	18.9	12.3	6.5
U.W. 101–1758	*H. naledi*	0.24–0.34	34.5	20.8	17.8	12.2	24.1	16.3	9.4
Jinniushan	*Homo*	0.26	40.3	24.3	18.6	13.1	–	–	–
Neandertals	*Homo*	0.03–0.2	43.7 ± 3.1 (n = 14)	26.4 ± 2.5 (n = 5)	–	–	29.1 ± 2.8 (n = 7)	22.0 ± 4.3 (n = 7)	–
KHS 1–45	*H. sapiens*	0.195	37.8	28.1	17.1	12.7	28.5	21.5	13.1
LB1/16	*H. floresiensis*	0.06	29.7	–	–	–	–	–	–
LB1/26	*H. floresiensis*	0.06	29.2	–	–	–	–	–	–

Note. ML, mediolateral; DP, dorsoplantar; PD, proximodistal. Data in this table from original fossils and measurements reported in Trinkaus, 1975; Latimer et al., 1982; Pearson, Royer, Grine, & Fleagle, 2008; Jungers, Larson, et al., 2009; Lu et al., 2011; Mersey, Jabbour, Brudvik, & Defleur, 2013; Harcourt-Smith et al., 2015; Pablos, Pantoja-Pérez, Martínez, Lorenzo, & Arsuaga, 2017. Only adult naviculars are shown in this table. Juvenile navicular DIK-1-1f (*A. afarensis*) is described elsewhere (DeSilva, Gill, et al., 2018) as are juvenile fossils from *H. naledi* (U.W. 101-910, U.W. 101-997; Harcourt-Smith et al., 2015). Naviculars from *Ardipithecus* (ARA-VP-6/503: White et al., 2009; Lovejoy et al., 2009), StW 623 (Clarke, 2013) and KNM-ER 64062 (Jungers et al., 2015) have been discussed in print but are not yet formally described. SWT/UNE-2 is an undated navicular from Swartkrans preliminarily announced by Throckmorton et al. (2015) and remains undescribed.

[a] Estimate that approximates the actual value.

comparative work as well as experimental studies that measure foot function as it pertains to an os peroneum and *M. peroneus longus* (Holowka & Lieberman, 2018).

The human cuboid differs from that of the apes in two functionally meaningful ways. First, the calcaneal process, or plantar beak, is larger and more medioplantarly (often called eccentrically) oriented (Harcourt-Smith, 2002). This positioning of the plantar beak is thought to stabilize the calcaneocuboid joint during bipedalism (Bojsen-Møller, 1979; Elftman & Manter, 1935). The *Ardipithecus ramidus* cuboid possesses the more primitive, ape-like position of the cuboid beak (Lovejoy et al., 2009); the OH 8 cuboid is more human-like (Day & Napier, 1964; Harcourt-Smith, 2002).

Additionally, the human cuboid is PD elongated relative to the mediolateral (ML) width of the bone. This change is thought to reflect a general elongation of the tarsal region in humans (Elftman & Manter, 1935; Keith, 1928; Schultz, 1963). And as with the other tarsal elements, Lovejoy et al. (2009) proposed that tarsal elongation might actually be the primitive form and that the apes independently foreshortened their cuboid. Interestingly, relative to the ML width of the bone, the PD length in *Pongo* is not substantially different from that in *Homo* (Figure 7). Furthermore, while there is some lateral pinching (PD narrowing) of the cuboid in *Pongo* compared with *Homo*, it is not nearly to the same extreme as that found in the African apes. We agree with Lovejoy et al. (2009) that the primitive form was a more generalized tarsal row, which became PD elongated in the human lineage (Table 5), and PD foreshortened in the individual African ape lineages over the course of their evolutionary histories (see also Morton, 1935).

Finally, the facets for the lateral metatarsals tend to be relatively flat on the human cuboid, but are—especially Mt4—quite concave in other primates. This anatomy is functionally related to the midtarsal break, which occurs primarily at the lateral tarsometatarsal joints (DeSilva, 2010). Stabilization of the lateral tarsometatarsal joint is a key bipedal innovation in early hominins (McNutt, Zipfel, & DeSilva, 2018) and thus the flattening of this joint in *Ardipithecus* (Lovejoy et al., 2009) supports its identification as a bipedal hominin.

2.5 | Medial cuneiform

The medial cuneiform articulates with the navicular proximally; the first metatarsal (Mt1) distally, and the intermediate cuneiform and second metatarsal (Mt2) laterally. It serves as the attachment for slips of *M. tibialis anterior* and in humans, but not in other apes, *M. peroneus longus*.

The proximal facet for the navicular is strongly concave in apes and is flatter (but still generally concave) in the human medial cuneiform. Though this curvature has not been quantified in any studies of hominin medial cuneiforms, it qualitatively appears to remain quite concave in StW 573 and A.L. 333-28, while flattening more in OH 8 and the medial cuneiforms from *H. naledi*. Plantolaterally, the human medial cuneiform possesses a rugosity for the insertion of *M. peroneus*

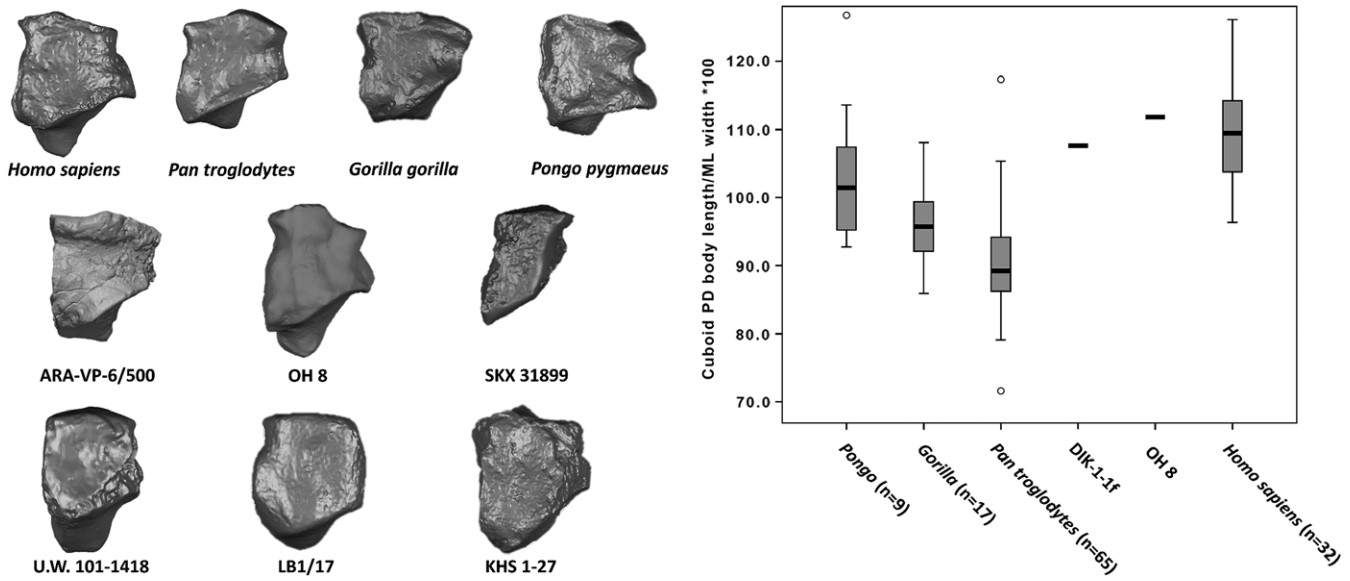

FIGURE 7 Cuboids from extant apes, modern human, and fossil hominins in dorsal view. Each bone is from the right side (mirrored if necessary) and has been scaled so that the mediolateral width of the dorsal cuboid is roughly the same. Notice that the African apes have a proximodistally squat cuboid that is particularly pinched laterally. Humans have a proximodistally elongated cuboid, with a more eccentrically oriented calcaneal beak. The cuboid is exceptionally rare in the hominin fossil record, and there is considerable variation in known cuboid morphology. Right: boxplot displaying the proximodistal length of the cuboid body relative to its mediolateral width in extant apes, modern humans, and two fossil hominins. Boxes span the interquartile ranges, with the horizontal center lines indicating median values. Whiskers indicate sample range, excluding outliers (dots). Notice that humans have a PD elongated cuboid body as do fossils from *A. afarensis* (juvenile DIK-1-1f) and OH 8. However, *Pongo* also possesses a proximodistally elongated cuboid, suggesting that the African apes have independently foreshortened the cuboid, especially laterally (Lovejoy et al., 2009). Image of *Ardipithecus ramidus* cuboid courtesy of Tim White and Gen Suwa

longus, which only inserts into the base of Mt1 in the apes. This insertion is present in StW 573, A.L. 333-28 (but see Susman, Stern, & Jungers, 1984), OH 8 and the medial cuneiforms from *H. naledi*. Laterally, the human medial cuneiform possesses an "L" shaped facet for continuous contact with the intermediate cuneiform, and viewed dorsally, this lateral facet is angled proximomedially to distolaterally, allowing the intermediate cuneiform to tuck into the medial cuneiform. In apes, there is a double facet for the intermediate cuneiform, which is more laterally directed and parallel to the long axis of the bone. Miocene ape and *Ardipithecus* medial cuneiforms are ape-like, consistent with a grasping hallux. *Australopithecus* and fossil *Homo* possess the angled, single "L" shaped facet for the intermediate cuneiform.

Functionally, one important aspect of the medial cuneiform is the distal facet for the Mt1 (Figure 8). This facet is strongly convex and medially oriented (relative to the navicular facet) in ape medial cuneiforms, though it is less medially directed and flatter in more terrestrial eastern gorillas compared with western gorillas (Schultz, 1930; Tocheri et al., 2011). Developmentally, the facet for the Mt1 is convex in both juvenile humans and apes; it flattens with age in humans, but remains convex in ape medial cuneiforms as they grow (Gill et al.,

TABLE 5 Comparative measurements of the cuboid in fossil hominins

Accession number	Taxon	Age (Ma)	Maximum ML width (mm)	Maximum PD medial length (mm)	Maximum PD lateral length (mm)
DIK-1-1f	*A. afarensis*	3.3	10.5	11.3	7.0
OH 8	*P. boisei*	1.85	20.4	22.8	11.6
Sima de los Huesos	*Homo*	0.43	27.2 ± 2.5 (*n* = 9)	–	–
U.W. 101-1023	*H. naledi*	0.24–0.34	–	23.1	–
U.W. 101-1418	*H. naledi*	0.24–0.34	–	24.4	12.3[a]
Neandertals	*Homo*	0.03-0.2	27.8 ± 3.8 (*n* = 9)	28.6 ± 5.0 (*n* = 9)	14.0 ± 2.6 (*n* = 8)
KHS 1–27	*H. sapiens*	0.195	25.9	26.1	14.9
LB1/17	*H. floresiensis*	0.06	–	18.5	–
LB1/27	*H. floresiensis*	0.06	–	18.4	–

Note. ML, mediolateral; DP, dorsoplantar; PD, proximodistal. Data in this table from original fossils and measurements reported in Trinkaus, 1975; Lu et al., 2011; Pablos et al., 2012; Harcourt-Smith et al., 2015; DeSilva, Gill, et al., 2018. Fossils too fragmentary to yield any of the measurements reported in this table include SKX 31899. Cuboids from *Ardipithecus* (ARA-VP-6/500–016, –081; White et al., 2009; Lovejoy et al., 2009), StW 638 (Clarke, 2013), and KNM-ER 64062 (Jungers et al., 2015) have been discussed in print but are not yet formally described. It is unclear to us what measurements are being reported for the Jinniushan specimen (Lu et al., 2011) and thus they are not included in this table. KB 3133 was identified as a hominin cuboid, but is not.
[a] Estimate that approximates the actual value.

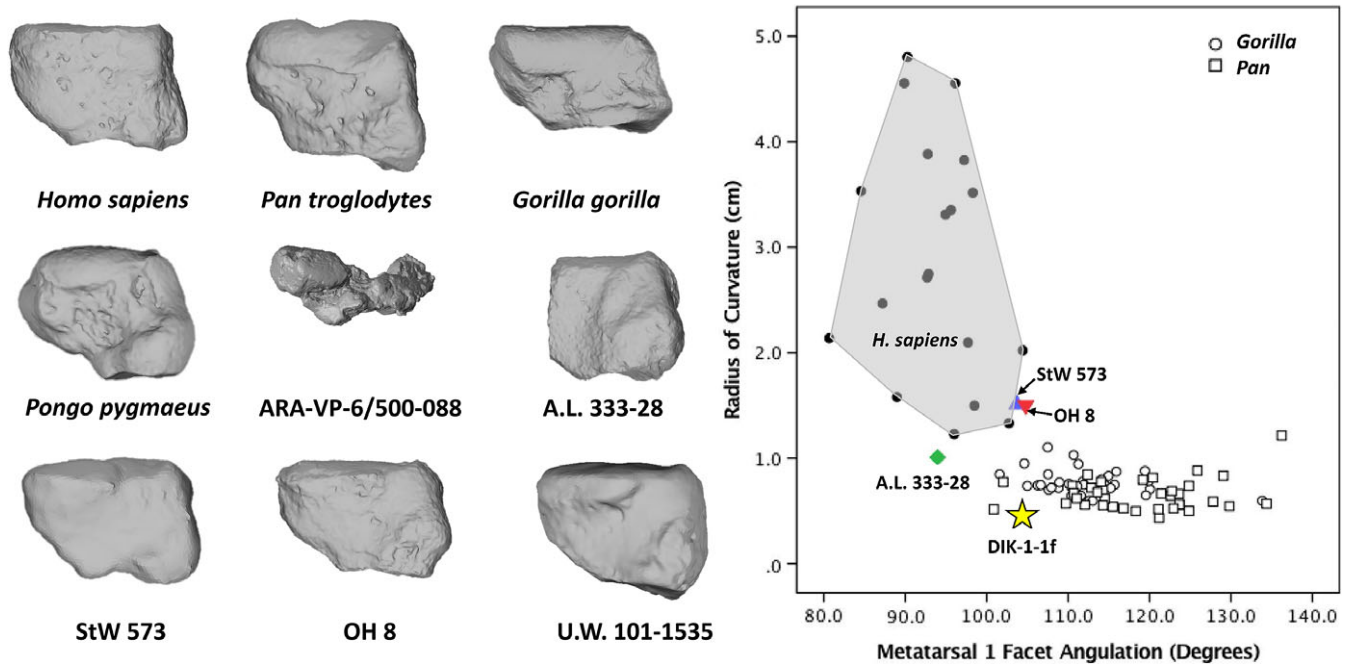

FIGURE 8 Medial cuneiforms from modern human, extant apes, and fossil hominins in medial view. Each bone is from the right side (mirrored if necessary) and has been scaled so that in medial view the bones are roughly the same in dorsoplantar height. Notice that the facet for the Mt1 spills onto the medial side and is quite convex in the extant apes and in *Ardipithecus ramidus* (ARA-VP-6/500-088). In *Australopithecus* (A.L. 333-28 and StW 573), OH 8 and *Homo*, the Mt1 facet is more human-like. Right: the curvature of the Mt1 facet is plotted against the angulation of the facet relative to the navicular facet. Data from Gill, Bredella, and DeSilva (2015) and DeSilva, Gill, et al. (2018). Notice that the DIK-1-1f juvenile is within the ape range for facet curvature and angulation; the adult *A. afarensis* specimen (A.L. 333-28) maintains a convex facet, but is angled distally as in human medial cuneiforms. StW 573 and OH 8 are within the human distribution for curvature, but overlap with apes in angulation. Image of *Ardipithecus* courtesy of T. White and G. Suwa

2015). The convex Mt1 facet can also be found in Miocene hominoids and in the *Ardipithecus* medial cuneiform, reflecting a divergent hallux capable of opposing the other pedal digits during grasping bouts. The flatter human facet faces more distally, reflecting an adducted, non-grasping, hallux. Interpreting this anatomy in fossil hominins has been challenging. The medial cuneiform Mt1 facet of juvenile *A. afarensis* (DIK-1-1f) is convex (Figure 8) and this curvature is retained in the adults (A.L. 333-28), falling on the low end of the modern ape range of Mt1 facet convexity (DeSilva, Gill, et al., 2018). We interpret this to reflect multidirectional loading and probably some degree of hallucal mobility in *A. afarensis* particularly in the juveniles. However, the distally directed Mt1 facet in *A. afarensis* demonstrates that the hallux, while more mobile than in humans today, was generally in a human-like adducted position (Latimer & Lovejoy, 1990a, 1990b). Claims that StW 573 possessed a divergent, grasping hallux (Clarke & Tobias, 1995) are not supported with additional analysis (Harcourt-Smith, 2002; McHenry & Jones, 2006; Gill et al., 2015; Figure 8). Interestingly, however, StW 573 and OH 8 possess more medially directed Mt1 facets than is typically the case in modern humans. However, articulation of the StW 573 and OH 8 foot bones unambiguously reveal a fully adducted hallux. The curvature of the Mt1 facets is reduced in StW 573 and OH 8 compared with A.L. 333-28 (Table 6), suggesting that these hominins may have had more restricted mobility of the hallux than did *A. afarensis*.

Latimer and Lovejoy (1990a) noted that the bursa for the *M. tibialis anterior* tendon inserted more dorsally in the human medial cuneiform and more plantarly in the ape one. This bursa position, they argued, would necessarily restrict any medial deviation of the Mt1 over the convex facet in *A. afarensis* and is further evidence for nongrasping in this taxon. However, the shape and convexity of the Mt1 facet on the medial cuneiform is not uniform along its dorsoplantar length (Dudas & Harcourt-Smith, 2017). In fact, the dorsal aspect of the facet is generally more convex than the plantar aspect and in some (*Pongo*, some gorillas, and *Ekembo*), the plantar aspect of the facet tapers and is not medially directed. Given that the all-important dorsal aspect of the A.L. 333-28 medial cuneiform is not preserved, we hesitate to agree that the dorsally positioned tibialis anterior bursa on A.L. 333-28 is definitive evidence for a nongrasping hallux in *A. afarensis*, and contend instead that while fully adducted, the hallux of *A. afarensis* possessed more mobility than that found in modern humans.

2.6 | Intermediate cuneiform

The intermediate cuneiform contacts the navicular proximally, the Mt2 distally, and the other two cuneiforms medially and laterally. It tends to be recessed into the tarsal row and to a greater degree in terrestrial primates, such as mountain gorillas and humans (Schultz, 1930), providing medial stability during terrestrial push-off. The plantar surface tapers to a narrow ridge and is the attachment for plantar ligaments, and a slip of the *M. tibialis posterior* tendon.

Ape and monkey intermediate cuneiforms have a strongly concave facet for the navicular, terminating in a proximally projecting lip of bone (Figure 9). This joint shape likely facilitates some mobility between the intermediate cuneiform and navicular as part of the

TABLE 6 Comparative measurements of the medial cuneiform in fossil hominins

Accession number	Taxon	Age (Ma)	Radius of curvature (cm)	Navicular angle (°)	PD length (mm)	DP height (mm)
StW 573	*A. prometheus*?	3.67?	1.51	103.7	17.6	25.0
DIK-1-1f	*A. afarensis*	3.3	0.42	104.4	–	10.5
A.L. 333-28	*A. afarensis*	3.2	1.01	94.0	21.4	29.5[a]
OH 8	*P. boisei*?	1.85	1.50	104.8	17.0	24.4
D4111	*Homo*	1.77	–	–	20.1	28.8
Sima de los Huesos	*Homo*	0.43	–	–	26.2 ± 1.2 (*n* = 7)	–
U.W. 101-1039	*H. naledi*	0.24–0.34	–	–	–	22.7[a]
U.W. 101-1062	*H. naledi*	0.24–0.34	–	–	17.3[a]	24.5
U.W. 101-1535	*H. naledi*	0.24–0.34	–	–	20.2	24.2
Jinniushan	*Homo*	0.26	–	–	–	32.3
Neandertals	*Homo*	0.03–0.2	–	–	25.0 ± 1.9 (*n* = 11)	–
KHS 1–46	*H. sapiens*	0.195	–	–	23.7	34.9
LB1/18	*H. floresiensis*	0.06	–	–	15.4	–

Note. PD, proximodistal; DP, dorsoplantar. Data in this table from original fossils and measurements reported in Latimer et al., 1982; Pearson et al., 2008; Jungers, Larson, et al., 2009; Jashashvili, Ponce de León, Lordkipanidze, & Zollikofer, 2010; Gill et al., 2015; Harcourt-Smith et al., 2015; DeSilva, Gill, et al., 2018. Medial cuneiform from *Ardipithecus* (ARA-VP-6/500-088: White et al., 2009; Lovejoy et al., 2009) has been discussed in print and is illustrated in Figure 8, but is not yet formally described. SKX 31117 was identified as a hominin medial cuneiform, but is not.
[a] Estimate that approximates the actual value.

medial component of the midtarsal break, though this remains to be tested. In humans, this joint is slightly concave to flat. Miocene ape intermediate cuneiforms all possess a concave joint surface and to a lesser degree so does StW 573. In OH 8, the facet is flatter and more human-like. In humans, the Mt2 facet is rather flat; whereas in apes and monkeys the lateral aspect of the facet spills laterally, complementing the Mt2 proximal surface which is often "V"-shaped and proximally projecting along the lateral side of the proximal facet.

Medially, the human intermediate cuneiform possesses a continuous, "L"-shaped facet for contact with the medial cuneiform (Figure 9).

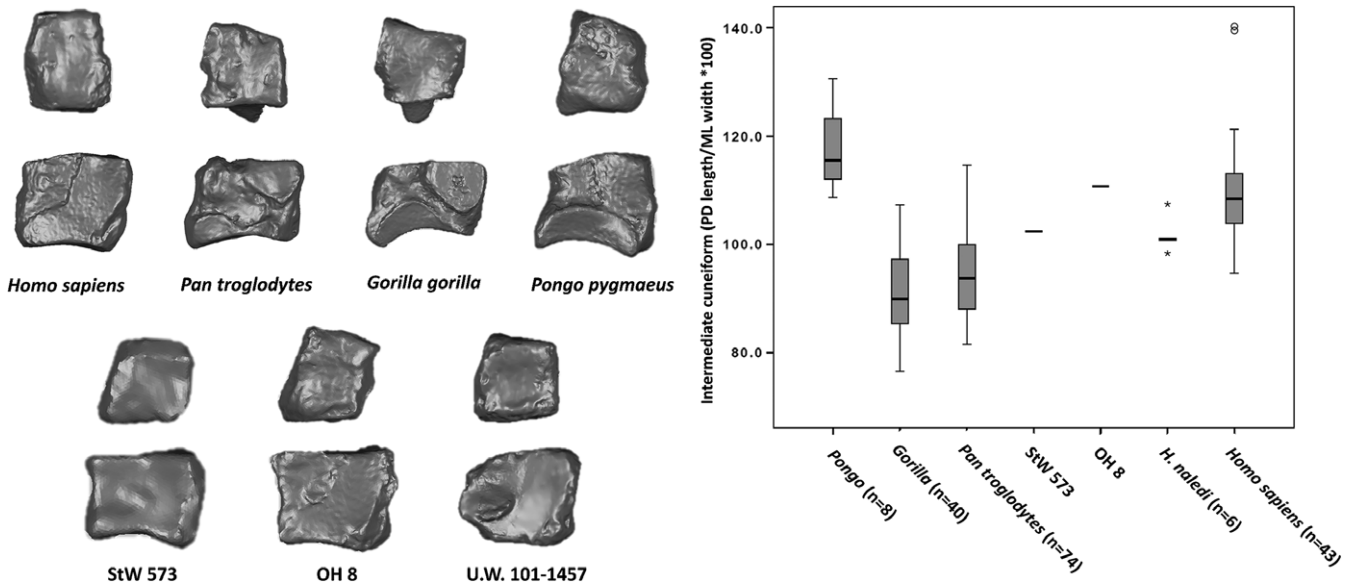

FIGURE 9 Intermediate cuneiforms from modern human, extant apes, and fossil hominins in dorsal view (top) and medial view (bottom). Each bone is from the right side (mirrored if necessary) and has been scaled so that in dorsal view the bones are roughly the same in mediolateral width and in medial view the same dorsoplantar length. Notice that the African apes have proximodistally foreshortened intermediate cuneiforms. The presence of the long intermediate cuneiform in *Pongo* may reduce Mt2 nesting into the tarsal row and make the medial forefoot more mobile. Notice that in comparison to the extant apes, humans have a dorsoplantarly flat navicular facet, and a single facet for the medial cuneiform (apes have a double facet). Right: boxplot of maximum intermediate cuneiform proximodistal length relative to mediolateral width. Boxes span the interquartile ranges, with the horizontal center lines indicating median values. Whiskers indicate sample range, excluding outliers (dots). Fossil intermediate cuneiforms are generally human-like in relative proximodistal elongation though StW 573 and some *H. naledi* specimens also fall within the African ape range

TABLE 7 Comparative measurements of the intermediate cuneiform in fossil hominins

Accession number	Taxon	Age (Ma)	Maximum ML width (mm)	Maximum PD length (mm)	Maximum DP height (mm)
ARA-VP-6/500-45	*Ar. ramidus*	4.4	13.9	–	20.0
ARA-VP-6/500-75	*Ar. ramidus*	4.4	13.9	–	20.0
StW 573	*A. prometheus?*	3.67?	12.3	12.6	15.4
DIK-1-1f	*A. afarensis*	3.3	4.9	6.3	–
OH 8	*P. boisei?*	1.85	11.2	12.4	15.1
Sima de los Huesos	*Homo*	0.43	–	15.4 ± 0.9 (n = 12)	–
U.W. 101-1242	*H. naledi*	0.24–0.34	10.7	10.8	13.8
U.W. 101-1457	*H. naledi*	0.24–0.34	12.0	12.1	14.0
U.W. 101-1534	*H. naledi*	0.24–0.34	12.3	12.4	18.3
U.W. 101-1618	*H. naledi*	0.24–0.34	12.2	12.0	15.0
U.W. 101-1682	*H. naledi*	0.24–0.34	8.7	8.8	10.2
U.W. 101-1695	*H. naledi*	0.24–0.34	12.1	13.0	13.3
Jinniushan	*Homo*	0.26	17.2	–	24.5
Neandertals	*Homo*	0.03–0.2	14.9 ± 1.4 (n = 7)	16.9 ± 1.3 (n = 16)	20.5 ± 2.2 (n = 5)
LB1/20	*H. floresiensis*	0.06	–	11.6	–

Note. ML, mediolateral; DP, dorsoplantar; PD, proximodistal. Data in this table from original fossils and measurements reported in Trinkaus, 1975; Lu et al., 2011; Pablos et al., 2012; Harcourt-Smith et al., 2015. Measurements of *Ardipithecus* intermediate cuneiforms courtesy of T. White and G. Suwa. Neandertal intermediate cuneiform width (ML) calculated as "navicular articular breadth" and height calculated as "metatarsal articular height" in Trinkaus, 1975. The intermediate cuneiform from KNM-ER 64062 (Jungers et al., 2015) is not yet formally described.

In apes and monkeys, this facet is divided into a distal facet and a proximal one that runs the dorsoplantar length of the bone. These double facets are present on the *Ardipithecus ramidus* intermediate cuneiforms (ARA-VP-6/500-45 and -75). StW 573 and OH 8 both possess the derived form of merged facets.

Perhaps most functionally relevant is the relative PD length of the intermediate cuneiform. In humans, the bone is PD elongated, which is thought to be part of a broader elongation of the tarsal row to convert the foot into a rigid lever without incurring bending strains across the metatarsal row (Keith, 1928; Elftman & Manter, 1935; Schultz, 1963; but see Holowka, O'Neill, Thompson, & Demes, 2017). However, the *Pongo* intermediate cuneiform is also PD elongated relative to the ML width of the bone, suggesting that this explanation is incomplete. In fact, monkeys, gibbons, *Pongo*, and humans all have longer intermediate cuneiforms relative to the width of the bone; only African apes do not. This observation is consistent with Lovejoy et al. (2009) who proposed that an elongated tarsal region represents the ancestral condition. If this evolutionary scenario is correct, then *Gorillas* and *Pan* have independently foreshortened the intermediate cuneiform, perhaps to increase medial midtarsal flexibility. *Pongo*'s retained PD elongated intermediate cuneiform may serve to increase medial foot mobility as it eliminates any recessing of the Mt2 into the tarsal row relative to the Mt3. Based on the roughly square-shaped intermediate cuneiforms in *Ardipithecus ramidus* (i.e., roughly equal ML and PD dimensions) and, to a lesser degree, the same condition in StW 573 and even *H. naledi* (Table 7), it is possible that the human-African ape last common ancestor (LCA) possessed a square-shaped intermediate cuneiform from which hominins evolved a slightly PD elongated bone, and African apes (independently) a foreshortened one.

2.7 | Lateral cuneiform

The lateral cuneiform contacts the navicular proximally, third metatarsal (Mt3) distally, cuboid laterally and intermediate cuneiform medially. In humans, the fourth metatarsal (Mt4) is often recessed into the tarsal row and contacts the distolateral corner of the lateral cuneiform. Plantarly, the lateral cuneiform tapers and provides insertion for a slip of the *M. tibialis posterior*, and is the origin of the lateral arm of *M. flexor hallucis brevis*.

Plantarly, the monkey and ape lateral cuneiform is dominated by a large and projecting hamulus. The hamulus receives a slip of the *M. tibialis posterior* tendon, and a distally (toward the Mt3) positioned plantar groove guides the tendon of *M. peroneus longus* across the plantar foot to the base of the Mt1 (Figure 10). The hamulus and distal groove is well-developed in most monkey and ape lateral cuneiforms, but only weakly developed in *Homo*, *Pongo*, and *Ateles*—primates that do not rely heavily on hallucal grasping, or have a relatively short hallux (e.g., Tuttle & Rogers, 1966). Interestingly, *Pongo* and *Ateles* have small navicular tuberosities (Prang, 2016c) and the reduction of both the navicular tuberosity and lateral cuneiform hamulus may be related to the relatively small size of *M. tibialis posterior* (Payne et al., 2006; Prang, 2016c; Zihlman, Mcfarland, & Underwood, 2011). In *Australopithecus* (A.L. 333-79 and StW 573), the hamulus is present, but the groove does not appear to be,[3] suggesting the presence of an os peroneum that would lift the *M. peroneus longus* out of the peroneal groove and orient it more obliquely across the foot. While Lovejoy et al. (2009) hypothesized that this reconfiguration of the *M. peroneus*

[3]There is damage to the A.L. 333-79 lateral cuneiform in this region though the overall anatomy in this region of the bone is not consistent with there having been a prominent groove for the *M. peroneus longus* tendon.

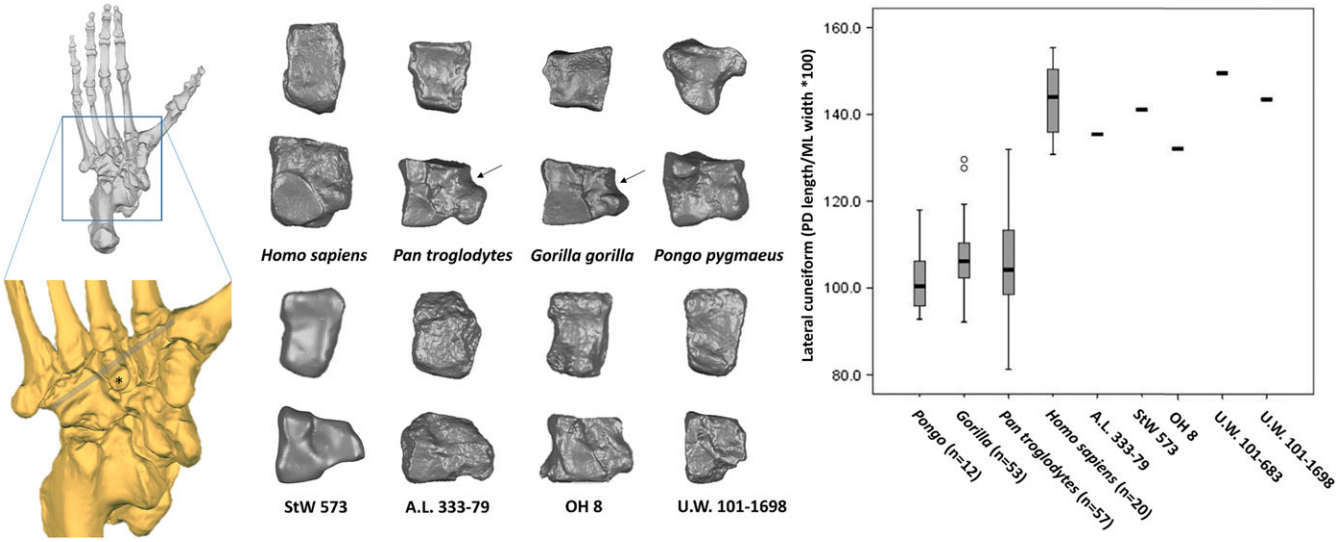

FIGURE 10 Left: A *Gorilla* foot shown plantarly so that the lateral cuneiform hamulus (asterisk) is shown as is the groove (gray line) for the tendon of *M. peroneus longus* in the cuboidal groove and a groove in the lateral cuneiform just distal to the hamulus. Middle: Lateral cuneiforms from modern human, extant apes, and fossil hominins in dorsal view (top) and lateral view (bottom). Each bone is from the right side (mirrored if necessary) and has been scaled so that in dorsal view the bones are roughly the same in mediolateral width and in lateral view the same dorsoplantar length. Notice that the African apes have a plantarly projecting hamulus and a distally positioned groove (arrow) for the tendon of *M. peroneus longus*. StW 573, A.L. 333-79, and OH 8 all possess a hamulus, but lack the prominent groove for the tendon of *M. peroneus longus*. Right: boxplot comparing the lateral cuneiform proximodistal length to mediolateral width. Boxes span the interquartile ranges, with the horizontal center lines indicating median values. Whiskers indicate sample range, excluding outliers (dots). Compared with extant great apes, humans and all known fossil hominins have a proximodistally elongated lateral cuneiform relative to the mediolateral width of the bone

longus tendon happened at some point in human evolution (and certainly by the time of OH 8), our analysis of the lateral cuneiform reveals that this reorientation of the *M. peroneus longus* occurred in early *Australopithecus*.

The distal facet for the Mt3 is flat in humans and African great apes. In *Pongo*, it possesses some medial convexity to complement a more concave Mt3 base (though not as concave as the Mt2). However, in gibbons and monkeys, the Mt3 facet is dorsoplantarly concave corresponding to a convex Mt3 base in these primates (Proctor, 2010a). This anatomy is also found in *Ekembo* lateral cuneiforms and is inferred for *Afropithecus* based on a convex Mt3 base. This concave/convex joint configuration at the lateral cuneiform/Mt3 junction in monkeys, gibbons, and early Miocene apes implies a degree of (and unique anatomical location for) midtarsal laxity not found in modern great apes or humans. Proximally, the square-shaped facet for the navicular is relatively flat in humans, but more convex in the African apes. In *Pongo* the facet is extremely convex and spills onto the medial side of the bone forming in some individuals a near ball and socket joint between the lateral cuneiform and the navicular. The proximal lateral cuneiform is flat in A.L. 333-79 (*A. afarensis*), StW 573, and OH 8.

As with the intermediate cuneiform, a PD elongated lateral cuneiform is part of general midfoot elongation that converts the human foot into a more effective lever for bipedal propulsion (Elftman & Manter, 1935; Keith, 1928; Schultz, 1963). The lateral cuneiform is PD short and squat in the extant apes (including *Pongo*), but this anatomy is hypothesized to be independently derived in the different apes to facilitate foot conformity around tree branches (Lovejoy et al., 2009). Additional lateral cuneiforms from the Middle to Late Miocene are needed to test this hypothesis. Notably, the newly announced lateral cuneiform from the Gona *Ardipithecus* partial skeleton is already human-like in dorsoplantar elongation (Simpson et al., 2018), as are other adult hominin lateral cuneiforms (Table 8).

2.8 | First metatarsal

The Mt1 articulates proximally with the medial cuneiform, distally with the hallucal proximal phalanx, and plantarly with medial and lateral sesamoids. In humans, the lateral base of the adducted Mt1 often contacts the proximolateral shaft of the Mt2 and can form a small facet (Singh, 1960). The plantolateral base is the insertion for the tendon of *M. peroneus longus* (Keith, 1928) and *M. tibialis anterior*. The Mt1 is relatively long and slender in the African apes; short and slender in *Pongo*; and robust in humans (Morton, 1926b), especially dorsoplantarly (Figure 11). The internal cortical shell is distributed to resist dorsoplantar bending forces (Jashashvili, Dowdeswell, Lebrun, & Carlson, 2015). The Mt1 is slender and ape-like in the Burtele foot (Haile-Selassie et al., 2012), and in StW 595 from Sterkfontein Member 4, but is more human-like and robust in a different Sterkfontein M4 specimen StW 562. Interestingly, the Mt1 is short and hyper-robust in the two Mt1s from Swartkrans (SKX 5017 and SK 1813), often assigned to *P. robustus*, and in OH 8 (Figure 11). Relative to the other digits, the Mt1 is also very short in *H. floresiensis* (Jungers, Harcourt-Smith, et al., 2009; Table 9).

Relative to the base, the shaft and head of the human Mt1 are neutrally positioned. Apes, in contrast, have an externally (laterally) torqued Mt1, which put the hallux in opposition with the lateral digits (Morton, 1922). In the transverse plane, the head of the human Mt1 has a slight valgus deviation, a laterally directed bony correction to medial weight transfer through the foot (Barnett, 1962).

TABLE 8 Comparative measurements of the lateral cuneiform in fossil hominins

Accession number	Taxon	Age (Ma)	Minimum ML width (mm)	Maximum PD length (mm)	Maximum DP height (mm)
StW 573	*A. prometheus?*	3.67?	11.7	16.7	20.1
DIK-1-1f	*A. afarensis*	3.3	7.1	9.4	–
A.L. 333-79	*A. afarensis*	3.2	14.8	18.7	24.2
OH 8	*P. boisei?*	1.85	11.2	15.6	22.7
Sima de los Huesos	*Homo*	0.43	–	18.2 ± 1.7 (*n* = 9)	–
U.W. 101-683	*H. naledi*	0.24–0.34	10.7	16.0	15.7
U.W. 101-1698	*H. naledi*	0.24–0.34	11.5	16.5	14.6
U.W. 101-1734	*H. naledi*	0.24–0.34	9.5[a]	13.9[a]	–
Neandertals	*Homo*	0.03–0.2	–	19.9 ± 2.3 (*n* = 12)	28.7 ± 3.9 (*n* = 4)
LB1/19	*H. floresiensis*	0.06	–	16.9	–
LB1/28	*H. floresiensis*	0.06	–	16.8	–

Note. ML, mediolateral; DP, dorsoplantar; PD, proximodistal. Lateral cuneiforms from *Ardipithecus* (ARA-VP-6/500–100; White et al., 2009) and Gona (Simpson et al., 2018), along with KNM-ER 64062 (Jungers et al., 2015) have been discussed in print but are not yet formally described. The Jinniushan foot (Lu et al., 2011) possesses a lateral cuneiform, but no measurements are reported. Data in this table from original fossils and measurements reported in Trinkaus, 1975; Latimer et al., 1982; Harcourt-Smith et al., 2015; Pablos et al., 2017.

[a] Estimate that approximates the actual value.

In humans, the Mt1 head rises dorsally above the plane of the shaft, creating a domed appearance, which has been suggested to be functionally related to the dorsiflexion of the hallucal proximal phalanx during bipedal push-off (Latimer & Lovejoy, 1990a, 1990b). *Ardipithecus ramidus* does not have a domed Mt1 (Lovejoy et al., 2009), nor does the Mt1 from the Burtele foot (Haile-Selassie et al., 2012), or StW 595 from Sterkfontein Member 4 (Figure 11). The Mt1 is dorsally domed in *A. afarensis* (A.L. 333-115), Mt1s assigned to *P. robustus* (SK 1813, SKX 5017), and one Mt1 assigned to *A. africanus* (StW 562). However, in these hominins, the dorsal articular surface is rounded and is not mediolaterally expanded and flat as is found in modern humans (e.g., Susman et al., 1984). This same anatomy—domed Mt1, but not mediolaterally expanded—is even present in the Mt1s from early *Homo* at Dmanisi (Pontzer et al., 2010). The dorsum is mediolaterally expanded in later *H. erectus* from Baringo, Kenya (BK 63) and from *H. naledi* (Harcourt-Smith et al., 2015).

The base of the Mt1 in humans is mediolaterally flat relative to the deeply concave, sigmoidal base shape (called "spiral concavity" by Lovejoy et al., 2009) in the ape Mt1. Functionally, the ape Mt1 base facilitates abduction and adduction of the Mt1 on the medial cuneiform in addition to some axial (lateral and medial) rotation at the hallucal tarsometatarsal joint. The flat Mt1 base in humans reflects the loss

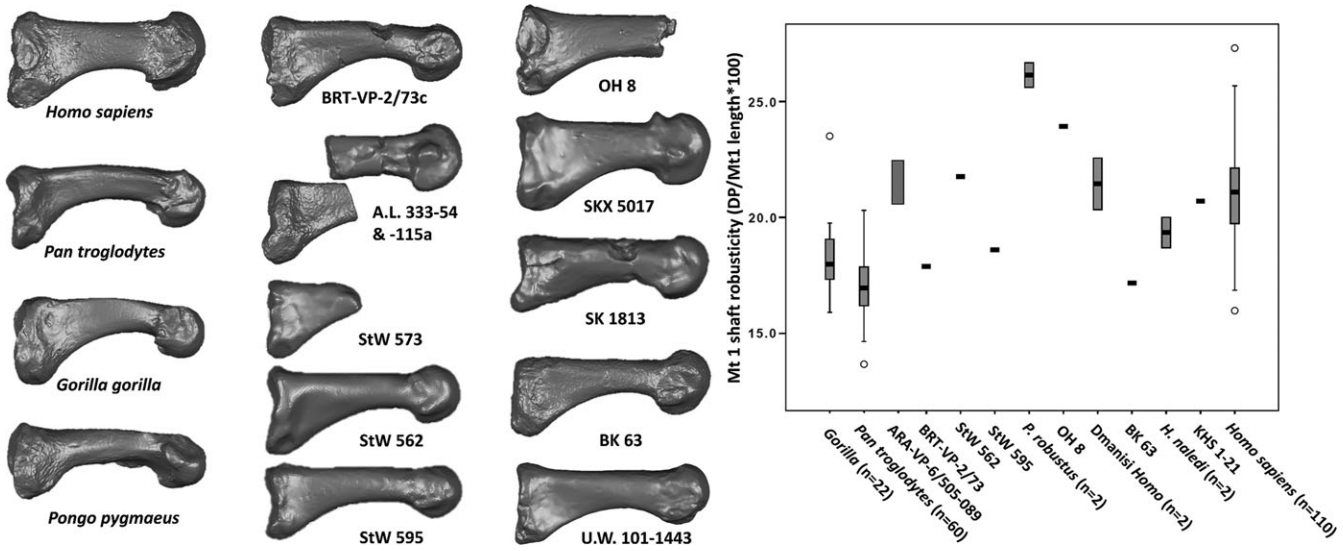

FIGURE 11 First metatarsal (Mt1) from modern human, extant apes, and fossil hominins in lateral view. Each bone is from the right side (mirrored if necessary) and has been scaled so that the bones are roughly the same proximodistal length. Notice that in humans, the Mt1 head is domed and the articular surface extends dorsally. This same anatomy can be found in most fossil hominin Mt1s, but not in BRT-VP-2/73c or StW 595. Right: boxplot depicting the dorsoplantar height of the Mt1 shaft relative to the length of the bone. Boxes span the interquartile ranges, with the horizontal center lines indicating median values. Whiskers indicate sample range, excluding outliers (dots). Human Mt1 are robust, whereas the Mt1 of the African apes is more gracile. The BRT Mt1 and StW 595 are ape-like; the Mt1 from *Ardipithecus*, StW 562, and fossil *Homo* (but not BK 63) are human-like. The robust australopith Mt1s (including OH 8) have quite short Mt1 shafts relative to the DP midshaft height

TABLE 9 Comparative measurements of the first metatarsal in fossil hominins

Accession number	Taxon	Age (Ma)	Length (mm)	Torsion (°)	Base ML width (mm)	Base DP height (mm)	Midshaft ML (mm)	Midshaft DP (mm)	Head ML width (mm)	Head DP height (mm)
ARA-VP-6/500-089	*Ar. ramidus*	4.4	55.6[a]	–	–	23–25	10.5–11.5	11.5–12.5	18.3[a]	14.5-15.5
StW 573	*A. prometheus*?	3.67?	–	–	12.5	20.4	9.4	10.2	–	–
BRT-VP-2/73c	Hominin sp.	3.4	50.3	–	14.6	22.7	9.1	9.0	16.7	14.5
A.L. 333-115a	*A. afarensis*	3.2	–	–	–	–	–	–	17.5	17.3
A.L. 333-54	*A. afarensis*	3.2	–	–	17.4	23.5	–	–	–	–
A.L. 333-21	*A. afarensis*	3.2	–	–	–	–	–	–	16.0	16.4[a]
StW 595	*A. africanus*?	2.0–2.6	45.7	−5.9	13.0	18.1	7.6	8.5	15.0	12.2
StW 562	*A. africanus*?	2.0–2.6	52.4	4.7	16.0	24.2	10.4	11.4	19.0	15.2
OH 8	*P. boisei*?	1.85	43.9[a]	10	15.9	21.3	10.6	10.5	–	–
D2671	*Homo*	1.77	47.2	3	–	–	–	10.6	–	–
D3442	*Homo*	1.77	–	15	–	–	–	9.6	–	–
SK 1813	*P. robustus*	1.1–2.0	41.4	7.5	13.3[a]	17.4[a]	10.3	10.6	10.8	14.6
SKX 5017	*P. robustus*	1.8–2.0	43.5	8.5	16.0	21.7	10.4	11.6	16.5	13.8
BK 63	*H. erectus*	0.5	60.0[a]	–	15.6[a]	22.5[a]	12.4	10.3	18.2	19.4
Sima de los Huesos	*Homo*	0.43	–	–	23.1 ± 2.4 (n = 4)	–	–	–	–	–
U.W. 101-496	*H. naledi*	0.24–0.34	–	–	–	–	11.9	10.6	14.2	–
U.W. 101-1019	*H. naledi*	0.24–0.34	55.1[a]	−5.2	–	–	10.9	10.3	13.8[a]	15.6[a]
U.W. 101-1443	*H. naledi*	0.24–0.34	50.0	−3.9	13.5	21.1	10.5	10.0	13.4	13.0
U.W. 101-1530	*H. naledi*	0.24–0.34	–	–	13.3	22.2	11.1[a]	10.3[a]	–	–
Jinniushan	*Homo*	0.26	55.7	–	–	–	–	–	20.5	21.1
Neandertals	*Homo*	0.03–0.2	55.4 ± 4.6 (n = 11)	17.1 ± 11.6 (n = 9)	19.9 ± 3.0 (n = 16)	29.5 ± 5.2 (n = 9)	14.9 ± 1.8 (n = 12)	12.4 ± 1.6 (n = 12)	24.1 ± 2.7 (n = 8)	21.1 ± 2.5 (n = 10)
KHS 1–21	*H. sapiens*	0.195	68.6	–	21.5	26.0	14.8	14.2	18.4	19.4
LB1/21	*H. floresiensis*	0.06	47.0	–	–	–	–	–	–	–

Note. ML, mediolateral; DP, dorsoplantar. Data in this table from original fossils and measurements reported in Trinkaus, 1975; Latimer et al., 1982; White and Suwa et al., 1987; Susman & de Ruiter, 2004; Lovejoy et al., 2009; Jungers, Larson, et al., 2009; Pontzer et al., 2010; Lu et al., 2011; Haile-Selassie et al., 2012; Drapeau & Harmon, 2013; Harcourt-Smith et al., 2015; Pablos et al., 2017. Only adult Mt1s are shown in this table. Juvenile Mt1s from *A. afarensis* (DIK-1-1f and A.L. 333-174) are described elsewhere (DeSilva, Gill, et al., 2018; Hillenbrand, 2009) as are juvenile fossils from *H. naledi* (U.W. 101-244; U.W. 101-1499; Harcourt-Smith et al., 2015). Juvenile KNM-WT 15000 included a skeletal fragment tentatively identified as a possible Mt1. It is probably not. Measurements in the table have not been Reported for LB1/29. Mt1s from *Ardipithecus* (ARA-VP-6/500–011; ARA-VP-1/1700: White et al., 2009) and Gona (Simpson et al., 2018), DNH 115 (Vernon, 2013), and KNM-ER 64062 (Jungers et al., 2015) have been discussed in print but are not yet described in detail.

[a] Estimate that approximates the actual value.

of a grasping big toe. The *Ardipithecus ramidus* Mt1 base is sigmoidal (Lovejoy et al., 2009), as is the base of the Mt1 in the Burtele foot (Haile-Selassie et al., 2012). This anatomy is consistent with mobility of the great toe in these early hominins. This sigmoidal shape is also moderately present in the Mt1s assigned to *P. robustus* SKX 5017 and SK 1813, raising the possibility that there was some grasping ability present in this robust lineage (Proctor, 2010b). The base of the Mt1 from *A. afarensis* (A.L. 333-54), which is also quite concave, is more difficult to interpret. In a geometric morphometrics study, it plots between human and ape (Proctor, 2010b), suggesting some mobility at this joint. Others regard the presence of a hilum and a nonarticular separation between the dorsal and plantar facets as evidence that there was no axial rotation possible at this joint in *A. afarensis* (Latimer & Lovejoy, 1990a, 1990b) and therefore little grasping potential. The base of the Mt1 from Dmanisi (Pontzer et al., 2010) and from OH 8 is flat and human-like. Related to the presence or absence of an abducent hallux is a contact area (and sometimes a facet) for the Mt2, which is unique to the human foot (Le Minor & Winter, 2003). This contact area is absent along the Mt1 base in *Ardipithecus* and the Burtele foot, but is present in some other australopiths and fossils assigned to early *Homo*. There is a particularly large facet on OH 8, effectively refuting any hypothesis for a divergent hallux in this foot.

2.9 | Second metatarsal

The Mt2 articulates medially and laterally with the first and third metatarsals respectively and with the intermediate cuneiform proximally. Distally, the Mt2 contacts the second proximal phalanx. Medially, the Mt2 also contacts the distolateral aspect of the medial cuneiform, and in humans, the adducted Mt1 often contacts the proximomedial shaft of the Mt2. Laterally, there is contact with the lateral cuneiform in humans and African apes, but typically not in orangutans where elongated intermediate cuneiforms force the Mt2 out of the tarsal row.

Human Mt2s are relatively short and straight; apes possess relatively longer Mt2s with greater longitudinal (proximodistal) curvature and some transverse plane (mediolateral) curvature. While some fossil Mt2s have longitudinal curvature (e.g., *Ardipithecus*, and StW 89), most are relatively straight (Figure 12). Only the Burtele Mt2 possesses the transverse plane curvature found in apes (Haile-Selassie et al., 2012).

Perhaps most notably, the human Mt2 head is neutrally oriented in the sagittal plane. Apes and monkeys possess strong internal (medial) torsion of the Mt2 in which the head of the metatarsal faces medially relative to the dorsoplantar orientation of the base. This morphology brings the head into opposition with the Mt1 and is functionally related to hallucal grasping (Drapeau & Harmon, 2013; Morton, 1922). *Ardipithecus* qualitatively possesses internal torsion (Lovejoy et al., 2009). The Burtele foot and StW 89 (Sterkfontein Member 4) both possess internal torsion as well (DeSilva et al., 2012; DeSilva, Proctor, & Zipfel, 2012; Haile-Selassie et al., 2012) though of magnitude slightly less than modern ape Mt2s. While these observations are consistent with hallucal grasping in *Ardipithecus* and the Burtele foot, the presence of high torsion in StW 89 is unexpected and discussed later in this review. Other hominin Mt2s (OH 8 and StW 377) have slight internal torsion (Drapeau & Harmon, 2013); in *H. naledi* the torsion is human-like (Harcourt-Smith et al., 2015).

The Mt2 head is DP tall in humans and the articular surface rises above the shaft, producing a domed appearance. There is often a sulcus between the head and the nonarticular dorsal surface of the Mt2, where the base of the proximal phalanx reaches expected, but not experimentally confirmed, maximum dorsiflexion during push-off. This anatomy is functionally correlated with dorsally canted proximal phalanges which dorsiflex during the terminal stance phase (i.e., heel up to toe-off) of walking when the forefoot becomes a propulsive lever (Latimer & Lovejoy, 1990b; but see Duncan, Kappelman, & Shapiro, 1994). In contrast, the ape Mt2 head lacks this dorsal doming and instead has an articular surface that is prolonged plantarly, functionally coincident with pedal grasping. The Mt2 head is unknown in *Ardipithecus*. In the Burtele foot, the head is slightly domed and there is a dorsal sulcus (Haile-Selassie et al., 2012), similar to the anatomy found in StW 89, which also possesses a more ape-like prolonged plantar surface (DeSilva, Proctor, & Zipfel, 2012). The Mt2 head in *A. afarensis* (A.L. 333-115 and A.L. 333-72) is quite human-like, with a dorsally domed surface and prominent sulcus (Fernández et al., 2016; Latimer & Lovejoy, 1990b).

In humans, the base of the metatarsal is DP tall and terminates in a strong ridge of bone for plantar ligaments, a bony anatomy hypothesized to be functionally correlated with a stiffening of the medial midfoot. Apes, in contrast, possess a DP short base. Relative to the total length of the bone, *Ardipithecus* has a tall Mt2 base (Lovejoy et al., 2009) whereas the Burtele foot and StW 89 from Sterkfontein M4 are both DP short and more ape-like (DeSilva, Proctor, & Zipfel, 2012; Haile-Selassie et al., 2012). By comparing the DP height of the base to its ML width (Table 10), more specimens can be included in an analysis of base height (Figure 12). Using this approach, *Ardipithecus*, the Burtele foot, and *Australopithecus* from South Africa (StW 573, and Sterkfontein M4) all have ape-like DP short bases. However, Mt2 fossils from Hadar, OH 8, and fossil *Homo* have tall, more human-like, bases (McNutt, Zipfel, & DeSilva, 2018).

In dorsal view, the base of the human Mt2 angles distomedially to proximolaterally, and the intermediate cuneiform facet is only mildly concave. African apes, in contrast, tend to have a less angled base, and more mediolateral concavity to the intermediate cuneiform facet. Additionally, the facet for the medial cuneiform is aligned with the long axis of the Mt2 in humans, but is angled proximolaterally to distomedially in the apes, which is consistent with medial divergence of the hallux. Most hominin fossils are human-like for these characters except *Ardipithecus*, which possesses the ape-like angulation for the medial cuneiform (Lovejoy et al., 2009; Figure 2).

Along the proximomedial shaft, there is often a small impression on the Mt2 of humans for contact with the Mt1. This contact facet is present in the proximal Mt2s from both South and Eastern African *Australopithecus*, including StW 573. However, it is neither detectable in the Burtele foot nor in *Ardipithecus*, consistent with a more divergent hallux.

Finally, Lovejoy et al. (2009) call attention to "paired chondral invaginations" on the dorsal surface of the base of the *Ardipithecus* Mt2 and propose that these impressions are the by-product of the

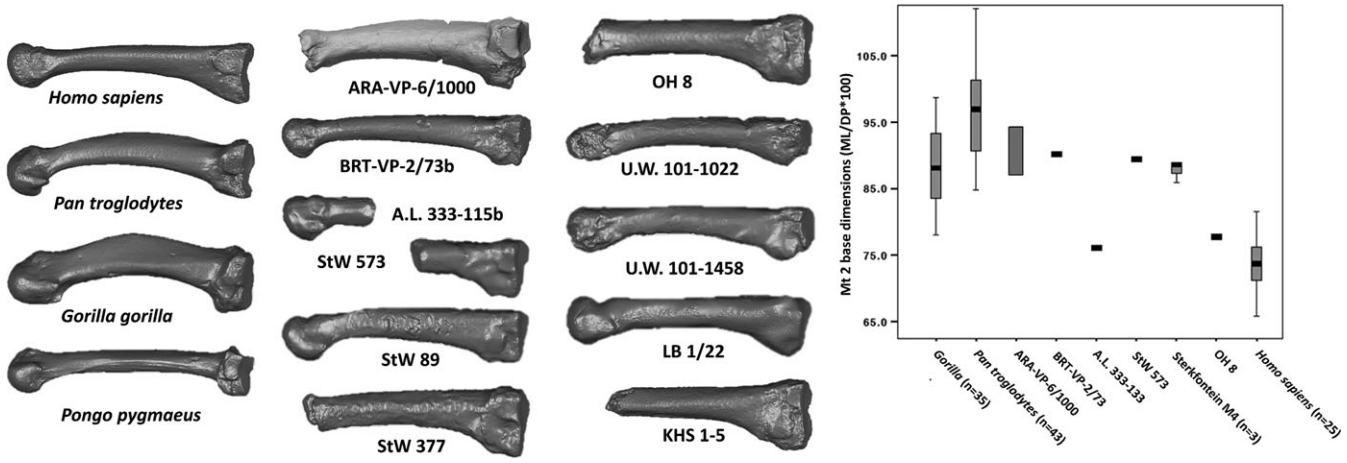

FIGURE 12 Second metatarsal (Mt2) from modern human, extant apes, and fossil hominins in medial view. Each bone is from the right side (mirrored if necessary) and has been scaled so that the bones are roughly the same proximodistal length. Notice that the human Mt2 is straight, with a dorsoplantarly tall base and a domed head. The ape Mt2 base is dorsoplantarly short and the head is internally rotated to face the Mt1. The Burtele Mt2 (BRT-VP-2/73b) and StW 89 both possess internally twisted heads and dorsoplantarly short bases relative to the total length of the Mt2. Right: boxplot displaying the mediolateral width of the Mt2 base relative to the dorspoplantar height. Boxes span the interquartile ranges, with the horizontal center lines indicating median values. Whiskers indicate sample range, excluding outliers (dots). Humans have a DP tall base, as does *A. afarensis* and OH 8. Mt2s from *Ardipithecus*, BRT, StW 573 and Sterkfontein member 4 (n = 3) are more ape-like. Reported measurements and image of ARA-VP-6/1000 courtesy of Tim White and Gen Suwa

dorsal capsule pressing into the surface of the bone during climbing (medial impression) and oblique axis bipedal propulsion (lateral impression). We note here that similar chondral invaginations are present in the second and third metatarsals of *Ekembo* and *Afropithecus*, and can occasionally be found in cercopithecoid Mt2s and Mt3s as well, demonstrating that they are not uniquely related to bipedalism per se, but as suggested by Lovejoy et al. (2009) relate to the joint capsule putting dorsal pressure on the bone during development when the foot rotates internally (for grasping) and externally (for some form of propulsion), though this hypothesis has yet to be experimentally confirmed.

2.10 | Third metatarsal

The third metatarsal (Mt3) articulates medially and laterally with the second and Mt4s respectively and with the lateral cuneiform proximally and third proximal phalanx distally. As with the Mt2, humans have short and straight Mt3s; whereas apes tend to have longer and more curved (longitudinally) Mt3s. The *Ardipithecus ramidus* Mt3 (ARA-VP-6/505) is short and slightly curved longitudinally (Lovejoy et al., 2009).

The Mt3 has internal (medial) torsion in apes, to assist with lateral toe opposability with the hallux (Morton, 1922). In monkeys, the Mt3 head torsion is more neutral; however, modern humans are unique amongst primates in exhibiting external (lateral) torsion of the Mt3 (Drapeau & Harmon, 2013). *Ardipithecus* has slight external torsion (Lovejoy et al., 2009) whereas OH 8 torsion falls within the human range (Pontzer et al., 2010). Interestingly, the Dmanisi Mt3s and those from *H. naledi* have external torsion considerably higher than is typically found in humans today (Harcourt-Smith et al., 2015; Pontzer et al., 2010). The functional explanation for this is unclear.

As with the Mt2, the Mt3 head is dorsally tall and domed in humans. Distal to the head is often a small sulcus where contact with the proximal phalanx is expected (though not yet experimentally confirmed) to occur during the push-off phase of bipedal walking. The *Ardipithecus ramidus* Mt3 (ARA-VP-6/505) possesses a human-like dorsally domed Mt3 head (Fernández et al., 2018; Lovejoy et al., 2009), as does the Burtele foot (BRT-VP-2/73; Haile-Selassie et al., 2012). In fact, the Mt3 is the most domed of any of the metatarsal heads in the perplexing Burtele foot. The Mt3 head of the A.L. 333-115 *A. afarensis* forefoot is not as domed as the other Mt heads and some analyses suggest it is more ape-like (Fernández et al., 2016), though there is extensive erosion around the dorsum of this fossil. Though there are six Mt3s from Sterkfontein Member 4 deposits, none preserve the metatarsal head, nor is it present in the OH 8 foot.

The Mt3 base is dorsoplantarly (DP) and mediolaterally (ML) flat in humans, and in African apes. In orangutans, the Mt3 base can be ML concave (as found in the Mt2 of apes). Interestingly, in gibbons (Proctor, 2010a) and in some cercopithecoids, the Mt3 base is DP convex. Furthermore, the contact facet between the Mt3 and Mt4 is flat in the apes. However, in gibbons and cercopithecoids, the Mt3 facet is concave, even cupped, for contact with a strongly convex Mt4 facet. These anatomies indicate considerable mobility of the Mt3 at both the tarsometatarsal and the lateral intermetatarsal joints in gibbons and monkeys that is absent in the great apes. Mt3 fossils of *Ekembo* and *Afropithecus* are gibbon and cercopithecoid-like for these anatomies. This anatomy may therefore be an important overlooked character distinguishing stem and crown great apes.

The base height of the Mt3 differs between hominins and the great apes (Figure 13). The base of the ape Mt3 is DP short relative either to the length of the metatarsal or to the ML width of the base. However, in all hominins (Table 11), from *Ardipithecus* through *Australopithecus* to *Homo*, the Mt3 base is DP tall (McNutt, Zipfel, & DeSilva, 2018; Figure 13). Functionally, the increase in Mt3 base height may be related to stiffening the lateral midfoot for bipedal propulsion,

TABLE 10 Comparative measurements of the second metatarsal in fossil hominins

Accession number	Taxon	Age (Ma)	Length (mm)	Torsion (°)	Base ML width (mm)	Base DP height (mm)	Midshaft ML (mm)	Midshaft DP (mm)	Head ML width (mm)	Head DP height (mm)
ARA-VP-6/1000	*Ar. ramidus*	4.4	–	–	18.4–18.8	19.5–21.6	–	–	–	–
StW 573	*A. prometheus?*	3.67?	–	–	13.5	15.1	7.5	8.5	–	–
BRT-VP-2/73b	Hominin sp.	3.4	66.9	−23	12.8	14.2	6.1	7.4	9.8	11.2
DIK-1-1f	*A. afarensis*	3.3	–	–	5.7	7.9	–	–	–	–
A.L. 333-72	*A. afarensis*	3.2	–	–	–	–	–	–	9.7	12.8
A.L. 333-115b	*A. afarensis*	3.2	–	–	–	–	–	–	9.9	11.8
A.L. 333-133	*A. afarensis*	3.2	–	–	12.1	15.9	–	–	–	–
StW 89	*A. africanus?*	2.0–2.6	61.1	−19.7	11.0	12.8	5.6	7.7	8.3	11.9
StW 377	*A. africanus*	2.0–2.6	54.9[a]	−11	13.2	14.9	6.1	7.2	–	–
StW 595c	*A. africanus?*	2.0–2.6	58.0[a]	–	11.7	13.2	6.3	6.8	–	–
Omo 323-1976-2117	*P. boisei?*	2.12	73.6	−12	16.7	19.8	8.1	10.5	10.6	15.2
OH 8	*P. boisei?*	1.85	55.6[a]	−7	11.2	14.4	6.3	7.2	–	–
ATD6-25	*H. antecessor*	0.77–0.95	–	–	14.6	19.2	–	–	–	–
ATD6-70+107	*H. antecessor*	0.77–0.95	79.0[a]	–	–	–	7.3	10.0	11.7	17.1
Arago XLIII	*Homo*	0.5	–	–	12.5	–	8.3	9.4	–	–
Sima de los Huesos	*Homo*	0.43	–	–	15.2 ± 0.9 (n = 4)	–	–	–	–	–
U.W. 101-459/461	*H. naledi*	0.24–0.34	58.0[a]		10.1	–	6.6	6.9	–	–
U.W. 101-1022	*H. naledi*	0.24–0.34	67.5	−8.7	–	–	7.6	7.2	–	–
U.W. 101-1458	*H. naledi*	0.24–0.34	63.4	6.7	11.5	–	6.3	6.8	–	11.5
U.W. 101-1499	*H. naledi*	0.24–0.34	–	–	9.7	11.3	–	–	–	–
Jinniushan	*Homo*	0.26	71.0	–	14.9	–	–	–	–	–
Neandertals	*Homo*	0.03–0.2	72.5 ± 5.5 (n = 14)	7.5 ± 4.0 (n = 4)	16.7 ± 2.4 (n = 18)	22.2 ± 2.1 (n = 12)	8.2 ± 0.9 (n = 18)	8.9 ± 1.0 (n = 18)	11.4 ± 1.7 (n = 6)	15.6 ± 2.3 (n = 9)
KHS 1–5	*H. sapiens*	0.195	–	–	15.3	21.1	7.5	8.8	–	–
LB1/22	*H. floresiensis*	0.06	63.0	–	–	–	–	–	–	–

Note. ML, mediolateral; DP, dorsoplantar. Data in this table from original fossils and measurements reported in Trinkaus, 1975; Latimer et al., 1982; Lamy, 1982; White & Suwa, 1987; Pearson et al., 2008; Pontzer et al., 2010; Lu et al., 2011; DeSilva, Proctor, & Zipfel, 2012; DeSilva, Zipfel, et al., 2012; Haile-Selassie et al., 2012; Pablos et al., 2012; Drapeau & Harmon, 2013; Pablos et al., 2017; Daver et al., 2018. Measurements reported for ARA-VP-6/1000 courtesy of T. White and G. Suwa. Measurements in the table have not been reported LB1/30. Mt2s from *Ardipithecus* (ARA-VP-6/500-042,-048; White et al., 2009), ASI-VP-2/1 (White et al., 2006), and KNM-ER 64062 (Jungers et al., 2015) have been discussed in print but are not yet described in detail.

[a] Estimate that approximates the actual value.

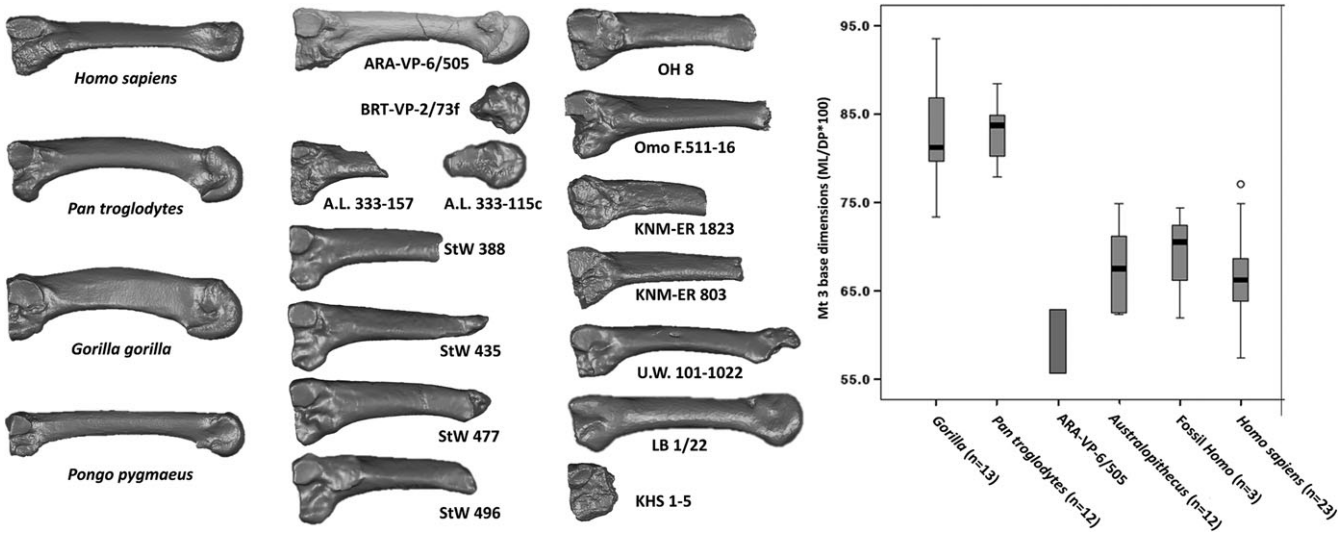

FIGURE 13 Third metatarsal (Mt3) from modern human, extant apes, and fossil hominins in lateral view. Each bone is from the right side (mirrored if necessary) and has been scaled so that the bones are roughly the same proximodistal length. Notice that the human Mt3 is straight, with a dorsoplantarly tall base and a domed head. Humans also have externally rotated heads; ape heads are more neutral. Right: boxplot showing the DP height of the Mt3 base relative to the ML width of the base. Boxes span the interquartile ranges, with the horizontal center lines indicating median values. Whiskers indicate sample range, excluding outliers (dots). All hominins, including *Ardipithecus*, have relatively tall Mt3 bases, a hominin synapomorphy. Reported measurements and image of ARA-VP-6/505 courtesy of Tim White and Gen Suwa

though this hypothesis remains to be experimentally tested. Nevertheless, we suggest that the Mt3 base height is a hominin synapomorphy potentially useful for identifying isolated pedal remains. Furthermore, Lovejoy et al. (2009) noted that ape Mt3 bases tend to have quite noticeable medial and lateral indentations for the transmission of intermetatarsal ligaments. These indentations are subtle in human Mt3s and in fossil hominins, including *Ardipithecus*.

Finally, along the distolateral shaft of many human Mt3s, there is the development of a prominent lateral tubercle, which is absent in the Mt3 of apes. This tubercle nestles into a concavity along the Mt4 shaft and gives rises to the M_{3-4} interosseous metatarsal ligament (Kelikian & Sarrafian, 2011). Functionally, it is proposed here (but remains untested) that this rugosity could be a bony correlate of the Mt3 and Mt4 moving as a functional unit during the propulsive phase of bipedal walking. This rugosity is not present in the *Ardipithecus* Mt3, but is variably present in *Australopithecus* (e.g., A.L. 333-157, StW 496).

2.11 | Fourth metatarsal

The Mt4 articulates with the Mt3 and Mt5 medially and laterally respectively and with the cuboid proximally and fourth proximal phalanx distally. In humans, but not in apes, the Mt4 is nestled into the tarsal row and often contacts the distolateral edge of the lateral cuneiform (Ward, Kimbel, & Johanson, 2011). As with the other metatarsals, the human Mt4 is relatively short and straight compared with the long and more curved (sagitally) Mt4 in the apes. The oldest known complete hominin Mt4s are from the Burtele foot (3.4 Ma) and from Hadar, Ethiopia (3.2 Ma), and sample quite different morphologies (Figure 14). The Burtele Mt4 is long and slender (Haile-Selassie et al., 2012); whereas the Hadar specimen (A.L. 333-160) is more human-like in being short and robust (Ward et al., 2011).

As with the other metatarsals, there are torsional differences between the ape and human Mt4 (Morton, 1922). In apes, the Mt4 torsion is roughly neutral. However, humans possess external (lateral) torsion which positions the head flush on the ground in a foot with a high transverse arch. While external torsion is certainly related to the presence of a transverse arch, the relationship between external torsion and a lateral longitudinal arch is unclear given that cercopithecoid monkeys also possess external torsion of the Mt4 (Drapeau & Harmon, 2013). Later hominins from OH 8, Dmanisi *Homo*, and later Pleistocene *Homo* have external torsion within the range of modern humans (Harcourt-Smith et al., 2015; Pontzer et al., 2010).

The human Mt4 head is dorsoplantarly (DP) tall and domed, with the articular surface rising above the dorsal surface of the shaft; a dorsal sulcus is typically present to facilitate metatarsophalangeal dorsiflexion during toe-off (Latimer & Lovejoy, 1990b). While the *Australopithecus* Mt4 head (known from A.L. 333-115 and A.L. 333-160) is domed (Ward et al., 2011), the shape may still retain some ape-like characteristics (Fernández et al., 2016, 2018).

As with other metatarsals, the human Mt4 base is DP tall relative both to the overall length of the bone, and to the ML width of the base. Apes, in contrast, have DP short bases. All known hominin Mt4s (Table 12) have tall DP bases (McNutt, Zipfel, & DeSilva, 2018), with the exception of the Burtele foot (Haile-Selassie et al., 2012). However, damage to the plantar base of the Mt4 of this specimen makes it difficult to assess this anatomy. Perhaps more important from a functional standpoint is the DP shape of the base (Figure 14). In humans, the base is typically either flat, or sinusoidal, reflecting stability at the lateral tarsometatarsal joint. Apes and monkeys, in contrast, have strongly convex bases, which are the result of tarsometatarsal dorsiflexion that occurs during the midtarsal break (DeSilva, 2010). The form: function link between the midtarsal break and Mt4 base shape is supported by an MRI study which found convex Mt4 bases in the occasional humans with a midtarsal break (DeSilva et al., 2015). *Ardipithecus ramidus* (ARA-VP-6/500-103) and the Burtele foot (BRT-VP-

TABLE 11 Comparative measurements of the third metatarsal in fossil hominins

Accession number	Taxon	Age (Ma)	Length (mm)	Torsion (°)	Base ML width (mm)	Base DP height (mm)	Midshaft ML (mm)	Midshaft DP (mm)	Head ML width (mm)	Head DP height (mm)
ARA-VP-6/505	*Ar. ramidus*	4.4	–	–	11.5–13.0	20.5–20.7	–	–	–	–
BRT-VP-2/73f	Hominin sp.	3.4	–	–	–	–	–	–	8.6[a]	13.2[a]
A.L. 333-115c	*A. afarensis*	3.2	–	–	–	–	–	–	9.2	13.2
A.L. 333-133	*A. afarensis*	3.2	–	–	11.0[a]	15.8	–	–	–	–
A.L. 333-157	*A. afarensis*	3.2	–	–	13.6	18.7	–	–	–	–
StW 238	*A. africanus*	2.0–2.6	–	–	12.1	16.3	6.3[a]	8.5[a]	–	–
StW 387	*A. africanus*	2.0–2.6	–	–	10.9	16.7	6.1[a]	7.9[a]	–	–
StW 388	*A. africanus*	2.0–2.6	–	14.7[a]	12.6	18.5	5.9[a]	8.9[a]	–	–
StW 435	*A. africanus*	2.0–2.6	–	–	13.3	20.1	6.2	8.7	–	–
StW 477	*A. africanus*	2.0–2.6	–	28.8[a]	12.0	16.5	5.8[a]	7.4[a]	–	–
StW 496	*A. africanus*	2.0–2.6	–	18.7[a]	10.9	16.8	5.7[a]	7.5[a]	–	–
SKX 38529	*P. robustus*?	1.8–2.0	–	–	12.1	–	–	–	–	–
KNM-ER 1500	*P. boisei*?	1.89	–	–	12	17.7	–	–	–	–
OH 8	*P. boisei*?	1.85	53.1[a]	24	11.9	16.0	6.6	8.8	–	–
OH 43	*Paranthropus*? *Homo*?	1.8	–	–	10.0	–	–	–	–	–
KNM-ER 997	*P. boisei*?	1.85	–	–	10.1	16.2	–	–	–	–
D3479	*H. erectus*	1.77	–	35.0	–	–	–	6.7	–	–
D2021	*H. erectus*	1.77	61[a]	38.0	–	–	–	9.0	–	–
Omo F.511-16	*Homo*?	1.7	–	–	14.6	20.7	7.6	10.2	–	–
KNM-ER 1823	*P. boisei*?	1.59	–	17	12.8	–	–	–	–	–
KNM-ER 803j	*H. erectus*	1.53	–	26	12.7	20.5	6.1	10.4		
SKX 247	*P. robustus*?	1.1–1.7	–	–	12.2	16.3	–	–	–	–
Sima de los Huesos	*Homo*	0.43	–	–	15.6 ± 1.0 (*n* = 6)	–	–	–	–	–
U.W. 101-552	*H. naledi*	0.24–0.34	60.0[a]	–	11.9	–	7.0	6.8	–	–
U.W. 101-1035	*H. naledi*	0.24–0.34	–	–	10.6	14.3	5.9[a]	6.9[a]	–	–
U.W. 101-1457	*H. naledi*	0.24–0.34	60.4	33.0	11.1	13.9	5.8	6.2	–	–
Neandertals	*Homo*	0.03–0.2	70.0 ± 3.3 (*n* = 5)	25.0 ± 7.8 (*n* = 3)	16.1 ± 2.0 (*n* = 18)	19.7 ± 1.7 (*n* = 8)	8.1 ± 0.9 (*n* = 10)	9.4 ± 1.7 (*n* = 11)	12.4 ± 1.4 (*n* = 3)	17.0 ± 2.7 (*n* = 4)
KHS 1–52	*H. sapiens*	0.195	–	–	14.5	22.3	–	–	–	–
LB1/23	*Homo floresiensis*	0.06	60.4	–	–	–	–	–	–	–

Note. ML, mediolateral; DP, dorsoplantar. Data in this table from original fossils and measurements reported in Day & Leakey, 1974; Trinkaus, 1975; White & Suwa, 1987; Jungers et al., 2009; Pontzer et al., 2010; Haile-Selassie et al., 2012; Ward, Kimbel, Harmon, & Johanson, 2012; Mersey et al., 2013; Harcourt-Smith et al., 2015; Measurements reported for ARA-VP-6/505 courtesy of T. White and G. Suwa. Only adult Mt3s are shown in this table. Juvenile Mt3 from *A. afarensis* (DIK-1-1f) is described elsewhere (DeSilva, Gill, et al., 2018) as is the juvenile Mt3 from *H. naledi* (U.W. 101-1500; Harcourt-Smith et al., 2015). Measurements in the table have not been reported LB1/31. Mt3s from Aramis *Ardipithecus* (ARA-VP-6/500–066, White et al., 2009) and Gona *Ardipithecus* (Simpson et al., 2018), StW 595d (Clarke, 2013), and KNM-ER 64062 (Jungers et al., 2015) have been discussed in print but are not yet described in detail.

[a] Estimate that approximates the actual value.

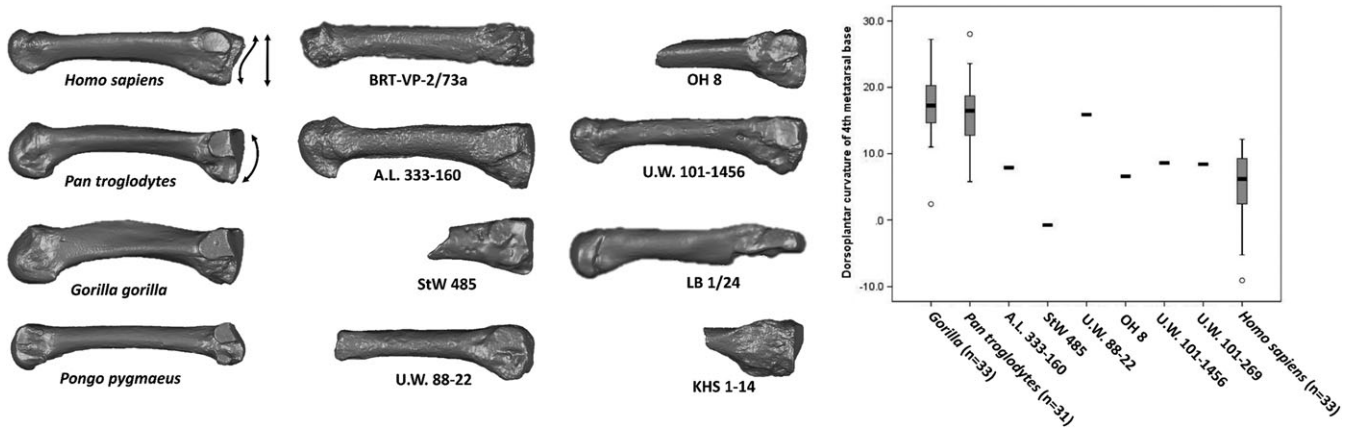

FIGURE 14 Fourth metatarsal (Mt4) from modern human, extant apes, and fossil hominins in medial view. Each bone is from the right side (mirrored if necessary) and has been scaled so that the bones are roughly the same proximodistal length. The base of the human Mt4 tends to be either flat or sinusoidal. Nonhuman anthropoids have convex Mt4 bases, a skeletal correlate of the midtarsal break. Right: boxplot quantifying the curvature of the base of the Mt4 (after DeSilva, 2010; DeSilva et al., 2013). Boxes span the interquartile ranges, with the horizontal center lines indicating median values. Whiskers indicate sample range, excluding outliers (dots). The Mt4 base is flat in all hominins (including *Ardipithecus* and Burtele—not shown in graph). However, the Mt4 base is uniquely convex in *A. sediba*—a function of a unique gait in this taxon

2/73a) both possess human-like dorsoplantarly sinusoidal or flat bases, demonstrating that the earliest known hominins had a stiff lateral midfoot for bipedal propulsion. This anatomy is found in early australopiths from Eastern Africa (A.L. 333-160) and South Africa (StW 485), and into genus *Homo*. Surprisingly, however, the base of the Mt4 from *A. sediba* is ape-like in its DP convexity (DeSilva et al., 2013), currently explained as a function of a relatively low arch (Prang, 2015b) and excessive medial weight transfer—two risk factors for a hypermobile midfoot in humans today (DeSilva et al., 2015).

In lateral view, humans tend to have Mt4s with a proximodorsal to distoplantarly angled base relative to the long axis of the shaft. This anatomy may be related to the presence of a longitudinal arch in humans and *A. afarensis* (Ward et al., 2011). This base angulation is more neutral or ape-like in *A. africanus* (StW 485) and *A. sediba* (U.W. 88-22). Finally, apes tend to have rounder midshaft dimensions; whereas the human Mt4 midshaft is DP taller and ML narrower. Hominin Mt4 midshafts are human-like with the exception of *A. sediba*, which has a round midshaft (DeSilva, Carlson, et al., 2018).

2.12 | Fifth metatarsal

The Mt5 articulates with the Mt4 medially, cuboid proximally, and fifth proximal phalanx distally. In apes, the Mt5 is long, slender and longitudinally curved in the sagittal plane and straight in the transverse plane. The human Mt5 is short and stout and often laterally deviates in the transverse plane. The only complete Mt5 in the early hominin fossil record (StW 114/115) from Sterkfontein Member 4 has a slight ape-like curve in the sagittal plane, but human-like transverse plane curvature (Zipfel, DeSilva, & Kidd, 2009; Figure 15). An earlier Mt5 from Hadar (A.L. 333-13) also displays human-like transverse plane curvature.

In both humans and apes, there is external torsion of the Mt5, with humans possessing a greater average value (Drapeau & Harmon, 2013). The Mt5 from *A. africanus* (StW 114/115) has human-like head torsion (Zipfel et al., 2009); whereas the Mt5 from Dmanisi *Homo* (D4058) is more chimpanzee-like (Pontzer et al., 2010; Table 13), though given the overlap in values between apes and humans, we do not regard these differences as functionally meaningful.

As with other metatarsal heads, the Mt5 of humans is dorsally domed and possesses a sulcus just proximal to the dorsal edge of the head, presumably for the rim of the proximal phalanx during metatarsophalangeal dorsiflexion (Latimer & Lovejoy, 1990b). *Australopithecus* Mt5 heads are human-like (Fernández et al., 2016; Zipfel et al., 2009). The cuboid and Mt4 facets of the Mt5 differ little in shape between humans and the apes (DeSilva, 2010; Proctor, 2013).

The human Mt5 midshaft is mediolaterally expanded compared to the more rounded shape of the Mt5 midshaft in apes. The diaphyseal strength relative to the articular area of the Mt5 head is greater in humans than in apes (Marchi, 2010). A CT-based study revealed that apes have more cortical bone in their metatarsals than humans (Marchi, 2005), and a more recent study found that in human Mt5s, the cortical bone is distributed in a manner that would resist dorsoplantarly bending forces, especially proximally (Dowdeswell et al., 2016).

Finally, compared with the human Mt5, apes tend to have a more projecting tuberosity, possibly reflecting an important role of *M. peroneus brevis* and the variably present *M. peroneus tertius*. *Australopithecus* Mt5s have a more human-like tuberosity, with the largest (most ape-like) tubersosity belonging to A.L. 333-13 (*A. afarensis*).

2.13 | Proximal phalanges

The human hallucal proximal phalanx (Table 14) is short and robust compared to that of African apes, which tend to be longer and more slender. Orangutans typically do not possess a hallucal proximal phalanx at all (Tuttle & Rogers, 1966). Human lateral proximal phalanges (PP) are relatively short and straight; whereas the lateral proximal phalanges of the apes are long and longitudinally curved (Trinkaus & Patel, 2016). Ontogenetic studies demonstrate that the curvature of the phalanges is related to grasping during development (Congdon, 2012). The shortening of the phalanges in the human lineage confers benefits during running (Rolian et al., 2009). The pedal phalanges of

Ardipithecus are long and curved (Lovejoy et al., 2009). Relative to *Ardipithecus*, the pedal phalanges of *Australopithecus* are shorter and less curved (Table 15; Figure 16). In *Homo*, the simple narrative of pedal phalanges becoming shorter and less curved is complicated by *H. floresiensis* and *H. naledi*, which possess long (*H. floresiensis*) or curved (*H. naledi*) proximal pedal phalanges (Harcourt-Smith et al., 2015; Jungers, Harcourt-Smith, et al., 2009).

Perhaps most notably, the base of human proximal phalanges is canted dorsodistally to plantoproximally; whereas great ape phalanges have opposite, plantar cants to the base of their proximal phalanges (Latimer & Lovejoy, 1990b; Figure 16). Dorsal canting is hypothesized to be part of a functional complex that includes dorsal doming of the metatarsal head functionally related to dorsiflexion of the toes during bipedal locomotion (Latimer & Lovejoy, 1990b). Fossil hominins from *Ardipithecus* through *Australopithecus* to *Homo* possess dorsally canted proximal phalanges (Haile-Selassie, 2001; Latimer & Lovejoy, 1990b), though the magnitude of dorsal canting may not be as high as found in modern humans (Duncan et al., 1994). However, dorsal canting alone does not indicate bipedalism: the proximal phalanges from *Proconsul* (*Ekembo*) *heseloni* possess dorsal canting as occasionally do lateral phalanges from gibbons and cercopithecoids (Begun, Teaford, & Walker, 1991; Griffin & Richmond, 2010; McNutt, Zipfel, & DeSilva, 2018).

Two other anatomies are worth noting: in apes, the base of the phalanx is mediolaterally broad whereas in humans, the base is dorsoplantarly tall and is curved along the dorsal rim (Stern & Susman, 1983). Preuschoft (1970) has suggested that the dorsoplantarly expanded base of the proximal phalanges may be related to the presence of the plantar aponeurosis and a windlass mechanism in the human foot (Hicks, 1953). Additionally, the plantar shaft of the ape phalanx possesses strong flexor ridges, which help keep the flexor tendons from pulling away from the plantar surface of the bone. In humans, the flexor ridges are not as well developed.

2.14 | Intermediate phalanges

As with the proximal phalanx, the ape intermediate phalanx is longer, more curved, and has a flatter base with more developed flexor ridges than the human intermediate phalanx. Similarly, as with the proximal phalanges, early hominin intermediate phalanges from *Ardipithecus* and *Australopithecus* are more ape-like in their length (McNutt, Zipfel, & DeSilva, 2018; Figure 17) and curvature; whereas those from later *Homo* tend to be shorter and less curved, though an exception to this trend is *H. naledi*, which has quite curved intermediate phalanges (Harcourt-Smith et al., 2015). Perhaps most notably, however, is the size differential in human intermediate phalanges. Unlike the proximal phalanges, which are only subtly decreasing in size from PP2 to PP5. The human intermediate phalanges (IP) reduce considerably in size from IP2 to IP5 (Elftman & Manter, 1935). *Australopithecus afarensis* (A.L. 333-115) retains long lateral intermediate phalanges (Stern & Susman, 1983), which would have been functionally beneficial for some degree of pedal grasping during bouts of climbing and infant clinging.

2.15 | Distal phalanges

Human distal phalanges are short and stout compared with ape distal phalanges, which tend to be longer and more slender. The most substantial functional differences can be found in the hallucal distal phalanx. In humans, the hallucal distal phalanx possesses, in the transverse plane, a lateral deflection of the long axis of the bone relative to the base (Barnett, 1962). This anatomy is present already at birth (Wilkinson, 1954). In apes, the long axis of the bone is perpendicular to the base. Furthermore, in the coronal plane, the human hallucal distal phalanx displays axial torsion (Figure 17), which is argued to be functionally related to hallucal push off (Barnett, 1962; Day & Napier, 1966). The OH 10 distal hallucal phalanx and *H. naledi* (U.W. 101-1551) are human-like in these characters, suggesting human-like bipedal propulsion (Day & Napier, 1966).

3 | HOMININ FOOT EVOLUTION

3.1 | Miocene

Although this review focuses on Plio-Pleistocene hominin foot evolution, genetic studies convincingly demonstrate that the human–chimpanzee divergence occurred in the Miocene (e.g., Moorjani, Amorim, Arndt, & Przeworski, 2016) and thus the earliest hominin foot fossils would derive from that time period. Two hominins from the Miocene—*Sahelanthropus tchadensis* (Brunet et al., 2002) and *Orrorin tugenensis* (Senut et al., 2001)—do not yet preserve any pedal remains. Therefore, although this review covers only hominin foot fossils from the Plio-Pleistocene, we are well aware that questions about the foot of the last common ancestor will be best addressed with pedal fossils from the Miocene, a time period currently devoid of confirmed hominin foot remains.

While it has been suggested that the Miocene ape *Oreopithecus* had a bipedal foot (Köhler & Moyà-Solà, 1997), our preliminary observations on these fossils along with the work of others (Susman, 2005) are skeptical of these claims and regard *Oreopithecus* as an arboreal hominoid (e.g., Harrison, 1991). Additionally, 5.7 Ma fossilized footprints from Crete may be from a bipedal hominin (Gierliński et al., 2017) or even a bipedal hominoid (Crompton, 2017). A biped from the Miocene of Crete truly would be paradigm altering and we look forward to the publication of the necessary information from these footprints (e.g., Falkingham et al., 2018) that can be used to either support or refute these extraordinary claims. Below, we detail what is currently known (and remains unknown) about the foot of Plio-Pleistocene hominins from species of *Ardipithecus* through *Australopithecus* and *Paranthropus* to *Homo*.

3.2 | *Ardipithecus kadabba* (Middle Awash, Ethiopia; 5.2 Ma)

Although much of the *Ar. kadabba* hypodigm derives from Late Miocene sediments (Haile-Selassie, 2001), the foot is represented by an early Pliocene (5.2 Ma) left fourth proximal pedal phalanx (AME-VP-1/71) from the Kuseralee Member (Sangantole Formation) of Amba East in the Middle Awash study area of Ethiopia (Haile-Selassie, 2001; Haile-Selassie, Suwa, & White, 2009). The anatomy discussed below is

TABLE 12 Comparative measurements of the fourth metatarsal in fossil hominins

Accession number	Taxon	Age (Ma)	Length (mm)	Torsion (°)	Base ML width (mm)	Base DP height (mm)	Midshaft ML (mm)	Midshaft DP (mm)	Head ML width (mm)	Head DP height (mm)
BRT-VP 2/73a	Hominin sp.	3.4	68.7	26–27	12.7	13.3[a]	5.4	9.2	10.5[a]	12.1[a]
DIK-1-1f	*A. afarensis*	3.3	–	30[a]	5.4	7.8	–	–	–	–
A.L. 333-115d	*A. afarensis*	3.2	–	–	–	–	–	–	9.5	14.0
A.L. 333-160	*A. afarensis*	3.2	59.9	17	13.1	17.1	6.1	9.1	8.5	13.4
StW 485	*A. africanus*	2.0–2.6	–		9.5	14.3	–	–	–	–
U.W. 88-22	*A. sediba*	1.98	56.0[a]	19[a]	9.3	13.4	5.5	6.5	–	–
OH 8	*P. boisei*?	1.85	51.7[a]	25	10.2	15.4	6.4	8.4	–	–
D2669	*H. erectus*	1.77	59.1	29	–	–	5.9	8.6	–	–
D4165	*H. erectus*	1.77	–	28	–	–	–	–	–	–
ATD6-24	*H. antecessor*	0.77–0.95	–	–	12.3	18.3	7.8	9.1	–	–
Sima de los Huesos	*Homo*	0.43	–	–	14.8 ± 0.4 (n = 4)	19.6 ± 0.3 (n = 3)	8.2 ± 0.2 (n = 4)	10.2 ± 0.9 (n = 4)	–	–
U.W. 101-248	*H. naledi*	0.24–0.34	–	–	–	9.2	–	–	–	–
U.W. 101-269	*H. naledi*	0.24–0.34	59.0	34.7	9.5	13.1	6.5	7.5	7.1	–
U.W. 101-1456	*H. naledi*	0.24–0.34	59.0	38.2	10.6	16.0	6.7	7.6	7.6[a]	12.6[a]
Neandertals	*Homo*	0.03-0.2	69.0 ± 5.0 (n = 9)	26.7 ± 8.3 (n = 6)	15.1 ± 1.2 (n = 14)	21.0 ± 2.2 (n = 8)	7.6 ± 0.8 (n = 21)	9.5 ± 1.3 (n = 20)	12.6 ± 1.2 (n = 5)	16.4 ± 2.2 (n = 6)
KHS 1–14	*H. sapiens*	0.195	–	–	12.4	18.8	–	–	–	–
LB1/24	*H. floresiensis*	0.06	58.3	–	–	–	–	–	–	–

Note. ML, mediolateral; DP, dorsoplantar. Data in this table from original fossils and measurements reported in Trinkaus, 1975; White & Suwa, 1987; Haile-Selassie et al., 2012; Pablos et al., 2012; Ward et al., 2012; Harcourt-Smith et al., 2015. Fossils too fragmentary to yield any of the measurements reported in this table include OH 43 and LB1/32. Mt4s from Aramis *Ardipithecus* (ARA-VP-6/500-102,-103, White et al., 2009) and Gona *Ardipithecus* (Simpson et al., 2018), StW 596 (Clarke, 2013), StW 628 (Proctor, 2013), and KNM-ER 64062 (Jungers et al., 2015) have been discussed in print but are not yet described in detail.

[a] Estimate that approximates the actual value.

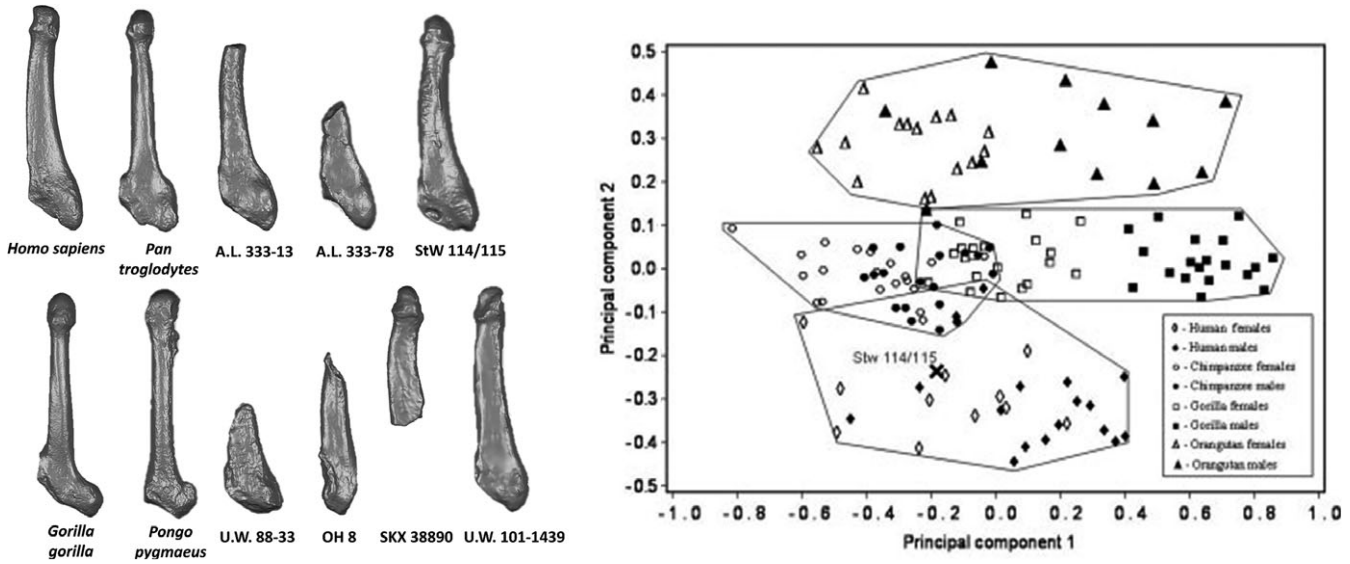

FIGURE 15 Fifth metatarsal (Mt5) from modern human, extant apes, and fossil hominins in dorsal view. Each bone is from the right side (mirrored if necessary) and has been scaled so that the bones are roughly the same proximodistal length. Notice that the human (and in general hominin) Mt5 curves laterally. Ape Mt5 tend to have a quite robust and projecting Mt5 tuberosity. Right: multivariate analysis of Mt5 of humans and apes. Notice that the complete *Australopithecus* Mt5 from Sterktontein M4 (StW 114/115) falls squarely within the human distribution (from Zipfel et al., 2009)

based primarily on Haile-Selassie (2001) and Haile-Selassie et al. (2009), and observations we made on the original fossil.

The phalanx is long, though it is relatively shorter than the PP4 of modern apes (Haile-Selassie et al., 2009). The longitudinal curvature falls within the range of modern chimpanzees (Deane & Begun, 2008). A most salient observation was the presence of a dorsally canted base (Haile-Selassie, 2001), which is found in hominin—but not African ape—pedal proximal phalanges and is functionally correlated with dorsiflexion during the toe-off phase of bipedal gait (Latimer & Lovejoy, 1990a, 1990b). This toe bone, therefore, is the earliest purported pedal evidence for upright walking on the African continent.

Begun (2004) suggested that dorsal canting also occurs in the phalanges of nonbipedal hominoids, including *Sivapithecus*, and cited Rose (1986). Haile-Selassie et al. (2009) responded that the *Sivapithecus* phalanges described in Rose (1986) are manual phalanges, rendering them irrelevant to a discussion about the foot. While an intermediate pedal phalanx from *Sivapithecus* (GSP 47583) is described as having a "ventrally inclined articular surface" (Madar, Rose, Kelley, MacLatchy, & Pilbeam, 2002), Begun (pers. comm.) informed us that he was also thinking about his own study of pedal phalanges in *Proconsul* (now *Ekembo* [McNulty, Begun, Kelley, Manthi, & Mbua, 2015]) *heseloni* (Begun et al., 1991) in which he documented dorsal canting in the lateral proximal phalanges of the KPS foot skeletons. We have since examined the KPS foot fossils and agree that the lateral proximal phalanges of *Ekembo* are dorsally canted (McNutt, Zipfel, & DeSilva, 2018). We are not suggesting that the Amba East *Ar. kadabba* proximal phalanx is not hominin, nor are we suggesting that this morphology precludes it from being bipedal. In fact, dorsally canted proximal phalanges and domed metatarsal heads form a functional complex found together in bipeds (Fernández et al., 2016, 2018; Haile-Selassie et al., 2009, 2012; Latimer & Lovejoy, 1990a, 1990b). However, given that dorsal canting can also be found in nonbipedal hominoids like *Ekembo* (Begun et al., 1991; McNutt, Zipfel, & DeSilva, 2018), we agree with the cautionary note in Haile-Selassie et al. (2009) that additional postcranial fossils will be necessary to assess the hypothesis that *Ar. kadabba* was bipedal.

3.3 | *Ardipithecus ramidus* (Aramis and Gona, Ethiopia; 4.4 Ma)

The pre-*Australopithecus* hominin foot is best known from 4.4 Ma pedal remains from Aramis and Gona, Ethiopia assigned to *Ardipithecus ramidus* (Lovejoy et al., 2009; Semaw et al., 2005; Simpson et al., 2018; White et al., 2009; White, Lovejoy, Asfaw, Carlson, & Suwa, 2015). Many of the foot fossils derive from a single skeleton—ARA-VP-6/500 ("Ardi"; Figure 18), though some key functional interpretations of the *Ardipithecus* foot come from isolated metatarsals ARA-VP-6/1000 (Mt2) and ARA-VP-6/505 (Mt3; Lovejoy et al., 2009). The Aramis foot skeleton is discussed below based on Lovejoy et al. (2009), White et al. (2015), and qualitative observations we made on the original fossil material. We end this section with some comments on the recently announced partial skeleton from Gona, Ethiopia (Simpson et al., 2018).

Unfortunately, the calcaneus is known only from a small fragment of the subtalar joint (White et al., 2009), which yields little functional information. However, the talus of the ARA-VP-6/500 skeleton is complete and exceptionally well preserved. In functionally meaningful ways, the talus appears quite African ape-like. The talar axis angle is high (14.5°; Lovejoy et al., 2009), indicating that, unlike in *Australopithecus*, the Aramis *Ardipithecus* foot had an inverted set to the ankle joint, adaptive for climbing. Qualitatively, the talar trochlea is quite wedged (Lovejoy et al., 2009 SOM Figure 1), indicating that *Ardipithecus* habitually loaded its ankle joint in dorsiflexion. A strongly wedged talar trochlea is found in wild hominoids and ateline monkeys that engage in flexed ankle vertical climbing (DeSilva, 2008, 2009), but not

TABLE 13 Comparative measurements of the fifth metatarsal in fossil hominins

Accession number	Taxon	Age (Ma)	Length including tuberosity (mm)	Torsion (°)	Base ML width (mm)	Base DP height (mm)	Midshaft ML (mm)	Midshaft DP (mm)	Head ML width (mm)	Head DP height (mm)
ARA-VP-6/500-067	*Ar. ramidus*	4.4	63.7[a]	–	–	–	–	–	–	–
A.L. 333-13	*A. afarensis*	3.2	–	–	18.1	12.1	9.4	7.3	–	–
A.L. 333-78	*A. afarensis*	3.2	–	–	15.7	11.0	7.0	6.4	–	–
A.L. 333-115e	*A. afarensis*	3.2	–	–	–	–	–	–	8.7	12.5
StW 114/115	*A. africanus*	2.0–2.6	60.7	12	16.5	11.0	8.7	7.4	8.7	12.6
U.W. 88-16	*A. sediba*	1.98	57.0[a]	–	–	–	6.9	4.8	–	–
U.W. 88-33	*A. sediba*	1.98	–	–	16.0	12.0	–	–	–	–
OH 8	*P. boisei*?	1.85	–	–	12.2	9.6	7.2	5.8	–	–
D4058	*H. erectus*	1.77	62.0[a]	7	–	–	–	6.8	–	–
KNM-ER 803f	*H. erectus*	1.53	–	–	20.3	12.0	–	–	–	–
SKX 33380	*P. robustus*?	1.0	–	–	–	–	8.9	7.3	8.1	11.2
Sima de los Huesos	*Homo*	0.43	–	–	23.4 ± 1.6 (*n* = 5)	–	–	–	–	–
U.W. 101-518	*H. naledi*	0.24–0.34	–	–	15.0	10.0	8.4	5.3	–	–
U.W. 101-1439	*H. naledi*	0.24–0.34	60.2	22.4	13.1	8.3	8.1	5.4	–	–
Neandertals	*Homo*	0.03–0.2	67.3 ± 4.2 (*n* = 7)	18.0 ± 8.2 (*n* = 5)	23.2 ± 2.3 (*n* = 17)	16.3 ± 1.6 (*n* = 11)	11.2 ± 1.3 (*n* = 12)	7.7 ± 1.1 (*n* = 12)	13.7 ± 1.8 (*n* = 5)	14.8 ± 1.8 (*n* = 5)

Note. ML, mediolateral; DP, dorsoplantar. Data in this table from original fossils and measurements reported in Trinkaus, 1975; Latimer et al., 1982; Zipfel et al., 2009; Lovejoy et al., 2009; Pontzer et al., 2010; Pablos et al., 2012; Harcourt-Smith et al., 2015. Only adult Mt5s are shown in this table. Juvenile Mt5 from *A. afarensis* (DIK-1-1f) is described elsewhere (DeSilva, Gill, et al., 2018). Measurements in the table have not been reported for LB1/25 and LB1/33. Mt5s from *Ardipithecus* (ARA-VP-6/960, White et al., 2009), StW 634 (Clarke, 2013), and KNM-ER 64062 (Jungers et al., 2015) have been discussed in print but are not yet described in detail.

[a] Estimate that approximates the actual value.

TABLE 14 Comparative measurements of the hallucal proximal phalanx in fossil hominins

Accession number	Element	Taxon	Age (Ma)	Length (mm)	Base ML	Base DP	Midshaft ML	Midshaft DP	Head ML	Head DP
BRT-VP-2/73g	PP1	Hominin sp.	3.4	25.2	13.1	9.7	8.5	6.1	12.2	6.5
A.L. 333-158	PP1	*A. afarensis*	3.2	–	14.5	12.7	–	–	–	–
A.L. 333-115f	PP1	*A. afarensis*	3.2	–	15.8	13.2	–	–	–	–
StW 470	PP1	*A. africanus*	2.0–2.6	23.2	14.9	11.6	10.6	7.8	13.0	7.3
SKX 45690	PP1	*P. robustus*?	1.8–2.0	23.3	14.4	12.1	9.7	6.4	11.7	6.9
KNM-ER 803q	PP1	*H. erectus*	1.53	–	–	–	9.9	8.5	–	–
ATD6-30	PP1	*H. antecessor*	0.77–0.95	36.6	18.0	16.7	11.8	10.5	15.0	10.7
ATD6-31	PP1	*H. antecessor*	0.77–0.95	34.3	18.3	17.0	11.0	9.9	16.1	10.8
Sima de los Huesos	PP1	*Homo*	0.43	–	–	–	–	–	17.6 ± 1.2 (n = 7)	–
U.W. 101-082	PP1	*H. naledi*	0.24–0.34	28.6	–	–	9.8	7.7	–	6.6
U.W. 101-1024	PP1	*H. naledi*	0.24–0.34	–	15.4	–	–	–	–	–
U.W. 101-1419	PP1	*H. naledi*	0.24–0.34	–	12.5	10.2	8.8	5.2	–	–
U.W. 101-1442	PP1	*H. naledi*	0.24–0.34	–	13.3	12.1	9.9	7.0	–	–
U.W. 101-1452	PP1	*H. naledi*	0.24–0.34	24.7	10.5	8.8	8.0	5.7	10.9	7.0
Jinniushan	PP1	*Homo*	0.26	29.1	–	–	–	–	–	–
Neandertals	PP1	*Homo*	0.03–0.2	26.2 ± 2.7 (n = 11)	19.9 ± 2.4 (n = 11)	16.5 ± 2.1 (n = 9)	12.9 ± 1.7 (n = 12)	9.8 ± 1.1 (n = 11)	17.5 ± 1.7 (n = 17)	9.5 ± 1.4 (n = 11)
KHS 1–25	PP1	*H. sapiens*	0.195	37.7	20.5	14.7	13.7	9.3	20.0	11.8
LB10	PP1	*H. floresiensis*	0.06	24.4	12.6	10.0	8.0	6.8	9.7	7.2

Note. ML, mediolateral; DP, dorsoplantar. Data in this table from original fossils and measurements reported in Trinkaus, 1975; Latimer et al., 1982; Lorenzo, Arsuaga, & Carretero, 1999; Pearson et al., 2008; Jungers et al., 2009; Lu et al., 2011; Haile-Selassie et al., 2012; Harcourt-Smith et al., 2015; Pablos et al., 2017. PP1s from *Ardipithecus* (ARA-VP-6/500-035, White et al., 2009), StW 595b (Clarke, 2013), KNM-ER 64062 (Jungers et al., 2015) have been discussed in print but are not yet described in detail.

TABLE 15 Comparative measurements of the lateral proximal phalanges in fossil hominins

Accession number	Element	Taxon	Age (Ma)	Length (mm)	Base ML	Base DP	Midshaft ML	Midshaft DP	Head ML	Head DP
AME-VP-1/71	PP4	*Ar. kadabba*	5.2	31.3	9.8	8.9	6.2	5.2	7.3	5.3
ARA-VP-6/500-094	PP4	*Ar. ramidus*	4.4	35.4	10.7	8.6	8.1	6.0	8.0	6.3
ARA-VP-6/500-017	PP4	*Ar. ramidus*	4.4	–	–	–	8.9[a]	5.9[a]	8.3	6.2
ARA-VP-6/500-047	PP2	*Ar. ramidus*	4.4	–	–	–	8.8	7.2	–	–
ARA-VP-6/500-047	PP2	*Ar. ramidus*	4.4	–	–	–	8.9[a]	7.4[a]	9.7	7.0
ARA-VP-6/500-008	PP3	*Ar. ramidus*	4.4	36.5[a]	12.1	10.9	–	–	–	–
ARA-VP-6/500-009	PP3	*Ar. ramidus*	4.4	–	–	–	9.3	6.6	–	–
ARA-VP-6/500-007	PP5	*Ar. ramidus*	4.4	–	10.9	9.3	–	–	–	–
ARA-VP-6/500-044	PP5	*Ar. ramidus*	4.4	30.9	10.9–12.1	9.8	–	–	8.2	5.7
GWM1/P37	PP	*Ar. ramidus*	4.3–4.5	–	9.2	7.8	–	–	–	–
KNM-ST 22944K	PP	*Australopithecus* sp.	3.5	–	9.7	9.0	–	–	–	–
BRT-VP-2/73e	PP2	Hominin sp.	3.4	29.7	10.9	9.6	6.4	6.0	8.0	5.3
BRT-VP-2/73d	PP4	Hominin sp.	3.4	28.7	10.3	8.6	5.3	5.2	7.9	5.4
A.L. 288-1y	PP	*A. afarensis*	3.2	22.7	9.2	7.4	5.5	4.3	6.3	4.3
A.L. 333w-25	PP	*A. afarensis*	3.2	–	11.2	9.6	8.4	6.4	–	–
A.L. 333w-51	PP	*A. afarensis*	3.2	–	11.8	10.1	9.2	6.5	–	–
A.L. 333-22	PP	*A. afarensis*	3.2	–	–	–	6.7	6.3	8.4	5.7
A.L. 333-102	PP	*A. afarensis*	3.2	30.5	10.6	10.2	6.8	5.7	9.3	5.7
A.L. 333-26	PP	*A. afarensis*	3.2	30.9	11.1	9.5	8.0	5.4	8.7	6.1
A.L. 333-60	PP	*A. afarensis*	3.2	27.9	10.9	10.0	6.2	4.8	8.2	6.0
A.L. 333-71	PP	*A. afarensis*	3.2	32.5	10.0	9.3	6.6	5.8	8.0	5.7
A.L. 333-168	PP	*A. afarensis*	3.2	32.9	10.7	9.8	6.2	5.4	7.6	5.6
A.L. 333-145	PP2	*A. afarensis*	3.2	29.6	10.6	9.8	6.1	5.8	7.2	5.2
A.L. 333-154	PP4	*A. afarensis*	3.2	27.4	9.9	8.9	5.4	5.2	6.8	5.3
A.L. 333-167	PP2	*A. afarensis*	3.2	29.6	10.3	10.2	5.8	5.8	7.5	5.6
A.L. 333-115g	PP2	*A. afarensis*	3.2	32.2	11.5	9.4	7.0	6.7	9.4	6.6
A.L. 333-115h	PP3	*A. afarensis*	3.2	34.5	13.6	10.6	8.0	6.1	9.0	5.7
A.L. 333-115i	PP4	*A. afarensis*	3.2	32.8	11.7	10.0	7.8	6.1	9.0	6.0
A.L. 333-115j	PP5	*A. afarensis*	3.2	28.6	10.1	8.9	6.0	6.0	8.0	5.4
StW 355	PP	*A. africanus*	2.0–2.6	24.6	9.1	7.8	5.9	5.0	7.1	4.5
DNH 117	PP	*P. robustus*	1.4–2.0	24.0	10.3	9.2	6.6	4.9	7.5	5.1
SKX 16699	PP	*Homo*?	~1.8	20.3	8.9	8.6	4.7	4.5	6.9	4.8
KNM-ER 803r	PP	*H. erectus*	1.53	–	–	–	6.9	6.1	9.0	6.3
ATD6-32	PP	*H. antecessor*	0.77–0.95	–	–	–	5.3	5.0	7.8	5.6
U.W. 101-504	PP	*H. naledi*	0.24–0.34	25.5	–	9.7	6.5	6.3	8.1	–

(*Continues*)

TABLE 15 (Continued)

Accession number	Element	Taxon	Age (Ma)	Length (mm)	Base ML	Base DP	Midshaft ML	Midshaft DP	Head ML	Head DP
U.W. 101-725	PP	*H. naledi*	0.24–0.34	–	6.8[a]	8.3[a]	5.8	5.1	7.4	–
U.W. 101-976	PP	*H. naledi*	0.24–0.34	23.6[a]	–	9.9	5.9	5.3	–	–
U.W. 101-1013	PP	*H. naledi*	0.24–0.34	22.4	–	8.4	5.5	5.1	6.4	4.9
U.W. 101-1034	PP	*H. naledi*	0.24–0.34	19.4	–	–	4.3	4.3	5.9	3.5
U.W. 101-1148	PP	*H. naledi*	0.24–0.34	21.5	7.9	8.9	4.9	5.5	6.3	4.5
U.W. 101-1395	PP	*H. naledi*	0.24–0.34	21.6	8.4	8.6	5.2	5.6	6.8	4.6
U.W. 101-1395b	PP	*H. naledi*	0.24–0.34	–	–	8.1[a]	4.9[a]	4.4[a]	–	–
U.W. 101-1441	PP	*H. naledi*	0.24–0.34	23.3	8.5	9.5	5.4	5.9	7.2	4.7
U.W. 101-1557	PP	*H. naledi*	0.24–0.34	–	–	–	–	–	5.1	3.3
U.W. 101-1657	PP	*H. naledi*	0.24–0.34	–	–	–	4.5	4.0	3.0	3.3
Jinniushan	PP3	*Homo*	0.26	26.4	13.3	–	–	–	–	–
Neandertals	PP	*Homo*	0.03–0.2	22.5 ± 2.2 (n = 31)	13.2 ± 2.1 (n = 37)	12.2 ± 1.6 (n = 37)	7.2 ± 1.3 (n = 38)	6.3 ± 1.0 (n = 36)	10.0 ± 1.3 (n = 35)	6.6 ± 1.0 (n = 36)
Denisova	PP	*Homo*	0.05	26.0[a]	12.0[a]	10.5	7.8	6.3	–	6.0[a]
LB1/38	PP	*H. floresiensis*	0.06	26.8	–	–	6.5	–	–	–
LB1/36	PP	*H. floresiensis*	0.06	26.2	–	–	6.8	–	–	–
LB1/37	PP	*H. floresiensis*	0.06	24.5	–	–	6.9	–	–	–
LB1/35	PP	*H. floresiensis*	0.06	23.9	–	–	6.4	–	–	–
LB1/34	PP	*H. floresiensis*	0.06	21.7	–	–	6.6	–	–	–
LB6/15	PP	*H. floresiensis*	0.06	20.0[a]	8.3	7.6	–	–	–	–

Note. Data in this table from original fossils and measurements reported in Day & Leakey, 1974; Latimer et al., 1982; Ward et al., 1999; Semaw, Simpson, Quade, & Renne, 2005; Mednikova, 2011; Haile-Selassie et al., 2012; Mersey et al., 2013; Vernon, 2013; Harcourt-Smith et al., 2015; Trinkaus and Patel, 2017. PPs from *Ardipithecus* (ARA-VP-1/2677, 6/1006, 6/1005: White et al., 2009), and from Gona (Simpson et al., 2018), and ASI-VP-2/215 (White et al., 2006) have been discussed in print but are not yet described in detail or are too fragmentary to yield the measurements listed above. Additionally, Pablos et al. (2017) referenced 78 proximal pedal phalanges from Sima de los Huesos but measurements are not yet available. PP, proximal phalanx; ML, mediolateral; DP, dorsoplantar.

[a] Estimate that approximates the actual value.

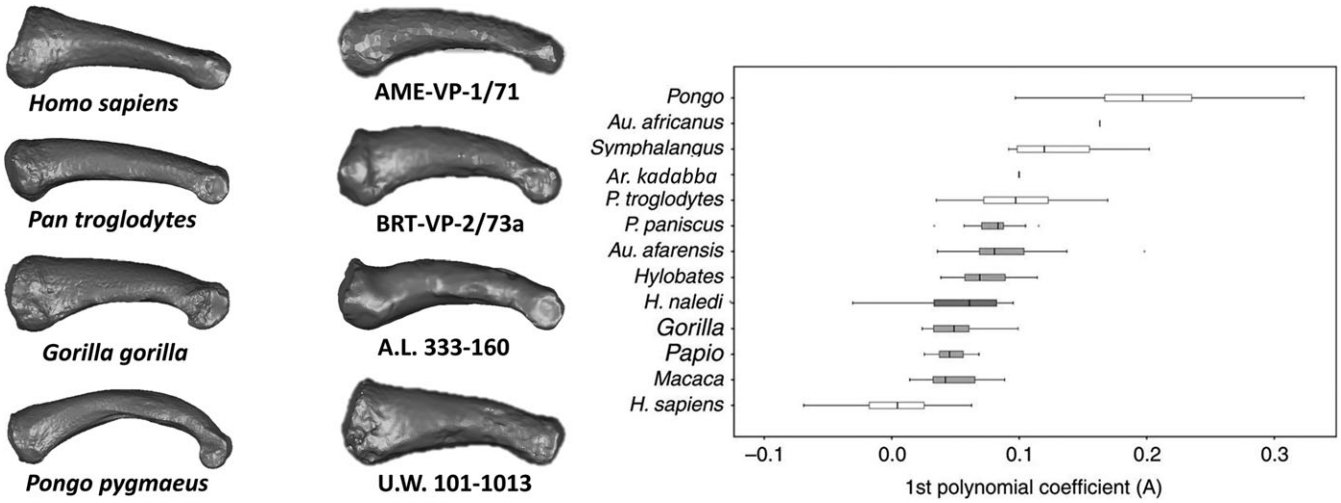

FIGURE 16 Proximal pedal phalanges from a modern human, extant apes, and fossil hominins (all PP4 except U.W. 101-1013 which is from an unknown digit). Note in lateral view that the human proximal pedal phalanx has a dorsally canted base and is relatively straight. While the fossil proximal pedal phalanges also possess dorsally canted bases, they display greater phalangeal curvature. Right: boxplot quantifying phalangeal curvature (from Harcourt-Smith et al., 2015). Boxes span the interquartile ranges, with the horizontal center lines indicating median values. Whiskers indicate sample range. AME-VP-1/71 from *Ar. kadabba*, and A.L. 333-115k are chimpanzee-like in their curvature, whereas the phalanges from *H. naledi* are gorilla-like

in zoo apes that may have been discouraged from climbing (Venkataraman, Kraft, DeSilva, & Dominy, 2013). We regard this as evidence for dorsiflexed ankle vertical climbing in *Ardipithecus ramidus*, an interpretation about *Ardipithecus* climbing behavior that differs from that originally proposed (Lovejoy et al., 2009; White et al., 2009, 2015). We agree with these authors that *Ardipithecus*

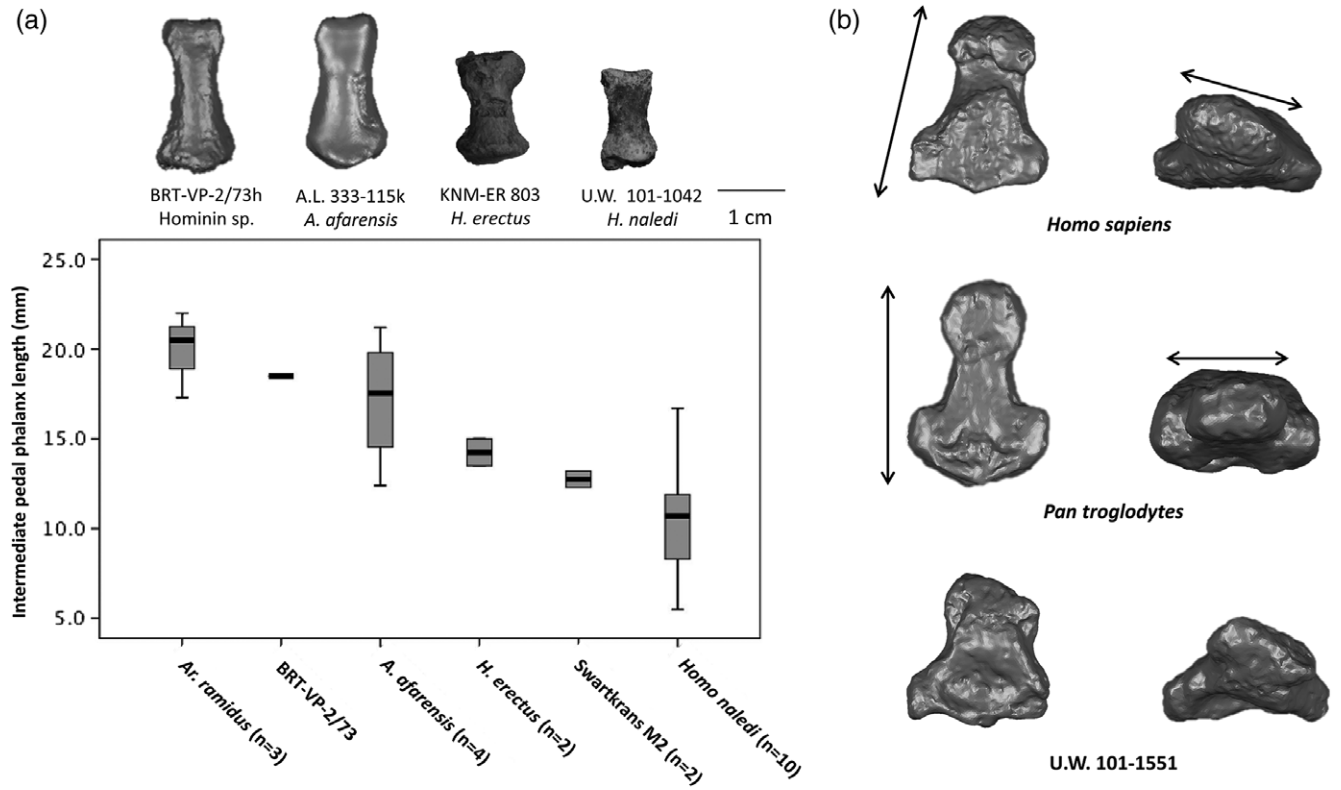

FIGURE 17 (a) Boxplot showing absolute length of intermediate phalanges in different hominins. Boxes span the interquartile ranges, with the horizontal center lines indicating median values. Whiskers indicate sample range. Intermediate phalanges have decreased in both relative and absolute length over evolutionary time (scale bar = 1 cm). This is particularly the case for the lateral digits, which were long in *Ardipithecus*, Burtele, and early *Australopithecus* and have since reduced to square-shape knobs of bone in *H. sapiens*. (b) Distal hallucal phalanges from a human, chimpanzee, and *H. naledi* (scaled to roughly the same mediolateral width). The distal hallucal phalanx is laterally angled (left) in humans compared to the apes, and possesses axial torsion (right)—both anatomies are thought to be associated with medial weight transfer and propulsion from the transverse axis of the foot. Note that U.W. 101-1551 (*H. naledi*) is human-like for both anatomies

TABLE 16 Comparative measurements of the intermediate proximal phalanges in fossil hominins

Accession number	Element	Taxon	Age (Ma)	Length (mm)	Base ML	Base DP	Midshaft ML	Midshaft DP	Head ML	Head DP
ARA-VP-6/500-021	IP4	*Ar. ramidus*	4.4	20.5	10.9	8.8	7.5	5.4	8.2	5.5
ARA-VP-6/500-004	IP5	*Ar. ramidus*	4.4	17.3	9.1	7.6	5.4	4.4	7.0	3.7
ARA-VP-6/500-128	IP3	*Ar. ramidus*	4.4	21.5–22.5	–	–	–	–	8.3	4.9
BRT-VP-2/73h	IP2	Hominin sp.	3.4	18.5	9.3	7.6	5.1	3.9	7.3	4.4
A.L. 333-21a	IP	*A. afarensis*	3.2	21.4	8.2	–	5.6	4.7	7.5	4.7
A.L. 333-21b	IP	*A. afarensis*	3.2	–	7.9	5.3	5.3	4.0	–	–
A.L. 333-w34	IP	*A. afarensis*	3.2	–	7.4	5.3	5.2	4.0	–	–
A.L. 333-115k	IP	*A. afarensis*	3.2	18.9	9.5	7.7	6.5	4.2	8.2	5.1[a]
A.L. 333-115l	IP	*A. afarensis*	3.2	16.5	7.7	7.0	5.2	4.2	7.7	4.5
A.L. 288-1z	IP	*A. afarensis*	3.2	12.5	6.7	5.5	4.6	3.4	5.6	3.6
SKX 344	IP	*Homo?*	1.1–1.7	13.2	8.5	6.7	7.4	4.3	7.5	4.8
SKX 1261	IP	*Homo?*	1.1–1.7	12.3	6.9	5.8	5.5	3.6	6.0	3.3
KNM-ER 803k	IP	*H. erectus*	1.53	13.5	9.0	7.9	5.3	4.5	8.5	6.2
KNM-ER 803l	IP	*H. erectus*	1.53	15.0	8.8	5.1	5.7	4.5	10.2	8.2
ATD6-33	IP	*H. antecessor*	0.77–0.95	14.9	9.6	8.5	7.3	5.6	9.5	5.1
ATD6-34	IP	*H. antecessor*	0.77–0.95	12.7	8.3	7.4	4.6	3.9	8.0	4.6
ATD6-35	IP	*H. antecessor*	0.77–0.95	10.6	7.4	6.6	5.7	4.2	7.7	3.9
U.W. 101-550	IP	*H. naledi*	0.24–0.34	12.7	–	5.6	5.5	3.7	7.1	4.2
U.W. 101-661	IP	*H. naledi*	0.24–0.34	10.6	6.8	4.6	4.5	3.1	5.5	3.9
U.W. 101-988	IP	*H. naledi*	0.24–0.34	11.5	6.8	–	5.1	3.5	6.6	3.5
U.W. 101-1042	IP	*H. naledi*	0.24–0.34	11.9	6.6	5.9	4.4	3.6	6.1	3.8
U.W. 101-1399	IP	*H. naledi*	0.24–0.34	16.7	9.3	6.9	6.0	4.4	7.1	4.3
U.W. 101-1438	IP	*H. naledi*	0.24–0.34	10.8	7.5	6.1	6.0	3.6	6.8	4.1
U.W. 101-1484	IP	*H. naledi*	0.24–0.34	8.6	5.9	4.7	4.7	3.7	5.8	3.5
U.W. 101-1549	IP	*H. naledi*	0.24–0.34	8.3	6.8	5.9	5.0	3.0	6.0	3.8
U.W. 101-1575	IP	*H. naledi*	0.24–0.34	–	–	–	–	–	6.0	3.6
U.W. 101-1587	IP	*H. naledi*	0.24–0.34	5.5	8.0	6.2	6.3	2.9	6.2	3.2
U.W. 101-1591	IP	*H. naledi*	0.24–0.34	–	7.0	6.1	–	–	–	–
U.W. 101-1594	IP	*H. naledi*	0.24–0.34	6.3	4.4[a]	3.1[a]	3.8	2.5	4.3[a]	2.1[a]
U.W. 101-1625	IP	*H. naledi*	0.24–0.34	–	–	–	5.1	3.2	5.2	2.9
Neandertals	IP	*Homo*	0.03–0.2	8.8 ± 1.5 (*n* = 5)	10.2 ± 0.4 (*n* = 6)	8.5 ± 0.6 (*n* = 6)	7.9 ± 0.7 (*n* = 6)	4.7 ± 0.4 (*n* = 6)	9.6 ± 0.4 (*n* = 6)	5.6 ± 0.9 (*n* = 6)
LB1/39	IP	*H. floresiensis*	0.06	14.7	–	–	5.9	–	–	–
LB1/56	IP	*H. floresiensis*	0.06	8.7	–	–	7.2	–	–	–
LB6/15	IP	*H. floresiensis*	0.06	11.1	7.2	–	5.1	–	7.0	–

Note. IP, intermediate phalanx; ML, mediolateral; DP, dorsoplantar. Data in this table from original fossils and measurements reported in Day & Leakey, 1974; Latimer et al., 1982; Susman, 1989; Lorenzo et al., 1999; Jungers, Larson, et al., 2009; Lovejoy et al., 2009; Haile-Selassie et al., 2012; Mersey et al., 2013; Harcourt-Smith et al., 2015. IPs from *Ardipithecus* (ARA-VP-6/1002, 6/1004, 6/500-012: White et al., 2009), Jinniushan (Lu et al., 2011), and 71 intermediate phalanges from Sima de los Huesos (Pablos et al., 2017) have been discussed in print but are not yet described in detail or are too fragmentary to yield the measurements listed above.

[a] Estimate that approximates the actual value.

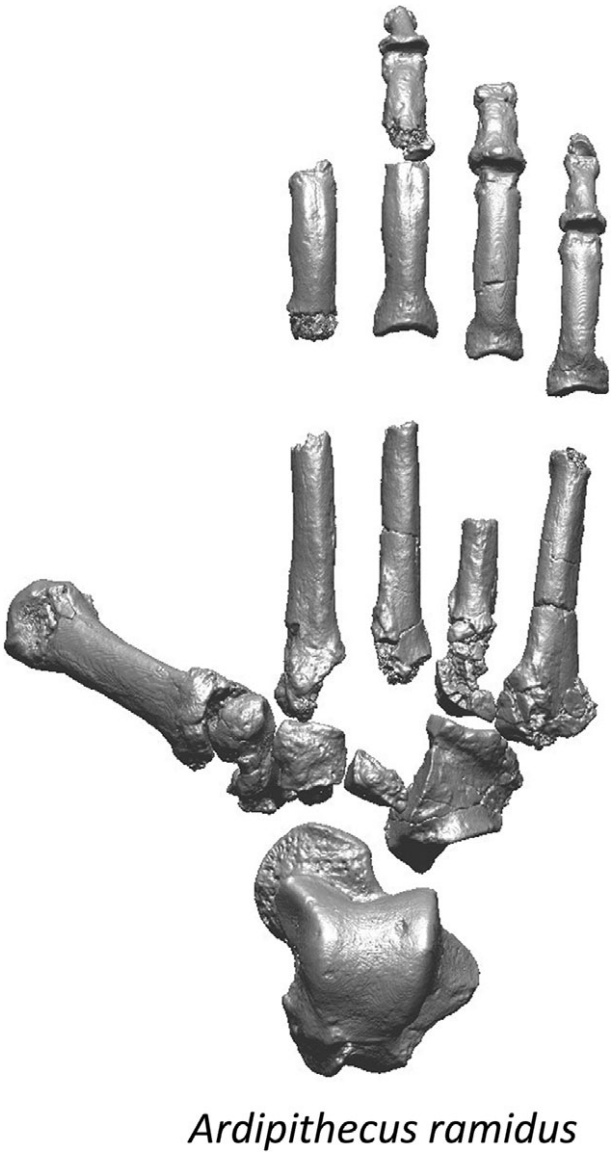

FIGURE 18 Foot of *Ardipithecus ramidus* (ARA-VP-6/500). Notice the ape-like wedging to the talar trochlea, divergent hallux, and long, curved phalanges. However, as in later hominins, the midfoot (cuboid) is proximodistally long. Image courtesy of Tim White and Gen Suwa

walked bipedally on the ground, and that *Ardipithecus* also could adeptly navigate an arboreal environment. The question then is how *Ardipithecus* moved from one substrate to the other. Given that both modern humans (Venkataraman, Kraft, & Dominy, 2013) and African apes (DeSilva, 2009) utilized flexed ankle vertical climbing to move between the forest floor and the canopy, we regard it as reasonable and probable that *Ardipithecus* did the same. Otherwise, it is unclear to us how *Ardipithecus* biomechanically moved from a terrestrial environment to an arboreal one.

The midtarsals of *Ardipithecus ramidus* are intermediate in relative proximodistal length between ape and human. White et al. (2009, 2015) and Lovejoy et al. (2009) interpret these anatomies as evidence that the foot of the last common ancestor was more generalized and that chimpanzees, gorillas, and orangutans have independently foreshortened their midtarsus for foot compliance during arboreal bouts. Others (Holowka & Lieberman, 2018; Pilbeam & Lieberman, 2018; Prang, 2018) interpret these anatomies in *Ardipithecus* as entirely consistent with an intermediate morphology between a chimpanzee-like ancestor and *Australopithecus*.

Qualitatively, the navicular body is *Australopithecus*-like and proximodistally thicker than the navicular body in the apes, but thinner than in modern humans (Lovejoy et al., 2009; Supporting Information Figure S3). Similarly, the cuboid is monkey-like in its relative elongation (Lovejoy et al., 2009; Supporting Information Figure S2; but see Prang, 2018); longer than that found in apes, but shorter than in humans. Lovejoy et al. (2009) note that the cuboid facet for the Mt4 is dorsoplantarly flat and therefore the lateral midfoot is rigid in *Ardipithecus* during bipedal propulsion, to which the authors credit the presence of the os peroneum. The os peroneum is a sesamoid found in the tendon of *M. peroneus longus* (Lovejoy et al., 2009), and in *Ardipithecus* this facet is located in the cuboidal groove (or offset laterally or posterolaterally), as it is in the feet of gibbons and cercopithecoid monkeys. Great apes typically do not have an os peroneum, and Lovejoy et al. (2009) proposed that they independently lost this sesamoid as chimpanzees, gorillas, and orangutans developed more flexible, arboreally adapted, feet. In humans (and OH 8), the os peroneum facet is perched proximolaterally to the cuboidal groove, which lifts the tendon of *M. peroneus longus* out of the cuboidal groove and directs it more obliquely across the midfoot. Lovejoy et al. (2009) described this anatomy in detail and proposed that this change in *M. peroneus longus* tendon orientation was related both to the loss of the divergent hallux and the evolution of the longitudinal arch. Furthermore, Lovejoy et al. (2009) proposed that the repositioning of the os peroneum out of the cuboidal groove was accompanied by the division of the plantar fascia into two components, which became the short plantar ligament and the derived long plantar ligament. Thus, considerable importance was subscribed to the evolution of this sesamoid (Lovejoy et al., 2009).

We agree that the lateral midfoot of *Ardipithecus* was stiff and adapted for bipedal propulsion. The base of the Mt4 (ARA-VP-6/500-103) is dorsoplantarly sinusoidal and does not have the convex shape found in primates (including some humans) with a midtarsal break (DeSilva, 2010; DeSilva et al., 2015). However, we do not think that the os peroneum is solely responsible, nor do we agree that a stiff lateral midfoot is the primitive condition. Monkeys and gibbons have an os peroneum in the cuboidal groove, but as pointed out elsewhere recently (Holowka & Lieberman, 2018; McNutt, Zipfel, & DeSilva, 2018; Pilbeam & Lieberman, 2018) monkeys, and most certainly gibbons (Vereecke & Aerts, 2008), do not have a stiff lateral midfoot and instead both possess a highly mobile tarsometatarsal joint during a midtarsal break (DeSilva, 2010). The os peroneum, by itself, is therefore not sufficient for stiffening the primate lateral midfoot. Furthermore, the base of the Mt4 and the Mt4 facet on the cuboid of Miocene apes (*Ekembo*, *Afropithecus*, and *Nacholapithecus*) is strongly convex/concave (unlike the sinusoidal anatomy found in *Ardipithecus*) and similar instead to that found in all Old World monkeys and apes. This observation is inconsistent with the idea that a stiff lateral midfoot is primitive. Instead, we regard the rigidity in the lateral midfoot of *Ardipithecus* as decidedly derived, and some of the strongest evidence for bipedal locomotion in this early hominin. This raises an

TABLE 17 Comparative measurements of the distal phalanges in fossil hominins

Accession number	Element	Taxon	Age (Ma)	Maximum length	Base ML	Base DP	Midshaft ML	Midshaft DP	Head ML	Head DP
ARA-VP-6/500-037	DiP	*Ar. ramidus*	4.4	13.3	9.3	6.6	–	–	–	–
A.L. 333-115m	DiP5	*A. afarensis*	3.2	–	7.8	7.2	–	–	–	–
StW 617	DiP1	*A. africanus*	2.0–2.6	15.4	13.8	6.4	9.6	4.4	9.5	5.1
OH 10	DiP1	*H. habilis*	1.8	17.5	18.3	–	–	–	–	–
KNM-ER 803m	DiP	*H. erectus*	1.53	9.4	8.6[a]	7.0[a]	4.2	4.3	6.8	3.0
ATD6-36	DiP	*H. antecessor*	0.77–0.95	–	–	–	–	–	8.0[a]	5.4[a]
ATD6-68	DiP	*H. antecessor*	0.77–0.95	11.1	9.1	6.3	5.3	5.0	6.6	5.0
Sima de los Huesos	DiP	*Homo*	0.43	–	–	–	–	–	14.6 ± 2.1 (n = 8)	–
U.W. 101-988	DiP	*H. naledi*	0.24–0.34	8.2	5.7	4.4	4.0	3.2	4.4	2.6
U.W. 101-1010	DiP	*H. naledi*	0.24–0.34	8.6	6.5	5.0	4.1	3.2	4.6	2.8
U.W. 101-1526	DiP	*H. naledi*	0.24–0.34	7.0	5.7	5.2	3.5	3.0	4.1	2.3
U.W. 101-1550	DiP	*H. naledi*	0.24–0.34	7.9	6.8	4.7	3.5	3.6	4.1	2.4
U.W. 101-1551	DiP1	*H. naledi*	0.24–0.34	15.5	–	–	9.5	6.5	–	5.3
U.W. 101-1576	DiP	*H. naledi*	0.24–0.34	4.9	6.5	5.8	6.1	4.3	5.9	3.5
Neandertals	DiP1	*Homo*	0.03–0.2	23.4 ± 1.3 (n = 6)	22.4 ± 4.7 (n = 2)	10.7 ± 2.1 (n = 5)	13.2 ± 2.2 (n = n = 5)	7.5 ± 0.6 (n = 5)	16.0 ± 3.2 (n = 5)	–
Neandertals	DiP2-5	*Homo*	0.03–0.2	11.7 ± 1.0 (n = 12)	10.7 ± 0.9 (n = 10)	8.6 ± 1.3 (n = 11)	6.8 ± 0.8 (n = 10)	6.3 ± 1.0 (n = 12)	9.4 ± 1.2 (n = 11)	–
KHS 1–26	DiP1	*H. sapiens*	0.195	–	11.9	6.6	–	–	–	–
LB1/43	DiP	*H. floresiensis*	0.06	8.5	8.5	–	–	–	–	–
LB1/57	DiP	*H. floresiensis*	0.06	9.8	9.8	–	–	–	–	–

Note. DiP, distal phalanx; ML, mediolateral; DP, dorsoplantar. Data in this table from original fossils and measurements reported in Day & Leakey, 1974; Trinkaus, 1975; Latimer et al., 1982; Day, 1986; Lorenzo et al., 1999; Pearson et al., 2008; Jungers, Larson, et al., 2009; Lovejoy et al., 2009; Mersey et al., 2013; Harcourt-Smith et al., 2015. DiPs from *Ardipithecus* (ARA-VP-6/500-033, -052, -099, 6/1008, 6/1009: White et al., 2009), Dmanisi (D2670 and D3877; Lordkipanidze et al., 2006; Patel et al., 2015), Jinniushan (Lu et al., 2011) have been discussed in print but are not yet described in detail or are too fragmentary to yield the measurements listed above.

[a] Estimate that approximates the actual value.

important question: if the os peroneum is not responsible for stiffening the lateral midfoot, what is? Holowka and Lieberman (2018) hypothesize that the *Ardipithecus* foot stiffened during push-off by contracting intrinsic foot muscles. We hypothesize (McNutt, Zipfel, & DeSilva, 2018) that the evolution of a long plantar ligament, which spans from the distal calcaneus to the lateral metatarsal bases and is absent in the ape foot (Gomberg, 1985), may have been one of the first anatomical innovations in the earliest upright walking hominins, and was central for stiffening the lateral midfoot during early hominin bipedal propulsion.

The medial cuneiform of ARA-VP-6/500 is crushed, but preserves enough of the distal articular surface to show that *Ardipithecus* had an ape-like grasping hallux (Figure 8). This anatomy of the medial cuneiform complements the deeply concave and sigmoidal proximal facet of the Mt1 (Lovejoy et al., 2009). The distal head lacks the dorsal doming found in some *Australopithecus* Mt1s (e.g., A.L. 333-115 and StW 562), and is similar instead to StW 595 and the Mt1 from the Burtele foot (Haile-Selassie et al., 2012). The *Ardipithecus* Mt1 head is divided dorsally by a nonsubchondral isthmus, which functionally delineates internal rotation of the hallucal proximal phalanx during arboreal grasping and external rotation during terrestrial propulsion (Lovejoy et al., 2009). In general, many aspects of the medial foot of *Ardipithecus* (talus, medial cuneiform, and Mt1) are quite ape-like and reflect the importance of arboreality, including vertical climbing (e.g., Wunderlich & Ischinger, 2017) to this early hominin.

The Mt2 (ARA-VP-6/1000) has a dorsoplantarly tall base relative to the length of the bone (Lovejoy et al., 2009), making its proportions even more human-like than the Mt2 from Burtele (Haile-Selassie et al., 2012) or StW 89 from Sterkfontein Member 4 (DeSilva, Proctor, & Zipfel, 2012). However, relative to the mediolateral width of the base, the dorsoplantar base of *Ardipithecus*, Burtele, and the South African australopiths are all ape-like (McNutt, Zipfel, & DeSilva, 2018). There is internal torsion of the Mt2 shaft, consistent with hallucal grasping in *Ardipithecus* (Lovejoy et al., 2009). Additionally, the dorsum of the base of the Mt2 possesses paired chondral invaginations hypothesized to be caused by pressure from the joint capsule during foot inversion (during climbing) and eversion (during walking; Lovejoy et al., 2009). The explanation is reasonable to us; however, as we noted earlier, these paired chondral invaginations are also present on the base of the Mt2 and Mt3 in *Ekembo* and *Afropithecus*, indicating that they alone are not indicators of bipedality. Though there is no Mt2 head yet known from *Ardipithecus*, Lovejoy et al. (2009) hypothesized that the Mt2 is the primary axis of propulsion during bipedal gait.

Laterally, the foot of *Ardipithecus* becomes more and more derived and *Australopithecus*-like. The Mt3 (ARA-VP-6/505) has a human-like, dorsoplantarly tall base relative to the length of the bone (Lovejoy et al., 2009) and relative to the mediolateral width of the base (McNutt, Zipfel, & DeSilva, 2018). A dorsoplantarly tall base is found in all hominin Mt3s and is probably a hominin synapomorphy (McNutt, Zipfel, & DeSilva, 2018; Figure 13). Distally, the head is dorsally domed, signifying phalangeal dorsiflexion during bipedal propulsion along the oblique axis of the foot (Lovejoy et al., 2009). However, unlike in later hominins, the Mt3 head exhibits only weak external torsion (Lovejoy et al., 2009), which would be consistent with the absence of a longitudinal arch in the *Ardipithecus* foot (Drapeau & Harmon, 2013; Lovejoy et al., 2009). Additionally, the Mt3 lacks any tubercle or rugosity along the lateral shaft that binds the Mt3 and lateral metatarsals into a rigid unit as is found in later hominins. As discussed earlier, the base of the cuboid facet of the fragmentary Mt4 is sinusoidal/flat and consistent with the absence of a midtarsal break in *Ardipithecus*.

Ardipithecus proximal and intermediate phalanges are long and *Gorilla*-like (Lovejoy et al., 2009). Phalangeal curvature is described as "moderate to large" (Lovejoy et al., 2009), reflecting the importance of arboreality to this early hominin. However, the bases of the phalanges are dorsally canted, which is functionally consistent with domed metatarsal heads and terrestrial bipedality (Lovejoy et al., 2009).

The 4.4 Ma *Ardipithecus ramidus* foot from Aramis, Ethiopia presents the paleoanthropological community with its first glimse of a pre-*Australopithecus* foot. In general, the medial foot is primitive, with a grasping hallux and ape-like talus. However, laterally, the foot is more derived, with evidence for a rigid tarsometarsal joint and bipedal propulsion along the oblique axis of the foot. Thus, the anatomy of the *Ardipithecus* foot suggests that, in general, the lateral aspect of the foot evolved bipedal adaptations before the medial (Fernández et al., 2016, 2018; Kidd, 1999; Lovejoy et al., 2009; Zipfel et al., 2009), a model that we also currently endorse (McNutt, Zipfel, & DeSilva, 2018).

However, recent discoveries have complicated this presentation of *Ardipithecus ramidus* foot anatomy. Simpson et al. (2018) announced a 4.3–4.6 Ma partial skeleton (GWM67/P2) of *Ardipithecus ramidus* from the Gona study area of Ethiopia. The foot of the Gona *Ardipithecus* includes a talus, fragmentary calcaneus, lateral cuneiform, distal Mt1, proximal Mts3–4, and pedal phalanges. As with the Aramis *Ardipithecus* foot skeleton, the Mt3 base is dorsoplantarly tall and the Mt4 base is dorsoplantarly tall and flat (Simpson et al., 2018), consistent with midfoot rigidity and the absence of a midtarsal break. Additionally, as in *Australopithecus*, the Mt4 is recessed into the tarsal row and the lateral cuneiform is proximodistally elongated (Simpson et al., 2018). However, the Mt1 head of the Gona foot is dorsoplantarly taller than the Aramis *Ardipithecus* or Burtele Mt1 (Simpson et al., 2018). Additionally, the Gona talus has a human-like talar axis angle, indicating that the foot was positioned in an everted set, and not as inverted as in the Aramis *Ardipithecus* individual (Simpson et al., 2018). The more human-like talar axis angle is a result of an elevated medial trochlear rim, which is distinctly different from the talar morphology in ARA-VP-6/500-023 (Simpson et al., 2018). While these differences could be interpreted as reflecting normal intraspecific variation, we are struck by differences in the Aramis and Gona *Ardipithecus* foot skeletons that have been hypothesized to have functional importance. It appears to us, therefore, that the Aramis *Ardipithecus* and Gona *Ardipithecus* would have walked in quite different ways, on quite different feet. The Aramis *Ardipithecus* would have walked on a more inverted foot and pushed off the oblique axis, utilizing the Mt1 primarily for grasping. The Gona *Ardipithecus* probably would have been a much better bipedal walker—landing on a more human-like, everted foot, and possibly even transferring weight medially toward the hallux during bipedal propulsion in a more australopith-type manner. It is difficult to know how to interpret this

variation at the current time. A future study should closely compare the similarities and differences in functional anatomy between not only the Aramis *Ardipithecus* and Gona *Ardipithecus*, but also the Burtele foot and Hadar material assigned to *A. afarensis*.

3.4 | *Australopithecus anamensis* (Asa Issie, Ethiopia; Kanapoi, Kenya; 4.1–4.2 Ma)

It is probable that key pedal adaptations occurred during the transition of *Ardipithecus* (or an *Ardipithecus*-like hominin) to *Australopithecus*. Unfortunately, frustratingly little is known about the foot anatomy of the earliest known *Australopithecus*, *A. anamensis*. There is an Mt2 shaft (ASI-VP-2/1) and a broken proximal foot phalanx (ASI-VP-2/215) from Asa Issie, Ethiopia, but both fossils are too fragmentary to yield much functional information (White et al., 2006). Therefore, the only fossil that currently yields any functional information about the *A. anamensis* foot is not even from the foot. KNM-KP 29285 is a tibia recovered in two pieces (proximal and distal) from 4.12 Ma deposits at Kanapoi, Kenya (Leakey, Feibel, McDougall, & Walker, 1995; Ward, Leakey, & Walker, 2001). Because the articular surface of the distal tibia mirrors the talar trochlea, and the *A. anamensis* talar articular surface is keeled, we can infer that the talus would possess a deep groove along the midline of the trochlea. Additionally, the talar articular suface is square-shaped, and lacks the mediolateral expansion of the distal (anterior) rim found in apes. It is probable, therefore, that the talus was not wedged in *A. anamensis* making it distinct from the talus in *Ardipithecus* and more like the talus in *A. afarensis* (DeSilva, 2009). Functionally, the absence of talar wedging implies that *A. anamensis* did not habitually load its ankle in dorsiflexion, as apes do and *Ardipithecus* probably did during vertical climbing bouts. Finally, the plane of the ankle joint is perpendicular to the long axis of the shaft, as is found in modern humans and in other *Australopithecus* fossils (Ward et al., 2001). This anatomy is correlated with a low talar axis angle, and functionally positions the foot in a human-like everted position directly under a valgus knee (DeSilva, 2009). In contrast, modern apes and the Aramis *Ardipithecus* foot possessed a high talar axis angle (Lovejoy et al., 2009) and an inverted set to the ankle joint.

Many questions remain about the foot of *A. anamensis* and in general about the foot of the earliest *Australopithecus*. Did they still possess an *Ardipithecus* or Burtele-like divergent hallux, or a more *Australopithecus*-like adducted hallux? Was the calcaneus adapted for heel-striking bipedalism as found in later *A. afarensis*, or was it more gracile and *A. sediba*-like? Additional fossil discoveries will be required to characterize this important transition from a more primitive *Ardipithecus*-like foot to a more derived *Australopithecus*-like one.

3.5 | Burtele foot (Woronso-Mille, Ethiopia; 3.4 Ma)

The Burtele foot (BRT-VP-2/73) was found in 3.4 Ma deposits in the Woronso-Mille study area of Ethiopia (Haile-Selassie et al., 2012). The partial foot skeleton consists of a complete Mt1, Mt2, and Mt4, an Mt3 head, and four phalanges (PP1, PP2, PP4, and IP2). While BRT-VP-2/73 was found in close proximity to craniodental fossils assigned to the newly named Pliocene hominin *A. deyiremeda* (Haile-Selassie et al., 2015), great care was taken to not directly attribute this foot to that taxon (Haile-Selassie et al., 2015). We thus review the functional anatomy of the Burtele foot without a taxonomic assignment. It is possible that this foot belongs to an early australopith like *A. deyiremeda*, but it is also possible that this foot is sampling a late occurring *Ardipithecus*. It is clearly not from *A. afarensis* (Figure 19), indicating that there were at least two forms of bipedal walking coexisting in the Pliocene of Eastern Africa (Haile-Selassie et al., 2012). Anatomies discussed below are based on Haile-Selassie et al. (2012) and observations we made on the original Burtele foot fossil.

Although the medial cuneiform was not discovered, the base of the Mt1 is concave and sigmoidal, as it is in apes and in *Ardipithecus ramidus* (Haile-Selassie et al., 2012). Additionally, the medial cuneiform facet is angled relative to the long axis of the Mt1 shaft, causing the Mt1 to deviate medially relative to the proximal facet. These anatomies together are evidence that the Burtele foot possessed at least a moderately abducent hallux and some grasping ability with the big toe. Relative to the other complete metatarsals (Mt2 and Mt4), the Mt1 is quite short and ape like in metatarsal proportions (Haile-Selassie et al., 2012). Additionally, the Mt1 shaft is gracile, lacking the dorsoplantarly expanded shaft found in humans and other hominins (McNutt, Zipfel, & DeSilva, 2018; Figure 11). This anatomy, combined with the absence of a dorsally domed Mt1 head indicate that the Burtele individual did not use the first digit during bipedal propulsion and instead pushed off the oblique axis of the foot (Haile-Selassie et al., 2012). The shape of the Burtele Mt1 head is strikingly different from the Mt1 of *A. afarensis*. The *A. afarensis* Mt1 head is tall, domed and mediolaterally tapers dorsally. The Burtele Mt1 head is short and not domed, but remains mediolaterally expanded dorsally (Figure 19).

The Mt2 (BRT-VP-2/73b) is curved in both the sagittal plane and the transverse plane. Internal head torsion (23°) and transverse plane curvature help position the Mt2 head in opposition to the Mt1—adaptations for pedal grasping. The base of the Mt2 is dorsoplantarly short relative to the ML width of the base, making it ape-like and similar to what is found in the Mt2 bases from Sterkfontein, South Africa, but not *A. afarensis* (Haile-Selassie et al., 2012; McNutt, Zipfel, & DeSilva, 2018; Figure 12). Relative to the overall length of the bone, the Mt2 base is dorsoplantarly shallow, making it more ape-like than even the *Ardipithecus ramidus* Mt2 (Lovejoy et al., 2009).

The Mt4 (BRT-VP-2/73a) is the longest of the metatarsals, which is unlike the anatomy found in apes or humans and instead recalls the condition in early Miocene hominoids like *Ekembo* (Haile-Selassie et al., 2012). The Mt4 base is damaged, but is dorsoplantarly flat, indicating that the Burtele foot was stiffened laterally and probably did not have a midtarsal break. As in other hominins (e.g., Ward et al., 2011), but also cercopithecoids (Drapeau & Harmon, 2013), the Mt4 exhibits strong external torsion of the head relative to the shaft (Haile-Selassie et al., 2012).

All three lateral metatarsal heads (Mts2–4) are dorsally domed and possess a sulcus proximal to the head, consistent with lateral digit dorsiflexion during bipedal propulsion using the oblique axis of the foot (Haile-Selassie et al., 2012). The linear dimensions of the lateral metatarsal heads of the Burtele foot are quite similar to the dimensions of the *A. afarensis* forefoot (A.L. 333-115; Tables 9–11). What

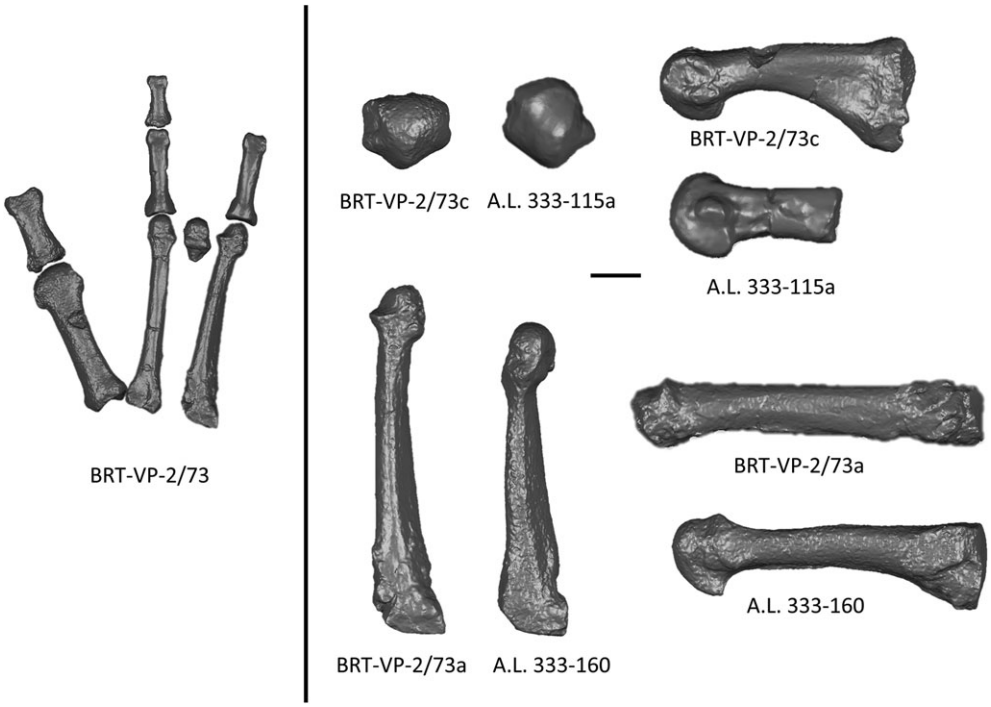

FIGURE 19 BRT-VP-2/73: a 3.4 Ma partial forefoot preserving Mt1-4, PP1-2,4, and IP2. While overlapping in time with *A. afarensis*, this foot is morphologically (and functionally) quite different. Notice the slightly divergent hallux (left). Right: compared with *A. afarensis* (A.L. 333-115 [mirrored to reflect right side]), the BRT Mt1 head is dorsoplantarly squat and is not dorsally domed. The Mt4 from BRT is long, gracile, and has weak dorsal doming of the head. The Mt4 from *A. afarensis* (A.L. 333-160 [mirrored to reflect right side]) is short, robust, and possesses both a dorsoplantarly tall base and a dorsally domed head. Scale bar = 1 cm

differ between these two feet are the relative size of the Mt1 head (dorsoplantarly much taller in *A. afarensis*) and the dimensions of the Mt bases, which are dorsoplantarly tall in *A. afarensis* and short and more ape-like in the Burtele foot.

The phalanges of the Burtele foot are similar to those found in *Ar. ramidus* and *A. afarensis* (Figures 16 and 17). They are relatively long (though shorter than chimpanzee pedal phalanges) and their curvature values are similar to those calculated for *A. afarensis* and within the lower range of modern chimpanzees (Haile-Selassie et al., 2012). Unlike in apes, the bases are dorsally canted which, combined with the domed metatarsal heads, form a functional complex consistent with dorsiflexion of the toes on the fixed metatarsal heads during the push-off phase of bipedal locomotion (Haile-Selassie et al., 2012; Latimer & Lovejoy, 1990a, 1990b).

The Burtele foot thus presents evidence for a hominin utilizing the medial forefoot for pedal grasping in an arboreal context, and the lateral forefoot for bipedal propulsion. In this way, the foot appears functionally similar to that described for the geologically older *Ar. ramidus* (Lovejoy et al., 2009). It is possible that the Burtele foot is a late occurring *Ardipithecus*—it will be important to systematically compare the Burtele foot to the pedal remains from both Aramis (Lovejoy et al., 2009) and Gona (Simpson et al., 2018). However, while the Burtele foot is broadly similar to *Ardipithecus*, there are important differences as well. While the Mt2 is proposed as the main axis of propulsion for the *Ardipithecus* foot (Lovejoy et al., 2009), in Burtele it is the Mt4 (Haile-Selassie et al., 2012). Anatomically related to this functional interpretation is the height of the base of the Mt2, which is dorsoplantarly tall relative to the estimated length of the bone in *Ardipithecus* and within the modern human distribution (Lovejoy et al., 2009), but is quite short in the Burtele foot, outside the human range and instead is chimpanzee-like (Haile-Selassie et al., 2012). The Burtele foot lacks the nonsubchondral isthmus separating the Mt1 head into distinct facets for walking and climbing in *Ardipithecus* (Lovejoy et al., 2009), a curious absence given that the Burtele foot is reconstructed as one performing both functions. Similarly, the paired chondral invaginations found on the dorsum of the base of the Mt2 in *Ardipithecus* and suggested to form as a result of pressure from the joint capsule during internal rotation (climbing) and external (walking; Lovejoy et al., 2009) are absent from the Burtele Mt2 (Haile-Selassie et al., 2012). Finally, the Mt1 head of the Gona *Ardipithecus* is dorsoplantarly taller than even the Burtele Mt1 (Simpson et al., 2018), making that *Ardipithecus* specimen more *Australopithecus*-like than the Burtele foot in this regard.

To further complicate matters, Haile-Selassie et al. (2012) calls attention to similarities between the Burtele foot and pedal fossils from South African australopiths—specifically the Mt1s StW 595 and the Mt2 StW 89 (discussed later in this review). We agree that these bones are remarkably similar to one another and suggest that future work continue to explore the uncanny resemblances between these foot fossils found 6,000 km apart in space and ~1 Ma apart in time from one another. Ultimately, the Burtele foot is a stunning discovery that reveals pedal diversity in the Pliocene and raises important questions about foot variation and function early in hominin evolution.

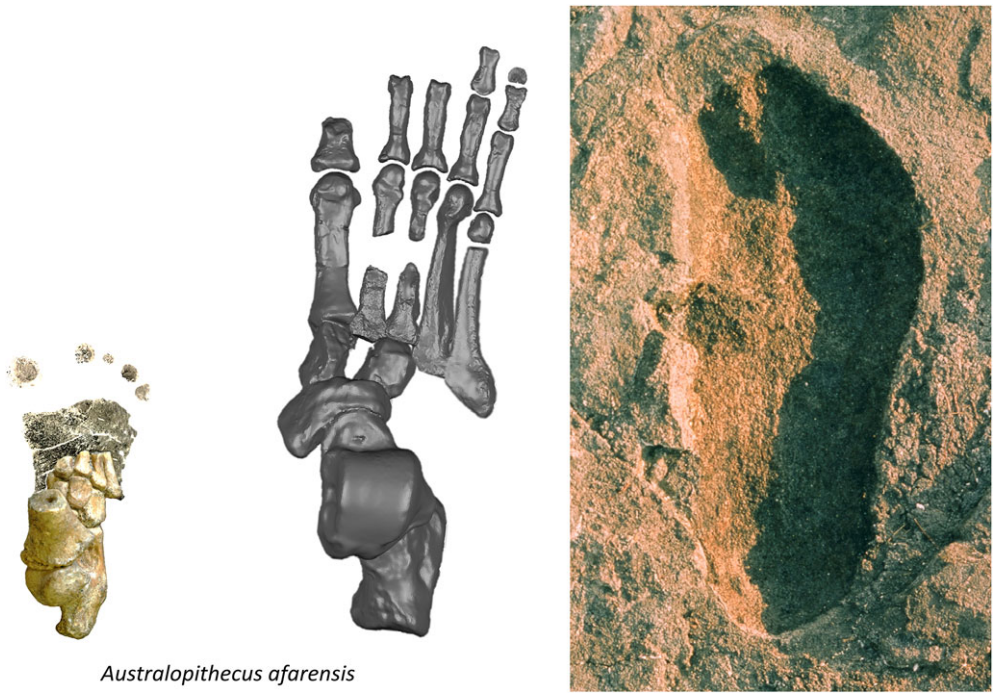

FIGURE 20 Foot of *Australopithecus afarensis*. Left: 3.32 Ma juvenile foot of DIK-1-1f (DeSilva, Gill, et al., 2018; mirrored to reflect right side) superimposed on a similarly sized footprint of a young modern *H. sapiens*. Middle: Composite foot skeleton from the Hadar 333 locality; any bones from the left side are reflected so that they all appear from a right foot. The bones of the forefoot (A.L. 333-115) are all associated and appear together except the Mt4, which has been replaced with the more complete A.L. 333-160, size-scaled to match Mt4 head dimensions of A.L. 333-115d. Other size-scaled elements are: calcaneus (A.L. 333-8), talus (A.L. 333-147), navicular (A.L. 333-36), medial cuneiform (A.L. 333-28), lateral cuneiform (A.L. 333-79), Mt1 base (A.L. 333-54), Mt2 base (A.L. 333-133), and Mt3 base (A.L. 333-157). Some of these elements probably belong to the same individual (see text). Notice the human-like rearfoot and midtarsal region, but long, lateral phalanges. Far right is a footprint often attributed to *A. afarensis* from the Laetoli G site. Photo by John Reader, courtesy of Science Photo Library

3.6 | *Australopithecus afarensis* (Hadar and Dikika, Ethiopia; Laetoli, Tanzania; 3.0–3.6 Ma)

The *Australopithecus afarensis* foot is the best-known early hominin foot (DeSilva, Gill, et al., 2018; Latimer et al., 1982; Ward et al., 2012). In fact, foot elements are not as well represented in a hominin taxon until the 430 kyr material from Atapuerca, Spain. All of the adult tarsals are represented except for the cuboid and the intermediate cuneiform; though these are known from the juvenile Dikika foot (DeSilva, Gill, et al., 2018). All metatarsals are represented, as are the phalanges, except for a few intermediate and distal phalanges. Both juvenile and adult elements are known, making it possible to characterize ontogenetic development of the foot in this taxon (DeSilva, Gill, et al., 2018). Futhermore, the G and S trails from Laetoli are generally attributed to *A. afarensis* (Day & Wickens, 1980; Masao et al., 2016; White & Suwa, 1987), giving researchers another tool for connecting foot form to function in this taxon (Figure 20).

However, interpretations of the *A. afarensis* pedal remains have been quite contentious, primarily pitting Stony Brook University anatomists Jack Stern and Randy Susman (Stern, 2000; Stern & Susman, 1983, 1991; Susman et al., 1984; Susman, Stern, & Jungers, 1985) against Cleveland Museum of Natural History and Kent State University anthropologists Owen Lovejoy and Bruce Latimer (Latimer, 1991; Latimer et al., 1987; Latimer & Lovejoy, 1989, 1990a, 1990b). Interpretations of the Hadar fossils and Laetoli footprints became quite polarized with the Stony Brook group emphasizing primitive, ape-like anatomies and the Ohio-based team highlighting the derived, human-like anatomies in *A. afarensis*. Ward (2002) noted that these teams were asking different questions of the fossils—Stern and Susman using anatomy to reconstruct the daily life of *A. afarensis* and Latimer and Lovejoy using this same anatomy to infer the direction of selection on the early hominin skeleton. Yet, these teams also have produced quite different reconstructions of arboreal tendencies and gait mechanics in *A. afarensis*. Anatomies discussed below are based on Latimer et al. (1982), Ward et al. (2012), and our studies of the original fossil material.

Although many of the foot bones from *A. afarensis* were found in isolation, some associated foot elements exist. A.L. 288-1 (Lucy) preserves a talus, proximal phalanx, and intermediate phalanx (Johanson et al., 1982). The A.L. 333-115 forefoot preserves the distal heads of all five metatarsals, all five proximal phalanges, intermediate phalanges 4 and 5, and a fragmentary distal phalanx 5 (Latimer et al., 1982). The juvenile Dikika foot preserves all 7 tarsals and the bases of all 5 metatarsals (Alemseged et al., 2006; DeSilva, Gill, et al., 2018). Based on congruent joint surfaces and a shared patina, the following associations are also proposed:

- A.L. 333-75 (talar head) and A.L. 333-47 (navicular)
- A.L. 333-36 (navicular) and A.L. 333-28 (medial cuneiform)
- A.L. 333-79 (lateral cuneiform) and A.L. 333-133 (Mts 2 and 3)

The calcaneus of *A. afarensis* is known from three adult fossils (A.L. 333-8, -37, -55) from Hadar, Ethiopia (Latimer et al., 1982;

Latimer & Lovejoy, 1989) and the juvenile DIK-1-1f (DeSilva, Gill, et al., 2018). It is possible that A.L. 333-8 and A.L. 333-55 are antimeres (Boyle et al., 2018). The general geometry of the proximal tuber is human-like, with a plantarly positioned lateral plantar process (Boyle et al., 2018; Latimer & Lovejoy, 1989). The lateral plantar process itself is relatively small (Stern & Susman, 1983), though this is probably a product of the small size of *A. afarensis* since the lateral plantar process size correlates with body weight in modern humans (Gill, Taneja, Bredella, Torriani, & DeSilva, 2014). Of presumed functional importance is the volume of the proximal tuber of the calcaneus in *A. afarensis*, which is human-like (Latimer & Lovejoy, 1989; Prang, 2015a; Zipfel et al., 2011) and evidence for heel-striking adaptations in this taxon. However, the calcaneus of the juvenile from Dikika is gracile and chimpanzee-like, indicating that the human-like robusticity happened developmentally in *A. afarensis* (DeSilva, Gill, et al., 2018). This change in calcaneal robusticity is in stark contrast to the growth of the calcaneus in humans, which is already robust at birth and maintained during development (DeSilva, Gill, et al., 2018). Thus, although both humans and *A. afarensis* have robust calcaneal tubers, they are acquired in developmentally different ways. This finding could imply canalization of this feature in later hominins, or homoplasy in calcaneal robusticity in *Homo* and *A. afarensis*.

The calcaneus of *A. afarensis* is human-like in other respects as well. The medial plantar process is flat in both the adults and the juvenile fossil, and lacks the breaking found in apes, atelines, *A. sediba* and the Omo calcaneus. The insertion for the Achilles tendon appears chimpanzee-like (Bramble & Lieberman, 2004); however, the large facet for the retrocalcaneal bursa makes it possible that *A. afarensis* instead had a long Achilles tendon, more like that of humans than that of apes (McNutt & DeSilva, 2016). The anterior talar facet of the *A. afarensis* calcaneus is relatively flat and human-like (Latimer & Lovejoy, 1989; Prang, 2016b; Zipfel et al., 2011), indicating reduced mobility at the subtalar joint compared with apes and with the South African australopiths (Prang, 2016b). A 3D geometrics morphometrics analysis of the hominoid calcaneus found that the most complete *A. afarensis* specimens (A.L. 333-8, -55) fall within the range of modern humans in general morphology (McNutt, Zipfel, & DeSilva, 2018; Figure 2).

However, the *A. afarensis* calcaneus also possesses some primitive, ape-like features as well (Deloison, 1985). The peroneal trochlea is large and projecting in both the juvenile foot and the adult calcanei (Figure 2), suggesting an important role for the peroneal musculature (Stern & Susman, 1983). The insertion for the calcaneofibular ligament manifests as a large, circular pit, as it does in apes. The distal and proximal portions of the bone are offset, with the distal portion angled medially relative to the proximal; this inflection happening at the peroneal trochlea (Deloison, 1985; Figure 3). This ape-like bend in the calcaneus is present in the juvenile from Dikika as well (DeSilva, Gill, et al., 2018). Finally, although the calcaneocuboid joint is not preserved in the adult calcanei (Latimer et al., 1982) and remains obscured in the Dikika foot (DeSilva, Gill, et al., 2018), enough of this region is preserved in A.L. 333-8 to infer a more ape-like pivot for the beak of the cuboid and more calcaneocuboid mobility than in modern humans, as suggested elsewhere (Gomberg & Latimer, 1984).

There are three adult tali from *A. afarensis*: the relatively complete A.L. 288-1, A.L. 333-147, and the fragmentary talar head A.L. 333-75 (Johanson et al., 1982; Latimer et al., 1982, 1987; Ward et al., 2012). These bones are generally found to be quite human-like: 3D geometric morphometric analyses position the *A. afarensis* tali within the shape space of modern humans (DeSilva, Carlson, et al., 2018; Harcourt-Smith, 2002). However, in a study of articular facet orientations, Parr et al. (2014) found the A.L. 288-1 fossil to fall outside the modern human distribution, implying different talar (and subsequently foot) geometry in *A. afarensis*. The talar axis angle is human-like (DeSilva, 2009) and indicates that *A. afarensis* possessed an everted foot and a tibia that moved vertically over a fixed foot during bipedal locomotion, as it does in humans (Latimer et al., 1987). The talar body lacks the extreme wedging and distal mediolateral expansion of the trochlea found in *Ardipithecus* and in modern apes, indicating that *A. afarensis* did not load its ankle in habitual dorsiflexion (DeSilva, 2009; Figure 4). Stern and Susman (1983) noted that the talar trochlea is distally prolonged in A.L. 288-1 suggesting that *A. afarensis* had ape-like ankle joint mobility; however the much larger talus A.L. 333-147 demonstrates that the subtended angle of the talar trochlea is a function of size (Ward, 2002; Ward et al., 2012). Nevertheless, the horizontal angle of the talar head and neck, torsion angle, and declination angles are all low and more ape-like (Prang, 2016b; Zipfel et al., 2011; Parr et al., 2014; Figure 5; Table 3), suggesting that the transverse tarsal joint may have had more mobility and the longitudinal arch may have been lower in *A. afarensis* than in modern humans. However, Prang (2015a) found that when articulated together, the facet angulation of the calcaneus and talus of *A. afarensis* angled in a more human-like way, and suggested that *A. afarensis* had at least a partially arched foot. The plantar portion of the talar heads all possess a smooth, triangular impression marking the plantar calcaneonavicular (spring) ligament, which supports the talus in an arched foot (Lamy, 1986; Latimer et al., 1982).

There are two naviculars known from the Hadar *A. afarensis* assemblage: A.L. 333-36 and A.L. 333-47 (Latimer et al., 1982). Both fossils possess a large, ape-like navicular tuberosity (Harcourt-Smith & Aiello, 2004; Figure 6). The body of the navicular is proximodistally thicker than in chimpanzees, but thinner than in modern humans (Harcourt-Smith, 2002), similar to the anatomy in *Ardipithecus* (Lovejoy et al., 2009). Susman (1983) noted that the *A. afarensis* naviculars are plantarly expanded where the plantar calcaneonavicular and cubonavicular ligaments insert, suggesting a well-supported medial midfoot. Additionally, these naviculars both possess large cuboid facets, which are typical in apes, and can occur in the human foot. However, this facet is typically much smaller in humans (and fossil *Homo*) than in the *A. afarensis* naviculars (Trinkaus, Wojtal, Wilczyński, Sázelová, & Svoboda, 2017). Sarmiento and Marcus (2000) proposed that the large cuboid facet on the navicular is evidence for foot inversion during vertical climbing in *A. afarensis*. A geometric morphometrics analysis of the Hadar naviculars found them to be intermediate between African ape and human, with the large navicular tuberosity evidence for medial weight bearing and therefore the absence of a longitudinal arch (Harcourt-Smith, 2002; Harcourt-Smith & Aiello, 2004). Berillon (2003, 2004) reached a similar conclusion based on

the ape-like angulation of the cuneiform facets on the Hadar naviculars. However, Prang (2016a, 2016b, 2016c) found the Hadar fossils to be more human-like, and questioned the relationship between navicular tuberosity size and arch development, suggesting instead that navicular tuberosity size was related to the *M. tibialis posterior*.

The cuboid and intermediate cuneiform are unknown in adult *A. afarensis*. A fragmentary cuboid (Gomberg & Latimer, 1984) has since been identified as nonhominin (Latimer, pers. comm.); we were unable to locate the original specimen in the National Museum of Ethiopia. These elements are therefore only known from the juvenile Dikika foot (DeSilva, Gill, et al., 2018). Both the cuboid and the intermediate cuneiform are dorsoplantarly long relative to their mediolateral width, as found in juvenile humans (DeSilva, Gill, et al., 2018) and indicative of an elongated midtarsus. The juvenile lateral cuneiform, however, is shorter dorsoplantarly, closer to the chimpanzee condition (DeSilva, Gill, et al., 2018). Yet, the adult lateral cuneiform (A.L. 333-79) is human-like in its proportions (Latimer et al., 1982; DeSilva, Gill, et al., 2018; Figure 10). Plantarly, the lateral cuneiform has a well-developed hamulus. Several scholars have noted that A.L. 333-79 has a plantar groove for the tendon of *M. peroneus longus*, which would indicate the absence of a human-like transverse arch (Sarmiento & Marcus, 2000; Ward et al., 2011). However, our observation of the original fossil reveals that although the hamulus is present and pronounced, there is damage precluding an assessment of the *M. peroneus longus* tendon groove.

Of great importance for interpreting the functional anatomy of the *A. afarensis* foot is a fragmentary medial cuneiform, A.L. 333-28. The specimen preserves the plantar two-thirds of the bone, but unfortunately the dorsal third has sheared away and there is erosion along the lateral rim of the Mt1 facet. The Mt1 facet was originally described as "markedly convex" (Latimer et al., 1982), which led to suggestions that *A. afarensis* had a mobile, perhaps even grasping, hallux (Stern & Susman, 1983; Susman et al., 1984). Quantification of the Mt1 facet reveals it to be more convex than modern human medial cuneiforms and slightly less convex than modern apes (Gill et al., 2015). The medial cuneiform of the Dikika juvenile is similarly convex (DeSilva, Gill, et al., 2018). However, the angulation of the Mt1 facet in A.L. 333-28 is more human-like, distally oriented, rather than medially oriented as it is in the apes (Berillon, 1999; Gill et al., 2015; Latimer & Lovejoy, 1990a); the facet angulation in the Dikika juvenile is more intermediate between apes and humans (DeSilva, Gill, et al., 2018). A.L. 333-28 is quite robust plantarly, which suggested to Sarmiento and Marcus (2000) that the medial cuneiform was weight-bearing and that the *A. afarensis* foot lacked a longitudinal arch. Plantarly, there is a large insertion area on A.L. 333-28 for the tendon of *M. peroneus longus* (but see Susman et al., 1984). The significance of this observation is that according to Lovejoy et al. (2009), insertion of this tendon into both the Mt1 base and the medial cuneiform would limit mobility of the Mt1 on a fixed medial cuneiform. Additionally, a well-developed bursa for the tendon of *M. tibialis anterior* abuts the Mt1 facet along the distoplantar corner of A.L. 333-28. Latimer and Lovejoy (1990a) argue that this bursa would preclude any medial deviation of the Mt1 on the medial cuneiform, though there is considerable variation in both humans and apes for this feature (Deloison, 1992). As mentioned earlier, the missing dorsal surface of the medial cuneiform would be more informative for addressing hallucal mobility in *A. afarensis*—a more complete adult specimen is sorely needed.

Complementing the morphology of the medial cuneiform is the Mt1, known from a proximal fragment (A.L. 333-54) and two distal heads (A.L. 333-115a, -21). Latimer and Lovejoy (1990a) note that an invagination of the proximal articular margin and raised hilus separating the proximal articular facet into dorsal and plantar regions would restrict axial rotation of the Mt1 on the medial cuneiform, thus preventing hallucal grasping in *A. afarensis*. Others note that despite this anatomy, the base of the Mt1 is strongly concave and ape-like (Deloison, 1991), and set at an angle that is consistent with some hallucal abducence (Berillon, 1999, 2004). Using a 3D geometrics morphometrics analysis, Proctor (2010a, 2010b) found A.L. 333–54 to be intermediate in shape between modern apes and humans. Latimer et al. (1982) wrote that there is "no indication of a facet for the Mt2", though Tuttle (1981) suggested that the base of the Mt1 probably contacted the Mt2. The Mt1 heads are dorsally domed indicating that the proximal hallucal phalanx dorsiflexed on the Mt1 head during bipedal push-off (Latimer & Lovejoy, 1990a; Figure 11). However, the dorsum of the Mt1 head mediolaterally narrows (Susman, 1983; Susman et al., 1984; Figure 19), and a geometric morphometrics study of the Mt1 head of *A. afarensis* found it to be more ape-like than human-like (Fernández et al., 2016) indicating that the bipedal push-off mechanism was less refined and less efficient than it is in modern humans. Wunderlich and Ischinger (2017) further regard the dorsally narrow (plantarly wide) Mt1 head to be consistent with vertical climbing in *A. afarensis*. Two juvenile Mt1s are known, and are generally described as human-like: A.L. 333-174 (Hillenbrand, 2009) and the proximal epiphysis from the Dikika foot (DeSilva, Gill, et al., 2018).

The Mt2 is known from a proximal base (A.L. 333-133) and two distal heads with partial shafts (A.L. 333-72, A.L. 333-115b). A.L. 333-72 was originally proposed as either an Mt2 or Mt3 (Latimer et al., 1982), but comparisons with A.L. 333-115, which preserves all five Mt heads, show it to be an Mt2. The Mt2 proximal base is dorsoplantarly expanded relative to its mediolateral width, making it quite human-like and unlike the more ape-like base in *Ardipithecus* and the Mt2s from *Australopithecus* at Sterkfontein Members 2 and 4 (McNutt, Zipfel, & DeSilva, 2018; Figure 12). Furthermore, there is a small contact facet on the proximomedial shaft of A.L. 333-133 for contact with the Mt1 (DeSilva, McNutt, Zipfel, & Kimbel, 2018). Distally, the Mt2 head is dorsally domed (Latimer & Lovejoy, 1990a, 1990b) and quite human-like in overall geometry (Fernández et al., 2016). Both Mt2s appear to have slight internal torsion of the head, though a more complete Mt2 will be necessary to quantify this anatomy in *A. afarensis*. The Mt3 is known from two proximal bases (A.L. 333-133, -157), and from a distal head (A.L. 333-115c). The bases are dorsoplantarly tall and human-like (Ward et al., 2012; McNutt, Zipfel, & DeSilva, 2018; Figure 13). The Mt3 head is intermediate in shape between apes and humans (Fernández et al., 2016).

The adult Mt4 is known from the only complete Hadar metatarsal: A.L. 333-160 (Ward et al., 2011), and from the distal head from the A.L. 333-115 forefoot (Latimer et al., 1982). The A.L. 333-160 metatarsal has a dorsoplantarly tall and relatively flat base, indicating human-like rigidity of the tarsometatarsal joint in *A. afarensis* (Ward et al., 2011; Figures 13 and 19). A contact facet between the base of

the Mt4 and the lateral cuneiform indicates that the Mt4 was nested into the tarsal row as it is in humans, but not apes (Ward et al., 2011, 2012). The Mt4 shaft is dorsoplantarly tall and quite mediolaterally narrow. The head exhibits external torsion, which was presented by Ward et al. (2011) as evidence for a lateral longitudinal arch in *A. afarensis*. This torsion is present already in the juvenile from Dikika (DeSilva, Gill, et al., 2018). However, external torsion of the Mt4 can be found in monkeys as well (Drapeau & Harmon, 2013), limiting its utility for characterizing the lateral longitudinal arch. However, additional evidence for an arch is the plantar declination of the shaft and head relative to the Mt base (Ward et al., 2011). The head is domed and there is a prominent gutter behind the head, indicating that the proximal phalanx dorsiflexed during bipedal propulsion (Ward et al., 2011, 2012). Fernández et al. (2016, 2018) found the Mt4 head of A.L. 333-115 and A.L. 333-160 to be more ape-like. Mitchell, Sarmiento, and Meldrum (2012) found aspects of the A.L. 333-160 fossil to be eastern gorilla-like; though a follow-up 3D analysis of A.L. 333-160 found it to group solidly with modern humans (Kuo, Ward, Kimbel, Congdon, & Johanson, 2016).

The *A. afarensis* Mt5 is represented by A.L. 333-13 and A.L. 333-78 (proximal bases and shafts), and the Mt5 head from A.L. 333-115. The bases are relatively flat dorsoplantarly and human-like (DeSilva, 2010). In the transverse plane, the A.L. 333-78 Mt5 exhibits a lateral bend typical of the human foot; A.L. 333-13 appears straighter but is not complete enough to accurately assess this anatomy. The Mt5 head (A.L. 333-115) is domed and human-like (Fernández et al., 2016; Latimer & Lovejoy, 1990b).

There are 18 proximal pedal phalanges and four intermediate pedal phalanges collected from Hadar (Johanson et al., 1982; Latimer et al., 1982; Ward et al., 2012). The proximal phalanges have a dorsal cant to the base, which is functionally related to dorsiflexion during the push-off phase of bipedal gait (Latimer & Lovejoy, 1990b). However, both Duncan et al. (1994) and Griffin and Richmond (2010) found that canting values of the Hadar proximal phalanges were intermediate between modern humans and African apes, especially gorillas. The proximal phalanges are relatively long compared to a modern human, but short compared with modern apes (Latimer & Lovejoy, 1990b; Susman et al., 1984). Additionally, the curvature of the pedal phalanges is found to be African ape-like when measuring either the included angle (Stern & Susman, 1983) or a polynomial curve fitting technique (Deane & Begun, 2008). The intermediate phalanges are similarly long and curved (Stern & Susman, 1983). Lovejoy et al. (2009) proposed that questions about the shortening of pedal digits should be focused on the intermediate, rather than the proximal phalanges since shorter intermediate phalanges would limit "tenting" of the interphalangeal joints during bipedal propulsion. Rolian et al. (2009) found that shorter toes had little impact on walking energetics, but helped reduce costs during running bouts. We note here, as others have done (e.g., Susman et al., 1984; Lovejoy et al., 2009; Supporting Information Table S1) that *A. afarensis* retained long intermediate phalanges. Most notable are the lateral intermediate phalanges (IP4–5), which are reduced to small, square-shaped bones in humans, but remain long in the apes (Elftman & Manter, 1935) and in *A. afarensis*. A fragmentary DP5 (A.L. 333-115) is the only distal phalanx known from *A. afarensis* and it yields little information.

Fortunately, the physical remains of *A. afarensis* can be measured against 3.66 Ma fossilized footprints preserved at Laetoli, Tanzania (Leakey & Harris, 1987). The first footprints discovered and suggested to be from a bipedal hominin were Laetoli "A", a set of 5 consecutive bipedal prints that were never fully excavated (Leakey, 1978; Leakey & Hay, 1979; White & Suwa, 1987). These prints were eventually hypothesized to either be from a hominin, or an ursid (Tuttle, 1987, 1990; Tuttle, Webb, Tuttle, & Baksh, 1992). McNutt et al. (2018) regards Laetoli "A" as more likely to be from a hominin than an ursid on the basis of data collected on semi-wild bipedal black bears, the narrow stride width of Laetoli "A", and more recently unearthed evidence for diversity in Pliocene hominin foot morphology.

The Laetoli "G" prints have been the primary focus of study (e.g., Clarke, 1979; Crompton et al., 2012; Day & Wickens, 1980; Leakey, 1979; Leakey & Hay, 1979; Tuttle, 1987, 1990; White & Suwa, 1987). The prints were produced by at least 3 hominins: one small individual (G1) and a second trail left by two individuals (G2/3), one walking in the prints of another. Musiba, Matthews, Noble, Kim, and Dominguez-Rodrigo (2011) have proposed that the G2/3 prints contain the prints of yet another individual, making them a composite of three feet. One of these prints has recently been digitally separated from the other(s) (Bennett, Reynolds, Morse, & Budka, 2016). Two other hominin bipedal trackways (Laetoli S1 and S2) have recently been discovered (Masao et al., 2016) and S1 is consistent with the "G" prints in inferred gait kinematics (Raichlen & Gordon, 2017) and foot form (Pelissero, 2017). The preservation of S2 impedes functional inferences.

The Laetoli G prints generally provide evidence for a hominin with a human-like gait (Raichlen, Gordon, Harcourt-Smith, Foster, & Haas Jr, 2010) and foot function, including a prominent heel-strike, a stiff lateral midfoot, incipient medial longitudinal arch, and adducted hallux (Crompton et al., 2012; Day & Wickens, 1980; White, 1980; White & Suwa, 1987). However, these superficial similarities belie some of the more interesting, albeit subtle, differences between modern human footprints and those at Laetoli. First, the Laetoli footprints were made by a hominin with a longitudinal arch that was intermediate in height between a human and ape, and would be considered "flat-footed" by modern standards (Bennett et al., 2009; Crompton et al., 2012; Hatala et al., 2016; Hatala, Demes, & Richmond, 2016). Furthermore, the prints reveal that there is less medial weight transfer than is typically found in modern humans (Crompton et al., 2012; Stern & Susman, 1983), though variation exists in humans (Hicks, 1953)

While many studies have highlighted the human-like, derived nature of the Laetoli footprints, others have pointed out the presence of primitive, ape-like features as well. Bennett et al. (2009) suggest that the Laetoli printmakers had a more divergent hallux than modern humans. Meldrum (2004, 2007) and Meldrum, Lockley, Lucas, and Musiba (2011) sees evidence for a midtarsal break in the footprints and the absence of both midfoot rigidity and a longitudinal arch. Stern and Susman (1983) noted that the lateral digits may be curled under the foot as can happen in apes walking bipedally, a hypothesis countered by both Tuttle (1985) and Berge, Penin, and Pellé (2006). However, Tuttle, Webb, Weidl, and Baksh (1990); Tuttle, Webb, and Baksh (1991) also regard the Laetoli footprints to be too human-like to have been made by *A. afarensis*, and instead proposes that they were made

by an as-of-yet undiscovered hominin with a more human-like foot, a hypothesis countered by White and Suwa (1987). Harcourt-Smith and Hilton (2005) have agreed with Tuttle et al. (1990, 1991) that the foot bones from Hadar do not match the footprints made at Laetoli.

To further complicate matters, recent work has challenged previous attempts to draw any direct connection between footprints and foot function. Numerous studies have revealed that substrate type and sediment erosion can impact footprint morphology and preservation, impacting any simple relationship between skeletal form, foot function, and footprint formation (Bates et al., 2013; D'Août, Meert, Van Gheluwe, De Clercq, & Aerts, 2010; Hatala et al., 2013a, 2013b; Hatala, Perry, & Gatesy, 2018; Morse et al., 2013; Wiseman & De Groote, 2018). These recent studies should give us pause interpreting fine details of foot function from the Laetoli prints, as extraordinary as they are.

Nevertheless, the wealth of data from the Hadar foot bones and the Laetoli footprints form a general picture of the *A. afarensis* foot (assuming of course that the Laetoli "G" and "S" prints were made by *A. afarensis*). The large robust heel of the calcanei from Hadar (Latimer & Lovejoy, 1990a, 1990b) is consistent with a prominent heel-strike during bipedal gait (as would the Laetoli trackways). The anatomy of the ankle joint demonstrates that a vertically oriented tibia swung over the foot as it does in modern humans, and that ankle dorsiflexion was limited, perhaps by an elongated Achilles tendon. Based on the relatively dorsoplantarly flat base of the Mt4 it is probable that at heel lift the foot would dorsiflex at the metatarsophalangeal joint, not at the tarsometatarsal joint as it does in other primates. Dorsoplantarly tall Mt2 and Mt3 bases would suggest that well developed deep plantar ligaments (e.g., long plantar ligament) helped stiffen the midfoot as the heel was lifting. In these respects, the *A. afarensis* foot was quite human-like.

However, there is evidence from the forefoot (Fernández et al., 2016; Susman et al., 1984) and from the Laetoli footprints that *A. afarensis* did not consistently push off the transverse axis of the foot and lacked the medial weight transfer onto the big toe that typifies modern human foot function. The doming of the Mt1 head implies foot versatility and occasional use of the transverse axis, but even then, the lack of a mediolaterally expanded dorsum of the head and the concave base of the Mt1/convex Mt1 facet on the medial cuneiform implies a push-off mechanism that is not as refined as in humans today. This could be a result of a thinner plantar aponeurosis and a weakened windlass mechanism (Griffin, Miller, Schmitt, & D'Août, 2015; Hicks, 1953). In this respect, we find great consistency between the pedal fossils from Hadar and the Laetoli footprints, which show less medial weight transfer and therefore less human-like push-off from the transverse axis of the foot. Furthermore, while the plantar arch has been dichotomized and scholars have argued that *A. afarensis* either had arches, or did not, we suggest that both the bones from Hadar and the Laetoli prints indicate that arches in this hominin were quite variable (DeSilva & Throckmorton, 2010) and neither human-like nor ape-like. We suggest that the current evidence best describes the *A. afarensis* longitudinal arch as present and better developed than in modern apes, but more flat and less developed than in modern humans (DeSilva, Gill, et al., 2018; Prang, 2015b).

We similarly suggest that arguments about arboreality in *A. afarensis* have become unnecessarily polarized, and regard the foot anatomy of *A. afarensis* to be consistent with more arboreality than accepted by some (e.g., Latimer, 1991), but less than proposed by others (e.g., Susman et al., 1984). The large peroneal trochlea indicates strong peroneal musculature in *A. afarensis*. Latimer and Lovejoy (1989) propose that the peroneals (*Mm. peroneus longus* and *brevis*) would operate as plantarflexors in the absence of a human-like *M. triceps surae*; however, we suspect that *A. afarensis* did possess an elongated Achilles tendon (McNutt & DeSilva, 2016). Furthermore, since the peroneals are foot everters in addition to secondary plantarflexors, if they contracted during heel-lift, one would expect *more* medial weight transfer during heel-lift (Jones, 1941), rather than less as is evidenced by the bones and footprints. Although we do note that because the proximal calcaneus is medially angled relative to the distal body of the calcaneus, the insertion of the *M. triceps surae* would be medial to the subtalar joint and could promote more inversion during contraction than in modern humans; it could be that simultaneous contraction of the *M. peroneus longus* could counterbalance the action of the *M. triceps surae* and produce a neutral foot position during heel lift (see Reeser, Susman, & Stern Jr, 1983). Nevertheless, even if the peroneals contracted during terrestrial gait in *A. afarensis*, we do find Stern and Susman's (1983) argument compelling that the strong peroneals would have also helped during bouts of arboreality (Langdon, 1985). Furthermore, the long(ish) and curved pedal phalanges—particularly the lateral IPs—are consistent with a reliance on the trees for food and/or survival, especially at night. However, these anatomies should not overshadow the strikingly human-like nature of the *A. afarensis* foot, which is—in our view—better adapted for terrestrial bipedalism than the foot of any other known australopith. Later in this review, we use a cladistics framework to demonstrate that the *A. afarensis* foot is the most human-like of any australopith.

Latimer and Lovejoy (1989, 1990a) have explained the presence of primitive features in the foot skeleton of *A. afarensis* as evidence for an arboreal past; their retention merely phylogenetic inertia. Recently, analysis of the Dikika foot skeleton provides a different perspective on the adult foot of *A. afarensis*. The Mt1 facet on the medial cuneiform is more medially directed in the juvenile than in the adult (DeSilva, Gill, et al., 2018). Perhaps more importantly, unlike in humans, the convexity of the Mt1 facet on the medial cuneiform was retained from the juvenile years through adulthood in *A. afarensis*, indicating multidirectional loading throughout life in *A. afarensis*. DeSilva, Gill, et al. (2018) hypothesized that juvenile *A. afarensis* was more arboreal than the adults and that developmentally plastic features of the foot skeleton (i.e., shape of the hallucal tarsometatarsal joint, phalangeal curvature) appear more ape-like in adult *A. afarensis* because of the arboreality of the juveniles and pedal grasping during infant carrying. Developmentally, the foot of *A. afarensis* became more human-like (e.g., calcaneal robusticity) illustrating the importance of terrestrial bipedality in this hominin. However, given the absence of controlled fire, *A. afarensis* almost certainly slept in trees at night and those long, curved toes would help grasp the substrate; Stern (2000) noted that the toes of A.L. 333-115 were the length of the fingers of 9- to 10-year-old humans, primates that also are known to occasionally climb. We envision *A. afarensis* climbing most often as youngsters,

and as adults less frequently, but kinematically like that observed in modern humans (Venkataraman, Kraft, & Dominy, 2013)—slowly, and carefully, without the acrobatics of a modern ape, but with slightly more hallucal mobility, longer lateral digits, and stronger peroneal musculature than in later, committed terrestrial hominins.

3.7 | *Australopithecus prometheus* (Sterkfontein Member 2; 3.67 Ma?)

Australopithecus prometheus was originally named based on craniodental material from Makapansgat, South Africa (Dart, 1948), but was subsequently sunk in to *A. africanus* (Robinson, 1954). However, Clarke (1988) has long argued that there was a mixed assemblage at Sterkfontein Member 4, and based on craniodental similarities between the Makapansgat material, some material from Sterkfontein Member 4 (discussed below under *Australopithecus africanus*), and the Member 2 partial skeleton "Little Foot" StW 573, this taxon has been resurrected (Clarke, 2008; Granger et al., 2015). Whether it remains one accepted by the scientific community will have to await a full publication and analysis of the StW 573 skeleton. For now, we utilize this nomenclature to describe the functional anatomy of the StW 573 "Little Foot" pedal remains, announced in 1995 (Clarke & Tobias, 1995) and fully described (Deloison, 2003). Additionally, the dating of these remains is contentious, with ranges from over 4 million (Partridge, Granger, Caffee, & Clarke, 2003) to ~2 million (Walker, Cliff, & Latham, 2006). In this review, we use the 3.67 Ma date currently proposed for the StW 573 remains (Granger et al., 2015), but note that this date is controversial and subject to alternative, geologically younger, interpretations (Kramers & Dirks, 2017). Observations below are based on Clarke and Tobias (1995), Deloison (2003) and primarily based on observations we have made on the original StW 573 foot fossil.

The circumstances of discovery of the StW 573 partial foot skeleton are discussed elsewhere (Clarke, 1998; Tobias, 1998). In short, Clarke identified several primate foot bones (talus, navicular, medial cuneiform, and Mt1) from Sterkfontein Member 2 in a faunal storage box at the Sterkfontein field laboratory. Preliminary analysis of these four bones suggested to Clarke and Tobias (1995) that this foot possessed the combination of a divergent hallux with a more human-like ankle joint. This interpretation led Clarke and Tobias (1995) to propose an evolutionary scenario for the foot in which the rearfoot (e.g., talus) evolved human-like anatomies before the forefoot. After publication, the intermediate cuneiform, lateral cuneiform (L and R), Mt2, and a fragmentary calcaneus were recovered and described (Deloison, 2003). While we do not agree that the partial calcaneus belongs with StW 573 and identify it instead as monkey based on the markedly mediolaterally concave cuboid facet typical of cercopithecoids, the other recovered fossils help form one of the most complete feet in the early hominin fossil record (Figure 21).

The talus of StW 573 was initially interpreted as being quite human-like (Clarke & Tobias, 1995; measurements in Deloison, 2003). It has roughly parallel trochlear rims and lacks the mediolateral expansion of the distal trochlear surface found in African ape tali (Figure 4). Damage to the fibular facet prevents an accurate assessment of the talar axis angle. However, both the horizontal and the head/neck torsion angles of the StW 573 talus are ape-like, suggesting mobility at

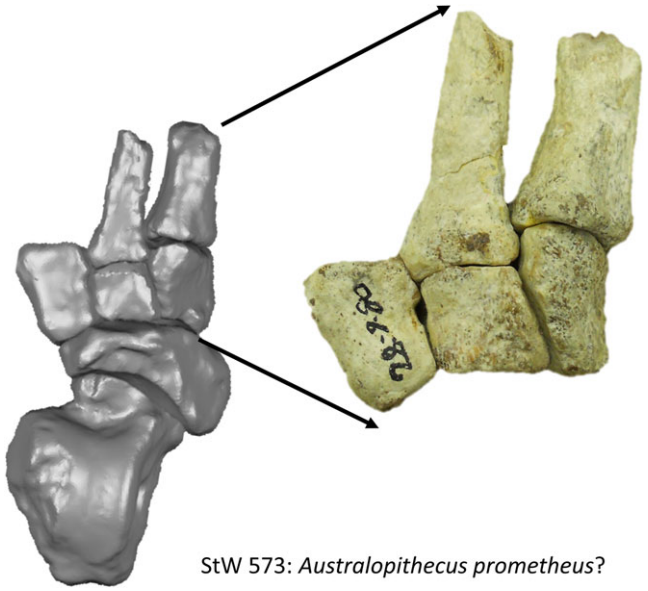

FIGURE 21 Left foot skeleton StW 573, attributed by some to *A. prometheus* (see text). The calcaneus may be from a cercopithecoid and is not included in this image. To the left is a surface scan rendering of articulated casts of StW 573; to the right is an enhanced image of the original fossil cuneiforms and preserved metatarsals (Mt1 and Mt2) in articulation. Note that the hallux is not divergent and instead is aligned with the Mt2, making StW 573 (at 3.67 Ma) the oldest known hominin foot fossil with an adducted hallux

the transverse tarsal joint (Kidd & Oxnard, 2005). A geometric morphometrics analysis found the StW 573 talus to cluster within the ape distribution and noted the deeply grooved and sloped trochlear surface (Harcourt-Smith, 2002).

The navicular of StW 573 has similarly yielded mixed interpretations. Clarke and Tobias (1995) noted the ape-like convex facet for the medial cuneiform and an ape-like angle between the facets for the cuneiforms. Deloison (2003) suggested that the navicular was chimpanzee-like and from an arboreally-adapted foot. Kidd and Oxnard (2005) used a multivariate analysis of linear metrics and found StW 573 to be generally African ape-like, with a relatively large tuberosity and proximodistally thin navicular body. However, Harcourt-Smith (2002) and Harcourt-Smith and Aiello (2004) used a geometric morphometrics analysis to conclude that the navicular was more human-like than these other scholars propose. Harcourt-Smith (2002) acknowledged that the tuberosity was larger and the body was more laterally pinched than is typical in modern humans (Figure 6), but that the overall geometry of the bone was more human-like than ape-like.

Of particular interest is the proposition that StW 573 possessed a divergent, grasping hallux. Clarke and Tobias (1995) noted that the medial cuneiform possessed a convex facet for the Mt1 that spilled onto the medial aspect of the bone. Many authors have challenged these preliminary assessments of the StW 573 medial cuneiform. Using a 3D geometric morphometrics approach to quantify the shape of the medial cuneiform, Harcourt-Smith (2002) and Harcourt-Smith and Aiello (2004) concluded that the medial cuneiform of Little Foot was human-like and was from a foot that had lost hallucal grasping potential. A canonical variates analysis of linear metrics also found the StW 573 medial cuneiform to be human-like (Kidd & Oxnard, 2005).

McHenry and Jones (2006) concurred in a study that quantified the degree to which the Mt1 facet spilled onto the medial aspect of the bone—they found that StW 573 was human-like. Lovejoy et al. (2009) noted that StW 573 did not have a divergent hallux, both because of a distally oriented Mt1 facet and because of the human-like attachment of *M. peroneus longus* to the plantar aspect of the medial cuneiform. Gill et al. (2015) quantified the curvature of the Mt1 facet and angulation between the navicular facet and the Mt1 facet on the StW 573 medial cuneiform and found that it fell well within the human range and was similar to the OH 8 medial cuneiform (Figure 8).

Furthermore, we note that when the StW 573 ft was comprised of a talus, navicular, medial cuneiform, and Mt1 (Clarke & Tobias, 1995) the arrangement of these bones could produce the illusion of a divergent hallux. However, with the recovery of the other cuneiforms and the Mt2 (Clarke, 1998; Deloison, 2003), the articulation of these elements produces a foot incapable of hallucal divergence (Figure 21). The intermediate cuneiform nestles into an angled medial cuneiform facet, as it does in humans, and the Mt2 is not only parallel to the Mt1 base, but has a small contact facet on its medial shaft for the adducted Mt1 (Singh, 1960; pattern 1). In sum, the hypothesis that StW 573 had a divergent hallux has been refuted. If the age of this fossil—3.67 Ma (Granger et al., 2015)—is accepted, the importance of this fossil is not that it had a divergent hallux (it did not), but that it would be the oldest known hominin foot fossil with an adducted great toe.

However, there still are primitive aspects to the medial forefoot. A geometric morphometric assessment of the base of the Mt1 found it to be intermediate in shape between apes and humans (Proctor, 2010b). Additionally, the base of the Mt2 is dorsoplantarly short, similar to that found in apes, the Burtele foot, and other Mt2 bases from Sterkfontein Member 4 (McNutt, Zipfel, & DeSilva, 2018; Figure 12). The proximal facet of the intermediate cuneiform for the navicular is quite concave (Figure 9), perhaps indicating some laxity of the medial midfoot. However, laterally, the foot is more human-like. The lateral cuneiform of StW 573 (metrics in Deloison, 2003) is proximodistally elongated (Figure 10), as is found in humans. Additionally, while there is a prominent plantar hamulus, there is no groove for the *M. peroneus longus* tendon, as can be found in ape lateral cuneiforms. This anatomy, in combination with smaller navicular tuberosity, would support the presence of at least an incipient longitudinal arch in the foot of StW 573 (Harcourt-Smith, 2002; Harcourt-Smith & Aiello, 2004).

With the unveiling of Little Foot, it appears that no additional foot bones were recovered from StW 573 and thus, the morphology of the calcaneus, cuboid, lateral metatarsals, and phalanges remain unknown. Assuming the 3.67 Ma age is correct (Granger et al., 2015; but see Kramers & Dirks, 2017), the StW 573 ft is the oldest on record with an adducted hallux, making it a critically important specimen for understanding the antiquity of human-like foot function. However, there remain primitive aspects of the foot (e.g., ape-like talar head torsion, grooved trochlea, short Mt2 base) that probably have functional and phylogenetic implications worthy of future study. To that end, it will be important to directly compare the StW 573 foot bones to the Sterkfontein Member 4 assemblage, which is quite heterogeneous and may sample two functionally distinct foot forms (see below). StW 573 will thus serve as an important template for correctly categorizing isolated pedal remains from Sterkfontein Member 4, and other localities in the Cradle of Humankind, South Africa.

3.8 | *Australopithecus africanus* (Sterkfontein Member 4; 2.0–2.6 Ma)

Most of what is known about the foot of *A. africanus* is based on isolated, unassociated fossils recovered from Member 4 deposits at Sterkfontein, South Africa. These include a calcaneus (StW 352); five tali (StW 88, 102, 347, 363, 486); two Mt1s (StW 562, 595); three Mt2s (StW 89, 377, 595); six Mt3s (StW 238, 387, 388, 435, 477, 496); three Mt4s (StW 485, 596, 628); one Mt5 (StW 114/115); one hallucal proximal phalanx (StW 470); one proximal phalanx (StW 355), and one distal hallucal phalanx (StW 617). There are no *Australopithecus africanus* skeletons definitively associated with any foot bones. The only possible exception to that statement is an Mt3 (StW 435), which may be associated with the StW 431 partial skeleton (Toussaint, Macho, Tobias, Partridge, & Hughes, 2003). StW 595 (Mt1-3; PP1) is assumed to be a partial foot based on a shared accession number (Clarke, 2013) though some of these bones remain undescribed. StW 377 (Mt2) and StW 485 (Mt4) may belong to the same foot, as might StW 388 (Mt3), StW 596 (Mt4), and StW 114/115 (Mt5; Deloison, 2004). As mentioned in the section on *Australopithecus prometheus* (StW 573) and discussed in more detail below, we suspect that the foot fossils from Sterkfontein Member 4 constitute a mixed assemblage and probably should not all be assigned to *A. africanus* (Figure 22). Anatomies discussed below are based on published sources and observations made on the original fossil material.

The calcaneus StW 352 (Deloison, 2003) preserves the talar facets and the distal two-thirds of the bone. The proximal tuber has been sheared away, exposing internal spongy bone. The peroneal trochlea appears quite large, but it has been artificially expanded by matrix infill and is affixed to the fossil too far distally (McNutt, Claxton, & Carlson, 2017). Although the proximal calcaneus is missing, the preserved cross-section is relatively small, suggesting that StW 352 had a gracile tuber, similar to U.W. 88-99 (*A. sediba*) and apes (Prang, 2015a), although the shape of the cross-section qualitatively appears more human-like (Zipfel et al., 2011). The anterior subtalar facet is strongly convex and ape-like (Prang, 2016b; Zipfel et al., 2011), suggesting considerable mobility at the subtalar joint in *A. africanus*. This anatomy is similar to that found in *A. sediba* (DeSilva et al., 2013; Zipfel et al., 2011), but contrasts with the more human-like flat subtalar joint of *A. afarensis* (Prang, 2016b). Internally, however, the trabecular bone underlying the subtalar joint is more human-like and consistent with stereotypic loading (Zeininger, Patel, Zipfel, & Carlson, 2016). Distally, the calcaneocuboid joint is damaged, but what is preserved is plantarly angled and appears human-like in external morphology. Internally, however, the orientation and density of the trabecular bone is more ape-like, suggesting multidirectional loading at the calcaneocuboid joint in *A. africanus* (Zeininger et al., 2016). It is unclear how to reconcile these contradictory signals from the external and internal anatomy of StW 352.

StW 88 and 363 are the best-preserved Sterkfontein Member 4 tali. The others have damage (StW 102—head missing; 347 and

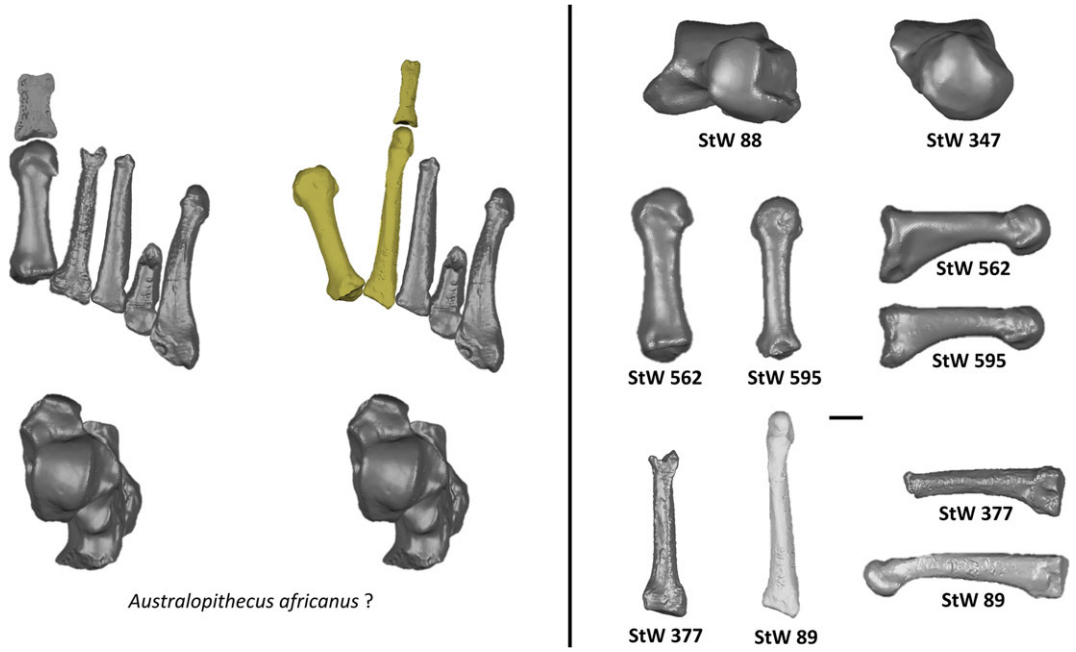

FIGURE 22 Left: Composite foot skeleton from the Sterkfontein Member 4 locality; any bones from the left side are reflected so that they all appear from a right foot. Elements shown here are: calcaneus (StW 352), talus (StW 88), Mt1 (StW 562), Mt2 (StW 377), Mt3 (StW 435), Mt4 (StW 485), Mt5 (StW 114/115), PP1 (StW 470). Shown to the immediate right of the composite foot are the same elements but with the Mt1 (StW 595), Mt2 (StW 89), and PP2 (StW 355) replaced and shown in yellow. These medial elements differ anatomically (and functionally) and probably derive from different taxa. However, it is unclear which rearfoot or lateral metatarsal elements are associated with these different medial forefoot skeletons. To the right are elements from Sterkfontein Member 4 that illustrate significant (and functionally important) differences that reflect taxonomic diversity in this assemblage. Talus StW 88 has an ape-like, low head/neck torsion angle whereas StW 347 has human-like torsion. Mt1 StW 562 is robust and has a domed head, whereas StW 595 is gracile and lacks human-like dorsal doming. Mt2 StW 377 is short, straight, and robust, whereas StW 89 is long, curved, gracile, and has internal torsion of the head. Scale bar = 1 cm

486—proximal body sheared away). StW 363 was found with a portion of the calcaneus adhered to the talus; one study suggests that this individual suffered a talar compression fracture in life (Fisk & Macho, 1992). In general, the talar trochlea are human-like; they have a low, human-like talar axis angle, which would position the foot in an everted set under the leg (DeSilva, 2009). Additionally, the tali are only moderately wedged, as is typical in fossil australopiths and humans (Figure 4), which would suggest that *A. africanus* did not load the ankle joint in extreme dorsiflexion as apes do (DeSilva, 2009). However, a geometric morphometrics study of the best-preserved Sterkfontein Member 4 talus (StW 88) found it to be considerably more ape-like in overall shape (Harcourt-Smith, 2002). StW 88 has a very low, ape-like head neck torsion angle and declination angle (Figure 5; Table 3), which may suggest that this hominin had a relatively low arch (declination angle) and some transverse tarsal joint mobility (low torsion angle). However, StW 347 has a high, human-like head/neck torsion (Prang, 2016b; Figure 22). Thus, the positioning of the head and neck relative to the trochlear body in *A. africanus* tali varies considerably, with some more primitive and ape-like (StW 88), and others more human-like (StW 347). Furthermore, studies of the internal trabecular architecture find that *A. africanus* tali differ from modern humans (DeSilva & Devlin, 2012; Su & Carlson, 2017). Su and Carlson (2017) argue that the trabecular microarchitecture of the *A. africanus* tali (StW 102, 363, 486) are consistent with loading of the lateral foot and the absence of human-like medial weight transfer during gait. A study of the internal trabecular bone of *A. africanus* distal tibiae suggests a more human-like loading of the ankle joint (Barak et al., 2013).

There are no other published tarsals from Sterkfontein Member 4 though Clarke (2013) lists an unpublished calcaneus (StW 643), navicular (StW 623), and cuboid (StW 638). There is no adult cuboid known from the genus *Australopithecus* making StW 638 of particular importance, though each of these bones promises to assist in our understanding the functional anatomy of the *A. africanus* foot.

There are two Mt1s known from Sterkfontein Member 4: StW 562 and StW 595. They are strikingly different from one another, strongly suggesting that they derive from different hominins with different foot mechanics (Zipfel, Kidd, & Clarke, 2010; Clarke, 2013; McNutt, Zipfel, & DeSilva, 2018; but see Deloison, 2003). StW 562 is generally human-like. It has a large head, which is dorsally domed with an articular surface that continues onto the dorsum of the bone (Figure 11; Figure 22), reflecting hallucal dorsiflexion during bipedal push-off. Unlike in modern humans, however, the dorsum is not mediolaterally expanded. Additionally, the Mt1 shaft has human-like robusticity (Figure 11). There is a well-developed contact facet for the Mt2 on the lateral rim of the base. The medial cuneiform facet, however, is quite convex and a geometric morphometrics analysis positions the base shape intermediate between human and ape (Proctor, 2010b). In contrast to StW 562 is the more ape-like StW 595, which is quite similar to the Mt1 from the Burtele foot (Haile-Selassie et al., 2012). The head of StW 595 is not dorsally domed, which reflects limited hallucal dorsiflexion (Clarke, 2013; Figure 22). Additionally, the

shaft is relatively long and gracile, similar to that found in the Burtele Mt1 and to modern ape Mt1 shafts (Figure 11) and suggests that the StW 595 hominin did not push off the hallux during bipedal gait, instead relying on the oblique axis of the foot for propulsion. We therefore agree with other findings (Clarke, 2013; Zipfel et al., 2010) that these anatomical differences are not just normal variation, but reflect functional differences in how the foot worked in StW 562 and StW 595, and therefore reflect two different hominins in the Sterkfontein Member 4 assemblage.

Similar differences are sampled in two Mt2s from Sterkfontein Member 4: StW 89 and StW 377 (DeSilva, Proctor, & Zipfel, 2012). While both bones have an ape-like dorsoplantarly short base relative to the mediolateral width (McNutt, Zipfel, & DeSilva, 2018; Figure 12), StW 377 displays a dorsoplantarly tall base relative to the estimated length of the bone, whereas StW 89 retains ape-like base dimensions found only in the Burtele foot amongst hominins (DeSilva, Proctor, & Zipfel, 2012; Haile-Selassie et al., 2012). Additionally, while both bones have internal torsion of the metatarsal head, torsion values in StW 89 are considerably higher and are similar to apes and to the Burtele foot, whereas StW 377 is more human-like (DeSilva, Proctor, & Zipfel, 2012; Drapeau & Harmon, 2013). An analysis combining the divergence angle (i.e., base angle relative to the shaft in the transverse plane), inclination angle (i.e., base angle relative to the shaft in the sagittal plane), and torsion angle positions StW 377 at the low end of the human range and StW 89 closer to the gorilla range with the Burtele Mt2 (Daver et al., 2018). StW 89 also possesses a more longitudinally curved shaft than StW 377, which is straighter and more human-like (DeSilva, Proctor, & Zipfel, 2012; Figure 22). The Mt2 from the StW 595 foot is missing a head, but the base is qualitatively similar to StW 89, suggesting StW 595 and StW 89 belong to feet that were functionally similar to one another (and different from the foot of StW 562 and StW 377; Figure 22).

There are six fragmentary proximal Mt3s from Sterkfontein Member 4. Little comparative work has been done on them (though metrics can be found in Deloison, 2003). We find these bones to be quite human-like and homogeneous, though Proctor (2010a) found the bases of StW 435 and 477 to be intermediate between human and ape, while the others were more human-like. All six bones preserve the base and part of the metatarsal shaft; none preserve the Mt3 head. The bases are all dorsoplantarly tall relative to the mediolateral width, which is a human-like characteristic found in the earliest hominins, including *Ardipithecus* and all known *Australopithecus* (McNutt, Zipfel, & DeSilva, 2018; Figure 13). The bones exhibit very little longitudinal curvature, but they do have lateral tubercles for contact with the Mt4 (these are particularly well developed in StW 238, 435, and 496), perhaps to stabilize the lateral column of the foot.

Three proximal Mt4s (StW 485, 596, 628) and a complete Mt5 (StW 114/115) represent the lateral metatarsals of *A. africanus*. We were only granted permission to study StW 485 and StW 114/115. The Mt4 (StW 485) is human-like in possessing a dorsoplantarly tall and flat (or sinusoidal) base, indicative of a stiff lateral midfoot and the absence of a midtarsal break (DeSilva, 2010; Proctor, 2013; DeSilva et al., 2015; Figure 14). There is an angulated contact facet medially for the lateral cuneiform, indicating that the Mt4 was nested into the tarsal row in *A. africanus* as it was in *A. afarensis* and in modern humans (Ward et al., 2011). Even though just the proximal portion of StW 485 is preserved, the shaft already exhibits external torsion typical of hominin Mt4s (Drapeau & Harmon, 2013; Pontzer et al., 2010; Ward et al., 2011). The complete StW 114/115 Mt5 is human-like in most respects (Zipfel et al., 2009; Figure 15). It is laterally curved in the transverse plane, has a small, human-like tuberosity, dorsoplantarly flat base, mediolaterally wide shaft, and a dorsally domed head. The only primitive aspect of the bone is some longitudinal curvature of the shaft. A multivariate analysis positions StW 114/115 well within the human range of variation (Zipfel et al., 2009; Figure 15). A study of the internal cortical structure found that StW 114/115 possessed thick, ape-like cortex distributed around the bone in a human-like manner (Dowdeswell et al., 2016). Together, the lateral metatarsals (Mts3–5) from Sterkfontein Member 4 are quite human-like and suggest that *A. africanus* had a human-like, stiff lateral midfoot that converted the foot into a lever during the propulsive phase of bipedal gait. Undescribed metatarsals (Mt4 StW 596, 628, and Mt5 StW 634) will help to test the functional hypothesis described here and reveal if any variation exists in the assemblage as we found in the medial forefoot.

There is a single proximal phalanx (StW 355) that is relatively long (Deloison, 2003; McNutt, Zipfel, & DeSilva, 2018) and the most curved of any known hominin pedal phalanx (Harcourt-Smith et al., 2015; Figure 16), similar to values in *Pongo* and *Symphalangus*. It may be associated with the Mt2 StW 89 (Kuman & Clarke, 2000), in which case there is ape-like plantarflexion possible at the metatarsophalangeal joint combined with the potential for human-like dorsiflexion (DeSilva, Proctor, & Zipfel, 2012). There is a hallucal proximal phalanx (StW 470) and distal phalanx (StW 617). StW 470 is quite robust and a ridge on the dorsal surface could be the result of dorsiflexion during toe-off. Deloison (2003), however, found StW 470 also to contain elements consistent with arboreality. StW 617 possesses slight lateral deviation, as found in human distal hallucal phalanges (Aiello & Dean, 1990), but does not possess the axial torsion the human DP1 has, consistent with push-off from the oblique axis of the foot.

It is difficult to synthesize the above information into a functionally cohesive narrative. The functionally relevant variation in the Sterkfontein Member 4 assemblage make it probable that the foot bones described above are not from a single taxon and it should also be noted that these sediments sample a large time range from 2.6 to 2.0 million years ago (Pickering et al., 2011). Based on the Mts3–5, we are confident that a hominin (and perhaps multiple hominins) at Sterkfontein had a stiff lateral midfoot. However, the medial midfoot appears to differ between hominins at Sterkfontein. One (represented by StW 595 and StW 89/355) possessed a more ape-like medial foot, with no dorsal doming of the Mt1, internal torsion of the Mt2, and ape-like phalangeal curvature. Together, these data would support the presence of an arboreal hominin with foot morphologies similar to those found in the Burtele foot (Haile-Selassie et al., 2012). Also present at Sterkfontein Member 4 is a foot (e.g., StW 562, StW 377) with a more human-like medial midfoot consistent with medial weight transfer and perhaps push-off from the transverse axis of the foot. Sterkfontein tali differ from one another in interesting ways (StW 88 has exceptionally low head/neck torsion; StW 347 has high torsion), but they are not as easily sorted as the medial metatarsals are.

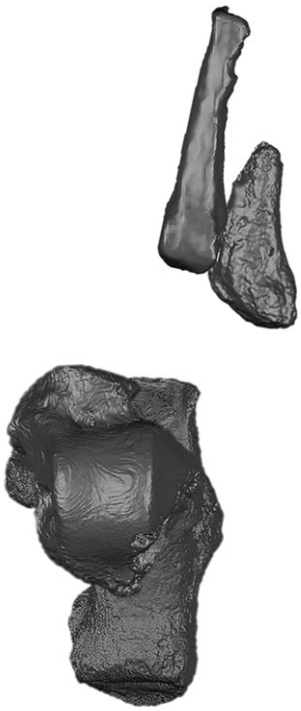

FIGURE 23 Elements currently known from the foot of *Australopithecus sediba*. These include the associated talus (U.W. 88-98) and calcaneus (U.W. 88-99) from the MH2 adult female skeleton, along with an isolated and currently unattributed Mt5 (U.W. 88-33) and an Mt4 (U.W. 88-22) from the MH1 juvenile male skeleton

The question of course is which foot belongs to *A. africanus*? And what hominin does the other foot represent? Associated foot bones, and a careful comparison between these remains and StW 573 (Little Foot) will be required to sort out the Sterkfontein Member 4 foot bones.

3.9 | *Australopithecus sediba* (Malapa, South Africa; 1.98 Ma)

Australopithecus sediba is currently known from the 1.98 Ma locality of Malapa, South Africa (Berger et al., 2010; Pickering et al., 2011). There are two partial skeletons (MH1 and MH2) that preserve pedal remains (DeSilva, Carlson, et al., 2018; Zipfel et al., 2011). MH1 preserves a calcaneal apophysis (U.W. 88-113), Mt4 (U.W. 88-22) and Mt5 (U.W. 88-16). MH2 preserves the talus (U.W. 88-98) and calcaneus (U.W. 88-97)—the only associated complete adult talus and calcaneus known from the genus *Australopithecus* (Figure 23). There is an isolated Mt5 (U.W. 88-33) that may be associated with MH2. A navicular and lateral cuneiform preliminarily reported to be hominin (DeSilva, Zipfel, et al., 2012) are not (DeSilva, Carlson, et al., 2018). Anatomies discussed below are based on published sources and observations we made on the original fossil material.

The Malapa calcaneus (U.W. 88-99) is surprisingly primitive (Zipfel et al., 2011; DeSilva et al., 2013; DeSilva, Carlson, et al., 2018; Figure 2). The lateral plantar process is dorsally positioned (Zipfel et al., 2011), most similar to that found in bonobos (Boyle et al., 2018), potentially making it ill-equipped for heel-striking bipedalism (DeSilva et al., 2015; Swanson, DeSilva, Boyle, Joseph, & McNutt, 2016; but see Holowka & Lieberman, 2018). This ape-like calcaneal tuber morphology found in *A. sediba* is quite distinct from the plantarly positioned, human-like, lateral plantar process of the geologically older *A. afarensis* calcanei (Boyle et al., 2018;Latimer & Lovejoy, 1989 ; Zipfel et al., 2011). Importantly, there is a calcaneal apophysis (U.W. 88-113) from a second individual (MH1), which preserves bony flanges for the plantar processes and is chimpanzee-like in its gracility and dorsally positioned flange for the lateral plantar process (Boyle et al., 2018; DeSilva, Carlson, et al., 2018; Zipfel et al., 2011). Furthermore, the overall tuber volume—hypothesized to be important for attenuating high forces incurred on the heel during bipedal walking (Latimer & Lovejoy, 1989) is quite low in the *A. sediba* calcaneus (Zipfel et al., 2011), and well within the ape range (Prang, 2015a). However, unlike in apes, the lateral body of the calcaneal tuber is dorsoplantarly tall and similar to the anatomy found in human and *Australopithecus* calcanei (Boyle et al., 2018).

As in modern apes, the U.W. 88-99 *A. sediba* calcaneus possesses a beaked medial process of the calcaneal tuberosity, perhaps to improve the mechanical advantage of the superficial head of *M. flexor digitorum brevis* (Sarmiento, 1983), and a large peroneal tubercle (Zipfel et al., 2011), which may indicate an important role for *M. peroneus longus* (Stern & Susman, 1983). Additionally, the subtalar joint is strongly convex and possesses a radius of curvature similar to that found in chimpanzees (DeSilva et al., 2013; Prang, 2016b; Zipfel et al., 2011). The calcaneocuboid joint is damaged, but the preserved facet is slightly plantarly angled, suggestive of an incipient lateral longitudinal arch (Heard-Booth, 2017; Zipfel et al., 2011), though Prang (2015a, 2015b) found that the orientation of the facets of the calcaneus and talus of *A. sediba* instead are consistent with a flat foot in this taxon. While primitive, ape-like anatomies abound in this calcaneus, *A. sediba* was a bipedal hominin and more human-like anatomies can be found as well. Plantarly, there is a palpable attachment for the long plantar ligament, which helps stabilize the midfoot during bipedal walking. Additionally, the attachment for the Achilles tendon is human-like in its orientation and in possessing a large retrocalcaneal bursa, suggesting that *A. sediba* is more likely to have possessed a long Achilles tendon than a short, ape-like, one (McNutt & DeSilva, 2016; Zipfel et al., 2011). A multivariate analysis found that the adult *A. sediba* calcaneus (U.W. 88-99) was intermediate in shape between modern apes and humans (Zipfel et al., 2011). A more detailed geometric morphometrics analysis yielded similar results in finding U.W. 88-99 positioned between modern apes and modern humans (McNutt, Zipfel, & DeSilva, 2018; DeSilva, Carlson, et al., 2018; Figure 2).

The talus of *A. sediba* (U.W. 88-98) similarly possesses a combination of human-like anatomies and those found in the apes. U.W. 88-98 has a relatively flat talar trochlea, unlike the grooved trochlea found in many Sterkfontein Member 4 tali (with the notable exception of StW 88, which is quite mediolaterally flat). The trochlea of U.W. 88-98 is human-like in lacking the wedged, mediolaterally expanded distal aspect (Figure 4) and therefore the ankle of *A. sediba* was not habitually loaded in dorsiflexion (DeSilva, 2009; Zipfel et al., 2011). This is consistent with a human-like Achilles tendon insertion,

which would limit ankle joint excursion (Myatt et al., 2011). The talar head and neck have one of the lowest torsion values of any known hominin (Table 3), well within the range of modern apes (DeSilva, Carlson, et al., 2018; Prang, 2016b; Zipfel et al., 2011). The horizontal angle is also high and ape-like, whereas the talar head and neck exhibits a more human-like declination angle (Zipfel et al., 2011; DeSilva, Carlson, et al., 2018; Figure 5; but see Prang, 2015b). This combination of having a rather high declination angle but low torsion angle is unknown in any other hominin talus; the functional implications remain unclear. The talar head of U.W. 88-99 is quite large relative to the trochlear body (Zipfel et al., 2011). DeSilva et al. (2013) hypothesized that this large talar head might facilitate motion along the medial column of the foot. However, Prang (2016a, 2016b, 2016c) found that the dorsoplantar curvature of the head was exceptionally low, suggesting that instead of mobility, the large talar head indicated a more rigid medial column of the foot in *A. sediba*—we have no objections to this interpretation. A multivariate analysis of talar dimensions found that the U.W. 88-98 talus was intermediate between apes and humans (Zipfel et al., 2011), and a geometric morphometrics study of the *A. sediba* talus positioned it just outside gorilla shape space (DeSilva, Carlson, et al., 2018). Prang (2016a, 2016b, 2016c) also found the *A. sediba* talus to be quite gorilla-like in multivariate shape space. Interestingly, in those same studies, the geologically older *A. afarensis* tali (A.L. 288-1 and A.L. 333-147) cluster with modern humans.

The base of the Mt4 (U.W. 88-22) is dorsoplantarly tall, as found in humans, but has ape-like convexity (Zipfel et al., 2011; DeSilva et al., 2013; Figure 14). Humans typically have a dorsoplantarly flat Mt4 base, as does every other early hominin Mt4 discussed in this review (DeSilva, 2010; Ward et al., 2011; Figure 14). A dorsoplantarly convex Mt4 is present in monkey and ape feet and is a skeletal correlate of the lateral tarsometatarsal dorsiflexion of a primate midtarsal break (DeSilva, 2010). While humans have long been thought to lack a midtarsal break (Elftman & Manter, 1935), more recent work finds that some humans can occasionally produce a midtarsal break (Bates et al., 2013; Crompton et al., 2012; DeSilva & Gill, 2013). Those humans that do produce a midtarsal break possess a more dorsoplantarly convex Mt4 than those with a more rigid lateral midfoot (DeSilva et al., 2015), indicating that *A. sediba* almost certainly possessed a midtarsal break.

While many foot elements of *A. sediba* remain undiscovered, what has been recovered is consistent with a foot well-adapted for arboreality, and functionally consistent with a unique form of bipedal walking. While the ankle is orthogonal to the long axis of the tibia, and the foot is everted, as it is in humans, the exceptionally thick medial malleoli of the distal tibia are evidence that *A. sediba* routinely loaded its foot in inversion (DeSilva et al., 2013; DeSilva, Carlson, et al., 2018; Zipfel et al., 2011), perhaps during climbing bouts. The high convexity of the subtalar joint is consistent with ape-like eversion and inversion; anatomies of the calcaneus and Mt5 suggest that *A. sediba* had well-developed *M. peroneus longus*, *M. flexor digitorum brevis*, *M. flexor digiti minimi*, and *M. abductor digiti minimi*, muscles that would assist a climbing *A. sediba* (DeSilva, Carlson, et al., 2018; Zipfel et al., 2011). Furthermore, a midtarsal break would help the foot mold around branches during arboreal travel (Meldrum, 1991). These foot anatomies are consistent with other anatomies of the upper limb that indicate climbing was an important part of the locomotor repertoire of *A. sediba* (Churchill et al., 2013; Rein, Harrison, Carlson, & Harvati, 2017).

However, adaptations for frequent and skilled climbing would necessarily impact terrestrial, bipedal gait mechanics. DeSilva et al. (2013) proposed that *A. sediba* hyperpronated when it walked. This model of walking hypothesizes that *A. sediba* inverted its foot during the swing phase of gait and landed on the outside edge of an inverted foot, maximizing substrate contact with the base of a gracile calcaneus and with the lateral midfoot. Ground reaction forces would rapidly pronate the foot, resulting in excessive medial weight transfer (toward the big toe). Hyperpronation relaxes the ligaments of the midfoot and is a predictor (along with a flat foot) of a midtarsal break in modern humans (DeSilva & Gill, 2013), perhaps helping explain the presence of the convex Mt4 base in *A. sediba*. In humans, a midtarsal break increases hallucal metatarsophalangeal dorsiflexion (i.e., the foot is "floppy"), making push-off less effective (Bates et al., 2013; DeSilva et al., 2015). A digital reconstruction of the proposed mechanism of gait in *A. sediba* can be visualized in Zhang and DeSilva (2018).

The *A. sediba* foot fossils are perplexing. Along with the Burtele foot (Haile-Selassie et al., 2012), they demonstrate that there were multiple foot forms, and biomechanically different modes of walking in the Plio-Pleistocene. While the hyperpronation hypothesis (DeSilva et al., 2013) appears internally consistent with the remains that have been recovered to date, it is subject to revision or refutation as new fossils are recovered and analyzed, and further experimental studies inform the functional implications of the *A. sediba* foot anatomy.

3.10 | *Paranthropus robustus* (Kromdraai, Swartkrans, Drimolen; 1.0–2.0 Ma)

The foot of *P. robustus* is known from a talus (TM 1517d), cuboid (SKX 31899), Mt1 (SK 5017, SK 1813, and DNH 115), Mt3 (SKX 247 and SKX 38529), Mt5 (SKX 33380), and pedal phalanges (SKX 45690, DNH 117, and TM 1517k). These remains are derived from the 1.0–2.0 Ma Kromdraai, Swartkrans, and Drimolen localities in South Africa. The talus and a possible hallucal distal phalanx (see below) were found in association with the type specimen (TM 1517) of *P. robustus* at Kromdraai, South Africa (Broom, 1938; Broom, 1943a, 1943b). The other fosils, however, were found in isolation and referral to *P. robustus* and not to *Homo* (also present at Swartkrans and Drimolen) is subject to scrutiny and reassessment as associated material is recovered. Anatomies discussed below are based on published sources and observations we made on the original fossil material. Several pedal remains originally hypothesized to be hominin are not. These include the following:

- TM 1517h,i,j,l,m,n,o—manual and pedal remains are cercopithecoid (Day & Thornton, 1986). Furthermore, the TM 1517k distal phalanx is treated by some as hallucal (e.g., Day & Thornton, 1986), but as a pollical by Kivell et al. (2015). We are unconvinced this is a hallucal distal phalanx.

FIGURE 24 Composite foot skeleton (mirrored when necessary to reflect right side) constructed with pedal remains often attributed to *Paranthropus robustus*. Little is known about the foot skeleton of *P. robustus* and the attribution of many of these remains (e.g., cuboid and Mt5) is tentative. Shown here are the talus (TM 1517d), cuboid (SKX 31899), Mt1 (SKX 5017), PP1 (SKX 42650), DP1 (TM 1517k), Mt3 (SKX 247), Mt5 (SKX 33380)

- Cuboid KB 3133 (Thackeray, de Ruiter, Berger, & van de Merwe, 2001) is from a cercopithecoid (Harcourt-Smith et al., 2014; Skinner, Kivell, Potze, & Hublin, 2013).
- Calcaneus KB 3297 (Thackeray et al., 2001) is from a cercopithecoid (Kuo et al., 2013; Skinner et al., 2013).
- Medial cuneiform SKX 31117 (Susman, 1989) is not a hominin medial cuneiform (see Jashashvili et al., 2010 and detailed notes in Ditsong Museum by W. Harcourt-Smith).

Attempts to infer the functional morphology of the *P. robustus* foot are complicated by relatively few confidently attributed pedal remains (Figure 24). Our descriptions below are based only on the Kromdraai and Swartkrans fossils; requests to access the Drimolen fossils were denied.

The talus of *P. robustus* (TM 1517d) is generally human-like (Le Gros Clark, 1947; but see Lisowski, Albrecht, & Oxnard, 1974), and possesses a low talar axis angle (DeSilva, 2009), which would position the foot in an everted set. The trochlear body is not wedged (DeSilva, 2008; Figure 4). However, the head/neck torsion angle is low and the horizontal angle high (ape-like; Table 3). Additionally, there is a well-developed trochlear keel (proximodistally oriented groove along the midline of the trochlear body) and the fibular facet flares laterally, similar to anatomies found in Koobi Fora, Kenya tali assigned to *P. boisei* and to OH 8 (Gebo & Schwartz, 2006). Christie (1990) also found the curvature of the talar trochlea to resemble OH 8. These anatomies differ from the SKX 42695 talus (Susman, de Ruiter, & Brain, 2001) making it probable that the Swartkrans talus belongs to *Homo*. The most notable anatomy of TM 1517 is the exceptionally large talar head, which is especially mediolaterally wide relative to the talar trochlear width (Figure 5). The functional implications of this anatomy remain unknown. Internal analysis of the trabecular bone of TM 1517 is generally ape-like, though highly oriented struts in the anteromedial portion of the talar body are consistent with human-like medial weight transfer toward the hallux and perhaps push-off from the transverse axis of the foot (Su & Carlson, 2017).

However, the Mt1—known from complete specimens SKX 5017 (Susman & Brain, 1988) and SK 1813 (Susman & de Ruiter, 2004)—complicates this human-like picture of gait in *P. robustus*. A multivariate analysis (Zipfel & Kidd, 2006) found the morphology of Mt1 fossils SK 1813 and SKX 5017 to be intermediate between apes and humans. While the Mt1 heads of SK 1813 and SKX 5017 are domed, the dorsum is mediolaterally narrow, implying a reduced role of the hallux in propulsion (Susman & Brain, 1988; Susman & de Ruiter, 2004), or at least a less developed windlass mechanism. Furthermore, a study of the trabecular architecture in the Mt1 heads of *P. robustus* (Komza, 2017) finds a pattern unlike that of modern humans and suggestive of a unique form of walking with a less stereotypical loading and possibly a more diverse locomotor repertoire. The Mt1 bases are also unlike that found in modern humans. A geometric morphometrics study (Proctor, 2010b; Proctor, Broadfield, & Proctor, 2008) found the bases of SK 1813 and SKX 5017 to be the most ape-like amongst fossil australopiths in curvature and oblique orientation. Vernon (2013) also found the base of the Mt1 from Drimolen DNH 115 to be gorilla-like. Proctor (2010a, 2010b) proposed that the hallux of *P. robustus* may have been moderately divergent and used for grasping, though we note the presence of a facet for the Mt2 on the base of SKX 5017, indicating that hallucal divergence, if present, would have been minimal. However, Haile-Selassie et al. (2012) also noted similarities between the quite primitive Mt1 from the Burtele foot and those assigned to *P. robustus*. Finally, we note that both SK 1813 and SKX 5017 are remarkably short and stout (Figure 11). While apes tend to have more slender Mt1s, these fossils are even more extreme in the human direction in measures of shaft robusticity (Pontzer et al., 2010; Figure 11). Thus, the Mt1 anatomy of *P. robustus* is unique amongst hominins, with an ape-like base, short stout shaft, and australopith-like domed (but ML narrow) head.

The lateral foot is generally human-like and derived in *P. robustus*. A damaged (burned; Pickering, Heaton, Throckmorton, Prang, & Brain, 2017) cuboid (SKX 31899) is human-like in possessing a dorsoplantarly flat Mt4 base, indicative of a stiff lateral midfoot. SKX 247 was originally identified as an Mt3 (Susman, 1989), but then proposed to be an Mt2 (Proctor, 2010a; Susman et al., 2001), and if so, it is quite ape-like (Proctor, 2010a). However, there is a single dorsal facet laterally and paired facets medially, a morphology more consistent with an Mt3 (Deloison, 2003). As an Mt3, SKX 247 possesses a relatively tall base (Figure 13). The Mt5 (SKX 33380) has a human-like laterally deflected shaft and a dorsally domed head behind which is a prominent sulcus. The shaft has thick, ape-like cortex, but human-like bending properties (Dowdeswell et al., 2016). Suggestions that this Mt5 has an insertion for *M. peroneus tertius* (Sarmiento, 1998; Susman, 1988) have been questioned (Eliot & Jungers, 2000).

FIGURE 25 Foot fossils we attribute to *Paranthropus aethiopicus/boisei*. Left: composite foot (mirrored when necessary to reflect right side) constructed using size-scaled calcaneus (Omo 33-74-896), talus (KNM-ER 1464), and Mt3 (KNM-ER 1823). To the right is the OH 8 foot, which is from the left side. As described in the text, this foot, often attributed to *Homo habilis*, has affinities with *Paranthropus* and in our view is more likely to be from *P. boisei*. These affinities are found primarily in the talus and the Mt1. Photo of OH 8 courtesy of Jackson Njau

Many questions remain about the foot of *P. robustus*, and these will require additional fossils to address (e.g., little is known about the tarsals). However, even based on the fossils currently assigned to this taxon, there are questions. Did *P. robustus* possess a grasping hallux (Proctor, 2010b) and what are we to make of the similarities between the Burtele Mt1 and those from *P. robustus* (Haile-Selassie et al., 2012)? In regards to medial weight transfer, why are mixed functional signals coming from the ankle joint and the Mt1? And perhaps most pressing is the question of whether all of these fossils have been correctly assigned to *P. robustus*. Associated material is sorely needed.

3.11 | *Paranthropus aethiopicus/boisei* (Omo, Koobi Fora, Olduvai; 1.6–2.3 Ma)

It is possible that *P. aethiopicus* and *P. boisei* are a single evolving lineage of Eastern African robust australopiths (e.g., Alemseged, Coppens, & Geraads, 2002) and are treated together here. As with *P. robustus*, it is difficult to confidently attribute any isolated pedal remains to an Eastern African robust hominin given spatial and temporal overlap with fossil *Homo*. Perhaps the most certain *P. boisei* pedal fossil is an Mt3 associated with the female robust skeleton KNM-ER 1500 (Grausz, Leakey, Walker, & Ward, 1988) though caution is urged in even assigning this partial skeleton to *P. boisei* (Wood & Constantino, 2007). After granting the uncertainty of assigning any of these fossils to *P. boisei*, we regard the following as probable pedal elements from the Eastern African robust hominin lineage: calcaneus (Omo-33-74-896); talus (KNM-ER 1464 and KNM-ER 1476); Mt2 (Omo 323-1976-2,117); Mt3 (KNM-ER 1500, KNM-ER 997, KNM-ER 1823, OH 43, Omo F.511-16); and Mt4 (OH 43). KNM-ER 1500t, a "calcaneus" (Leakey & Leakey, 1978) associated with the possible *P. boisei* partial skeleton is not a hominin calcaneus (pers. obs.; note from M. Hausler in KNM). Additionally, as we discuss below, we agree with others (Gebo & Schwartz, 2006; Wood, 1974a) that the OH 8 ft is more likely to be from a *P. boisei* than from *H. habilis*, as is traditionally suggested (e.g., Leakey et al., 1964; Figure 25). Anatomies discussed below are based on published sources and observations we made on the original fossil material.

Omo-33-74-896 is a 2.36 Ma calcaneus from the Omo-Shunguru Formation in Ethiopia (Figure 2; Table 2), suggested by some to belong to *Paranthropus* (Deloison, 1986; Howell, Haesaerts, & de Heinzelin, 1987). At this age, it would be attributed to *P. aethiopicus* (Suwa, White, & Howell, 1996). Others suggest it may belong to *Homo*, however (Gebo & Schwartz, 2006). The calcaneus is well preserved distally, but the proximolateral portion of the tuber is sheared away, preventing any characterization of the position or size of the lateral

plantar process. The peroneal tubercle is large and quite proximally positioned. On the original bone, there is a palpable retrotrochlear eminence forming just lateral to the peroneal trochlea and deflecting proximoplantarly, suggesting to us that the lateral plantar process (if preserved) would have been plantarly positioned as it is in humans (Latimer & Lovejoy, 1989; Zipfel et al., 2011). However, the medial plantar process is large and beak-shaped, as is the case in the apes, and proposed to be functionally related to an enhanced role for the superficial head of *M. flexor digitorum brevis* during pedal grasping (Sarmiento, 1983). The groove for the tendon of *M. flexor hallucis longus* is also quite wide. The preserved portion of the tuber is gracile, making it more like apes and *A. sediba* than humans and *A. afarensis*, though relative to the size of the posterior talar facet, the cross-sectional area of the tuber falls within the human distribution (Prang, 2015a). The posterior talar facet is relatively flat and human-like, suggesting reduced mobility at the subtalar joint (Prang, 2016b; Zipfel et al., 2011). The orientation of the sustentaculum tali (Harcourt-Smith et al., 2015) and the plantar tilt of the calcaneocuboid joint (Berillon, 2003) are both consistent with a longitudinally arched foot, though the cuboid facet would indicate a low arch by modern human standards (Heard-Booth, 2017). An anterolateral process and proximally prolonged facet for the cuboid beak are evidence for a human-like locking mechanism at the calcaneocuboid joint (Bojsen-Møller, 1979; Elftman & Manter, 1935) though these anatomies are not as well-developed in Omo-33-74-896 as in humans today (Gebo & Schwartz, 2006).

There are four complete fossil tali from the 1.6–1.88 Ma KBS formation of Koobi Fora, Kenya: KNM-ER 813, KNM-ER 1464, KNM-ER 1476, and KNM-ER 5428. KNM-ER 813 is similar to the human talus (Wood, 1974b) and probably belongs to fossil *Homo*. KNM-ER 5248 is from *H. erectus* (Boyle & DeSilva, 2015) based on its large size, human-like anatomies, and similarities to the KNM-ER 803 fragmentary talus from the *H. erectus* partial skeleton (Day & Leakey, 1974). In contrast, KNM-ER 1464 and KNM-ER 1476 are quite distinct from ER 813 and ER 5428. They both possess deeply grooved trochlear surfaces, laterally flaring fibular facets, and a medial twist to the head and neck relative to the long axis of the trochlear body (Figure 4). KNM-ER 1464 was discovered at the 1.59 Ma Ileret locality 6A (McDougall et al., 2012), which only has yielded *Paranthropus* craniodental remains (Grausz et al., 1988). Most, therefore, regard these tali as belonging to *Paranthropus* (e.g., Gebo & Schwartz, 2006; Wood & Constantino, 2007; Wood & Leakey, 2011; Boyle & DeSilva, 2015). These tali have a high horizontal angle, intermediate torsion angle, and low declination angle (Figure 5; Table 3). The deeply grooved trochlea may be evidence for an osteological, rather than a ligamentous, means of stabilizing the ankle in the robust australopiths compared with *Homo* (DeSilva, 2008). The internal trabecular bone of KNM-ER 1464 is ape-like in many respects, though it has a decidedly human-like anteromedial region corresponding to medial weight transfer through the ankle (Su, Wallace, & Nakatsukasa, 2013) as was also evident in the *P. robustus* talus TM 1517 (Su & Carlson, 2017). Trabecular bone was not quantifiable in KNM-ER 1476 (Su et al., 2013). These tali (ER 1464 and ER 1476) share features (e.g., deeply keeled trochlea, medial twist to head and neck; relatively large talar head) with OH 8, suggesting that the Olduvai foot is also from a robust australopith (Gebo & Schwartz, 2006; Wood, 1974a).

A newly described Mt2 (Omo 323-1976-2117) is human-like in base robusticity, and base angulation in both the transverse and sagittal planes (Daver et al., 2018). Only head torsion is low and just outside the human range (Daver et al., 2018); internal head torsion has been suggested to be a skeletal indicator of a relatively low medial longitudinal arch in early hominins (DeSilva, Proctor, & Zipfel, 2012), a hypothesis supported by recent data correlating Mt2 torsion with flat-footedness (Kitashiro et al., 2017).

Third metatarsals from Koobi Fora (KNM-ER 997, ER 1823) may belong to *Homo* or *Paranthropus*, though ER 1823 was recovered at Ileret 6A, which has only yielded *Paranthropus* craniodental remains (Grausz et al., 1988; Wood & Constantino, 2007). KNM-ER 1823 has a slightly mediolaterally concave base, which makes it look like an Mt2, and some have suggested it is (e.g., Daver et al., 2018). While it is possible, we regard the high external torsion of the shaft as evidence that it is an Mt3 (Day et al., 1976). The base of the Mt3 of KNM-ER 1500 is dorsoplantarly tall and slightly convex; whereas the third metatarsal from Omo F.511-16, which may be from *Homo* (Coppens, 1975), has a similarly dorsoplantarly tall base, and a prominent lateral tubercle to help stabilize the lateral column of the foot. Two very small, and quite fragmentary left Mts3–4 were also found in Bed I of FLKNN at Olduvai (Day, 1973; Njau & Blumenschine, 2012; Wood, 1974a) but they yield very little information at the current time.

There is no partial foot skeleton definitively attributed to *P. boisei*. However, the similarities between the *P. boisei* tali KNM-ER 1464 and KNM-ER 1476 to the OH 8 talus have suggested to some that OH 8 is best allocated to *P. boisei* and not *H. habilis* (Gebo & Schwartz, 2006; Wood, 1974a). We agree and regard the preliminary announcement of KNM-ER 64062, the 1.82–1.86 fossil *Homo* foot from Ileret, Kenya (Jungers et al., 2015) as further evidence that OH 8 is not from *Homo* and is instead a *P. boisei* foot. Both the Ileret foot and the early *Homo* talus from Dmanisi (D4110) lack the deeply grooved trochlea and medial twist to the head and neck that characterizes *P. boisei* and OH 8 (Jungers et al., 2015; Pontzer et al., 2010). We may be wrong, but we proceed as though OH 8 is a robust australopith foot and present the current understanding of this historically important fossil below.

3.12 | OH 8

OH 8 was first announced in 1960 (Leakey, 1960) and included in the *H. habilis* hypodigm (Leakey et al., 1964). After decades of using modern primate models to infer human foot evolution, the OH 8 foot finally gave paleoanthropologists insight into the anatomy of the foot of early hominins. It is comprised of all of the tarsals (though the proximal calcaneus has been torn away), and all metatarsals (all missing the distal ends; Figure 24). No phalanges were recovered. The anatomy was preliminarily described by Day and Napier (1964) and OH 8 has been intensively studied by scholars of human foot evolution for the last half century, though a proper anatomical description of OH 8 has never been done. While Day and Napier (1964) found the OH 8 foot to be quite human-like and others have concurred (Susman, 1983;

Susman & Stern, 1982), Oxnard and Lisowski (1980) claimed to find errors in the original reconstruction and regard the foot as more ape-like, as did Lewis (1980c). While most scholars find the Day and Napier (1964) interpretation of OH 8 to be compelling, there is an opportunity to use modern scanning and reconstruction techniques to assess these two competing OH 8 models. The anatomy described below is based on published scholarship and on our observation of the original fossil.

OH 8 is regarded by many to belong to *H. habilis* (Leakey et al., 1964; Susman, 2008; Susman & Stern, 1982); we regard it as more likely to be the foot of *P. boisei*, as others have suggested (Gebo & Schwartz, 2006; Wood, 1974a). The anatomical basis for this assignation is discussed in more detail below, but it is based primarily on the talus and the Mt1. There is also a related disagreement regarding the chronological age of the OH 8 individual. Some have proposed that OH 8 is a juvenile and that it is associated with the subadult *H. habilis* type OH 7, and with OH 35 (Susman, 2008; Susman, Patel, Francis, & Cardoso, 2011; Susman & Stern, 1982). While superficially the OH 8 foot and the OH 35 tibia appear to articulate well, the joint surfaces are not congruent (Aiello, Wood, Key, & Wood, 1998; Wood, Aiello, Wood, & Key, 1998) and geologically, they were found in different horizons, 300 yards from one another (Day & Napier, 1964; Njau & Blumenschine, 2012).

Nevetheless, the thrust of the argument is that OH 8 is associated with OH 7, and is therefore a juvenile *H. habilis*. This interpretation of the material is based on what are perceived to be unfused metatarsal heads of the Mt2 and Mt3 (Susman, 2008). However, these metatarsals have carnivore tooth marks on them, just millimeters from the missing metatarsal heads (Njau & Blumenschine, 2012; Figure 24), making it probable that the metatarsal heads are missing not because OH 8 was a juvenile, but because the heads (and toes) were torn off and consumed by a predator. Furthermore, while variation surely exists (Susman et al., 2011), at the developmental age of OH 7, the base of the OH 8 Mt1 should be either unfused or in the process of fusing, but instead the proximal epiphysis is fully fused and the epiphyseal line is obliterated (DeSilva et al., 2010; Weiss, DeSilva, & Zipfel, 2012). Additionally, there are osteophytic growths along the cotylar fossa, the dorsum of the lateral cuneiform, and along the lateral intermetatarsal facets, consistent with age-related osteoarthritis (Weiss, 2012). We therefore are of the opinion that OH 8 is an adult foot (Day, 1986; Leakey, 1971), though others strongly disagree (Susman et al., 2011). The importance of characterizing the age of this individual lies not only in accurately interpreting the functional anatomy, but also in assessing the likelihood that the OH 8 foot is associated with OH 7, the type of *H. habilis*. Morphology aside (but see below) if OH 8 was a juvenile, given the proximity of these bones to the OH 7 hand and craniodental material, we agree that it would most reasonably be assigned to that individual (and that taxon). However, as an adult, and therefore a different individual from the juvenile OH 7, it is no more likely to be from *H. habilis*, than from *P. boisei*, also known from Olduvai FLKNN Bed I.

The OH 8 calcaneus is badly damaged proximally and plantarly, but preserves most of the subtalar joint and all of the calcaneocuboid joint. A multivariate analysis of the subtalar joint complex found OH 8 to be human-like (Prang, 2016b). The cuboid facet is plantarly angled as in the arched human foot (Berillon, 2003; Heard-Booth, 2017), has a dorsolateral overhang and a proximomedially prolonged facet for the beak of the cuboid, which would lock the calcaneocuboid joint during bipedal propulsion (Bojsen-Møller, 1979; Day & Napier, 1964; Kidd et al., 1996; Lewis, 1980c; Susman & Stern, 1982). The cuboid is human-like in 3D shape space (Harcourt-Smith, 2002); it is proximodistally elongated (Figure 7), has an eccentrically positioned beak, flat, human-like facets for the lateral metatarsals, and a human-like os peroneum facet (Lovejoy et al., 2009).

However, the talus is quite different from both the modern human talus, and Early Pleistocene tali assigned to *Homo* (see below), including Omo 323-76-898 (Gebo & Schwartz, 2006), KNM-ER 813 (Wood, 1974b), KNM-ER 5428 (Boyle & DeSilva, 2015), KNM-ER 803 (Leakey, 1973), and D4110 (Pontzer et al., 2010). Instead, the OH 8 talus is similar to two tali typically assigned to *P. boisei* (KNM-ER 1464 and ER 1476), and to TM 1517 from *P. robustus*. The trochlear body is deeply grooved and has a high lateral rim, as does the KNM-ER 1464 talus (Boyle & DeSilva, 2015; Gebo & Schwartz, 2006; Pontzer et al., 2010). Additionally, the head and neck are medially twisted relative to the trochlear body, as in KNM-ER 1464 and KNM-ER 1476 (Boyle & DeSilva, 2015). Day and Wood (1968) noted that the horizontal and declination angles of OH 8 were more ape-like, and that unlike either humans or apes, the curvature of the lateral and medial rims would lead to foot adduction, rather than abduction, during dorsiflexion. In the first multivariate study of the OH 8 talus, Lisowski et al. (1974) found it grouped with TM 1517 and amongst modern taxa, closer to orangutans than to modern humans. More recent work clusters the OH 8 talus closer to humans, but still outside the range of modern variation and near KNM-ER 1464 (Harcourt-Smith, 2002); while a study of the angulation of the facets found OH 8 to be within the human distribution (Parr et al., 2014). However, Lewis (1980c) and Kidd et al. (1996) regarded the horizontal angle to be so ape-like as to indicate a semi-divergent hallux, a suggestion that is not widely accepted (see below).

The OH 8 navicular is generally human-like (Harcourt-Smith, 2002; Aiello and Harcourt-Smith, 2004, but see Kidd et al., 1996). The facets for the cuneiforms angle in a manner that is consistent with a longitudinal arch of the foot (Berillon, 2003), and the plantar portion of the navicular is well-developed for the insertion of the spring ligament (Susman & Stern, 1982). Prang (2016b) found the talonavicular joint to be human-like in OH 8 and later (Prang, 2016c) applied a geometric morphometrics analysis on the OH 8 navicular and found it to be quite modern human-like as well. The lateral cuneiform is proximodistally expanded (Susman & Stern, 1982; Figure 10), as is the intermediate cuneiform (Figure 9). The medial cuneiform possesses a distally oriented and mildly convex facet for the Mt1 (Gill et al., 2015), consistent with an adducted hallux (Day & Napier, 1964; Preuschoft, 1971; Susman & Stern, 1982; Figure 8; Table 6; but see Lewis, 1972; Lewis, 1980c).

Day and Napier (1964) reported that the OH 8 ft had an unusual pattern of metatarsal robusticity: 1 > 5 > 3 > 4 > 2, and used these data to suggest that the modern human striding gait "had not yet been achieved." It is typical in humans for the lateral digits (Mt4 and Mt5) to be more robust than Mt2 or Mt3. However, Archibald, Lovejoy, and Heiple (1972) described greater variation in human metatarsal

robusticity patterns and found the OH 8 ft to be fully consistent with a human-like gait. More recently, Patel et al. (2018) have revisited this problem with a larger sample and a μCT approach that permitted the quantification of cross-sectional properties and found the OH 8 pattern to most commonly be 1 > 3 > 5 > 4 > 2, which is different from the typical human condition (1 > 4/5 > 2/3) or ape one, suggesting that OH 8 loaded its foot in a biomechanically unique manner.

The Mt1 of OH 8 has a human-like base (Proctor, 2010b) and a large contact facet for the Mt2 (Le Minor & Winter, 2003). However, the reconstructed length of the Mt1 (White & Suwa, 1987) is quite short and dorsoplantarly robust (Pontzer et al., 2010), most similar to SK 1813 and SKX 5017 (McNutt, Zipfel, & DeSilva, 2018; Figure 11), Mt1s assigned to *Paranthropus robustus*. The Mt2 and Mt3 have dorsoplantarly tall bases, similar to the modern human condition (McNutt, Zipfel, & DeSilva, 2018; Figures 12 and 13), and torsion values close to that of modern humans (Pontzer et al., 2010). The Mt4 has a dorsoplantarly tall and flat base, consistent with tarsometatarsal rigidity (DeSilva, 2010). The Mt5 is damaged laterally and medially possesses a large osteophytic growth (DeSilva et al., 2010), which has been hypothesized to be the result of trauma (Susman & Stern, 1982).

For a foot that has been known for over a half century (Day & Napier, 1964), it is remarkable how much disagreement swirls around OH 8. For some, OH 8 is a subadult *H. habilis* (e.g., Susman, 2008); for others, an adult *P. boisei* (DeSilva et al., 2010; this article). Nevertheless, most agree that OH 8 was human-like in many respects, and had an adducted hallux, locking calcaneocuboid joint, and a longitudinal arch (but see Lewis, 1980c). However, the large talar head (Figure 4), deeply grooved talar trochlea (Gebo & Schwartz, 2006; Figure 5), short Mt1 (McNutt, Zipfel, & DeSilva, 2018; Figure 11), and unique robusticity pattern (Patel et al., 2018) may suggest a unique loading regime and perhaps different gait kinematics. The relationship between these anatomies and foot function should be examined regardless of whether OH 8 is early *Homo* or *Paranthropus*. The Ileret foot (KNM-ER 64062) will make an important functional and taxonomic comparison to OH 8, given that they have both been attributed to early *Homo* and are roughly contemporaneous. Yet, given the possibility of multiple early *Homo* species (Leakey et al., 2012), our failure to securely identify the OH 8 foot demonstrates how valuable a *P. boisei* skeleton will be to our science.

3.13 | Early *Homo*

The origins of our genus remain quite a contentious topic; craniodental evidence suggests that *Homo* may have originated in the late Pliocene (Villmoare et al., 2015). However, there is relatively little known about the foot of the earliest members of our genus prior to ~2 Ma. Furthermore, in the absence of partial skeletons, there is the difficulty of assigning isolated pedal remains to either *Paranthropus* or *Homo* as best illustrated by OH 8 (see above). And even if isolated remains can be reasonably assigned to *Homo*, the increasing likelihood of taxonomic diversity within early *Homo* (e.g., Leakey et al., 2012) makes it even more difficult to assign pedal remains to *H. habilis*, *H. rudolfensis*, or early *H. erectus* (=*ergaster*). Unfortunately, the best represented early *Homo* skeleton—KNM-WT 15000—does not preserve any foot bones (a fragmentary and admittedly dubious "Mt1" [Walker & Leakey, 1993] is probably not). Below, we review what is known about the foot of early *Homo* from three partial foot skeletons/assemblages: KNM-ER 64062, Dmanisi, and KNM-ER 803, and then conclude the section by discussing isolated fossils that we suspect belong to the genus *Homo*. Anatomies discussed below are based on published sources and observations we made on the original fossil material, with the exception of KNM-ER 64062, which is still under study, and the fossils from Dmanisi.

KNM-ER 64062 is a partial foot skeleton from 1.84 Ma deposits at Ileret, Kenya (Jungers et al., 2015). Although the fossil has not yet been fully published, it promises to help resolve important questions about the foot of early members of genus *Homo*. Preserved are all of the tarsals except for the medial cuneiform, all of the metatarsals, and the proximal hallucal phalanx (Figure 26). A preliminary announcement of the fossil (Jungers et al., 2015) reveals that the calcaneus is derived and human-like in possessing a large, robust tuber and a plantarly positioned lateral plantar process. The cuboid is also described as human-like. The talus and Mt1 are described as being similar to the Dmanisi fossils (Jungers et al., 2015). Jungers (pers. comm.) informs us that while the Mt1 is adducted and has a domed head, it lacks the mediolaterally expanded dorsum typical of modern humans and instead is dorsally narrow, like the Dmanisi Mt1s and those from australopiths. Furthermore, the navicular is quite primitive and possesses an enlarged navicular tuberosity and has a dorsoplantarly narrow lateral navicular body (Jungers et al., 2015), even more so than that found in StW 573 and LB1 (Jungers, pers. comm.). A geometric morphometrics study of the metatarsal heads finds the Mt2 and Mt3 to be human-like, while the Mt1 is just outside the modern human range (Fernández et al., 2018). Comparisons between this Ileret foot and partial foot skeletons from *H. floresiensis*, *H. naledi*, and OH 8 (historically called *H. habilis*, but here hypothesized to be from *P. boisei*) will yield important insights into the foot of the earliest members of our genus, and diversity in foot forms throughout the Pleistocene.

If, as we suggest above, OH 8 is not from early *Homo*, then until the Ileret foot is published (see above), our best understanding of the foot of early *Homo* is from the 1.77 Ma site of Dmanisi, Georgia (Lordkipanidze et al., 2007; Pontzer et al., 2010). A partial adult foot is comprised of a talus (D4110), Mts3–5 (D2021, D4165, D4058) and distal phalanx (D3877; Lordkipanidze et al., 2007; Pontzer et al., 2010). Subadult foot bones (Mt1 D2671; Mt4 D2669; DP1 D2670) are associated with the D2700 juvenile skull (Lordkipanidze et al., 2007; Pontzer et al., 2010). A medial cuneiform (D4111) and Mt1 (D3442) are associated (Jashashvili et al., 2010; Lordkipanidze et al., 2007; Pontzer et al., 2010). There is finally an isolated Mt3 (D3479; Gabunia, Vekua, & Lordkipanidze, 1999; Lordkipanidze et al., 2007; Figure 26).

The talus (D4110) is human-like in most respects (Lordkipanidze et al., 2007; Pontzer et al., 2010). The talar trochlea is mediolaterally flat, as is common in fossils from *Homo*, but differs from the trochlear surface in OH 8 and KNM-ER 1464 (Pontzer et al., 2010). The head/neck horizontal angle is similar to that found in other fossil *Homo* (26°), on the high end of the modern human range (Lordkipanidze et al., 2007). The talus has a human-like declination angle, consistent with a longitudinal arch (Pontzer et al., 2010). The head/neck torsion angle has not been reported. There is some moderate flaring of the

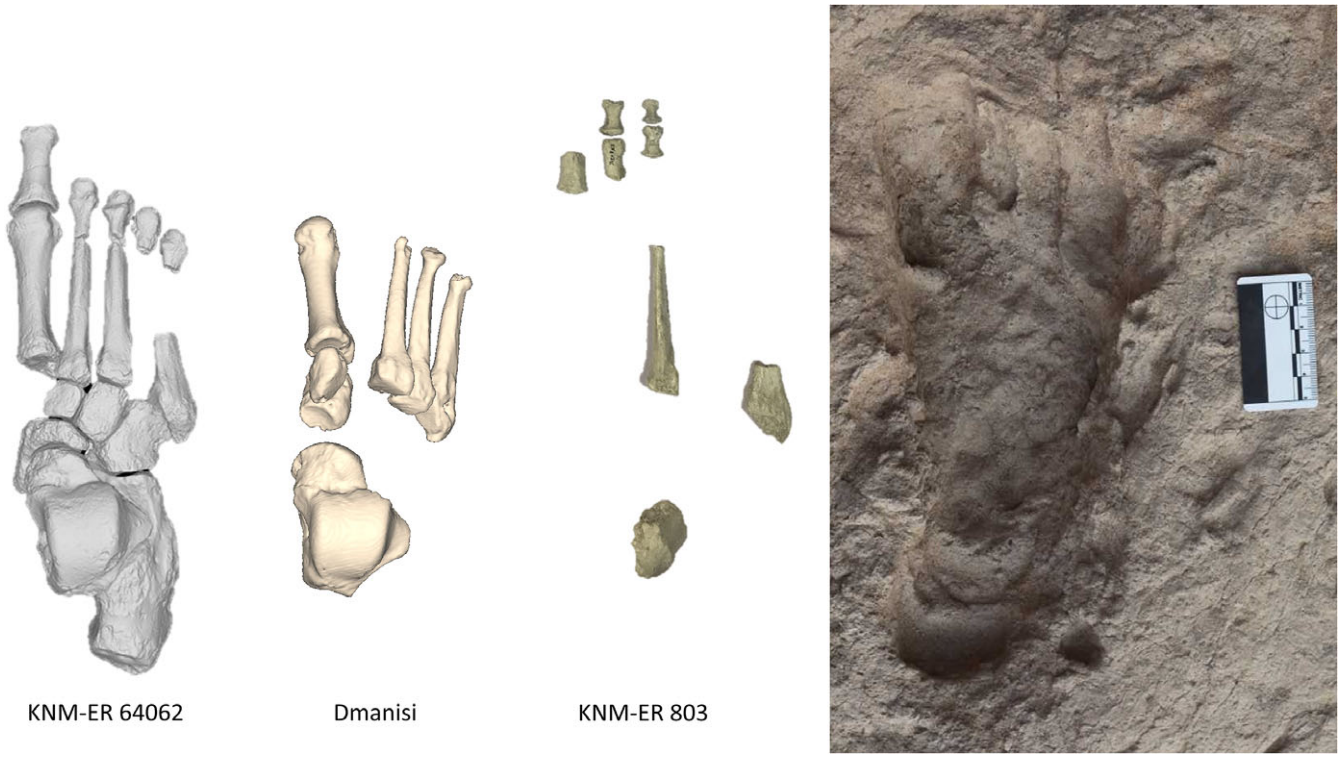

FIGURE 26 Foot of early *Homo*. The foot skeleton of the earliest members of the *Homo* genus are known from KNM-ER 64062, the 1.77 Ma Dmanisi fossil locality, and KNM-ER 803. The fossil feet have been scaled so that they are roughly the same size and reversed (if necessary) to present the right side. To the far right is a single right footprint from the 1.55 Ma Ileret track way, thought to have been made by *H. erectus*. KNM-ER 64062 image thanks to W. Jungers and the Turkana Basin Institute. Dmanisi image courtesy of C. Zollikofer and M. Ponce de León. The Ileret footprint photo was provided by K. Hatala

fibular facet (Pontzer et al., 2010), and well-developed proximoplantar tubercles at the base of an obliquely oriented groove for *M. flexor hallucis longus* (Lordkipanidze et al., 2007), though this feature is highly variable in human tali (Pontzer et al., 2010).

The medial cuneiform (D4111) is bipartite, which happens, but is unusual, in modern human medial cuneiforms (Jashashvili et al., 2010). Although it is consistent with an adducted hallux, D4111 is said to differ in shape from modern human medial cuneiforms (Jashashvili et al., 2010). The base of the Dmanisi Mt1 is divided into plantar and dorsal facets similar to the morphology of A.L. 333-54 (Pontzer et al., 2010); though the Dmanisi Mt1 base is much flatter. The base is dorsoplantarly tall, indicating the presence of strong plantar ligaments (Lordkipanidze et al., 2007). However, the Mt1s are short compared with the lateral metatarsals (Pontzer et al., 2010). Furthermore, although the shafts have human-like robusticity, the heads are dorsally narrow (Lordkipanidze et al., 2007; Pontzer et al., 2010), similar to the anatomy found in australopith Mt1s (e.g., Susman & Brain, 1988) and quite different from later *Homo* (BK 63), Mt1s from *H. naledi* (Harcourt-Smith et al., 2015) and *H. floresiensis* (Jungers, Harcourt-Smith, et al., 2009; Figure 11).

The lateral metatarsals (Mt3 and Mt4 especially) possess human-like external torsion (Lordkipanidze et al., 2007; Pontzer et al., 2010), demonstrating that the Dmanisi hominins had strongly developed transverse arches of the foot, and according to Pontzer et al. (2010) longitudinal arches as well. However, the shaft robusticity of these lateral metatarsals is quite different from that found in modern humans. The Mt3 has relatively high robusticity (Gabunia et al., 1999), in the range of modern chimpanzees (Pontzer et al., 2010); the Mt4 is similarly robust, unlike chimpanzees or humans (Pontzer et al., 2010); the Mt5 has quite low shaft robusticity, making it ape-like as well (Pontzer et al., 2010). A more detailed examination of the cortical structure of the Mt5 (D4058) found that the thickness and distribution of cortex was ape-like, though the cortex tapered distally as it does in humans (Dowdeswell et al., 2016). No detailed analyses of the pedal phalanges (D3877, D2670) have been published though Patel, Jashashvili, Trinkaus, Susman, and Lordkipanidze (2015) noted that D2670, a hallucal distal phalanx, possesses moderate axial torsion, but lacks human-like lateral deviation.

The early *Homo* foot as represented by the Dmanisi material is generally human-like. The morphology of the ankle joint is consistent with a human-like tibia moving primarily in the sagittal plane over a foot with an adducted hallux and a well-developed longitudinal arch. However, the head of the Mt1 suggests that early *Homo* from Dmanisi may not have possessed human-like push off capabilities, perhaps because the windlass mechanism was not fully developed. Furthermore, the lesser metatarsal shaft robusticity indicates that the foot was loaded in a different manner than in humans today. The low Mt5 (but high Mt3 and Mt4) robusticity may be related to the placement of the foot relative to the direction of travel, though this remains speculative and requires additional testing (Pontzer et al., 2010). Nevertheless, the Dmanisi fossils are important additions to our understanding of early *Homo* foot evolution. They raise important questions

about the relationship between metatarsal torsion and plantar arches—a correlation that still remains unclear. Additionally, direct comparisons between similarly aged foot material from Ileret (Jungers et al., 2015), and chronologically later material from *H. floresiensis* (Jungers, Harcourt-Smith, et al., 2009) and *H. naledi* (Harcourt-Smith et al., 2015) will help test functional and even phylogenetic hypotheses about foot evolution in the earliest members of our genus.

KNM-ER 803 (Figure 26) is a partial skeleton from 1.53 Ma deposits at Koobi Fora, Kenya regarded by most (based on associated craniodental remains) to be from *H. erectus* (e.g., Antón, 2003). The partial foot skeleton includes a fragmentary talus, Mt3 (without the head), proximal Mt5, and five pedal phalanges (Day & Leakey, 1974; Leakey, 1973; Leakey & Leakey, 1978). The talus preserves only the lateral (fibular) half, but is quite human-like. The trochlear surface is mediolaterally flat (Boyle & DeSilva, 2015), and the fibular facet is vertically inclined. The base of the Mt3 is dorsoplantarly tall relative to the mediolateral width (Figure 13). The Mt5 preserves only the base; the cuboid facet is dorsoplantarly flat and the tuberosity is only weakly developed, both morphologies found in modern human Mt5s. Perhaps most interesting about this foot are the phalanges. The intermediate phalanges are relatively (Trinkaus & Patel, 2016) and absolutely (McNutt, Zipfel, & DeSilva, 2018; Figure 17) very short, and represent some of the earliest known evidence for shortening of the intermediate phalanges from the more primitive australopith condition. Rolian et al. (2009) has collected experimental evidence that phalangeal shortening reduces energy output during running (but not walking); the toes of KNM-ER 803 would thus support hypotheses for running adaptations in *H. erectus* (Bramble & Lieberman, 2004; Holowka & Lieberman, 2018).

In addition to these three assemblages (KNM-ER 64062, Dmanisi, and KNM-ER 803) there are a number of isolated fossils that we suspect belong to the genus *Homo*. These include four tali, and four phalanges from sites in both Eastern and South Africa.

The oldest foot fossil purported to belong to the genus *Homo* is a 2.2 Ma talus (Omo 323-76-898) from the Omo Shungura formation, Ethiopia (Gebo & Schwartz, 2006). This catalogue name (Omo 323-76-898) has also mistakenly been used for a *Paranthropus* cranium (Falk, 1986; Kimbel, 1984; Kimbel & Rak, 1985), which is Omo 323-76-896 (Wood & Leakey, 2011). Gebo and Schwartz (2006) find the Omo 323-76-898 talus to be quite human-like and we agree and regard it as most likely belonging to the genus *Homo*. The trochlea is mediolaterally flat with roughly equal medial and lateral margins, giving it a human-like talar axis angle (Figure 5). The head has human-like torsion, but the Omo talus lacks the declination angle found in modern human tali, suggesting that this individual had a low arch (Peeters et al., 2013).

Similarly, the 1.85 Ma talus KNM-ER 813 is typically assigned to *Homo* (Leakey, 1973; Wood, 1974b), and more specifically *H. rudolfensis* (McHenry, 1994; Wood, 1992). A multivariate analysis of the specimen finds it securely within the modern human distribution (Wood, 1974b), making it more human-like than the similarly aged OH 8 talus (Day & Wood, 1968). The talar trochlea is human-like in its general curvature (Christie, 1990), though we note that the mediolateral surface is more grooved than in most humans. The trochlea has mild wedging (Figure 4), and roughly equal medial and lateral sides. Both the horizonatal angle and the head/neck torsion values are modern human-like (Figure 5; Table 3). The declination angle is low for a modern human, but higher than most australopiths. The internal trabecular bone is not preserved well enough for study at the current time (Su & Carlson, 2017).

A large, chronologically later (1.6 Ma) talus (KNM-ER 5428) is also from *Homo*, and more specifically *H. erectus* (Boyle & DeSilva, 2015). KNM-ER 5428 is human-like in almost all respects, clustering in a principal components analysis with modern humans (Boyle & DeSilva, 2015). It posseses a human-like trochlea that is mildly wedged and mediolaterally flat (Figure 4), making it more like KNM-ER 803 (*H. erectus*) and unlike the deeply grooved tali of KNM-ER 1464 and OH 8 (presumed *P. boisei*). The head has human-like torsion and declination, the latter anatomy suggesting a human-like longitudinal arch (Figure 5). The talus is also quite large, estimated to be from a nearly 90 kg individual (Boyle & DeSilva, 2015; McHenry, 1994). KNM-ER 5428 differs from a modern human talus in having a dorsoplantarly low body—a talar anatomy that persists right through early *H. sapiens* (Boyle & DeSilva, 2015; McNutt, Zipfel, & DeSilva, 2018). Unfortunately, the internal trabecular bone could not be isolated (Su & Carlson, 2017).

One final talus that is probably from *Homo* is SKX 42695, a fragmentary talar body without a head from the lower bank of Member 1 Swartkrans, South Africa. SKX 42695 differs from the TM 1517 talus (*P. robustus*) in its larger size, mediolaterally flatter trochlea and less flared fibular facet (Susman et al., 2001). Furthermore, the internal trabecular architecture is similar to that found in humans (DeSilva & Devlin, 2012).

In addition to these tali, there are three phalanges from Swartkrans, South Africa that are short and human-like. SKX 16699 is a proximal phalanx that is both relatively and absolutely short and straight (Trinkaus & Patel, 2016). Additionally, it has a dorsoplantarly expanded base, which may signifiy a thick plantar aponeurosis and modern human-like windlass mechanism (Trinkaus & Patel, 2016). SKX 16699 differs in these respects from DNH 117, which is longer and more curved, making it reasonable that the Swartkrans specimen is from *Homo* and the Drimolen phalanx from *P. robustus*. Additionally, intermediate phalanges SKX 344 and 1261 from Swartkrans Member 2 are very short—shorter (absolutely) than australopith intermediate phalanges, and even the *H. erectus* intermediate phalanges from KNM-ER 803 (McNutt, Zipfel, & DeSilva, 2018; Figure 17), making it reasonable to propose that they are from *Homo*. Finally, there is a distal hallucal phalanx from Olduvai (OH 10). Historically, this fossil is of importance since it harkens back to the days when early hominin fossils were so rare that an isolated distal hallucal phalanx could be published in *Nature* (Day & Napier, 1966), and more importantly, it was the first fossil subjected to a multivariate analysis (Day, 1967). OH 10 possesses both the lateral (valgus) angulation in the transverse plane of 2°, and the axial torsion (13°) associated with hallucal propulsion found in modern humans (Day, 1986; Day & Napier, 1966), making it quite human-like (Wood, 1974a). In his multivariate analysis, Day (1967) found OH 10 to cluster distinctly with modern humans, though Oxnard (1972) found OH 10 to be distinct from both humans and apes. Little additional work has been done on this fossil since.

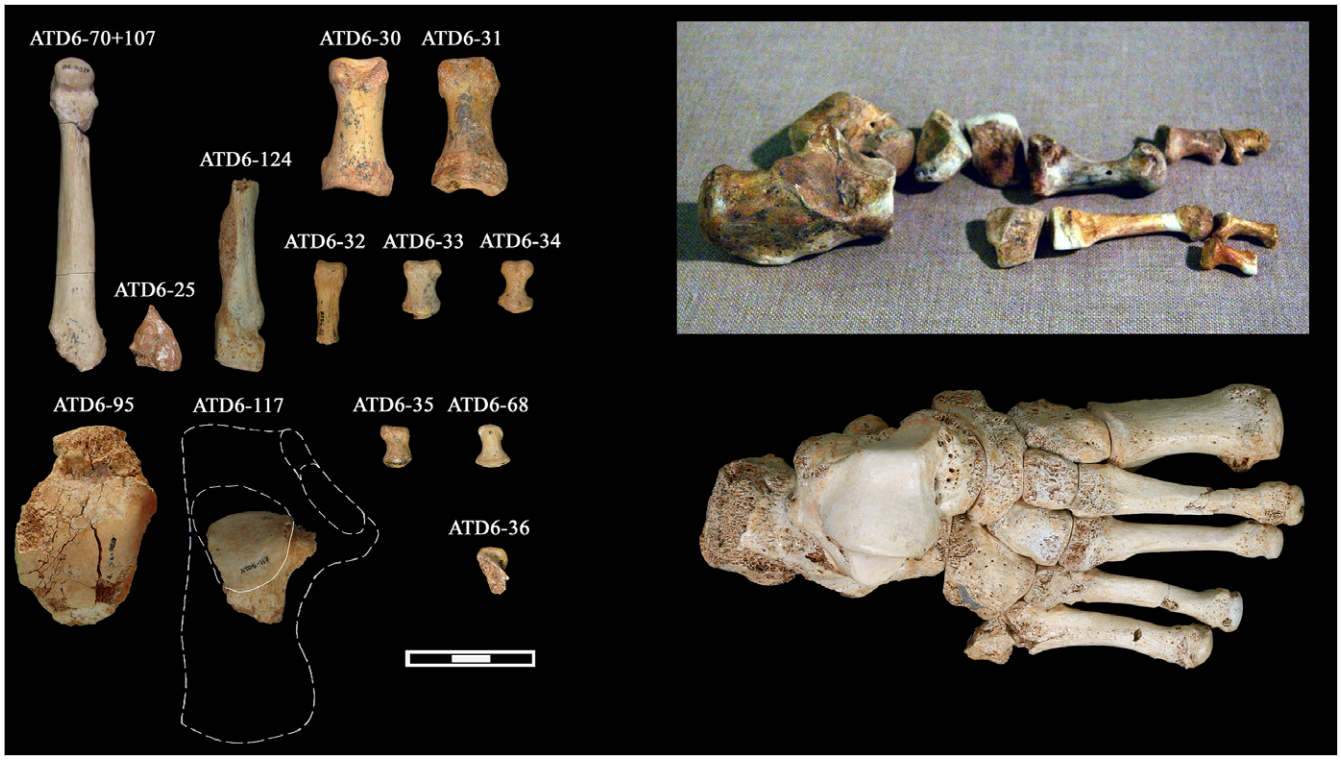

FIGURE 27 Left: Foot fossils assigned to *Homo antecessor* from the Gran Dolina locality at Atapuerca, Spain (Image courtesy of A. Pablos). Upper right: right partial foot skeleton from Jinniushan, China. Bottom right: articulated foot skeleton from Sima de los Huesos, Atapuerca, Spain (Image taken by J. Trueba, courtesy of Science Photo Library)

Fossilized footprints have been recovered in 1.4–1.5 Ma deposits at two localities near the town of Ileret in northern Kenya: GaJi10 (Behrensmeyer & Laporte, 1981) and FwJj14E (Bennett et al., 2009). Analyses of these prints (Figure 26), attributed by most to *H. erectus*, are consistent with the functional anatomy of the pedal remains—they reveal a foot with a fully adducted hallux and longitudinal arch, walking with human-like medial weight transfer (Bennett et al., 2009; Hatala et al., 2017; Hatala, Demes, & Richmond, 2016; Hatala, Roach, et al., 2016).

3.14 | Late early/middle Pleistocene *Homo*

To the best of our knowledge, there are only three pedal fossils from Africa known from the roughly 1.2 million year span separating the 1.53 Ma foot bones of the KNM-ER 803 *H. erectus* skeleton and the numerous pedal remains from the 236- to 335-kyr-old South African hominin *H. naledi* (described below). A fragmentary, unprepared and undescribed talus (BOU-VP-2/95) has been recovered from the ~1.0 Ma sediments at Daka, Ethiopia (Gilbert & Asfaw, 2008). Another talus (LZH-01) was recovered from undated (possibly Middle Pleistocene?) sediments from Luangwa, Zambia and found to resemble modern humans in a geometric morphometrics analysis (Bishop et al., 2016). Additionally, from ~0.5 Ma Kapthurin Formation deposits at Baringo, Kenya (Deino & McBrearty, 2002), there is an Mt1 (BK 63) which has never been formally described.

The base of BK 63 is weathered around the edges, but appears generally human-like. Distally, the head is domed (Figure 11), and our observations on the original are that the head is mediolaterally wide dorsally, as it is in modern humans. However, Lu et al. (2011) find the contours of the head to be unlike modern humans and similar to both the chronologically later Jinniushan Mt1, and much earlier *Paranthropus* fossils from Swartkrans. We regard BK 63 as possessing a much more human-like Mt1 head than SKX 5017 or SK 1813. Nevertheless, Fisher and McBrearty (2002) and Meldrum (2007) have commented on the gracility of the shaft of BK 63 and we concur. Relative to the length of the bone, the shaft is surprisingly dorsoplantarly shallow (Figure 11), seemingly poorly constructed to resist the high bending forces on the Mt1 during hallucal propulsion. Meldrum (2007) and Lu et al. (2011) regard this as evidence that Middle Pleistocene hominins still had not acquired a modern human-like gait. Significantly more evidence will be needed from this poorly sampled time period to better understand Middle Pleistocene foot evolution in Africa. Despite the near absence of foot fossils in Africa during this time period, there are nearly a dozen footprints at the 700-kyr-old site of Gombore II-2, Melka Kunture, Ethiopia (Altamura, Bennett, D'Août, et al., 2018). The best-preserved are described by the authors as generally similar to the presumed *H. erectus* prints from Ileret, Kenya, and perhaps most interestingly, there are prints preserved from both adults and children thought to be as young as 12 months old (Altamura et al., 2018).

In Europe, at least, there are over a dozen foot bones from the 772 to 949 ka (Duval et al., 2018) site of Gran Dolina, Spain (Figure 27), attributed to the taxon *H. antecessor* (De Castro et al., 1997). We were unable to study the original fossils and base our comments on published scholarship. There is a talus (ATD6-95), fragmentary calcaneus (ATD6-117), two Mt2s (ATD6-25 and ATD 6-70 + 107), Mt4 (ATD6-124), and eight phalanges (ATD6-30-36,68). In general, the bones are human-like and according to Pablos

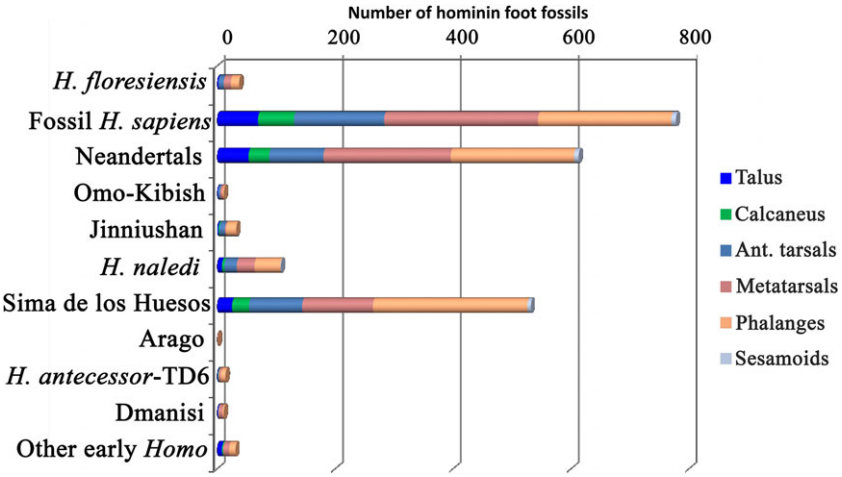

FIGURE 28 Absolute number of foot fossils (values across the top of the graph) attributed to members of the genus *Homo*. Note that there are only a small number of pedal remains for localities older than Sima de los Huesos. However, the Sima de los Huesos, Spain collection contains more than 500 foot fossils, far more than what is known for any other Pleistocene *Homo* group except for Neandertals and *Homo sapiens*. Image courtesy of A. Pablos; modified from "The foot in the *Homo* fossil record" by Pablos, 2015, *Mitteilungen der Gesellschaft für Urgeschichte*, *24*, 11

et al. (2012) would be in a foot employing a human-like gait. The phalanges are short, straight and robust (Lorenzo et al., 1999); the metatarsals are similarly human-like in proportion (Lorenzo et al., 1999; Pablos et al., 2012). The Mt4 base is mediolaterally wide, as found in fossils from Sima de los Huesos and Neandertals (Pablos et al., 2012). Additionally, the Mt4 (ATD6-124) preserves evidence for a healed stress fracture (Martin-Francés, Martinon-Torres, Gracia-Téllez, & Bermúdez de Castro, 2015). Unfortunately, the calcaneus only preserves the anterior talar facet and little can be gleaned from it. The talus (ATD6-95), while eroded, contains valuable information. It is a very large talus—one of the largest known from the Pleistocene (Pablos et al., 2012). The trochlear body is quite narrow mediolaterally, a trait the ATD6-95 specimen shares in common with Neandertals, but not with the Sima de los Huesos tali, which possess wider trochlear surfaces. The trochlear body is long; the talar neck quite short—an inverse relationship previously hypothesized to exist in Neandertal tali (Rhoads & Trinkaus, 1977). In a principal components analysis, the Gran Dolina talus plots outside the shape space occupied by humans, Neandertals, and the Sima de los Huesos tali (Pablos et al., 2012). Functionally, whether these different talar dimensions are of any consequence is unclear and may just reflect population-level differences in Pleistocene *Homo*. Nearly 50 fossilized footprints from Happisburgh, UK were (they have since eroded) the oldest known from Europe (~0.78–1.0 Ma) and preserved the movements of a group attributed to *H. antecessor* (Ashton et al., 2014). They were not adequately preserved to draw functional inferences from internal morphology.

3.15 | Eurasian Middle Pleistocene *Homo*

Prior to 1997, the only Middle Pleistocene *Homo* foot fossil known was an Mt2 (Arago XLIII) from France (Day, 1986; Lamy, 1982). There are now close to 600 fossils as a result of discoveries on the western and eastern edges of the Eurasian landmass: Sima de los Huesos in the Atapuerca Mountains, Spain has yielded over 500 foot fossils from 16 individuals (Pablos et al., 2017; Figure 27). The fossils are ~430 kyr old (Arsuaga et al., 2014) and represent a population closely related to, or even ancestral to, Neandertals (Meyer et al., 2014). We were unable to study the original material and base our report below on published studies. Sima de los Huesos is, by far, the largest collection of foot fossils known from any one locality (Pablos et al., 2017; Figure 28). To the east, the Jinniushan, China locality has yielded two (left and right) partial foot skeletons of a ~260 kyr old female (Lu et al., 2011; Figure 27). Furthermore, there are two known footprint sites from this time. At Terra Amata, France (~400 kyr old), there is a single footprint (De Lumley, 1969), and at Roccamonfina, Italy, there are three 325–385 kyr old trackways preserving quite human-like prints (Mietto, Avanzini, & Rolandi, 2003). These foot bones and footprints are generally human-like, and thus attention is paid below to those anatomies that deviate from the modern human or Neandertal condition.

The Sima de los Huesos foot bones have been partially described (Pablos et al., 2017), with the most detailed descriptions and analyses done thus far on the talus (Pablos et al., 2013) and calcaneus (Pablos et al., 2014). There are 29 calcanei known from 15 different individuals from Sima de los Huesos (Pablos et al., 2014). The fossils are modern human-like, though they are more robust, with large articular surfaces, recalling the Neandertal calcaneus (Pablos et al., 2014). Additionally, the tubers are relatively long, though not as long as those found in Neandertals (Pablos et al., 2014, 2017), an anatomy that would compromise running efficiency (Raichlen et al., 2011). Unlike in any other Pleistocene calcanei, the Sima fossils have an unusually projected sustentaculum tali (Pablos et al., 2014), a feature already present in the juveniles (Pablos et al., 2017). It is possible that this morphology indicates that the Sima individuals had a greater range of motion at the subtalar joint (Pablos et al., 2014).

The Sima de los Huesos fossil assemblage has also produced an astounding 25 tali from 14 different individuals (Pablos et al., 2013). These tali are generally human like, though a multivariate analysis groups the Sima tali in a different shape space than either Neandertals or modern humans (Pablos et al., 2013). The Sima tali have vertically short bodies (unlike the vertically tall talar body of Late Pleistocene

humans), unwedged talar trochlea, broad fibular facets, short talar necks, and short middle calcaneal facets—similar to the tali of Neandertals. However, the Sima specimens have exceptionally broad fibular facets, and a uniquely mediolaterally short talar head (Pablos et al., 2013; Figure 4). This mediolateral width of the head also scales differently in the Sima tali compared with Neandertals—as the talus gets larger, the head gets proportionally narrower in Sima compared with Neandertals (Pablos et al., 2017). The combination of a uniquely short talar head with projecting sustentaculum tali may be worth additional functional consideration.

The remaining foot bones are partially described in Pablos et al. (2017). There are an extraordinary number of tarsal bones: navicular (n = 25), cuboid (n = 22), medial cuneiform (n = 14), intermediate cuneiform (n = 15), and lateral cuneiform (n = 12). The navicular is robust, and the cuboid narrow, anatomies similar to those found in Neandertals (Pablos et al., 2017). Unique to the Sima population is a proximodistally short intermediate cuneiform, which in conjunction with the other cuneiforms, would result in a more recessed and presumably more stable Mt2 (Pablos et al., 2017). The metatarsals and phalanges are generally robust, similar to the anatomy of the Neandertal foot. The Mt1 (n = 18), Mt3 (n = 16), Mt4 (n = 12), and Mt5 (n = 11) all possess proximal bases slightly broader than Neandertal fossils (Pablos et al., 2017), indicating a wider midfoot in the Sima population. The Mt2 (n = 13) is relatively narrow in the Sima fossils, perhaps related to the recessed, stable medial midfoot discussed above. The phalanges (hallucal proximal n = 28; hallucal distal n = 21; nonhallucal proximal n = 78; intermediate n = 71; nonhallucal distal n = 63) are broad and robust, with distal breadths similar to those found in Neandertal feet (Pablos et al., 2017). The distal hallucal phalanges have slight valgus deviation (Pablos et al., 2017).

A female partial skeleton recovered from the ~260 kyr old site of Jinniushan, China (Rosenberg, Lü, & Ruff, 2006), includes most of both feet (Lu et al., 2011). The left foot is better preserved with all of the tarsals present, minus the navicular (which is preserved from the right side; Figure 27). There is an Mt1 and Mt2, in addition to numerous phalanges (Lu et al., 2011). The Jinniushan foot is generally human-like, though Lu et al. (2011) noted several differences that they regard as functionally significant and evidence for a gait that differs from that of modern humans. All of the anatomy described below is from Lu et al. (2011). Only one of us (BZ) was able to see the Jinniushan fossil, but only through a glass case.

The calcaneus is large and robust with a plantarly positioned lateral plantar process. Lu et al. (2011) noted the extreme distal position of the LPP, though this is not uncommon in modern human calcanei. The calcaneocuboid joint is quite human-like, with a plantomedial cuboid facet and dorsal overhang (Elftman & Manter, 1935), which locks the eccentrically positioned cuboid beak into a stable calcaneocuboid joint (Bojsen-Møller, 1979). The talus is human-like with medial and lateral rims of equal height, a mediolaterally ungrooved trochlear surface, a facet on the plantar head for the spring ligament and high head neck torsion (46°; Lu et al., 2011). The horizontal head neck angle is also quite high (30°; Lu et al., 2011). The navicular tuberosity is large and projecting, which is interpreted by Lu et al. (2011) as evidence for weight-bearing in a flat foot. The robust plantar base of the medial cuneiform is interpreted the same way. Lu et al. (2011) draw attention to a groove on the plantar lateral cuneiform they describe as "proximally" positioned for the tendon of *M. peroneus longus*, which would indicate a rather low transverse and longitudinal arch. We note that this groove for *M. peroneus longus* is distally positioned. The Mt1 facet on the medial cuneiform is distally oriented and only slightly convex mediolaterally. The Mt1 head itself is dorsally domed and is mediolaterally wide dorsally. However, a shape analysis clusters this bone outside the human range and with the Middle Pleistocene Kenyan fossil BK 63, suggesting that the Jinniushan individual did not possess a modern human toe-off mechanism (Lu et al., 2011). The pedal phalanges are short, straight, and robust. The distal hallucal phalanx has minimal valgus deviation or axial torsion (Lu et al., 2011).

While generally human-like, Lu et al. (2011) emphasize differences in the Jinniushan foot compared with modern humans and argue that this individual would not have possessed a human-like gait. The foot would have been rigid, but would have lacked a longitudinal arch, which may have compromised endurance (Lu et al., 2011). The hallucal metatarsophalangeal joint was also not entirely human-like, suggesting that Jinniushan did not toe-off as humans do today (Lu et al., 2011).

3.16 | *Homo naledi*

Homo naledi is known from 236 to 335 kyr old sediments (Dirks et al., 2017) recovered from the Dinaledi (Berger et al., 2015) and Lesedi (Hawks et al., 2017) chambers of the Rising Star cave system in South Africa. The foot is known only from the Dinaledi chamber and consists of 107 fully published pedal elements (Figure 28), including five partial foot skeletons (Harcourt-Smith et al., 2015; Figure 29). The anatomy discussed below is based primarily on Harcourt-Smith et al. (2015) and observations we have made on the original fossil material.

The foot of *H. naledi* is generally human-like, but differs in having curved pedal phalanges and in morphologies hypothesized to be related to the arch of the foot (Harcourt-Smith et al., 2015). The calcaneus is human-like in having a flat subtalar joint, a medially positioned facet for the beak of the cuboid, a human-like angulation of the retrotrochlear eminence (and inferred position of the lateral plantar process), and a small peroneal trochlea. However, the tuber is quite gracile, outside of the range of modern humans (Figure 2; Table 2). Additionally, the angulation of the sustentaculum tali is more ape-like, a morphology that has been correlated with arch development (Harcourt-Smith et al., 2015; Morton, 1935). The talus of *H. naledi* is generally human-like as well (Figure 4). The trochlea is mediolaterally flat and possesses subequal medial and lateral rims, as is found in the human talus. There is pronounced human-like head/neck torsion (Figure 5), indicative of midtarsal stability (Kidd, 1999). The horizontal angle of the head and neck is intermediate between human and ape; however, the declination angle of the head and neck is decidedly ape-like, a morphology that has been hypothesized to be related to arch height (Day & Wood, 1968) and has more recently been found to correlate with flatfootedness in modern humans (Peeters et al., 2013). A geometric morphometrics analysis of the tali from *H. naledi* position them just on the edge of the modern human distribution (Harcourt-Smith et al., 2015).

FIGURE 29 Feet from *Homo naledi* (from Harcourt-Smith et al., 2015). To the far left are two partial juvenile feet. To the right are more complete adult *H. naledi* foot skeletons, including (far right) the almost complete Foot 1

The midtarsus (cuboid, lateral cuneiform, intermediate cuneiform) is proximodistally elongated, and a facet on the lateral cuneiform indicates that the Mt4 was recessed into the tarsal row as in modern humans (Harcourt-Smith et al., 2015). The published naviculars are poorly preserved (Harcourt-Smith et al., 2015); however, there is a newly recovered specimen (U.W. 101-1758) that possesses a large navicular tuberosity and pinching of the lateral body similar to that found in australopiths and *H. floresiensis* (Figure 6). This will be an important specimen for understanding navicular evolution.

The medial cuneiform is human-like, with a relatively flat and distally directed facet for the Mt1. Additionally, the intermediate cuneiform facet is "L-shaped" as it is in humans. These anatomies of the medial cuneiform are consistent with an adducted hallux in *H. naledi* (Figure 8). A geometric morphometrics analysis finds *Homo naledi* to be quite similar to OH 8, just on the edge of the modern human distribution (Harcourt-Smith et al., 2015).

Metatarsal robusticity in *H. naledi* is 1 > 5 > 4 > 3 > 2, which is quite human-like (Archibald et al., 1972; Harcourt-Smith et al., 2015; Patel et al., 2018). Additionally, the relative lengths of the metatarsals are within the human range (Harcourt-Smith et al., 2015) in contrast to the condition found in *H. floresiensis* (Jungers, Harcourt-Smith, et al., 2009; Jungers, Larson, et al., 2009). Unlike the condition found in fossils assigned to early *Homo* (Jungers et al., 2015; Pontzer et al., 2010), the *H. naledi* Mt1 head is mediolaterally expanded dorsally, consistent with a human-like toe-off and fully developed windlass mechanism (Harcourt-Smith et al., 2015; Figure 11). The metatarsal bases are dorsoplantarly tall (though the Mt3 is on the low end of the human and fossil hominin range; Figure 13), and metatarsal torsion is within the range of modern humans (Harcourt-Smith et al., 2015). Human-like torsion of the Mt3 (Drapeau & Harmon, 2013; Pontzer et al., 2010) and Mt4 (Pontzer et al., 2010; Ward et al., 2011) have been proposed as skeletal correlates of a longitudinally arched foot in early hominins. The talus and calcaneus of *H. naledi* would indicate a hominin with a flat foot, while the metatarsals would suggest one with an arched foot; clearly more work needs to be done to understand the skeletal correlates of arch height. The Mt5 is externally quite human-like (Figure 15), and internally possesses human-like cortical gracility (Dowdeswell et al., 2016). However, the distribution of cortex indicates more ape-like resistance to bending forces and the Mt5 cortical structure lacks the distal tapering that is present in OH 8 and SKX 33380 (Dowdeswell et al., 2016).

The lateral metatarsal heads are dorsally domed and possess human-like dorsal canting of the proximal phalangeal bases (Harcourt-Smith et al., 2015; Trinkaus & Patel, 2016), consistent with human-like toe-off during bipedal gait. Furthermore, the phalanges are both absolutely (McNutt, Zipfel, & DeSilva, 2018) and relatively (Trinkaus & Patel, 2016) short. However, the proximal pedal phalanges are *Gorilla*-like in curvature, suggesting some retained grasping ability in this taxon (Harcourt-Smith et al., 2015; Figure 17). Throckmorton et al. (2017) has documented healed fractures in two *H. naledi* proximal pedal phalanges.

The *H. naledi* foot functioned in much the same manner as a modern human foot. After initial contact with the ground, the tibia would swing in the sagittal plane over a fixed ankle joint. The midfoot is elongated and stiff; head/neck torsion of the talus and a locking calcaneocuboid joint would render the foot rigid during heel lift. The human-like metatarsal head is consistent with medial weight transfer and a human-like windlass mechanism. However, there are some anatomies of the *H. naledi* foot that are unlike those found in most modern human feet: a relatively gracile calcaneus, evidence for a low longitudinal arch, and curved pedal phalanges. Given the small lower limb joints of *H. naledi* (Walker et al., 2015) and a reduced longitudinal pedal arch (Harcourt-Smith et al., 2015), it is possible that *H. naledi* would not have had the endurance to travel (walk or run) over long distances without exhaustion or risk of injury and may have had rather small home ranges. Future work should address how these more primitive anatomies, in an otherwise quite human-like foot, may impact gait mechanics or efficiency in *H. naledi*.

Given the extraordinary number of juvenile elements in the *H. naledi* assemblage (Harcourt-Smith et al., 2015), there is an opportunity to examine foot ontogeny in this taxon—an approach that has already yielded important insights into the functional anatomy of the hominin foot (e.g., DeSilva, Gill, et al., 2018). Finally, *H. naledi* is yet another example of Pleistocene hominin foot mosaicism, with

potential insights into the foot of early *Homo*. To understand both the functional and phylogenetic significance, it will be critical to directly compare the foot fossils of *H. naledi* to the early *Homo* foot fossils from Dmanisi (Lordkipanidze et al., 2007), Ileret (Jungers et al., 2015), and later Pleistocene—but anatomically more primitive—foot fossils from *H. floresiensis* (Jungers, Harcourt-Smith, et al., 2009; Jungers, Larson, et al., 2009).

3.17 | *Homo floresiensis*

Homo floresiensis is an insular species from the Indonesian island of Flores (Brown et al., 2004) known from 60 to 100 kyr old deposits in the Liang Bua cave (Sutikna et al., 2016). The foot is known primarily from the LB1 skeleton (Jungers, Harcourt-Smith, et al., 2009; Figure 30), though additional pedal remains not associated with LB1 have been recovered and described (Jungers, Larson, et al., 2009). The anatomy discussed below is based on published descriptions and analysis (Jungers, Harcourt-Smith, et al., 2009; Jungers, Larson, et al., 2009) combined with observations we have made on 3D printouts of high-resolution scans of the original material made available by M. Tocheri.

All of the tarsals were recovered except for the calcaneus; all five metatarsals are represented, as are many of the pedal phalanges (Jungers, Harcourt-Smith, et al., 2009; Jungers, Larson, et al., 2009). Relative to the length of the lower limb, the foot of *H. floresiensis* is remarkably long (i.e., 70% the length of the femur), making it more ape-like than human-like (Jungers, Harcourt-Smith, et al., 2009).

The talus has a human-like trochlear surface—it is only moderately wedged, has even medial and lateral margins, and possesses a mediolaterally flat articular surface with the tibia (Jungers, Harcourt-Smith, et al., 2009; Figure 4). The head and neck form a 23° horizontal angle with the body, which is similar to other tali of fossil *Homo*. However, the head/neck torsion angle (26°) is quite low and outside the range of humans (Jungers, Harcourt-Smith, et al., 2009), suggesting some mobility at the transverse tarsal joint (Figure 5). However, this observation contradicts Prang's (2016a, 2016b, 2016c) finding that the head of the LB1 talus was dorsoplantarly flat, and less mobile in the sagittal plane than in modern humans. It is unclear how to reconcile these observations, which notably are also found in the *A. sediba* talus. There is some damage to the plantar aspect of the talar head, but there appears to be a small facet for the spring ligament (Jungers, Larson, et al., 2009). A geometric morphometrics study found the LB1 talus to be intermediate in shape space between human and African ape tali (Jungers, Harcourt-Smith, et al., 2009).

The LB1 naviculars (left and right) are surprisingly primitive. They possess a large tuberosity suggestive of a flat foot and the lateral body is proximodistally reduced, producing a wedged appearance (Jungers, Harcourt-Smith, et al., 2009; Figure 6). A geometric morphometrics study found them to be decidedly ape-like (Jungers, Harcourt-Smith, et al., 2009). Plantarly, there are well-developed insertions for the spring ligament (Jungers, Larson, et al., 2009); this may imply that the *H. floresiensis* foot was functionally rigid, even though it was structurally flat. The medial cuneiform has a relatively flat and distally directed facet for the adducted Mt1, and a human-like "L-shaped" facet for the intermediate cuneiform (Jungers, Larson, et al., 2009).

FIGURE 30 Foot of *Homo floresiensis*. Notice the short Mt1, long lateral metatarsals and long phalanges relative to the midfoot. Image courtesy of W. Jungers

The cuboid is proximodistally elongated, as in other hominins (Figure 7). However, it has only a weakly developed calcaneal process with a rather flat articular surface (Jungers, Harcourt-Smith, et al., 2009). This morphology, in combination with the low talar head/neck torsion, might imply that the transverse tarsal joint was more mobile in *H. floresiensis* than in modern humans. However, the facets for the lateral metatarsals are dorsoplantarly flat (Jungers, Larson, et al., 2009), indicating that *H. floresiensis* did not possess a midtarsal break.

The forefoot of *H. floresiensis* possesses an unusual combination of features. The relative robusticity of the metatarsal row is human like (1 > 5 > 4 > 3 > 2). However, their relative lengths are decidedly not (Jungers, Harcourt-Smith, et al., 2009). The LB 1 foot possesses a short Mt1 and relatively long Mt2 and Mt3—proportions that match the foot of chimpanzees (Jungers, Harcourt-Smith, et al., 2009). The Mt1 is 74.6% the length of the Mt2 in *H. floresiensis*, an ape-like ratio matched among hominin fossils only by the Burtele foot (Mt1 75.2% the length of Mt2). While the shortness of the Mt1 contributes to this ratio, the length of the bone (47.0 mm) matches that of the Dmanisi Mt1s (47.0 for D3442 and 47.2 for D2671). *H. floresiensis*, therefore, possessed extraordinarily long lateral metatarsals, ape-like in their length relative to the midtarsus of LB1 (Jungers, Harcourt-Smith, et al., 2009).

The Mt1 possesses a flat base, consistent with an adducted hallux. Oddly, there are no plantar grooves for the sesamoids of *M. flexor hallucis brevis* (Jungers, Larson, et al., 2009). However, the Mt1 head is human-like (Figure 11) and possesses a mediolaterally wide dorsum similar to the anatomy of *H. naledi* and modern humans, but different from that found in early *Homo* (Dmanisi and Ileret) or australopiths

FIGURE 31 Foot remains from middle to late Pleistocene *Homo*. Far left: the Denisovan proximal pedal phalanx (image courtesy of B. Viola); scale bar = 1 cm. Middle: Kiik-Koba Neandertal foot. Right: La Ferrassie Neandertal foot. Note the short, robust phalanges on the Neandertal feet. Kiik-Koba and La Ferrassie images courtesy of E. Trinkaus

(Jungers, Harcourt-Smith, et al., 2009). The lateral metatarsal heads have some damage, but are dorsally domed.

Relative to the length of the metatarsals (which themselves are relatively long), the proximal phalanges are long, within the low end of the modern ape range (Jungers, Harcourt-Smith, et al., 2009). However, they have human-like robust bases and shafts, and dorsal canting consistent with dorsiflexion at the metatarsophalangeal joint (Jungers, Harcourt-Smith, et al., 2009). Phalangeal curvature is varied and overlaps with the human range, though one specimen (LB1/38) is australopith-like in its curvature (Jungers, Larson, et al., 2009).

Homo floresiensis had long toes on the ends of long metatarsals in a foot that was long compared with its leg. Thus, toe clearance might have been problematic during the swing phase of walking and *H. floresiensis* walked with altered gait kinematics involving either more flexion at the hip, knee, and/or ankle or less hip extension during the terminal part of stance phase (Jungers, Harcourt-Smith, et al., 2009). Additionally, there is skeletal evidence for a flattened longitudinal plantar arch (Jungers, Harcourt-Smith, et al., 2009), which could imply that *H. floresiensis* was ill equipped for endurance walking or running, and subsequently may have had a small home range. Nevertheless, the Mt1 head would suggest that *H. floresiensis* transferred weight to the hallux and had a well-developed plantar aponeurosis to engage the windlass mechanism during the push-off phase of walking. The dorsoplantarly large and flat talar head (Prang, 2016a) implies some midtarsal rigidity, while the lower torsion head and weakly developed cuboid beak suggests the opposite—a fascinating contradiction within the foot of *H. floresiensis* that requires additional study.

Ultimately, a remaining question about the foot (and indeed the entire body) of *H. floresiensis* is whether it represents a dwarfed version of *H. erectus*, or instead whether it better represents an early form of *Homo* (Jungers, Larson, et al., 2009). As mentioned previously, the LB1 foot needs to be systematically compared with that of early *Homo* (Dmanisi, Ileret), and *H. naledi* to better understand Pleistocene *Homo* foot evolution.

3.18 | Late Pleistocene *Homo*: Denisovans and Neandertals

Besides *H. floresiensis* (already discussed above), there are three known populations of human from the Late Pleistocene: Denisovans, Neandertals, and modern humans. Denisovans are known primarily from their genetics (e.g., Reich et al., 2010) and little is actually known about their anatomy, including the foot. There is one ~50 kyr old quite robust proximal pedal phalanx (Mednikova, 2011) attributed to the Denisovans. The majority of fossils from the Late Pleistocene are either Neandertal or anatomically modern human.

All of the bones of the foot are represented in the Neandertal fossil record, and there have been several associated partial foot skeletons discovered, including from La Ferrassie, Kiik-Koba, Tabun, and Shanidar (Trinkaus, 1983b; Pablos, 2015; Pablos et al., 2017; Figure 31). In general, the Neandertal foot strongly resembles that of modern humans, through subtle differences can be found (Trinkaus, 1983b). The foot proportions are modern human-like, though Neandertal feet are more robust and have larger joint surfaces—morphologies thought to be reflective of increased biomechanical loads. Both Shanidar 1 and 3 exhibit extensive osteoarthritis (Trinkaus, 1983b; Trinkaus & Zimmerman, 1982).

The Neandertal calcaneus is robust, with a mediolaterally wide tuber, broad sustentaculum tali, large talar facets and a human-like, locking, calcaneocuboid joint (Pablos, 2015; Pablos et al., 2014; Trinkaus, 1983a, b). Compared with modern humans, the proximal calcaneal body is elongated, which would increase the moment arm for

FIGURE 32 Foot of early *Homo sapiens*. Shown is the left side of each foot and footprint. Far left: ~115 ka foot from the juvenile Skhul VIII. (© 2019 President and Fellows of Harvard College, Peabody Museum of Archaeology and Ethnology, PM# 46-49-60/N7448.0). Middle: the oldest foot fossil assigned to *H. sapiens* from the 195 ka Omo-Kibish partial skeleton (mirrored to be from the same [left] side at the Skhul juvenile foot and the footprint). The Omo foot is indistinguishable from a modern human foot with the one notable exception of the talus being dorsoplantarly squat. Far right: One of the oldest known footprints attributed to *H. sapiens* from Langebaan Lagoon, South Africa (Image courtesy of W. Black ©Iziko Museums of South Africa)

M. triceps surae (Pablos et al., 2014; Trinkaus, 1983a, 1983b). While this anatomical arrangement may make walking more energetically efficient, it would reduce the elastic energy storage capacity of the Achilles tendon and compromise endurance running (Raichlen et al., 2011). Plantarly, the medial plantar process is hypertrophied, perhaps as a result of a strong plantar aponeurosis in Neandertal feet (Trinkaus, 1983a).

Neandertal tali are robust, with a large trochlea, and tibial and fibular facets (Rhoads & Trinkaus, 1977; Rosas et al., 2017; Trinkaus, 1983a). The talar body tends to be quite square-shaped (Pablos et al., 2012; Pomeroy et al., 2017; Rosas et al., 2017). There is an inverse relationship between the length of the talar body and the talar neck, with Neandertals possessing long talar bodies and short talar necks (Pablos et al., 2012; Pomeroy et al., 2017; Rhoads & Trinkaus, 1977), but Rosas et al. (2017) found that Neandertal talar necks are short independent of talar body length. Squatting facets, which form on the talar neck as a result of habitual dorsiflexion, are common on the talar neck (Mersey et al., 2013; Trinkaus, 1975a, 1975b). There is human-like head torsion, which would stiffen the medial midfoot (Trinkaus, 1983a, after Elftman, 1960), and the head is mediolaterally broad compared with modern human tali (Pablos et al., 2012; Pomeroy et al., 2017; Rosas et al., 2017). Early reconstructions of Neandertals (Boule, 1911, 1912, 1913) equipped them with a slightly divergent hallux based on what was perceived as more ape-like horizontal angles of the head and neck of the talus. However, more recent work shows that these angles are within the normal human distribution (Trinkaus, 1983a). Hallucal divergence proposed by Boule (1911, 1912, 1913) was also based on the mediolaterally convex surface of the medial cuneiform and the corresponding concavity of the Mt1, though the convex/concave surface of the Neandertal hallucal tarsometatarsal joint does not approach that found in apes and is also within the normal human range of variation (Trinkaus, 1983a, 1983b).

The naviculars of Neandertals are robust, with large tuberosities for the insertions of the plantar calcaneonavicular (spring) ligament and the tendon of *M. tibialis posterior* (Harvati et al., 2013; Heim, 1982; McCown & Keith, 1939; Mersey et al., 2013; Pomeroy et al., 2017; Trinkaus, 1983a, b), important musculoligamentous supporters of the longitudinal arch. There are typically small, ovoid contact facets between the navicular and the cuboid (Trinkaus, 1983b). Large insertions for plantar ligaments and slips of the *M. tibialis posterior* can be found on the plantar surface of the lateral cuneiforms.

Neandertal metatarsals are robust compared with modern human metatarsals (Mersey et al., 2013; Trinkaus, 1983a). The Mt1 and Mt5 are the most robust (as is typical in modern humans; Trinkaus, 1983b), and they possess human-like torsion (Trinkaus, 1983a). The Mt1 has a large insertion for the *M. peroneus longus* tendon (Trinkaus, 1983a). However, compared with the modern human foot, the Neandertal proximal phalanges are relatively short and robust (i.e., they are mediolaterally wide; Trinkaus, 1983a; Trinkaus & Hilton, 1996; Mersey et al., 2013), whereas the intermediate and distal phalanges are long (Trinkaus, 1983a), such that the relative toe length of Neandertals is the same as in modern humans, but the proportions of the phalanges within a ray differ. The wide proximal phalanges have been proposed as a means by which Neandertal feet could resist mediolateral directed forces on the toes, perhaps during movement over rugged terrain (Trinkaus, 1983b). The base of the proximal phalanges is enlarged,

perhaps a result of a well-developed plantar aponeurosis in Neandertal feet (Trinkaus, 1983a).

A single human-like footprint from 62 kyr old deposits in Vârtop Cave, Romania has been attributed to a Neandertal (Onac et al., 2005).

3.19 | *Homo sapiens*

The oldest foot fossil attributed to *Homo sapiens* is the 195 kyr old partial foot skeleton from Omo-Kibish, Ethiopia (Pearson et al., 2008; Figure 32). This foot consists of a talus, navicular, medial cuneiform, cuboid, metatarsals 1–4, the hallucal proximal phalanx, and a fragment of the distal hallucal phalanx (Day, Twist, & Ward, 1991; Pearson et al., 2008). The foot is almost identical to that found in modern humans today. However, there is one difference that we could detect: the talar body is dorsoplantarly short, unlike the dorsoplantarly tall talar body found in modern *H. sapiens* (Boyle & DeSilva, 2015; McNutt, Zipfel, & DeSilva, 2018; Pablos et al., 2012; Rosas et al., 2017). The functional reason (if any) for the increase in talar trochlear body height in Late Pleistocene *H. sapiens* remains unclear.

The ~100 ka site of Klasies River Mouth, South Africa has yielded three metatarsals: an Mt1 (KRM 20272[B]), Mt2 (SAM-AP 6386), and Mt5 (SAM-AP 6385). These have been described as human-like in all respects (Grine, Wurz, & Marean, 2017; Rightmire, Deacon, Schwartz, & Tattersall, 2006; Zipfel & Kidd, 2008). The oldest foot fossils assigned to *H. sapiens* that are not on the African continent are from Qafzeh skeletons 3, 8, and 9, and Skhul skeletons 3–9 (McCown & Keith, 1939; Van der Meersch, 1981). Other pedal fossils of note are the 67 ka Mt3 from Callao Cave, Phillipines (Mijares et al., 2010), and the quite small phalanges (IP and DP 5) from the 45–65 ka Diepkloof Rock Shelter in South Africa (Verna, Texier, Rigaud, Poggenpoel, & Parkington, 2013). For a more complete list of Upper Paleolithic human foot remains, see Pablos et al. (2017).

Footprints attributed to *H. sapiens* abound. The oldest are between 90 and 125 ka and are all from South Africa: Nahoon (~125 ka; Mountain, 1966; Jacobs & Roberts, 2009), Langebaan Lagoon (~117 ka; Roberts & Berger, 1997; Figure 32) and along the Cape south coast (~90 ka; Helm et al., 2018). Given the likelihood that *H. naledi* continued to live in South Africa during the late Middle Pleistocene, it should not be a given that these all belong to *H. sapiens*, however. An extraordinary collection of hundreds of prints is preserved at the ~20 ka site of Engare Sero, Tanzania (Liutkus-Pierce et al., 2016). Other footprint localities of note are ~36 ka site of Ciur-Izbuc Cave in Romania (Webb et al., 2014) and the oldest *H. sapiens* prints on the continents of Asia (Jeju Island, Korea: 19–25 ka; Kim, Kim, Kim, Lee, & Lim, 2009; Kim, Kim, Kim, & Lim, 2010); Australia (Willandra Lakes: ~20 ka; Webb, Cupper, & Robins, 2006) and North America (Calvert Island, Canada: ~13 ka; McLaren et al., 2018).

The human foot had achieved its current form by the Late Pleistocene; however, the use of footware has had an impact on the recent human foot skeleton. The oldest direct evidence for footware comes from sites in North America that date to ~7,500–9,000 years old (Kuttruff, DeHart, & O'Brien, 1998). However, there is more ancient skeletal evidence for shoes. Trinkaus (2005) found that the intermediate phalanges become more gracile in Middle Upper Paleolithic (~30 ka) human remains compared with earlier fossils. In fact, the oldest evidence of footware (based on phalangeal gracility) comes from the ~40 ka Tianyuan site in China (Trinkaus & Shang, 2008).

In addition to phalangeal gracility, footware is also associated with an increase in forefoot pathologies (Zipfel & Berger, 2007). Compared with shod populations, some unshod humans tend to have a wider forefoot (D'Août, Pataky, De Clercq, & Aerts, 2009, but see Thompson & Zipfel, 2005), and a relatively narrow stride width (Tuttle et al., 1990). Unshod humans also heel strike with less force (Wallace, Koch, Holowka, & Lieberman, 2018) and have more evenly distributed pressure throughout the foot (D'Août et al., 2009). Many studies have found an association between childhood footware and the prevalence of flatfootedness (e.g., Rao & Joseph, 1992; Sachithanandam & Joseph, 1995). A more recent study revealed that the unshod Tarahumara population possessed stronger plantar musculature and stiffer longitudinal arches (Holowka, Wallace, & Lieberman, 2018), a finding consistent with Miller, Whitcome, Lieberman, Norton, and Dyer (2014) who found that shod humans can strengthen their instrinsic foot musculature and stiffen the longitudinal arch by converting to minimal footware. Extreme cases of the impact of shoes on the foot are clear from foot-binding practices (Cummings, Ling, & Stone, 1997).

4 | CLADISTICS ANALYSIS

In order to help understand the evolution of foot skeletal morphology in hominins, a cladistic analysis was run on the fossils discussed in this review using anatomical characters described throughout and listed in Supporting Information Table S1. Taxa included in the cladistic analysis represent three genera of modern great apes (*Pan*, *Gorilla*, and *Pongo*) as well as most hominins discussed in this review. Recently announced material from the 4.3 to 4.6 Ma As Duma locality at Gona, Ethiopia was preliminarily characterized based on Simpson et al. (2018). The Sterkfontein Member 4 fossils were treated as two distinct groups, with one possessing more primitive characters and one more derived—this will require reanalysis as more associated fossils are recovered. Fossil *Homo* included material from Dmanisi, isolated foot bones from Omo-Shungura and Koobi Fora (see review of early *Homo* for detail), and what has been preliminarily announced about the Ileret foot (Jungers et al., 2015). Fossil *Homo* does not include chronologically later material from the Middle Pleistocene, or Neandertals.

The analysis was rooted with *Ekembo* based on observations of original material. The tree will need to be re-rooted should new material from the Miocene be recovered. The data matrix (80 characters; 19 taxa) was treated under the assumption of the minimal model of unweighted parsimony, using PAUP.4b1 (Swofford, 2002), with a Branch and Bound search (exhaustive search; addition sequence = furthest). The results were then visualized using Win Clada (Nixon, 2002). All characters were treated as unordered and equally weighted. The branch support was assessed by calculating the Bremer index (Bremer, 1994) with the same software. In addition, a principal coordinate analysis (PCoA) using the Bray–Curtis similarity index was run on the same dataset using the software PAST (Hammer, Harper, & Ryan, 2001), removing *P. boisei* from the sample as some critical missing data were creating pairs of rows with no common values, though given the results of the cladistic analysis, OH 8 is probably a *P. boisei*. Though

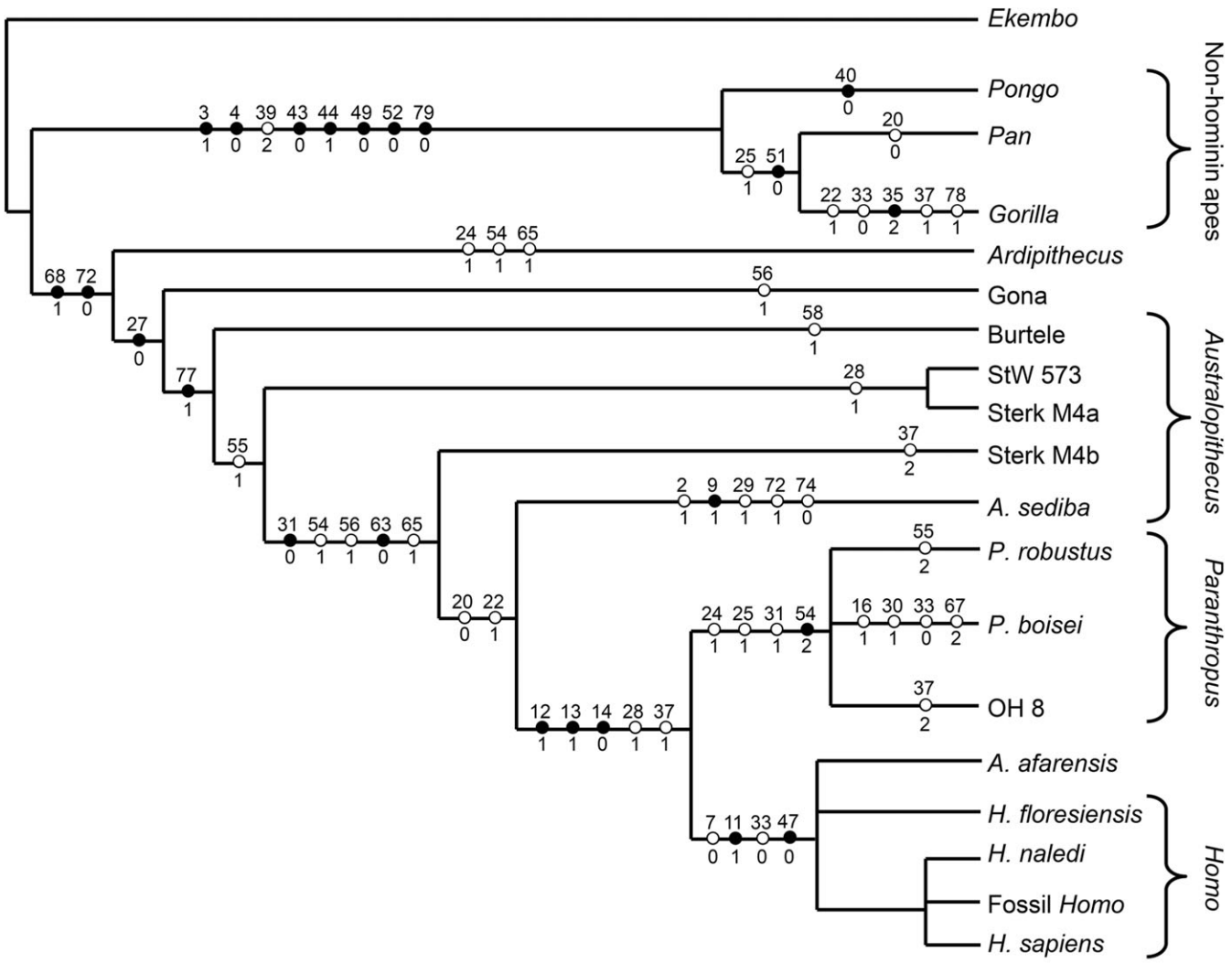

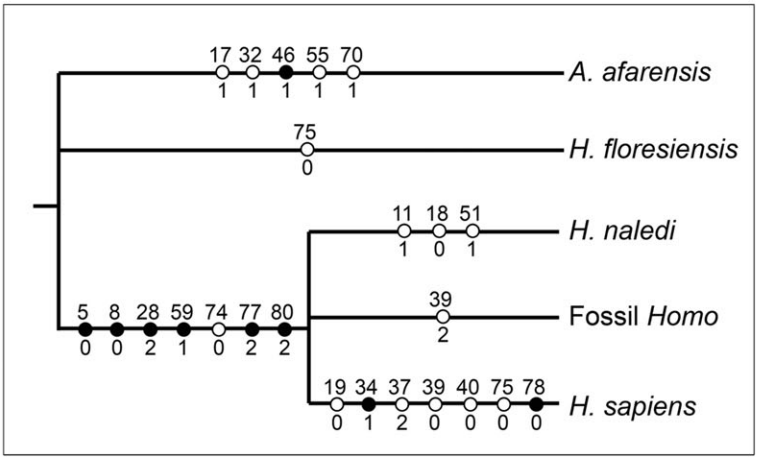

FIGURE 33 Cladistics analysis performed on morphologies of the foot (n = 80) from 19 taxa. The numbers positioned along the branches correspond to traits listed in Supporting Information Table S1, and reflect evolutionary changes to the foot in those lineages. Note the following: (1) the modern apes cluster together, possibly reflecting homoplasy in the evolution of the ape foot; (2) the earliest hominin foot fossils (*Ardipithecus*, Gona *Ardipithecus*, Burtele, StW 573) do not cluster together and instead represent distinct branches reflecting mosaic foot evolution and perhaps bipedal experimentation early in the hominin lineage; (3) a mixed assemblage at Sterkfontein member 4 is supported here, with some fossils (Sterk M4a) aligned with StW 573; (4) OH 8 is positioned within the *Paranthropus* clade, indicating that this foot probably belongs to *P. boisei*; (5) the *A. afarensis* foot is quite derived and clusters with *Homo*, which may indicate homoplasy in the evolution of the foot of *A. afarensis* and *Homo*

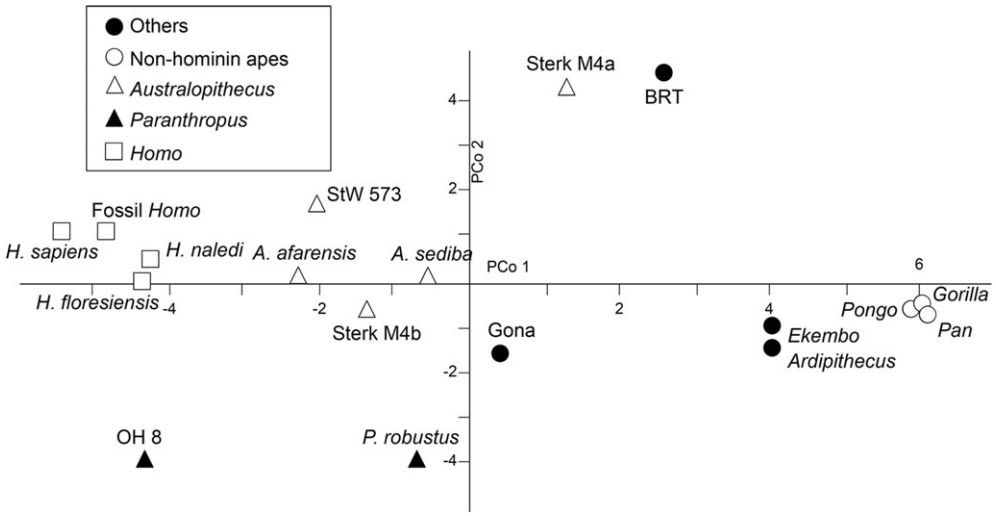

FIGURE 34 Principal components analysis (PCoA) performed on the data matrix (n = 80 characters) from fossil hominin foot fossils, extant apes, and *Ekembo* (outgroup). PC1 explains 48% of the variation and sorts taxa generally along a continuum thought to reflect adaptations for arboreality, with the extant great apes on the far right next to *Ekembo* and the Aramis *Ardipithecus* foot skeleton. The Burtele foot (BRT), Gona *Ardipithecus*, and feet from *Australopithecus* and *Paranthropus* are in the middle of PC1 and to the far left are members of the genus *Homo* and OH 8. PC 2 explains 14% of the variance

PCoA deals with the presence–absence data, the results read like those of a principal component analysis.

The cladistic analysis (Figure 33) resulted in four equally parsimonious trees (tree length = 159). The homoplasy index is low (0.34), the consistency and rescaled consistency indices are 0.66 and 0.52, respectively, and the retention index is 0.78, which indicates an overall reliable result. The robusticity is also supported by the fact that almost every branch is suported by at least one unambiguous synapomorphy, although all clades are supported by a Bremer index of 1 only, except the clade gathering *Pan*, *Gorilla* and *Pongo* which has a Bremer support of 4. The strict consensus tree displays three irresolutions. The first is the position of OH 8, which clusters either with *P. boisei* or with *P. robustus* (but not with *Homo*). The second irresolution occurs at the base of the genus *Homo*, with either the Hadar *A. afarensis* foot sister to all *Homo* or *H. floresiensis* sister to the clade consisting of *A. afarensis* and *Homo* (Figure 33). The third unresolved relationship within the *Homo* clade is the result of the two different positions of *H. naledi* which alternatively cluster either with *H. sapiens* or more basal as the sister clade to *H. sapiens* and fossil *Homo*.

We find *Homo* and *Paranthropus* to be sister clades, a result also supported using craniodental characters (Dembo et al., 2016; Strait, Grine, & Fleagle, 2015; Villmoare, 2018). The australopiths branch in a pectinate manner at the base of the *Homo-Paranthropus* clade, *A. sediba* being the sister group of the latter. *Ardipithecus* is the sister group of all other hominins. The basal branching of *Ardipithecus* and the derived position of *A. sediba* have been supported in other phylogenetic analyses using cranial and dental characters (e.g., Berger et al., 2010; Dembo et al., 2016; Dembo, Matzke, Mooers, & Collard, 2015; Strait et al., 2015). A noticeable result that does not conform to the current phylogenetic consensus is the gathering of *Pan*, *Gorilla* and *Pongo* into a single clade. This creates a dichotomy within the tree between animals adapted to an "arboreal" lifestyle (i.e., nonhominin apes) and those adapted to "bipedal" locomotion (i.e., hominins). This strongly suggests that this dichotomy is more likely based on characters reflecting adaptations to two different locomotory repertoires than actual phylogenetically shared derived traits. It is noteworthy that the first axis of the PCoA (which explains 48% of the variance) also appears to reflect this dichotomy between "bipedal" and "arboreal" taxa as the nonhominin apes and *Ekembo* and *Ardipithecus* are found on one side of the scatter plot whereas representatives of the genus *Homo* are found on the other. Australopiths, *Paranthropus* and *Ardipithecus* (Gona) are spread in-between. Axis two accounts for 14% of the variance (Figure 34).

There are five salient observations to make about the results of this analysis:

1. The two characters that define the root of the hominin lineage are dorsal doming of the Mt3 and dorsoplantar flattening of the Mt4 base. These traits functionally correlate with a stiff lateral midfoot and bipedal propulsion off the oblique axis of the foot. We regard this as strong evidence that these early hominins were at least occasionally bipedal and that the lateral midfoot was the initial target of selection on the foot of the earliest bipeds (e.g., Fernández et al., 2018; Fernández, Mongle, Patel, Tocheri, & Jungers, 2017; Kidd, 1999; Lovejoy et al., 2009; McNutt, Zipfel, & DeSilva, 2018; Morton, 1935).
2. The base of the hominin tree is pectinate, with the Aramis *Ardipithecus* foot, the Gona *Ardipithecus*, the Burtele foot, and the earliest known australopith foot (StW 573) occupying four distinct, nonclustering, branches. We interpret this result as evidence for variation at the base of the lineage, with different hominins evolving different foot morphologies and practicing different forms of bipedal walking (e.g., Haile-Selassie et al., 2012), and/or different amounts of arboreality. This diversity in walking biomechanics continued into the Plio-Pleistocene (e.g., DeSilva et al., 2013; Harcourt-Smith & Aiello, 2004; Napier, 1964; Robinson, 1972), but this is the first study to demonstrate that experiments in bipedal walking probably characterized the beginnings of the lineage as well.

3. We admittedly arbitrarily divided the Sterkfontein Member 4 material into two clusters: one that contained more primitive foot bones (e.g., StW 89 and StW 595) and another that contained more derived material (e.g., StW 563 and StW 377). Interestingly, they did not cluster together (as they would if they represented a single taxon: *A. africanus*). Instead, the more primitive group clustered with StW 573. These results support Clarke (2008, 2013) who has hypothesized that Sterkfontein Member 4 consists of two distinct hominins and that one is *A. prometheus* (e.g., StW 573). Whether that taxonomic assignment stands remains to be seen; but we are in agreement with Clarke (2008) that Sterkfontein Member 4 samples two different foot forms and one resembles StW 573.
4. OH 8 does not cluster with fossil *Homo*, and instead clearly groups with the robust australopiths, making it a foot of *Paranthropus boisei*. Others have suggested this (e.g., Gebo & Schwartz, 2006; Wood, 1974a), but here we present a more thorough analysis that clusters OH 8 clearly with *P. boisei*. No longer should the OH 8 foot be used to characterize foot anatomy in the earliest members of our genus. We look instead to the forthcoming description of the KNM-ER 64062 Ileret foot for that information.
5. Despite possessing some primitive anatomies (e.g., distally deflected calcaneal body, some Mt1 mobility; long lateral toes) the Hadar foot of *A. afarensis* is remarkably derived, clustering with *Homo*. This finding is driven primarily by a quite human-like calcaneus, talus, and midfoot. There are two ways to interpret these findings. The first is that the shared derived foot anatomies in *A. afarensis* and *Homo* descend from a common ancestor with a similarly derived foot. Given recent craniodental cladistics work arguing against an *A. afarensis-Homo* clade (e.g., Dembo et al., 2016; Strait et al., 2015), an alternative interpretation is homoplasy in the foot bones of *A. afarensis* and fossil *Homo*, including the independent evolution of a large calcaneal tuber and mediolaterally flat talar trochlea (e.g., Prang, 2015a). We note in this context that the large calcaneal tuber is obtained in developmentally different ways in *A. afarensis* and in modern humans (DeSilva, Gill, et al., 2018).

5 | CONCLUSION

Paleoanthropology is a young science. Only 50 years ago, the human foot fossil record consisted of the OH 8 foot (thought then to be from *H. habilis*) and foot bones from Neandertals. A decade later, the Hadar *A. afarensis* remains were recovered (Latimer et al., 1982) and foot evolution could be characterized as a linear progression from the chimpanzee foot through *A. afarensis*, OH 8 and Neandertals to modern humans (Susman, 1983). The discoveries of the last 20 years have shown that foot evolution was more complicated, and more interesting. However, we should expect more surprises from the fossil record. It could be that new fossils will show that the burgeoning variation of the hominin foot fossil record is indeed evidence for hominin diversity and experimentation in bipedalism. We currently support that view. However, we are aware that new fossils may also increase intraspecific variation in ways that render some interspecific morphological differences presented in this review as functionally irrelevant noise. We certainly need more fossils. However, we also need a better understanding of what these morphological differences mean functionally, and to better evaluate whether these features have actually been the target of natural selection (Grabowski & Roseman, 2015).

Nevertheless, based on the current evidence, we are impressed with the morphological variation of the hominin foot fossil record. We interpret this variation as others have done (Harcourt-Smith & Aiello, 2004) and regard both the detailed examination of the functional anatomy of the hominin foot fossil record presented in this review and the cladistical analysis presented above as strong evidence that hominins had different foot forms throughout the Plio-Pleistocene. Early in hominin evolution (e.g., Aramis *Ardipithecus*, Gona *Ardipithecus*, Burtele), there were distinct foot morphologies, with different combinations of bony anatomies that—in our opinion—would have resulted in quite distinct manners (and frequency) of walking, and differential use of arboreal substrates. Within the australopiths themselves, there are considerable differences in foot morphologies, resulting in *A. afarensis*, *A. prometheus*, fossils allocated to *A. africanus*, *A. sediba* and *Paranthropus* failing to cluster in the foot cladogram and supporting the view that there was locomotor diversity—both in terms of walking kinematics, and use of arboreal substrates—throughout the Plio-Pleistocene (DeSilva et al., 2013; Harcourt-Smith & Aiello, 2004; Robinson, 1972). The same probably continued in *Homo* (e.g., Harcourt-Smith, 2016; Harcourt-Smith et al., 2015; Jungers, Harcourt-Smith, et al., 2009).

However, while the hominin foot fossil record has grown considerably in the last 50 years, we also recognize that these findings are still based on a limited number of remains from a limited number of individuals and that future work may (and should) retest and revise our results. Furthermore, it is difficult to incorporate normal intraspecific variation into a cladistical analysis and we are well aware that considerable variation probably existed for many of these features and that without large samples, we simply cannot yet quantify that variation. Finally, given that each foot consists of 26 bones, we cannot discount the possibility that although individual bony elements may differ between different hominins, the overall function of the foot may still have retained equivalency in its basic kinematics (e.g., Bennett et al., 2016; Throckmorton, 2013). More work is clearly needed to better understand how (and whether) intraspecific differences in foot anatomy corresponded to actual kinematic differences (e.g., DeSilva et al., 2015), and differences in gait performance (e.g., Raichlen et al., 2011; Rolian et al., 2009), throughout human evolution.

ACKNOWLEDGEMENTS

The authors are grateful to curators and colleagues who provided access to all of the hominin foot fossils discussed in this article. The authors thank A. Kwekason and P. Msemwa, and the Tanzanian Commission for Science and Technology for the opportunity to study the OH 8 ft at the National Museum of Tanzania. The authors thank F. Kyalo Manthi, J. Kibii, E. Mbua, and the National Museum of Kenya. The authors are grateful to D. Abebaw, Z. Alemseged, Y. Assefa, M. Endalamaw, T. Getachew, Y. Haile-Selassie, B. Asfaw, T. White, B. Kimbel, and C. Ward for the opportunity to study fossil pedal material at the National Museum of Ethiopia. The authors thank the Evolutionary Studies Institute and University of the Witwatersrand Fossil

Access Advisory Panel for permitting our study of fossil material housed at the ESI in Johannesburg, South Africa. The authors thank L. Costeur and the Naturhistorisches Museum Basel for the opportunity to study the *Oreopithecus* material. The authors thank S. Potze for her assistance at the Ditsong Museum of Natural History (Pretoria, South Africa). For access to skeletal material of extant apes and modern humans, we are grateful to B. Billings (University of the Witwatersrand), E. Westwig (AMNH), L. Jellema (CMNH), O. Lovejoy (Libben; Kent State), J. Chupasko and M. Omura (MCZ), and D. Pilbeam, M. Morgan, O. Herschensohn (Harvard Peabody), L. Gordon (NMNH), K. Zyskowski (Yale Peabody), B. Stanley, and M. Schulenberg (Chicago Field Museum), and S. Hinshaw (UofM Museum of Zoology). The authors thank G. Voegele for her assistance with the dissection of a *Pan troglodytes* foot. In the last decade, we have benefitted enormously from discussions about foot evolution with W. Harcourt-Smith, R. Kidd, B. Latimer, L. MacLatchy, C. Ward, S. Gill, W. Jungers, Z. Throckmorton, D. Proctor, C. Prang, N. Griffin, R. Wunderlich, M. Drapeau, O. Lovejoy, Y. Haile-Selassie, S. Simpson, T. White, G. Suwa, F. Thackeray, L. Berger, M. Wolpoff, R. Susman, D. Gebo, E. Boyle, K. Carlson, D. Lieberman, C. Gill, Z. Alemseged, B. Patel, J. Meldrum, R. Clarke, K. Hatala, A. Pablos, K. Congdon, and A. Deane. The authors are grateful to P. Tobias for insightful conversations about foot anatomy and evolution and are lucky to have learned in his presence. The authors thank J. Reader, J. Trueba, and the Science Photo Library for images appearing in Figures 20 and 27. G. Suwa and T. White generously provided the *Ardipithecus* foot image for Figures 8 and 18. The authors thank J. Njau for the OH 8 image used in Figure 24. The authors thank C. Zollikofer, W. Jungers and the Turkana Basin Institute, and K. Hatala for images in Figure 26. The authors thank A. Pablos for permission to use foot images in Figure 27 and for providing permission to replicate Figure 28. B. Viola and E. Trinkaus provided images in Figure 31. W. Black (Iziko Museum) provided the footprint image in Figure 32. T. White and G. Suwa provided measurements on the *Ardipithecus* foot graphed in Figures 12 and 13. Thanks to B. DeSilva for providing a footprint for Figure 20. Funding for this study was provided by the National Research Foundation, African Origins Platform, Leakey Foundation, and Dartmouth College. T. White and G. Suwa provided useful comments on this manuscript. This article benefitted from the careful read and constructive comments of two anonymous reviewers, and the associate editor. We dedicate this article to the memory of Michael Day: his are the giant shoulders we humbly stand upon.

ORCID

Jeremy DeSilva https://orcid.org/0000-0001-7010-1155

REFERENCES

Ackermann, R. R., & Cheverud, J. M. (2004). Detecting genetic drift versus selection in human evolution. *Proceedings of the National Academy of Sciences of the United States of America*, *101*, 17946–17951.

Aiello, L., & Dean, C. (1990). *An introduction to human evolutionary anatomy*. San Diego, CA: Academic Press.

Aiello, L., Wood, B., Key, C., & Wood, C. (1998). Laser scanning and paleoanthropology. An example from Olduvai Gorge, Tanzania. In E. Strasser, J. Fleagle, A. Rosenberger, & H. McHenry (Eds.), *Primate locomotion. Recent advances*. New York, NY: Plenum Press.

Alemseged, Z., Coppens, Y., & Geraads, D. (2002). Hominid cranium from Omo: Description and taxonomy of Omo-323-1976-896. *American Journal of Physical Anthropology*, *117*, 103–112.

Alemseged, Z., Spoor, F., Kimbel, W. H., Bobe, R., Geraads, D., Reed, D., & Wynn, J. G. (2006). A juvenile early hominin skeleton from Dikika, Ethiopia. *Nature*, *443*, 296–301.

Altamura, F., Bennett, M. R., D'Août, K., Gaudzinski-Windheuser, S., Melis, R. T., Reynolds, S. C., & Mussi, M. (2018). Archaeology and ichnology at Gombore II-2, Melka Kunture, Ethiopia: Everyday life of a mixed-age hominin group 700,000 years ago. *Scientific Reports*, *8*, 2815.

Antón, S. C. (2003). Natural history of *Homo erectus*. *Yearbook of Physical Anthropology*, *122*, 126–170.

Archibald, J. D., Lovejoy, C. O., & Heiple, K. G. (1972). Implications of relative robusticity in the Olduvai metatarsus. *American Journal of Physical Anthropology*, *37*, 93–95.

Arsuaga, J. L., Martínez, I., Arnold, L. J., Aranburu, A., Gracia-Téllez, A., Sharp, W. D., … Carbonell, E. (2014). Neandertal roots: Cranial and chronological evidence from Sima de los Huesos. *Science*, *344*, 1358–1363.

Ashton, N., Lewis, S. G., De Groote, I., Duffy, S. M., Bates, M., Bates, R., … Stringer, C. (2014). Hominin footprints from early Pleistocene deposits at Happisburgh, UK. *PLoS One*, *9*, e88329.

Barak, M. M., Lieberman, D. E., Raichlen, D., Pontzer, H., Warrener, A. G., & Hublin, J. J. (2013). Trabecular evidence for a human-like gait in *Australopithecus africanus*. *PLoS One*, *8*, e77687.

Barnett, C. H. (1955). Some factors influencing the angulation of the neck of the mammalian talus. *Journal of Anatomy*, *89*, 225–230.

Barnett, C. H. (1962). Valgus deviation of the distal phalanx of the great toe. *Journal of Anatomy*, *96*, 171.

Bates, K. T., Collins, D., Savage, R., McClymont, J., Webster, E., Pataky, T. C., … Crompton, R. H. (2013). The evolution of compliance in the human lateral mid-foot. *Proceedings of the Royal Society B: Biological Sciences*, *280*, 20131818.

Begun, D. R. (2004). The earliest hominins--is less more? *Science*, *303*, 1478–1480.

Begun, D. R., Teaford, M. F., & Walker, A. (1991). Comparative and functional anatomy of *Proconsul* phalanges from the Kaswanga primate site, Rusinga Island, Kenya. *Journal of Human Evolution*, *26*, 89–165.

Behrensmeyer, A. K., & Laporte, L. F. (1981). Footprints of a Pleistocene hominid in northern Kenya. *Nature*, *289*, 167–169.

Bennett, M. R., Harris, J. W., Richmond, B. G., Braun, D. R., Mbua, E., Kiura, P., … Huddart, D. (2009). Early hominin foot morphology based on 1.5 million-year-old footprints from Ileret, Kenya. *Science*, *323*(5918), 1197–1201.

Bennett, M. R., Reynolds, S. C., Morse, S. A., & Budka, M. (2016). Laetoli's lost tracks: 3D generated mean shape and missing footprints. *Scientific Reports*, *6*, 21916.

Berge, C., Penin, X., & Pellé, E. (2006). New interpretations of Laetoli footprints using an experimental approach and Procrustes analysis: Preliminary results. *Comptes Rendus Palevol*, *5*, 561–569.

Berger, L. R., de Ruiter, D. J., Churchill, S. E., Schmid, P., Carlson, K. J., Dirks, P. H. G. M., & Kibii, J. M. (2010). Australopithecus sediba: A new species of Homo-like Australopith from South Africa. *Science*, *328*, 195–204.

Berger, L. R., Hawks, J., de Ruiter, D. J., Churchill, S. E., Schmid, P., Delezene, L., … Zipfel, B. (2015). *Homo naledi*, a new species of the genus *Homo* from the Dinaledi chamber, South Africa. *eLife*, *4*, e09560.

Berillon, G. (1999). Geometric pattern of the hominoid hallucal tarsometatarsal complex. Quantifying the degree of hallux abduction in early hominids. *Comptes Rendus de l'Académie des Sciences-Series IIA*, *328*, 627–633.

Berillon, G. (2003). Assessing the longitudinal structure of the early hominid foot: A two-dimensional architectural analysis. *Human Evolution*, *18*, 113–122.

Berillon, G. (2004). In what manner did they walk on two legs? In D. J. Meldrum & C. E. Hilton (Eds.), *From biped to strider* (pp. 85–100). Boston, MA: Springer.

Bishop, L. C., Barham, L., Ditchfield, P. W., Elton, S., Harcourt-Smith, W. E., & Dawkins, P. (2016). Quaternary fossil fauna from the Luangwa Valley, Zambia. *Journal of Quaternary Science*, *31*, 178–190.

Bojsen-Møller, F. (1979). Calcaneocuboid joint and stability of the longitudinal arch of the foot at high and low gear push off. *Journal of Anatomy*, *129*, 165.

Boule, M. (1911). L'homme fossile de la Chapelle-aux-Saints. *Annales de Paléontologie*, *6*, 111–172.

Boule, M. (1912). L'homme fossile de la Chapelle-aux-Saints. *Annales de Paléontologie*, *7*, 21–56.

Boule, M. (1913). L'homme fossile de la Chapelle-aux-Saints. *Annales de Paléontologie*, *8*, 1–70.

Boyle, E., & DeSilva, J. M. (2015). A large *Homo erectus* talus from Koobi fora, Kenya (KNM-ER 5428), and Pleistocene hominin talar evolution. *Paleoanthropology*, *2015*, 1–13.

Boyle, E. K., McNutt, E. J., Sasaki, T., Suwa, G., Zipfel, B., & DeSilva, J. M. (2018). A quantification of calcaneal lateral plantar process position with implications for locomotion in Australopithecus. *Journal of Human Evolution*, *123*, 24–34.

Bramble, D. M., & Lieberman, D. E. (2004). Endurance running and the evolution of Homo. *Nature*, *432*, 345–352.

Bremer, K. (1994). Branch support and tree stability. *Cladistics*, *10*, 295–304.

Broom, R. (1938). Further evidence on the structure of the South African Pleistocene anthropoids. *Nature*, *142*, 897–899.

Broom, R. (1943a). Further evidence on the structure of the south African Pleistocene anthropoids. *Nature*, *142*, 897–899.

Broom, R. (1943b). An ankle-bone of the ape-man *Paranthropus robustus*. *Nature*, *152*, 689–690.

Brown, P., Sutikna, T., Morwood, M. J., Soejono, R. P., JatmikoWayhu Saptomo, E., & Due, R. A. (2004). A new small-bodied hominin from the late Pleistocene of Flores, Indonesia. *Nature*, *431*, 1055–1061.

Brunet, M., Guy, F., Pilbeam, D., Mackaye, H. T., Likius, A., Ahounta, D., … De Bonis, L. (2002). A new hominid from the upper Miocene of Chad, Central Africa. *Nature*, *418*, 145–151.

Butler, A. M., & Walsh, W. R. (2004). Mechanical responses of ankle ligaments at low loads. *Foot and Ankle International*, *25*, 8–12.

Christie, P.W. (1990). *Mathematical representation and analysis of articular surfaces: Application to the functional anatomy and palaeoanthropology of the ankle joint*. Ph.D. Thesis, University of Witwatersrand, Johannesburg, South Africa.

Churchill, S. E., Holliday, T. W., Carlson, K. J., Jashashvili, T., Macias, M. E., Mathews, S., … Berger, L. R. (2013). The upper limb of *Australopithecus sediba*. *Science*, *340*, 1233477.

Čihák, R. (1972). Ontogenesis of the skeleton and intrinsic muscles of the human hand and foot. *Ergebnisse der Anatomie und Entwicklungsgeschichte*, *46*, 1–194.

Clarke, R. J. (1979). Early hominid footprints from Tanzania. *South African Journal of Science*, *75*, 148–149.

Clarke, R. J. (1988). A new Australopithecus cranium from Sterkfontein and its bearing on the ancestry of Paranthropus. In F. E. Grine (Ed.), *Evolutionary history of the "robust" australopithecines* (pp. 285–292). New York: Aldine de Gruyter.

Clarke, R. J. (1998). First ever discovery of a well-preserved skull and associated skeleton of *Australopithecus*. *South African Journal of Science*, *94*, 460–463.

Clarke, R. J. (2008). Latest information on Sterkfontein's *Australopithecus* skeleton and a new look at *Australopithecus*. *South African Journal of Science*, *104*, 443–449.

Clarke, R. J. (2013). *Australopithecus* from Sterkfontein caves, South Africa. In K. E. Reed, J. G. Fleagle, & R. E. Leakey (Eds.), *The Paleobiology of Australopithecus* (pp. 105–124). New York: Springer.

Clarke, R. J., & Tobias, P. V. (1995). Sterkfontein member 2 foot bones of the oldest south African hominid. *Science*, *269*, 521–524.

Congdon, K. A. (2012). Interspecific and ontogenetic variation in proximal pedal phalangeal curvature of great apes (*Gorilla gorilla*, *Pan troglodytes*, and *Pongo pygmaeus*). *International Journal of Primatology*, *33*, 418–427.

Coppens, Y. (1975). Évolution des hominidés et de leur environment au cours du Plio-Pléistocène dans la basse vallèe de l'Omo en Éthiopie. *Comptes Rendus de l'Académie des Sciences - Series D - Sciences Naturelles*, *281*, 1693–1696.

Crompton, R. H. (2017). Making the case for possible hominin footprints from the late Miocene (c. 5.7 ma) of Crete? *Proceedings of the Geologists' Association*, *128*, 692–693.

Crompton, R. H., Pataky, T. C., Savage, R., D'Août, K., Bennett, M. R., Day, M. H., … Sellers, W. I. (2012). Human-like external function of the foot, and fully upright gait, confirmed in the 3.66 million year old Laetoli hominin footprints by topographic statistics, experimental footprint-formation and computer simulation. *Journal of the Royal Society Interface*, *9*, 707–719.

Cummings, S. R., Ling, X., & Stone, K. (1997). Consequences of foot binding among older women in Beijing, China. *American Journal of Public Health*, *87*, 1677–1679.

D'Août, K., & Aerts, P. (2008). The evolutionary history of the human foot. In *Advances in plantar pressure measurements in clinical and scientific research* (pp. 44–68). Maastricht, Shaker Publishing.

D'Août, K., Meert, L., Van Gheluwe, B., De Clercq, D., & Aerts, P. (2010). Experimentally generated footprints in sand: Analysis and consequences for the interpretation of fossil and forensic footprints. *American Journal of Physical Anthropology*, *141*, 515–525.

D'Août, K., Pataky, T. C., De Clercq, D., & Aerts, P. (2009). The effects of habitual footwear use: Foot shape and function in native barefoot walkers. *Footwear Science*, *1*, 81–94.

Dart, R. A. (1948). The Makapansgat proto-human australo-pithecus prometheus. *American Journal of Physical Anthropology*, *6*, 259–284.

Darwin, C. (1859). *On the origin of species by means of natural selection*. London: Murray.

Daver, G., Berillon, G., Jacquier, C., Ardagna, Y., Yadeta, M., Maurin, T., … Boisserie, J. R. (2018). New hominin postcranial remains from locality OMO 323, Shungura formation, lower Omo Valley, southwestern Ethiopia. *Journal of Human Evolution*, *122*, 23–32.

Day, M. H. (1967). Olduvai Hominid 10: A multivariate analysis. *Nature*, *215*, 323–324.

Day, M. H. (1973). Locomotor features of the lower limb in hominids. *Symposia of the Zoological Society of London*, *33*, 29–51.

Day, M. H. (1986). *Guide to fossil man*. Chicago, IL: University of Chicago Press.

Day, M. H., & Leakey, R. E. F. (1974). New evidence of the genus Homo from east Rudolf, Kenya (III). *American Journal of Physical Anthropology*, *41*, 367–380.

Day, M. H., Leakey, R. E. F., Walker, A. C., & Wood, B. A. (1976). New hominids from East Turkana, Kenya. *American Journal of Physical Anthropology*, *45*, 369–435.

Day, M. H., & Napier, J. R. (1964). Hominid fossils from bed 1, Olduvai George, Tanganyika: Fossil foot bones. *Nature*, *201*, 969–970.

Day, M. H., & Napier, J. R. (1966). A hominid toe bone from bed 1, Olduvai Gorge, Tanzania. *Nature*, *211*, 929–930.

Day, M. H., & Thornton, C. M. B. (1986). The extremity bones of *Paranthropus robustus* from Kromdraai B, east formation member 3, Republic of South Africa—A reappraisal. *Anthropos (Brno)*, *23*, 91–99.

Day, M. H., Twist, M. H. C., & Ward, S. (1991). Les vestiges post-crâniens d'Omo I (Kibish). *L'Anthropologie*, *95*, 595–610.

Day, M. H., & Wickens, E. H. (1980). Laetoli Pliocene hominid footprints and bipedalism. *Nature*, *286*, 385–387.

Day, M. H., & Wood, B. A. (1968). Functional affinities of the Olduvai hominid 8 talus. *Man*, *3*, 440–455.

De Castro, J. B., Arsuaga, J. L., Carbonell, E., Rosas, A., Martınez, I., & Mosquera, M. (1997). A hominid from the lower Pleistocene of Atapuerca, Spain: Possible ancestor to Neandertals and modern humans. *Science*, *276*(5317), 1392–1395.

De Lumley, H. (1969). A Paleolithic camp at Nice. *Scientific American*, *220*(5), 42–51.

Deane, A. S., & Begun, D. R. (2008). Broken fingers: Retesting locomotor hypotheses for fossil hominoids using fragmentary proximal phalanges and high-resolution polynomial curve fitting (HR-PCF). *Journal of Human Evolution*, *55*(4), 691–701.

Deino, A. L., & McBrearty, S. (2002). 40Ar/39Ar dating of the Kapthurin formation, Baringo, Kenya. *Journal of Human Evolution*, *42*(1–2), 185–210.

Deloison, Y. (1985). Comparative study of calcanei of primates and pan-Australopithecus-Homo relationship. In P. V. Tobias (Ed.), *Hominid evolution: Past, present and future* (pp. 143–147). New York: Liss.

Deloison, Y. (1986). Description d'un calcanéum fossile de Primate et sa comparison avec des calcanéums de Pongidés, d'Australopithèques et d'*Homo*. *Comptes Rendus des Séances de l'Académie des Sciences Paris, Série III*, *302*, 257–262.

Deloison, Y. (1991). Les australopithe`ques marchaient-ils comme nous? In B. Senut & Y. Coppens (Eds.), *Origine(s) de la bipe´die chez les Hominide's* (pp. 177–186). Paris, France: CNRS.

Deloison, Y. (1992). Empreintes de pas à Laetoli (Tanzanie). Leur apport à une meilleure connaissance de la locomotion des Hominidés fossiles. *Comptes Rendus des Séances de l'Académie des Sciences Paris, Série I*, *315*, 103.

Deloison, Y. (2003). Anatomie des os fossils de pieds des hominids d'Afrique du sud dates entre 2,4 et 3,5 millions d'annés. Interprétation quant à leur mode de locomotion. *Biométrie Humaine et Anthropologie*, *21*, 189–230.

Deloison, Y. (2004). A new hypothesis on the origin of hominoid locomotion. In D. J. Meldrum & C. E. Hilton (Eds.), *From biped to strider* (pp. 35–47). Boston, MA: Springer.

Dembo, M., Matzke, N. J., Mooers, A. Ø., & Collard, M. (2015). Bayesian analysis of a morphological supermatrix sheds light on controversial fossil hominin relationships. *Proceedings of the Royal Society B*, *282*, 20150943.

Dembo, M., Radovčić, D., Garvin, H. M., Laird, M. F., Schroeder, L., Scott, J. E., … Collard, M. (2016). The evolutionary relationships and age of Homo Naledi: An assessment using dated Bayesian phylogenetic methods. *Journal of Human Evolution*, *97*, 17–26.

DeSilva, J.M. (2008). *Vertical climbing adaptations in the anthropoid ankle and midfoot: Implications for locomotion in Miocene catarrhines and Plio-Pleistocene hominins.* Doctoral Dissertation, University of Michigan, Michigan, MI.

DeSilva, J. M. (2009). Functional morphology of the ankle and the likelihood of climbing in early hominins. *Proceedings of the National Academy of Sciences of the United States of America*, *106*, 6567–6572.

DeSilva, J. M. (2010). Revisiting the "midtarsal break". *American Journal of Physical Anthropology*, *141*, 245–258.

DeSilva, J. M., Bonne-Annee, R., Swanson, Z., Gill, C. M., Sobel, M., Uy, J., & Gill, S. V. (2015). Midtarsal break variation in modern humans: Functional causes, skeletal correlates, and paleontological implications. *American Journal of Physical Anthropology*, *156*, 543–552.

DeSilva, J. M., Carlson, K. J., Claxton, A., Harcourt-Smith, W. E. H., McNutt, E., Sylvester, A. D., … Berger, L. R. (2018). The anatomy of the lower limb skeleton of *Australopithecus sediba*. *PaleoAnthropology* (in press).

DeSilva, J. M., & Devlin, M. (2012). A comparative study of the trabecular bony architecture of the talus in humans, non-human primates, and *Australopithecus*. *Journal of Human Evolution*, *63*, 536–551.

DeSilva, J. M., Gill, C., Prang, C., Bredella, M., & Alemseged, Z. (2018). A nearly complete foot from Dikika, Ethiopia and its implications for the ontogeny and function of *Australopithecus afarensis*. *Science Advances*, *4*, eaar7723.

DeSilva, J. M., & Gill, S. (2013). Brief communication: A midtarsal (midfoot) break in the human foot. *American Journal of Physical Anthropology*, *151*, 495–499.

DeSilva, J. M., Holt, K. G., Churchill, S. E., Carlson, K. J., Walker, C. S., Zipfel, B., & Berger, L. R. (2013). The lower limb and mechanics of walking in *Australopithecus sediba*. *Science*, *340*, 1232999.

DeSilva, J.M., McNutt, E., Zipfel, B., & Kimbel, W. (2018). *Associated Australopithecus afarensis second and third metatarsals (A.L. 333–133) from Hadar, Ethiopia.* Paper presented at the meeting of the American Association of Physical Anthropologists, Austin, TX.

DeSilva, J. M., Proctor, D. J., & Zipfel, B. (2012). A complete second metatarsal (StW 89) from Sterkfontein member 4, South Africa. *Journal of Human Evolution*, *63*, 497–496.

DeSilva, J. M., & Throckmorton, Z. J. (2010). Lucy's flat feet: The relationship between the ankle and rearfoot arching in early hominins. *PLoS One*, *5*, e14432.

DeSilva, J. M., Zipfel, B., Kidd, R., Carlson, K., Churchill, S., & Berger, L. (2012). The primitive aspects of the foot and ankle of *Australopithecus sediba*. *American Journal of Physical Anthropology*, *S54*, 129.

DeSilva, J. M., Zipfel, B., Van Arsdale, A. P., & Tocheri, M. W. (2010). The Olduvai hominid 8 foot: Adult or subadult? *Journal of Human Evolution*, *58*, 418–423.

Dirks, P. H., Roberts, E. M., Hilbert-Wolf, H., Kramers, J. D., Hawks, J., Dosseto, A., … Berger, L. R. (2017). The age of *Homo naledi* and associated sediments in the rising star cave, South Africa. *eLife*, *6*, e24231.

Dowdeswell, M. R., Jashashvili, T., Patel, B. A., Lebrun, R., Susman, R. L., Lordkipanidze, D., & Carlson, K. J. (2016). Adaptation to bipedal gait and fifth metatarsal structural properties in Australopithecus, Paranthropus, and Homo. *Comptes Rendus Palevol*, *16*(5–6), 585–599.

Drapeau, M. S. M., & Harmon, E. H. (2013). Metatarsal torsion in monkeys, humans and australopiths. *Journal of Human Evolution*, *64*, 93–108.

Dudas, M., & Harcourt-Smith, W. E. H. (2017). Using 4th order polynomial curve fitting to assess curvature and allometry of the hallucal facet in extant hominoids and fossil hominins. *American Journal of Physical Anthropology*, *162*, 167.

Duncan, A. S., Kappelman, J., & Shapiro, L. J. (1994). Metatarsophalangeal joint function and positional behavior in Australopithecus afarensis. *American Journal of Physical Anthropology*, *93*(1), 67–81.

Dunn, R. H., Tocheri, M. W., Orr, C. M., & Jungers, W. L. (2014). Ecological divergence and talar morphology in gorillas. *American Journal of Physical Anthropology*, *153*, 526–541.

Duval, M., Grün, R., Parés, J. M., Martín-Francés, L., Campaña, I., Rosell, J., … de Castro, J. M. B. (2018). The first direct ESR analysis of a hominin tooth from Atapuerca gran Dolina TD-6 (Spain) supports the antiquity of Homo antecessor. *Quaternary Geochronology.*, *47*, 120–137.

Elftman, H. (1960). The transverse tarsal joint and its control. *Clinical Orthopaedics*, *16*, 41–45.

Elftman, H., & Manter, J. (1935). Chimpanzee and human feet in bipedal walking. *American Journal of Physical Anthropology*, *20*, 69–79.

Eliot, D. J., & Jungers, W. L. (2000). Fifth metatarsal morphology does not predict presence or absence of fibularis tertius muscle in hominids. *Journal of Human Evolution*, *38*(2), 333–342.

Falk, D. (1986). Evolution of cranial blood drainage in hominids: Enlarged occipital/marginal sinuses and emissary foramina. *American Journal of Physical Anthropology*, *703*, 311–324.

Falkingham, P. L., Bates, K. T., Avanzini, M., Bennett, M., Bordy, E. M., Breithaupt, B. H., … Belevedere, M. (2018). A standard protocol for documenting modern and fossil ichnological data. *Palaeontology*, *61*, 469–480.

Fernández, P. J., Holowka, N. B., Demes, B., & Jungers, W. L. (2016). Form and function of the human and chimpanzee rearfoot: Implications for early hominin bipedalism. *Scientific Reports*, *30532*, 1–10.

Fernández, P. J., Mongle, C. S., Leakey, L., Proctor, D. J., Orr, C. M., Patel, B. A., … Jungers, W. L. (2018). Evolution and function of the hominin forefoot. *Proceedings of the National Academy of Sciences of the United States of America*, *115*, 8746–8751.

Fernández, P. J., Mongle, C. S., Patel, B. A., Tocheri, M. W., & Jungers, W. L. (2017). Functional morphology and evolution of the early hominin forefoot. *American Journal of Physical Anthropology*, *162*, 179.

Fisher, R., & McBrearty, S. (2002). The comparative morphology of hominin postcranial remains from the Kapthurin formation, Baringo District, Kenya. *American Journal of Physical Anthropology*, *117*, 70.

Fisk, G. R., & Macho, G. A. (1992). Evidence of a healed compression fracture in a Plio-Pleistocene hominid talus from Sterkfontein, South Africa. *International Journal of Osteoarchaeology*, *2*, 325–332.

Gabunia, L., Vekua, A., & Lordkipanidze, D. (1999). A hominid metatarsal from Dmanisi (eastern Georgia). *Anthropologie (1962)*, *37*, 163–166.

Gebo, D. L. (1992). Plantigrady and foot adaptation in African apes: Implications for hominin origins. *American Journal of Physical Anthropology*, *89*, 29–58.

Gebo, D. L., & Schwartz, G. T. (2006). Foot bones from Omo: Implications for hominid evolution. *American Journal of Physical Anthropology*, *129*, 499–511.

Gierliński, G. D., Niedźwiedzki, G., Lockley, M. G., Athanassiou, A., Fassoulas, C., Dubicka, Z., … Ahlberg, P. E. (2017). Possible hominin footprints from the late Miocene (c. 5.7 ma) of Crete? *Proceedings of the Geologists' Association*, *128*(5), 697–710.

Gilbert, W. H., & Asfaw, B. (2008). *Homo erectus: Pleistocene evidence from the Middle Awash, Ethiopia* (Vol. 1). Berkeley, CA: University of California Press.

Gill, C., Taneja, A., Bredella, M., Torriani, M., & DeSilva, J. (2014). Osteogenic relationship between the lateral plantar process and the peroneal tubercle in the human calcaneus. *Journal of Anatomy*, *224*, 173–179.

Gill, C. M., Bredella, M. A., & DeSilva, J. M. (2015). Skeletal development of hallucal tarsometatarsal joint curvature and angulation in extant apes and modern humans. *Journal of Human Evolution*, *88*, 137–145.

Gomberg, D.N. (1981). *Form and function of the hominoid foot*. Ph.D. Thesis. University of Massachusetts, Amherst.

Gomberg, D. N. (1985). Functional differences of three ligaments of the transverse tarsal joint in hominoids. *Journal of Human Evolution*, *14*, 553–562.

Gomberg, D. N., & Latimer, B. (1984). Observations on the transverse tarsal joint of *Australopithecus afarensis* and some comments on the interpretation of behavior from morphology. *American Journal of Physical Anthropology*, *63*, 164.

Grabowski, M., & Roseman, C. C. (2015). Complex and changing patterns of natural selection explain the evolution of the human hip. *Journal of Human Evolution*, *85*, 94–110.

Granatosky, M. C., Laird, M. R., Kuo, S., Alemseged, Z., & Ross, C. F. (2018). An XROMM analysis of midfoot mobility in non-human primates. *American Journal of Physical Anthropology*, *165*, 104.

Granger, D. E., Gibbon, R. J., Kuman, K., Clarke, R. J., Bruxelles, L., & Caffee, M. W. (2015). New cosmogenic burial ages for Sterkfontein member 2 *Australopithecus* and member 5 Oldowan. *Nature*, *522*, 85–88.

Grausz, H. M., Leakey, R. E., Walker, A. C., & Ward, C. V. (1988). Associated cranial and postcranial bones of *Australopithecus boisei*. In F. E. Grine (Ed.), *Evolutionary history of the "robust" australopithecines* (pp. 127–132). New Brunswick: Aldine.

Gregory, W. K. (1928). The upright posture of man: A review of its origin and evolution. *Proceedings of the American Philosophical Society*, *67*, 339–377.

Griffin, N. L., Miller, C. E., Schmitt, D., & D'Août, K. (2015). Understanding the evolution of the windlass mechanism of the human foot from comparative anatomy: Insights, obstacles, and future directions. *American Journal of Physical Anthropology*, *156*, 1–10.

Griffin, N. L., & Richmond, B. G. (2010). Joint orientation and function in great ape and human proximal pedal phalanges. *American Journal of Physical Anthropology*, *141*, 116–123.

Grine, F. E., Wurz, S., & Marean, C. W. (2017). The middle stone age human fossil record from Klasies River Main site. *Journal of Human Evolution*, *103*, 53–78.

Haile-Selassie, Y. (2001). Late Miocene hominids from the middle awash, Ethiopia. *Nature*, *412*, 178–181.

Haile-Selassie, Y., Gibert, L., Melillo, S. M., Ryan, T. M., Alene, M., Deino, A., … Saylor, B. Z. (2015). New species from Ethiopia further expands middle Pliocene hominin diversity. *Nature*, *521*, 483–488.

Haile-Selassie, Y., Saylor, B. Z., Deino, A., Levin, N. E., Alene, M., & Latimer, B. M. (2012). A new hominin foot from Ethiopia shows multiple Pliocene bipedal adaptations. *Nature*, *483*, 565–569.

Haile-Selassie, Y., Suwa, G., & White, T. D. (2009). Hominidae. In Y. Haile-Selassie & G. WoldeGabriel (Eds.), *Ardipithecus kadabba. Late Miocene evidence from the middle awash, Ethiopia* (pp. 159–236). Berkeley, CA: University of California Press.

Hammer, Ø., Harper, D. A. T., & Ryan, P. D. (2001). Past: Paleontological statistics software package for education and data analysis. *Palaeontologia Electronica*, *4*(1), 9.

Harcourt-Smith, W., Thomas, O., DeSilva, J., Frost, S., Patel, B., & Orr, C. (2014). The Kromdraai "hominin" cuboid KB 3133. A new assignation based on comparative anatomical techniques and 3D geometric morphometrics. *American Journal of Physical Anthropology*, *S58*, 136.

Harcourt-Smith, W.E.H. (2002). *Form and function in the hominoid tarsal skeletal structure*. Ph.D. Dissertation, University College London, London.

Harcourt-Smith, W. E. H. (2016). Early hominin diversity and the emergence of the genus *Homo*. *Journal of Anthropological Sciences*, *94*, 19–27.

Harcourt-Smith, W. E. H., & Aiello, L. C. (2004). Fossils, feet, and the evolution of human bipedal locomotion. *Journal of Anatomy*, *204*, 403–416.

Harcourt-Smith, W. E. H., & Hilton, C. (2005). Did *Australopithecus afarensis* make the Laetoli footprint trail? New insights into an old problem. *American Journal of Physical Anthropology*, *126*(S40), 112.

Harcourt-Smith, W. E. H., Throckmorton, Z., Congdon, K. A., Zipfel, B., Deana, A. S., Drapeau, M. S. M., … DeSilva, J. M. (2015). The foot of *Homo naledi*. *Nature Communications*, *6*, 8432.

Harrison, T. (1991). The implications of Oreopithecus bambolii for the origins of bipedalism. In Y. Coppens & B. Senut (Eds.), *Origine (s) de la bipédie chez les hominidés*, *Cahiers de Paléoanthropologie* (pp. 235–244). Paris, France: CNRS.

Harvati, K., Dalas, A., Bailey, S., Rein, T. R., El Zaatari, S., Fiorenza, L., … Psathi, E. (2013). New Neanderthal remains from Mani peninsula, southern Greece: The Kalamakia middle Paleolithic cave site. *Journal of Human Evolution*, *64*, 486–499.

Hatala, K. G., Demes, B., & Richmond, B. G. (2016). Laetoli footprints reveal bipedal gait biomechanics different from those of modern humans and chimpanzees. *Proceedings of the Royal Society B: Biological Sciences*, *283*, 2016020235.

Hatala, K. G., Dingwall, H. L., Wunderlich, R. E., & Richmond, B. G. (2013a). Variation in foot strike patterns during running among habitually barefoot populations. *PLoS One*, *8*, e52548.

Hatala, K. G., Dingwall, H. L., Wunderlich, R. E., & Richmond, B. G. (2013b). The relationship between plantar pressure and footprint shape. *Journal of Human Evolution*, *65*, 21–28.

Hatala, K. G., Perry, D. A., & Gatesy, S. M. (2018). A biplanar X-ray approach for studying the 3D dynamics of human track formation. *Journal of Human Evolution*, *121*, 104–118. https://doi.org/10.1016/j.jhevol.2018.03.006

Hatala, K. G., Roach, N. T., Ostrofsky, K. R., Wunderlich, R. E., Dingwall, H. L., Villmoare, B. A., … Richmond, B. G. (2017). Hominin track assemblages from Okote member deposits near Ileret, Kenya, and their implications for understanding fossil hominin paleobiology at 1– 5 Ma. *Journal of Human Evolution*, *85*, 75–93.

Hatala, K. G., Roach, N. T., Ostrofsky, K. R., Wunderlich, R. E., Dingwall, H. L., Villmoare, B. A., … Richmond, B. G. (2016). Footprints reveal direct evidence of group behavior and locomotion in *Homo erectus*. *Scientific Reports*, *28766*, 1–9.

Hawks, J., Elliot, M., Schmid, P., Churchill, S. E., de Ruiter, D. J., Roberts, E., … Berger, L. R. (2017). New fossil remains of *Homo naledi* from the Lesedi chamber, South Africa. *eLife*, *6*, e24232.

Heard-Booth, A.N. (2017). *Morphological and functional correlates of variation in the human longitudinal arch*. Doctoral Dissertation, Department of Anthropology, University of Texas, Austin, TX.

Heim, J. L. (1982). Les hommes fossiles de La Ferrassie II. *Archives de l'Institut de Paléontologie Humaine*, *38*, 1–272.

Helm, C. W., McCrea, R. T., Cawthra, H. C., Lockley, M. G., Cowling, R. M., Marean, C. W., … Hattingh, S. (2018). A new Pleistocene hominin Tracksite from the cape south coast, South Africa. *Scientific Reports*, *8*(1), 3772.

Hicks, J. H. (1953). The mechanics of the foot. I. The joints. *Journal of Anatomy*, *83*, 345–357.

Hillenbrand, H.A. (2009). *An Australopithecus afarensis infant first metatarsal from Hadar, Ethiopia*. Honors Thesis, Miami University, Oxford, OH.

Holowka, N. B., & Lieberman, D. E. (2018). Rethinking the evolution of the human foot: Insights from experimental research. *Journal of Experimental Biology*, *221*, jeb174425.

Holowka, N. B., O'Neill, M. C., Thompson, N. E., & Demes, B. (2017). Chimpanzee and human midfoot motion during bipedal walking and the evolution of the longitudinal arch of the foot. *Journal of Human Evolution*, *104*, 23–31.

Holowka, N. B., Wallace, I. J., & Lieberman, D. E. (2018). Foot strength and stiffness are related to footwear use in a comparison of minimally- vs. conventionally-shod populations. *Scientific Reports*, *8*(1), 3679.

Howell, F. C., Haesaerts, P., & de Heinzelin, J. (1987). Depositional environments, archaeological occurrences and hominids from members E and F of the Shungura formation (Omo basin, Ethiopia). *Journal of Human Evolution*, *16*, 665–700.

Huxley, T. H. (1863). *Man's place in nature*. London: Routledge.

Inman, V. T. (1976). *The joints of the ankle*. Baltimore: Williams & Wilkins.

Jacobs, Z., & Roberts, D. L. (2009). Last interglacial age for aeolian and marine deposits and the Nahoon fossil human footprints, southeast coast of South Africa. *Quaternary Geochronology*, *4*(2), 160–169.

Jashashvili, T., Dowdeswell, M. R., Lebrun, R., & Carlson, K. J. (2015). Cortical structure of hallucal metatarsals and locomotor adaptations in hominoids. *PLoS One*, *10*(1), e0117905.

Jashashvili, T., Ponce de León, M. S., Lordkipanidze, D., & Zollikofer, C. P. (2010). First evidence of a bipartite medial cuneiform in the hominin fossil record: A case report from the early Pleistocene site of Dmanisi. *Journal of Anatomy*, *216*(6), 705–716.

Johanson, D. C., Lovejoy, C. O., Kimbel, W. H., White, T. D., Ward, S. C., Bush, M. E., … Coppens, Y. (1982). Morphology of the Pliocene partial hominid skeleton (AL 288-1) from the Hadar formation, Ethiopia. *American Journal of Physical Anthropology*, *57*, 403–451.

Jones, F. W. (1916). *Arboreal man*. London: Longmans.

Jones, R. L. (1941). The human foot. An experimental study of its mechanics, and the role of its muscles and ligaments in the support of the arch. *Developmental Dynamics*, *68*(1), 1–39.

Jungers, W. L., Grine, F. E., Leakey, M. G., Leakey, L., Brown, F., Yang, D., & Tocheri, M. W. (2015). New hominin fossils from Ileret (Kolom Odiet), Kenya. *American Journal of Physical Anthropology*, *156*, 181.

Jungers, W. L., Harcourt-Smith, W. E. H., Wunderlich, R. E., Tocheri, M. W., Larson, S. G., Sutikna, T., … Morwood, M. J. (2009). The foot of *Homo floresiensis*. *Nature*, *459*, 81–84.

Jungers, W. L., Larson, S. G., Harcourt-Smith, W. E. H., Morwood, M. J., Sutikna, T., Awe, R. D., & Djubiantono, T. (2009). Descriptions of the lower limb skeleton of *Homo floresiensis*. *Journal of Human Evolution*, *57*, 538–554.

Kachlik, D., Baca, V., Cepelik, M., Hajek, P., Mandys, V., & Musil, V. (2008). Clinical anatomy of the calcaneal tuberosity. *Annals of Anatomy – Anatomischer Anzeiger*, *190*, 284–291.

Keith, A. (1928). The history of the human foot and its bearing on orthopaedic practice. *Journal of Bone and Joint Surgery*, *11*, 10–32.

Kelikian, A. S., & Sarrafian, S. K. (2011). *Sarrafian's anatomy of the foot and ankle: Descriptive, topographic, functional*. New York: Lippincott Williams & Wilkins.

Kidd, R. (1999). Evolution of the rearfoot. A model of adaptation with evidence from the fossil record. *Journal of the American Podiatric Medical Association*, *89*, 2–17.

Kidd, R. S., O'Higgins, P., & Oxnard, C. E. (1996). The OH 8 foot: A reappraisal of the functional morphology of the hindfoot utilizing a multivariate analysis. *Journal of Human Evolution*, *31*, 269–291.

Kidd, R. S., & Oxnard, C. (2005). Little foot and big thoughts—A re-evaluation of the StW 573 foot from Sterkfontein, South Africa. *Journal of Comparative Human Biology*, *55*, 189–212.

Kim, C. B., Kim, J. Y., Kim, K. S., & Lim, H. S. (2010). New age constraints for hominid footprints found on Jeju Island, South Korea. *Journal of Archaeological Science*, *37*, 3338–3343.

Kim, K. S., Kim, J. Y., Kim, S. H., Lee, C. Z., & Lim, J. D. (2009). Preliminary report on homind and other vertebrate footprints from the late quaternary strata of Jeju Island, Korea. *Ichnos*, *16*, 1–11.

Kimbel, W. H. (1984). Variation in the pattern of cranial venous sinuses and hominid phylogeny. *American Journal of Physical Anthropology*, *63*(3), 243–263.

Kimbel, W. H., & Rak, Y. (1985). Functional morphology of the asterionic region in extant hominoids and fossil hominids. *American Journal of Physical Anthropology*, *66*(1), 31–54.

Kitashiro, M., Ogihara, N., Kokubo, T., Matsumoto, M., Nakamura, M., & Nagura, T. (2017). Age-and sex-associated morphological variations of metatarsal torsional patterns in humans. *Clinical Anatomy*, *30*, 1058–1063.

Kivell, T. L., Deane, A. S., Tocheri, M. W., Orr, C. M., Schmid, P., Hawks, J., … Churchill, S. E. (2015). The hand of *Homo naledi*. *Nature Communications*, *6*, 8431.

Klenerman, L., & Wood, B. (2006). *The human foot*. London: Springer.

Knigge, R. P., Tocheri, M. W., Orr, C. M., & McNulty, K. P. (2015). Three-dimensional geometric morphometric analysis of talar morphology in extant gorilla taxa from highland and lowland habitats. *The Anatomical Record*, *298*, 277–290.

Köhler, M., & Moyà-Solà, S. (1997). Ape-like or hominid-like? The positional behavior of *Oreopithecus bambolii* reconsidered. *Proceedings of the National Academy of Sciences of the United States of America*, *94*(21), 11747–11750.

Komza, K. (2017). *A unique form of locomotion in Swartkrans hominins: An analysis of the trabecular structure of the first metatarsal*. MScRes thesis. University of Kent, Canterbury, England.

Kramers, J. D., & Dirks, P. H. (2017). The age of fossil StW573 ('little foot'): An alternative interpretation of 26Al/10Be burial data. *South African Journal of Science*, *113*, 1–8.

Kuman, K., & Clarke, R. J. (2000). Stratigraphy, artifact industries and hominin associations for Sterkfontein, member 5. *Journal of Human Evolution*, *38*, 827–847.

Kuo, S., DeSilva, J. M., Devlin, M., McDonald, G., & Morgan, E. (2013). The effect of the Achilles tendon on trabecular structure in the primate calcaneus. *The Anatomical Record*, *296*, 1509–1517.

Kuo, S., Ward, C. V., Kimbel, W. H., Congdon, K. A., & Johanson, D. C. (2016). Functional morphology of the fourth metatarsal in monkeys, apes, and *Australopithecus afarensis*. *American Journal of Physical Anthropology*, *159*, 198–199.

Kuttruff, J. T., DeHart, S. G., & O'Brien, M. J. (1998). 7500 years of prehistoric footward from Arnold research cave, Missouri. *Science*, *281*, 72–75.

Lamy, P. (1982). Le metatarsien Arago XLIII. L'*Homo erectus* et la place de l'homme de Tautavel parmi les hominidés fossils: Congrès international de paléontologie humaine, 1er Congrès. *Nice*, *1–2*, 319–336.

Lamy, P. (1986). The settlement of the longitudinal plantar arch of some African Plio-Pleistocene hominins: A morphological study. *Journal of Human Evolution*, *15*, 31–46.

Langdon, J. H. (1985). Fossils and the origin of bipedalism. *Journal of Human Evolution*, *14*, 615–635.

Langdon, J. H. (1986). Functional morphology of the Miocene hominoid foot. *Contribution to Primatology*, *22*, 1–225.

Langdon, J. H., Bruckner, J., & Baker, H. H. (1991). Pedal mechanics and bipedalism in early hominins. In Y. Coppens & B. Senut (Eds.), *Origine (s) de la Bipédie chez les Homininés* (pp. 159–167). Paris: Centre National de la Recherche Scientifique.

Latimer, B. (1991). Locomotor adaptations in Australopithecus afarensis: The issue of arboreality. In Y. Coppens & B. Senut (Eds.), *Origine(s) de la Bipédie chez les Hominidés* (pp. 169–176). Paris: Centre National de la Recherche Scientifique.

Latimer, B. M., & Lovejoy, C. O. (1989). The calcaneus of Australopithecus afarensis and its implications for the evolution of bipedality. *American Journal of Physical Anthropology*, *78*, 369–386.

Latimer, B. M., & Lovejoy, C. O. (1990a). Metatarsophalangeal joints of *Australopithecus afarensis*. *American Journal of Physical Anthropology*, *83*, 13–23.

Latimer, B. M., & Lovejoy, C. O. (1990b). Hallucal tarsometatarsal joint in *Australopithecus afarensis*. *American Journal of Physical Anthropology*, *82*, 125–133.

Latimer, B. M., Lovejoy, C. O., Johanson, D. C., & Coppens, Y. (1982). Hominid tarsal, metatarsal, and phalangeal bones recovered from the Hadar formation: 1974-1977 collections. *American Journal of Physical Anthropology*, *57*, 701–719.

Latimer, B. M., Ohman, J. C., & Lovejoy, C. O. (1987). Talocrural joint in African hominoids: Implications for *Australopithecus afarensis*. *American Journal of Physical Anthropology*, *74*, 155–175.

Le Gros Clark, W. E. (1947). Observations on the anatomy of the fossil Australopithecinae. *Journal of Anatomy*, *81*, 300–333.

Le Minor, J. M., & Winter, M. (2003). The intermetatarsal articular facet of the first metatarsal bone in humans: A derived trait unique within primates. *Annals of Anatomy*, *185*, 359–365.

Leakey, L. S. B. (1960). Recent discoveries at Olduvai gorge. *Nature*, *188*(4755), 1050–1052.

Leakey, L. S. B., Tobias, P. V., & Napier, J. R. (1964). A new species of genus Homo from Olduvai Gorge. *Nature*, *202*, 7–9.

Leakey, M. D. (1971). *Olduvai Gorge. Excavations in beds I and II. 1960–1963*. Cambridge: Cambridge University Press.

Leakey, M. D. (1978). Pliocene footprints at Laetolil, northern Tanzania. *Antiquity*, *52*(205), 133.

Leakey, M. D. (1979). Footprints in the ashes of time. *National Geographic*, *155*, 446–457.

Leakey, M. D., & Hay, R. L. (1979). Pliocene footprints in the Laetolil beds at Laetoli, northern Tanzania. *Nature*, *278*(5702), 317–323.

Leakey, M. G., & Harris, J. M. (1987). Laetoli: A Pliocene Site in Northern Tanzania. Oxford: Clarendon Press.

Leakey, M. G., Feibel, C. S., McDougall, I., & Walker, A. C. (1995). New four-million-year-old hominid species from Kanapoi and Allia bay, Kenya. *Nature*, *376*, 565–571.

Leakey, M. G., & Leakey, R. E. (1978). *Koobi Fora research project, volume 01: The fossil hominids and an introduction to their context, 1968–1974*. Oxford, UK: Clarendon Press.

Leakey, M. G., Spoor, F., Dean, M. C., Feibel, C. S., Antón, S. C., Kiarie, C., & Leakey, L. N. (2012). New fossils from Koobi fora in northern Kenya confirm taxonomic diversity in early Homo. *Nature*, *488*(7410), 201–204.

Leakey, R. E. F. (1973). Further evidence of lower Pleistocene hominids from east Rudolf, North Kenya, 1972. *Nature*, *242*, 170–173.

Leakey, R. E. F., & Wood, B. A. (1973). New evidence of the genus Homo from east Rudolf, Kenya. II. *American Journal of Physical Anthropology*, *39*(3), 355–368.

Lewis, O. J. (1972). The evolution of the hallucial tarsometatarsal joint in the anthropoidea. *American Journal of Physical Anthropology*, *37*, 13–33.

Lewis, O. J. (1980a). The joints of the evolving foot. Part I. the ankle joint. *Journal of Anatomy*, *130*, 527–543.

Lewis, O. J. (1980b). The joints of the evolving foot. Part II. The intrinsic joints. *Journal of Anatomy*, *130*, 833–857.

Lewis, O. J. (1980c). The joints of the evolving foot. Part III. The fossil evidence. *Journal of Anatomy*, *131*, 275–298.

Lewis, O. J. (1981). Functional morphology of the joints of the evolving foot. *Symposia of the Zoological Society of London*, *46*, 169–188.

Lewis, O. J. (1989). *Functional morphology of the evolving hand and foot*. Oxford: Clarendon Press.

Lieberman, D. E., Castillo, E. R., Otarola-Castillo, E., Sang, M. K., Sigei, T. K., Ojiambo, R., … Pitsiladis, Y. (2015). Variation in foot strike patterns among habitually barefoot and shod runners in Kenya. *PLoS One*, *10*, e0131354.

Lieberman, D. E., Venkadesan, M., Werbel, W. A., Daoud, A. I., D'Andrea, S., Davis, I. S., … Pitsiladis, Y. (2010). Foot strike patterns and collision forces in habitually barefoot versus shod runners. *Nature*, *463*, 531–535.

Lisowski, F. P., Albrecht, G. H., & Oxnard, C. E. (1974). The form of the talus in some higher primates: A multivariate study. *American Journal of Physical Anthropology*, *41*, 191–216.

Liutkus-Pierce, C. M., Zimmer, B. W., Carmichael, S. K., McIntosh, W., Deino, A., Hewitt, S. M., … Rossi, V. (2016). Radioisotopic age, formation, and preservation of late Pleistocene human footprints at Engare Sero, Tanzania. *Palaeogeography, Palaeoclimatology, Palaeoecology*, *463*(1), 68–82.

Lordkipanidze, D., Jashashville, T., Vekua, A., Ponce de Léon, M. S., Zollikofer, C. P. E., Rightmire, G. P., … Rook, L. (2007). Postcranial evidence from early *Homo* from Dmanisi, Georgia. *Nature*, *449*, 305–310.

Lorenzo, C., Arsuaga, J. L., & Carretero, J. M. (1999). Hand and foot remains from the gran Dolina early Pleistocene site (sierra de Atapuerca, Spain). *Journal of Human Evolution*, *37*, 501–522.

Lovejoy, C. O. (1975). Biomechanical perspectives on the lower limb of early hominids. In R. Tuttle (Ed.), *Primate functional morphology and evolution* (pp. 291–326). The Hague: Mouton Publishers.

Lovejoy, C. O. (1978). A biomechanical review of the locomotor review of early hominids. In C. J. Jolly (Ed.), *Early hominids of Africa* (pp. 403–429). New York: St. Martins Press.

Lovejoy, C. O., Latimer, B. M., Suwa, G., Asfaw, B., & White, T. D. (2009). Combining prehension and propulsion: The foot of *Ardipithecus ramidus*. *Science*, *326*, 72e1–72e8.

Lu, Z., Meldrum, D. J., Huang, Y., He, J., & Sarmiento, E. E. (2011). The Jinniushan hominin pedal skeleton from the late middle Pleistocene of China. *HOMO - Journal of Comparative Human Biology*, *62*(6), 389–401.

Madar, S. I., Rose, M. D., Kelley, J., MacLatchy, L., & Pilbeam, D. (2002). New *Sivapithecus* postcranial specimens from the Siwaliks of Pakistan. *Journal of Human Evolution*, *42*, 705–752.

Manter, J. T. (1941). Movements of the subtalar and transverse tarsal joints. *The Anatomical Record*, *80*, 397–410.

Marchi, D. (2005). The cross-sectional geometry of the hand and foot bones of the Hominoidea and its relationship to locomotor behavior. *Journal of Human Evolution*, *49*, 743–761.

Marchi, D. (2010). Articular to diaphyseal proportions of human and great ape metatarsals. *American Journal of Physical Anthropology*, *143*, 198–207.

Martin, R. L. (2011). The ankle and foot complex. In P. K. Levangie & C. C. Norkin (Eds.), *Joint structure and function* (5th ed., pp. 440–481). New York, NY: McGraw-Hill.

Martin-Francés, L., Martinon-Torres, M., Gracia-Téllez, A., & Bermúdez de Castro, J. M. (2015). Evidence of stress fracture in a *Homo antecessor* metatarsal from gran Dolina site (Atapuerca, Spain). *Int J Osteoarch.*, *25*, 564–573.

Masao, F. T., Ichumbaki, E. B., Cherin, M., Barili, A., Boschian, G., Iurino, D., … Manzi, G. (2016). New footprints from Laetoli (Tanzania) provide evidence for marked body size variation in early hominins. *eLife*, *5*, e19568.

McCown, T., & Keith, A. (1939). *The stone age of Mt. Carmel*. Oxford: Clarendon Press.

McDougall, I., Brown, F. H., Vasconcelos, P. M., Cohen, B. E., Theide, D. S., & Buchanan, M. J. (2012). New single crystal 40Ar/39Ar ages improve time scale for deposition of the Omo group, Omo–Turkana Basin, East Africa. *Journal of the Geological Society of London*, *169*, 213–226.

McHenry, H. M. (1994). Early hominid postcrania. In R. S. Corruccini & R. L. Ciochon (Eds.), *Integrative paths to the past* (pp. 251–268). Englewood Cliffs, NJ: Prentice Hall.

McHenry, H. M., & Jones, A. L. (2006). Hallucial convergence in early hominids. *Journal of Human Evolution*, *50*, 534–539.

McLaren, D., Fedje, D., Dyck, A., Mackie, Q., Gauvreau, A., & Cohen, J. (2018). Terminal Pleistocene epoch human footprints from the Pacific coast of Canada. *PLoS One*, *13*, e0193522.

McNulty, K. P., Begun, D. R., Kelley, J., Manthi, F., & Mbua, E. N. (2015). A systematic revision of *Proconsul* with the description of a new genus of early Miocene hominoid. *Journal of Human Evolution*, *84*, 42–61.

McNutt, E. J., Claxton, A. G., & Carlson, K. J. (2017). Revisiting the peroneal trochlea of the StW 352 calcaneus. *South African Journal of Science*, *113*, 1–5.

McNutt, E. J., & DeSilva, J. M. (2016). The relationship between superior calcaneal facet area and Achilles tendon length in primates. *American Journal of Physical Anthropology*, *159*, 226.

McNutt, E. J., & DeSilva, J. M. (2018). Geometric morphometric analysis of the hominin calcaneus. *American Journal of Physical Anthropology*, *165*, 173.

McNutt, E.J., Kilham, B., Casana, J., Hatala, K., Hill, A.C., Johnson, C., Kilham, P., Reader, J., Thompson, N., & DeSilva, J.M. (2018). *Reassessing the Ursid hypothesis for the Laetoli "a" bipedal trackway*. Annual Meeting of the Paleoanthropological Society, Austin, TX.

McNutt, E. J., Zipfel, B., & DeSilva, J. M. (2018). Evolution of the human foot. *Evolutionary Anthropology*, *27*, 197–217.

Mednikova, M. B. (2011). A proximal pedal phalanx of a Paleolithic hominin from denisova cave, Altai. *Archaeology, Ethnology and Anthropology of Eurasia*, *39*(1), 129–138.

Meldrum, D. J. (1991). Kinematics of the cercopithecine foot on arboreal and terrestrial substrates with implications for the interpretation of hominin terrestrial adaptations. *American Journal of Physical Anthropology*, *84*, 273–289.

Meldrum, D. J. (2004). Fossilized Hawaiian footprints compared with Laetoli hominid footprints. In D. J. Meldrum & C. E. Hilton (Eds.), *From biped to strider* (pp. 63–83). Boston, MA: Springer.

Meldrum, D. J. (2007). Letter to the editor: Hyperbipeds-or- from biped to strider. *American Journal of Physical Anthropology*, *134*, 292–294.

Meldrum, D. J., Lockley, M. G., Lucas, S. G., & Musiba, C. (2011). Ichnotaxonomy of the Laetoli trackways: The earliest hominin footprints. *Journal of African Earth Sciences*, *60*(1–2), 1–12.

Mersey, B., Jabbour, R. S., Brudvik, K., & Defleur, A. (2013). Neanderthal hand and foot remains from Moula-Guercy, Ardèche, France. *American Journal of Physical Anthropology*, *152*(4), 516–529.

Meyer, M., Fu, Q., Aximu-Petri, A., Glocke, I., Nickel, B., Arsuaga, J. L., … Pääbo, S. (2014). A mitochondrial genome sequence of a hominin from Sima de los Huesos. *Nature*, *505*(7483), 403–406.

Midlo, C. (1934). Form of hand and foot in primates. *American Journal of Physical Anthropology*, *19*, 337–389.

Mietto, P., Avanzini, M., & Rolandi, G. (2003). Palaeontology: Human footprints in Pleistocene volcanic ash. *Nature*, *422*(6928), 133.

Mijares, A. S., Détroit, F., Piper, P., Grün, R., Bellwood, P., Aubert, M., … Dizon, E. (2010). New evidence for a 67,000-year-old human presence at Callao cave, Luzon, Philippines. *Journal of Human Evolution*, *59*(1), 123–132.

Miller, E. E., Whitcome, K. K., Lieberman, D. E., Norton, H. L., & Dyer, R. E. (2014). The effect of minimal shoes on arch structure and instrinsic foot muscle strength. *Journal of Sport and Health Science*, *3*, 74–85.

Mitchell, P. J., Sarmiento, E. E., & Meldrum, D. J. (2012). The AL 333-160 fourth metatarsal from Hadar compared to that of humans, great apes, baboons and proboscis monkeys: Non-conclusive evidence for pedal arches or obligate bipedality in Hadar hominins. *HOMO-Journal of Comparative Human Biology*, *63*(5), 336–367.

Moorjani, P., Amorim, C. E. G., Arndt, P. F., & Przeworski, M. (2016). Variation in the molecular clock of primates. *Proceedings of the National Academy of Sciences of the United States of America*, *113*, 10607–10612.

Morse, S. A., Bennett, M. R., Liutkus-Pierce, C., Thackeray, F., McClymont, J., Savage, R., & Crompton, R. H. (2013). Holocene footprints in Namibia: The influence of substrate on footprint variability. *American Journal of Physical Anthropology*, *151*(2), 265–279.

Morton, D. J. (1922). Evolution of the human foot. *American Journal of Physical Anthropology*, *5*, 305–336.

Morton, D. J. (1924). Evolution of the human foot II. *American Journal of Physical Anthropology*, *7*, 1–52.

Morton, D. J. (1926a). The significant characteristics of the Neanderthal foot. *Natural History*, *26*, 310–314.

Morton, D. J. (1926b). Evolution of man's erect posture (preliminary report). *Journal of Morphology*, *43*(1), 147–179.

Morton, D. J. (1935). *The human foot: Its evolution, physiology, and functional disorders*. New York: Columbia University Press.

Mountain, E. D. (1966). Footprints in calcareous sandstone at Nahoon point. *South African Journal of Science*, *62*(4), 103.

Musiba, C., Matthews, N., Noble, T., Kim, J., & Dominguez-Rodrigo, M. (2011). How many individuals left their footprints at Laetoli? Reinterpretation of the trackways based on recently acquired 3d data. *Journal of Vertebrate Paleontology*, *31*, 164.

Myatt, J. P., Schilling, N., & Thorpe, S. K. (2011). Distribution patterns of fibre types in the triceps surae muscle group of chimpanzees and orangutans. *Journal of Anatomy*, *218*(4), 402–412.

Napier, J. R. (1964). The evolution of bipedal walking in the hominids. *Archives de Biology*, *75*, 673–708.

Nixon, K. C. (2002). *WinClada* ver. 1.00. 08. Published by the author, Ithaca, NY, 2002. 628, 2002. On simultaneous analysis. KC Nixon, JM carpenter. *Cladistics*, *12*(3), 221–241.

Njau, J. K., & Blumenschine, R. J. (2012). Crocodylian and mammalian carnivore feeding traces on hominid fossils from FLK 22 and FLK NN 3, Plio-Pleistocene, Olduvai Gorge, Tanzania. *Journal of Human Evolution*, *63*, 408–417.

Oishi, M., Ogihara, N., Shimizu, D., Kikuchi, Y., Endo, H., Une, Y., … Ichihara, N. (2018). Multivariate analysis of variations in intrinsic foot musculature among hominoids. *Journal of Anatomy*, *232*, 812–823.

Onac, B. P., Viehmann, I., Lundberg, J., Lauritzen, S. E., Stringer, C., & Popiță, V. (2005). U–Th ages constraining the Neanderthal footprint at Vârtop cave, Romania. *Quaternary Science Reviews*, *24*(10–11), 1151–1157.

Oxnard, C. E. (1972). Some African fossil foot bones: A note on the interpolation of fossils into a matrix of extant species. *American Journal of Physical Anthropology*, *37*(1), 3–12.

Oxnard, C. E., & Lisowski, F. P. (1980). Functional articulation of some hominoid foot bones: Implications for the Olduvai (hominin 8) foot. *American Journal of Physical Anthropology*, *52*, 107–117.

Pablos, A. (2015). The foot in the *Homo* fossil record. *Mitteilungen der Gesellschaft für Urgeschichte*, *24*, 11.

Pablos, A., Lorenzo, C., Martínez, I., Bermúdez de Castro, J. M., Martinón-Torres, M., Carbonell, E., & Arsuaga, J. L. (2012). New foot remains from the gran Dolina-TD6 early Pleistocene site (sierra de Atapuerca, Burgos, Spain). *Journal of Human Evolution*, *63*, 610–623.

Pablos, A., Martínez, I., Lorenzo, C., Gracia, A., Sala, N., & Arsuaga, J. L. (2013). Human talus bones from the middle Pleistocene site of Sima de los Huesos (sierra de Atapuerca, Burgos, Spain). *Journal of Human Evolution*, *65*(1), 79–92.

Pablos, A., Martínez, I., Lorenzo, C., Sala, N., Gracia-Téllez, A., & Arsuaga, J. L. (2014). Human calcanei from the middle Pleistocene site of Sima de los Huesos (sierra de Atapuerca, Burgos, Spain). *Journal of Human Evolution*, *76*, 63–76.

Pablos, A., Pantoja-Pérez, A., Martínez, I., Lorenzo, C., & Arsuaga, J. L. (2017). Metric and morphological analysis of the foot in the middle Pleistocene sample of Sima de los Huesos (sierra de Atapuerca, Burgos, Spain). *Quaternary International*, *433*, 103–113.

Parr, W. C. H., Soligo, C., Smaers, J., Chatterjee, H. J., Ruto, A., Cornish, L., & Wroe, S. (2014). Three-dimensional shape variation of talar surface morphology in hominoid primates. *Journal of Anatomy*, *225*(1), 42–59.

Partridge, T. C., Granger, D. E., Caffee, M. W., & Clarke, R. J. (2003). Lower Pliocene hominid remains from Sterkfontein. *Science*, *300*, 607–612.

Patel, B., Jashashvili, T., Bui, S. H., Carlson, K. J., Griffin, N. L., Wallace, I. J., … Susman, R. L. (2018). Inter-ray variation in metatarsal strength properties in humans and Africa apes: Implications for inferring bipedal biomechanics in the Olduvai hominid 8 foot. *Journal of Human Evolution*, *121*, 147–165. https://doi.org/10.1016/j.jhevol.2018.02.013

Patel, B. A., Jashashvili, T., Trinkaus, E., Susman, R. L., & Lordkipanidze, D. (2015). A hallucal distal phalanx from Dmanisi, Georgia: Implications for early *Homo* foot biomechanics and evolution. *American Journal of Physical Anthropology*, *156*, 247.

Payne, R. C., Crompton, R. H., Isler, K., Savage, R., Vereecke, E. E., Günther, M. M., … D'Août, K. (2006). Morphological analysis of the hindlimb in apes and humans. II. Moment arms. *Journal of Anatomy*, *208*, 725–742.

Pearson, O. M., Royer, D. F., Grine, F. E., & Fleagle, J. G. (2008). A description of the Omo 1 postcranial skeleton, including newly discovered fossils. *Journal of Human Evolution*, *55*(3), 421–437.

Peeters, K., Schreuer, J., Burg, F., Behets, C., Van Bouwel, S., Dereymaeker, G., … Jonkers, I. (2013). Alterated talar and navicular bone morphology is associated with pes planus deformity: A CT-scan study. *Journal of Orthopaedic Research*, *31*(2), 282–287.

Pelissero, A. J. (2017). *A comparative analysis of newly discovered Pliocene hominin footprints from Laetoli, Tanzania*. Denver, CO: University of Colorado at Denver.

Pickering, R., Dirks, P. H., Jinnah, Z., De Ruiter, D. J., Churchill, S. E., Herries, A. I., … Berger, L. R. (2011). *Australopithecus sediba* at 1.977 ma and implications for the origins of the genus *Homo*. *Science*, *333*(6048), 1421–1423.

Pickering, T. R., Heaton, J. L., Throckmorton, Z. J., Prang, T. C., & Brain, C. K. (2017). A burned primate cuboid from Swartkrans cave, South Africa. *Annals of the Ditsong National Museum of Natural History*, *7*, 1–7.

Pilbeam, D. R., & Lieberman, D. E. (2018). Reconstructing the last common ancestor of chimpanzees and humans. In M. N. Muller, R. W. Wrangham, & D. R. Pilbeam (Eds.), *Chimpanzees and human evolution* (pp. 22–142). Cambridge, MA: Belknap Press.

Pomeroy, E., Lahr, M. M., Crivellaro, F., Farr, L., Reynolds, T., Hunt, C. O., & Barker, G. (2017). Newly discovered Neanderthal remains from Shanidar cave, Iraqi Kurdistan, and their attribution to Shanidar 5. *Journal of Human Evolution*, *111*, 102–118.

Pontzer, H., Rolian, C., Rightmire, G. P., Jashavili, T., Ponce de León, M. S., Lordkipanidze, D., & Zollikofer, C. P. E. (2010). Locomotor anatomy and biomechanics of the Dmanisi hominins. *Journal of Human Evolution*, *58*(6), 492–504.

Pontzer, H., Suchman, K., Raichlen, D. A., Wood, B. M., Mabulla, A. Z., & Marlowe, F. W. (2014). Foot strike patterns and hind limb joint angles during running in Hadza hunter-gatherers. *Journal of Sport and Health Science*, *3*, 95–101.

Prang, T. C. (2015a). Calcaneal robusticity in Plio-Pleistocene hominins: Implications for locomotor diversity and phylogeny. *Journal of Human Evolution*, *80*, 135–146.

Prang, T. C. (2015b). Rearfoot posture of *Australopithecus sediba* and the evolution of the hominin longitudinal arch. *Scientific Reports*, *5*, 17677.

Prang, T. C. (2016a). Conarticular congruence of the hominoid subtalar joint complex with implications for joint function in Plio-Pleistocene hominins. *American Journal of Physical Anthropology*, *160*, 446–457.

Prang, T. C. (2016b). The subtalar joint complex of *Australopithecus sediba*. *Journal of Human Evolution*, *90*, 105–119.

Prang, T. C. (2016c). Reevaluating the functional implications of *Australopithecus afarensis* navicular morphology. *Journal of Human Evolution*, *97*, 73–85.

Prang, T. C. (2018). Multivariate analysis of foot proportions in *Ardipithecus ramidus*. *American Journal of Physical Anthropology*, *159*, 314.

Preuschoft, H. (1970). Functional anatomy of the lower extremity. In G. H. Bourne (Ed.), *The chimpanzee* (Vol. 3, pp. 221–294). Basel: Karger.

Preuschoft, H. (1971). Body posture and mode of locomotion in early Pleistocene hominins. *Folia Primatologica*, *14*, 209–240.

Proctor, D. J. (2010a). *Three-dimensional morphometrics of the proximal metatarsal articular surfaces of gorilla, pan, Hylobates, and shod and unshod humans*. Iowa City, IA: The University of Iowa.

Proctor, D. J. (2010b). Brief communication: Shape analysis of the Mt 1 proximal articular surface in fossil hominins and shod and unshod *Homo*. *American Journal of Physical Anthropology*, *143*, 631–637.

Proctor, D. J. (2013). Proximal metatarsal articular surface shape and the evolution of a rigid lateral foot in hominins. *Journal of Human Evolution*, *65*(6), 761–769.

Proctor, D. J., Broadfield, D., & Proctor, K. (2008). Quantitative three-dimensional shape analysis of the proximal hallucial metatarsal articular surface in Homo, pan, gorilla, and Hylobates. *American Journal of Physical Anthropology*, *135*(2), 216–224.

Raichlen, D. A., Armstrong, H., & Lieberman, D. E. (2011). Calcaneus length determines running economy: Implications for endurance running performance in modern humans and Neandertals. *Journal of Human Evolution*, *60*(3), 299–308.

Raichlen, D. A., & Gordon, A. D. (2017). Interpretations of footprints from site S confirms human-like bipedal biomechanics in Laetoli hominins. *Journal of Human Evolution*, *107*, 134–138.

Raichlen, D. A., Gordon, A. D., Harcourt-Smith, W. E. H., Foster, A. D., & Haas, W. R., Jr. (2010). Laetoli footprints preserve earliest direct evidence of human-like bipedal biomechanics. *PLoS One*, *5*, e9769.

Rao, U. B., & Joseph, B. (1992). The influence of footwear on the prevalence of flat foot. A survey of 2300 children. *Bone & Joint Journal*, *74*, 525–527.

Rasmussen, O., Kromann-Anderson, C., & Boe, S. (1983). Deltoid ligament. Functional analysis of the medial collateral ligamentous apparatus of the ankle joint. *Acta Orthopaedica Scandinavica*, *54*, 36–44.

Reeser, L. A., Susman, R. L., & Stern, J. T., Jr. (1983). Electromyographic studies of the human foot: Experimental approaches to hominid evolution. *Foot & Ankle*, *3*, 391–407.

Reich, D., Green, R. E., Kircher, M., Krause, J., Patterson, N., Durand, E. Y., … Pääbo, S. (2010). Genetic history of an archaic hominin group from Denisova cave in Siberia. *Nature*, *486*, 1053.

Rein, T. R., Harrison, T., Carlson, K. J., & Harvati, K. (2017). Adaptation to suspensory locomotion in *Australopithecus sediba*. *Journal of Human Evolution*, *104*, 1–12.

Rhoads, J. G., & Trinkaus, E. (1977). Morphometrics of the Neandertal talus. *American Journal of Physical Anthropology*, *46*(1), 29–43.

Rightmire, G. P., Deacon, H. J., Schwartz, J. H., & Tattersall, I. (2006). Human foot bones from Klasies River main site, South Africa. *Journal of Human Evolution*, *50*(1), 96–103.

Roberts, D., & Berger, L. R. (1997). Last interglacial (c. 117 kyr) human footprints from South Africa. *South African Journal of Science*, *93*(8), 349–350.

Robinson, J. T. (1954). The genera and species of the Australopithecinae. *American Journal of Physical Anthropology*, *12*(2), 181–200.

Robinson, J. T. (1972). *Early hominid posture and locomotion*. Chicago: University of Chicago Press.

Rolian, C., Lieberman, D. E., Hamill, J., Scott, J. W., & Werbel, W. (2009). Walking, running and the evolution of short toes in humans. *Journal of Experimental Biology*, *212*(5), 713–721.

Rosas, A., Ferrando, A., Bastir, M., García-Tabernero, A., Estalrrich, A., Huguet, R., … de la Rasilla, M. (2017). Neandertal talus bones from El Sidrón site (Asturias, Spain): A 3D geometric morphometrics analysis. *American Journal of Physical Anthropology*, *164*(2), 394–415.

Rose, M. D. (1986). Further hominoid postcranial specimens from the late Miocene Nagri formation of Pakistan. *Journal of Human Evolution*, *15*(5), 333–367.

Rosenberg, K. R., Lü, Z., & Ruff, C. B. (2006). Body size, body proportions, and encephalization in a middle Pleistocene archaic human from northern China. *Proceedings of the National Academy of Sciences of the United States of America*, *103*(10), 3552–3556.

Sachithanandam, V., & Joseph, B. (1995). The influence of footwear on the prevalence of flat foot. A survey of 1846 skeletally mature persons. *Bone & Joint Journal*, *77*(2), 254–257.

Sarmiento, E. E. (1983). The significance of the heel process in anthropoids. *International Journal of Primatology*, *4*, 127–152.

Sarmiento, E. E. (1998). Generalized quadrupeds, committed bipeds, and the shift to open habitats: An evolutionary model of hominid divergence. *American Museum Novitates*, *3250*, 1–78.

Sarmiento, E. E., & Marcus, L. F. (2000). The os navicular of humans, great apes, OH 8, Hadar, and Oreopithecus: Function, phylogeny, and multivariate analyses. *American Museum Novitates*, *3288*, 1–38.

Saunders, J. B. M., Inman, V. T., & Eberhart, H. D. (1953). The major determinants in normal and pathological gait. *Journal of Bone and Joint Surgery (Am.)*, *35*(3), 543–558.

Schroeder, K. L., Rosser, B. W., & Kim, S. Y. (2014). Fiber type composition of the human quadratus plantae muscle: A comparison of the lateral and medial heads. *Journal of Foot and Ankle Research*, *7*, 54.

Schultz, A. H. (1930). The skeleton of the trunk and limbs of higher primates. *Human Biology*, *2*, 303–438.

Schultz, A. H. (1963). Relations between the lengths of the main parts of the foot skeleton in primates. *Folia Primatol (Basel)*, *1*, 150–171.

Semaw, S., Simpson, S. W., Quade, J., & Renne, P. R. (2005). Early Pliocene hominids from Gona, Ethiopia. *Nature*, *433*, 301–305.

Senut, B., Pickford, M., Gommery, D., Mein, P., Cheboi, K., & Coppens, Y. (2001). First hominid from the Miocene (Lukeino formation, Kenya). *Comptes Rendus de l'Académie des Sciences-Series IIA-Earth and Planetary Science*, *332*(2), 137–144.

Sewell, R. (1904). A study of the astragalus. *Journal of Anatomy*, *38*, 233–247.

Shipman, P. (2002). *The man who found the missing link: Eugene Dubois and his lifelong quest to prove Darwin right*. Cambridge, MA: Harvard University Press.

Simpson, S. W., Levin, N. E., Quade, J., Rogers, M. J., & Semaw, S. (2018). Postcranial fossils of *Ardipithecus ramidus* from Gona, Ethiopia. *American Journal of Physical Anthropology*, *165*, 253.

Singh, I. (1960). Variations in the metatarsal bones. *Journal of Anatomy*, *94*, 345.

Skinner, M. M., Kivell, T. L., Potze, S., & Hublin, J. J. (2013). Microtomographic archive of fossil hominin specimens from Kromdraai B, South Africa. *Journal of Human Evolution*, *64*, 434–447.

Sobczak, S., Vereecke, E., Rooze, M., Van Sint Jan, S., D'Août, K., Lescrenier, K., … De Clercq, D. (2008). Functional anatomy of the foot. Part a: The modern human foot. In K. D'Août, K. Lescrenier, B. Van Gheluwe, & D. De Clercq (Eds.), *Advances in Plantar Pressure Measurements in Clinical and Scientific Research* (pp. 69–91). Maastricht: Shaker Publishing.

Stern, J. T. (2000). Climbing to the top: A personal memoir of *Australopithecus afarensis*. *Evolutionary Anthropology*, *9*, 113–133.

Stern, J. T., & Susman, R. L. (1983). The locomotor anatomy of *Australopithecus afarensis*. *American Journal of Physical Anthropology*, *60*, 279–317.

Stern, J. T., & Susman, R. L. (1991). Total morphological pattern versus the "magic trait": Conflicting approaches to the study of early hominid bipedalism. In Y. Coppens & B. Senut (Eds.), *Origine(s) de la Bipédie chez les Homininés* (pp. 99–112). Paris: Centre National de la Recherche Scientifique.

Strait, D., Grine, F. E., & Fleagle, J. G. (2015). Analyzing hominin hominin phylogeny: Cladistic approach. In W. Henke & I. Tattersall (Eds.), *Handbook of paleoanthropology* (pp. 1989–2014). Berlin: Springer.

Straus, W. L., Jr. (1949). The riddle of man's ancestry. *The Quarterly Review of Biology*, *24*, 200–223.

Su, A., & Carlson, K. J. (2017). Comparative analysis of trabecular bone structure and orientation in south African hominin tali. *Journal of Human Evolution*, *106*, 1–18.

Su, A., Wallace, I. J., & Nakatsukasa, M. (2013). Trabecular bone anisotropy and orientation in an early Pleistocene hominin talus from East Turkana, Kenya. *Journal of Human Evolution*, *64*, 667–677.

Susman, R. L. (1983). Evolution of the human foot: Evidence from Plio-Pleistocene hominids. *Foot & Ankle*, *3*, 365–376.

Susman, R. L. (1988). New postcranial remains from Swartkrans and their bearing on the functional morphology and behavior of *Paranthropus robustus*. In F. E. Grine (Ed.), *Evolutionary history of the "robust" australopithecines* (pp. 149–172). New York: Aldine de Gruyter.

Susman, R. L. (1989). New hominid fossils from the Swartkrans formation (1979-1986 excavations): Postcranial specimens. *American Journal of Physical Anthropology*, *79*, 451–474.

Susman, R. L. (2005). *Oreopithecus*: Still apelike after all these years. *Journal of Human Evolution*, *49*(3), 405–411.

Susman, R. L. (2008). Brief communication: Evidence bearing on the status of *Homo habilis* at Olduvai Gorge. *American Journal of Physical Anthropology*, *137*, 356–361.

Susman, R. L., & Brain, T. M. (1988). New first metatarsal (SKX 5017) from Swartkrans and the gait of *Paranthropus robustus*. *American Journal of Physical Anthropology*, *77*, 7–15.

Susman, R. L., & de Ruiter, D. J. (2004). New hominin first metatarsal (SK 1813) from Swartkrans. *Journal of Human Evolution*, *47*, 171–181.

Susman, R. L., de Ruiter, D. J., & Brain, C. K. (2001). Recently identified postcranial remains of *Paranthropus* and early *Homo* from Swartkrans cave, South Africa. *Journal of Human Evolution*, *41*, 607–629.

Susman, R. L., Patel, B. A., Francis, M. J., & Cardoso, H. F. (2011). Metatarsal fusion pattern and developmental morphology of the Olduvai hominid 8 foot: Evidence of adolescence. *Journal of Human Evolution*, *60*(1), 58–69.

Susman, R. L., & Stern, J. T. (1982). Functional morphology of *Homo habilis*. *Science*, *217*, 931–934.

Susman, R. L., Stern, J. T., & Jungers, W. L. (1984). Arboreality and bipedality in the Hadar hominids. *Folia Primatologica*, *43*, 113–156.

Susman, R. L., Stern, J. T., & Jungers, W. L. (1985). Locomotor adaptations in the Hadar hominids. In E. Delson (Ed.), *Ancestors: The hard evidence* (pp. 184–192). New York: Alan R. Liss, Inc..

Sutikna, T., Tocheri, M. W., Morwood, M. J., Saptomo, E. W., Awe, R. D., Wasisto, S., … Roberts, B. G. (2016). Revised stratigraphy and chronology for *Homo floresiensis* at Liang Bua in Indonesia. *Nature*, *532*(7599), 366–369.

Suwa, G., White, T. D., & Howell, F. C. (1996). Mandibular postcanine dentition from the Shungura formation, Ethiopia: Crown morphology, taxonomic allocations, and Plio-Pleistocene hominid evolution. *American Journal of Physical Anthropology*, *101*, 247–282.

Swanson, Z. S., DeSilva, J. M., Boyle, E. K., Joseph, K. M., & McNutt, E. J. (2016). Variation in lateral plantar process position and functional implications in living humans. *American Journal of Physical Anthropology*, *159*, 308.

Swofford, D. L. (2002). *PAUP*. Phylogenetic analysis using parsimony (and other methods). Version 4*. Sunderland, MA: Sinauer Associates.

Thackeray, J. F., de Ruiter, D. J., Berger, L. R., & van de Merwe, N. (2001). Hominid fossils from Kromdraai: A revised list of specimens discovered since 1938. *Annals of the Transvaal Museum*, *38*, 158–169.

Thompson, A. L. T., & Zipfel, B. (2005). The unshod child into womanhood—Forefoot morphology in two populations. *The Foot*, *15*, 22–28.

Thompson, N. E., Holowka, N. B., O'Neill, M. C., & Larson, S. G. (2014). Brief communication: Cineradiographic analysis of the chimpanzee (pan troglodytes) talonavicular and calcaneocuboid joints. *American Journal of Physical Anthropology*, *154*(4), 604–608.

Throckmorton, Z. (2013). *Variation and non-adaptive evolution of the hominin foot and ankle*. Ph.D. thesis. University of Wisconsin, Madison, MI.

Throckmorton, Z., Pickering, T., Heaton, J., Sutton, M., Senjem, J., Prang, C., & C. Brain (2015). *New hominin tarsals from Swartkrans, South Africa*. 24th Annual Paleoanthropology Society Meeting. San Francisco, California.

Throckmorton, Z., Zipfel, B., Randolph-Quinney, P., Odes, E., Congdon, K., DeSilva, J., Harcourt-Smith, W., & Berger, L. (2017). *Homo naledi's* pedal pathologies. *American Journal of Physical Anthropology*, *162*, 381.

Tobias, P. V. (1998). History of the discovery of a fossilised little foot at Sterkfontein, South Africa, and the light that it sheds on the origins of hominin bipedalism. *Mitteilungen der Berliner Geselschaft für Anthropologische, Ethnologische und Urgeschichte*, *19*, 47–56.

Tocheri, M. W., Solhan, C. R., Orr, C. M., Femiani, J., Frohlich, B., Groves, C. P., … Jungers, W. L. (2011). Ecological divergence and medial cuneiform morphology in gorillas. *Journal of Human Evolution*, *60*, 171–184.

Toussaint, M., Macho, G. A., Tobias, P. V., Partridge, T. C., & Hughes, A. R. (2003). The third partial skeleton of a late Pliocene hominin (Stw 431) from Sterkfontein, South Africa. *South African Journal of Science*, *99*(5–6), 215–223.

Trinkaus, E. (1975a). Squatting among the Neandertals: A problem in the behavioral interpretation of skeletal morphology. *Journal of Archaeological Science*, *2*(4), 327–351.

Trinkaus, E. (1975b). *A functional analysis of the Neanderthal foot*. Ph.D. thesis. University of Pennsylvania, Philadelphia, PA.

Trinkaus, E. (1983a). Functional aspects of Neandertal pedal remains. *Foot & Ankle*, *3*, 377–390.

Trinkaus, E. (1983b). *The shanidar neandertals*. New York: Academic Press.

Trinkaus, E. (2005). Anatomical evidence for the antiquity of human footwear use. *Journal of Archaeological Science*, *32*, 1515–1526.

Trinkaus, E., & Hilton, C. E. (1996). Neandertal pedal proximal phalanges: Diaphyseal loading patterns. *Journal of Human Evolution*, *30*(5), 399–425.

Trinkaus, E., & Patel, B. A. (2016). An early Pleistocene human pedal phalanx from Swartkrans, SKX 16699, and the antiquity of the human lateral forefoot. *Comptes Rendus Palevol*, *15*, 978–987.

Trinkaus, E., & Shang, H. (2008). Anatomical evidence for the antiquity of human footwear: Tianyuan and Sunghir. *Journal of Archaeological Science*, *35*, 1928–1933.

Trinkaus, E., Wojtal, P., Wilczyński, J., Sázelová, S., & Svoboda, J. (2017). Palmar, patellar, and pedal human remains from Pavlov. *PaleoAnthropology*, *15*, 73–101.

Trinkaus, E., & Zimmerman, M. R. (1982). Trauma among the Shanidar Neandertals. *American Journal of Physical Anthropology*, *57*(1), 61–76.

Tuttle, R., Webb, D., Weidl, E., & Baksh, M. (1990). Further progress on the Laetoli trails. *Journal of Archaeological Science*, *17*(3), 347–362.

Tuttle, R. H. (1981). Evolution of hominid bipedalism and prehensile capabilities. *Philosophical Transactions of the Royal Society of London B: Biological Sciences*, *292*(1057), 89–94.

Tuttle, R. H. (1985). Ape footprints and Laetoli impressions: A response to the SUNY claims. In P. V. Tobias (Ed.), *Hominid evolution: Past, present, and future* (pp. 129–133). New York: Alan R. Liss.

Tuttle, R. H. (1987). Kinesiological inferences and evolutionary implications from Laetoli bipedal trails G-1, G-2/3, and A. In M. D. Leakey & J. Harris (Eds.), *Laetoli: A Pliocene site in northern Tanzania* (pp. 503–523). Oxford: Clarendon Press.

Tuttle, R. H. (1990). The pitted pattern of Laetoli feet. *Natural History*, *99*(3), 64.

Tuttle, R. H., & Rogers, C. M. (1966). Genetic and selective factors in reduction of the hallux in Pongo pygmaeus. *American Journal of Physical Anthropology*, *24*, 191–198.

Tuttle, R. H., Webb, D. M., & Baksh, M. (1991). Laetoli toes and *Australopithecus afarensis*. *Human Evolution*, *6*, 193–200.

Tuttle, R. H., Webb, D. M., Tuttle, N. I., & Baksh, M. (1992). Footprints and gaits of bipedal apes, bears, and barefoot people: Perspectives on Pliocene tracks. *Topics in Primatology*, *3*, 221–242.

Van der Meersch, B. (1981). *Les hommes fossiles de Gafzeh (Israël)*. Paris, France: Centre National de la Recherche Scientifique.

Venkataraman, V. V., Kraft, T. S., DeSilva, J. M., & Dominy, N. J. (2013). Phenotypic plasticity of climbing-related traits in the ankle joint of great apes and rainforest hunter-gatherers. *Human Biology*, *85*, 309–328.

Venkataraman, V. V., Kraft, T. S., & Dominy, N. J. (2013). Tree climbing and human evolution. *Proceedings of the National Academy of Sciences of the United States of America*, *110*(4), 1237–1242.

Vereecke, E., Van Sint Jan, S., D'Août, K., Lescrenier, K., Van Gheluwe, B., & De Clercq, D. (2008). Functional anatomy of the foot. Part B: The ape foot. In K. D'Août, K. Lescrenier, B. Van Gheluwe, & D. De Clercq (Eds.), *Advances in Plantar Pressure Measurements in Clinical and Scientific Research* (pp. 92–109). Maastricht: Shaker Publishing.

Vereecke, E. E., & Aerts, P. (2008). The mechanics of the gibbon foot and its potential for elastic energy storage during bipedalism. *Journal of Experimental Biology*, *211*(23), 3661–3670.

Verna, C., Texier, P. J., Rigaud, J. P., Poggenpoel, C., & Parkington, J. (2013). The middle stone age human remains from Diepkloof rock shelter (Western cape, South Africa). *Journal of Archaeological Science*, *40*(9), 3532–3541.

Vernon, D.S. (2013). *A morphometric analysis of the phalanges and a fragmentary first metatarsal from the Drimolen hominin site, South Africa.* Ph. D. Dissertation, University of Johannesburg, Johannesburg.

Villmoare, B. (2018). Early *Homo* and the role of the genus in paleoanthropology. *American Journal of Physical Anthropology*, *165*, 72–89.

Villmoare, B., Kimbel, W. H., Seyoum, C., Campisano, C. J., DiMaggio, E. N., Rowan, J., … Reed, K. E. (2015). Early *Homo* at 2.8 ma from Ledi-Geraru, Afar, Ethiopia. *Science*, *347*, 1352–1355.

Walker, A. C., & Leakey, R. E. F. (Eds.). (1993). *The Nariokotome Homo erectus skeleton*. Cambridge, MA: Harvard University Press.

Walker, C.S., DeSilva, J., Holliday, T.W., Marchi, D., Garvin, H.M., Cofran, Z., Hawks, J., Berger, L.R., & Churchill, S.E. (2015). *Relative length of the immature Homo naledi tibia U.W. 101–1070: evidence for elongation of the leg*. Paper presented at the meeting of the American Association of Physical Anthropologists, Atlanta.

Walker, J., Cliff, R. A., & Latham, A. G. (2006). U-Pb isotopic age of the StW 573 hominid from Sterkfontein, South Africa. *Science*, *314*, 1592–1594.

Wallace, I. J., Koch, E., Holowka, N. B., & Lieberman, D. E. (2018). Heel impact forces during barefoot versus minimally shod walking among Tarahumara subsistence farmers and urban Americans. *Royal Society Open Science*, *5*, 180044.

Ward, C. V. (2002). Interpreting the posture and locomotion of *Australopithecus afarensis*: Where do we stand? *American Journal of Physical Anthropology*, *119*, 185–215.

Ward, C. V., Kimbel, W. H., Harmon, E. H., & Johanson, D. C. (2012). New postcranial fossils of *Australopithecus afarensis* from Hadar, Ethiopia (1990-2007). *Journal of Human Evolution*, *63*, 1–51.

Ward, C. V., Kimbel, W. H., & Johanson, D. C. (2011). Complete fourth metatarsal and arches in the foot of *Australopithecus afarensis*. *Science*, *318*, 750–753.

Ward, C. V., Leakey, M. G., Brown, B., Brown, F., Harris, J., & Walker, A. C. (1999). South Turkwel: A new Pliocene hominid site in Kenya. *Journal of Human Evolution*, *36*, 69–95.

Ward, C. V., Leakey, M. G., & Walker, A. C. (2001). Morphology of *Australopithecus anamensis* from Kanapoi and Allia bay, Kenya. *Journal of Human Evolution*, *41*, 255–368.

Webb, D., Robu, M., Moldovan, O., Constantin, S., Tomus, B., & Neag, I. (2014). Ancient human footprints in Ciur-Izbuc cave, Romania. *American Journal of Physical Anthropology*, *155*(1), 128–135.

Webb, S., Cupper, M. L., & Robins, R. (2006). Pleistocene human footprints from the Willandra Lakes, southeastern Australia. *Journal of Human Evolution*, *50*, 405–413.

Webber, J. T., & Raichlen, D. A. (2016). The role of plantigrady and heel-strike in the mechanics and energetics of human walking with implications for the evolution of the human foot. *Journal of Experimental Biology*, *219*(23), 3729–3737.

Weidenreich, F. (1923). Evolution of the human foot. *American Journal of Physical Anthropology*, *6*, 1–10.

Weiss, E. (2012). Olduvai hominin 8 foot pathology: A comparative study attempting a differential diagnosis. *HOMO-Journal of Comparative Biology*, *63*, 1–11.

Weiss, E., DeSilva, J., & Zipfel, B. (2012). Brief communication. Radiographic study of metatarsal one basal epiphyseal fusion: A note of caution on age determination. *American Journal of Physical Anthropology*, *147*, 489–492.

White, T. D. (1980). Evolutionary implications of Pliocene hominid footprints. *Science*, *208*, 175–176.

White, T. D., Asfaw, B., Beyene, Y., Haile-Selassie, Y., Lovejoy, C. O., Suwa, G., & WoldeGabriel, G. (2009). *Ardipithecus ramidus* and the paleobiology of early hominids. *Science*, *326*, 64–86.

White, T. D., Lovejoy, C. O., Asfaw, B., Carlson, J. P., & Suwa, G. (2015). Neither chimpanzee nor human, *Ardipithecus* reveals the surprising ancestry of both. *Proceedings of the National Academy of Sciences of the United States of America*, *112*, 4877–4884.

White, T. D., & Suwa, G. (1987). Hominid footprints at Laetoli: Facts and interpretations. *American Journal of Physical Anthropology*, *72*, 485–514.

White, T. D., WoldeGabriel, G., Asfaw, B., Ambrose, S., Beyene, Y., Bernor, R. L., … Hart, W. K. (2006). Asa Issie, Aramis and the origin of *Australopithecus*. *Nature*, *440*, 883–889.

Wilkinson, J. L. (1954). The terminal phalanx of the great toe. *Journal of Anatomy*, *88*, 537.

Wiseman, A. L., & De Groote, I. (2018). A three-dimensional geometric morphometric study of the effects of erosion on the morphologies of modern and prehistoric footprints. *Journal of Archaeological Science: Reports*, *17*, 93–102.

Wood, B. A. (1974a). Olduvai bed 1 post-cranial fossils: A reassessment. *Journal of Human Evolution*, *3*, 373–378.

Wood, B. A. (1974b). Evidence on the locomotor pattern of *Homo* from early Pleistocene of Kenya. *Nature*, *251*, 135–136.

Wood, B. A. (1992). Origin and evolution of the genus *Homo*. *Nature*, *355*, 783–790.

Wood, B. A., Aiello, L., Wood, C., & Key, C. (1998). A technique for establishing the identity of 'isolated'fossil hominin limb bones. *The Journal of Anatomy*, *193*(1), 61–72.

Wood, B. A., & Constantino, P. (2007). *Paranthropus boisei*: Fifty years of evidence and analysis. *American Journal of Physical Anthropology*, *134*, 106–132.

Wood, B. A., & Leakey, M. (2011). The Omo-Turkana Basin fossil hominins and their contribution to our understanding of human evolution in Africa. *Evolutionary Anthropology: Issues, News, and Reviews*, *20*(6), 264–292.

Wunderlich, R. E., & Ischinger, S. B. (2017). Foot use during vertical climbing in chimpanzees (pan troglodytes). *Journal of Human Evolution*, *109*, 1–10.

Zeininger, A., Patel, B. A., Zipfel, B., & Carlson, K. J. (2016). Trabecular architecture in the StW 352 fossil hominin calcaneus. *Journal of Human Evolution*, *97*, 145–158.

Zhang, A., & DeSilva, J. M. (2018). Computer animation of walking mechanics in *Australopithecus sediba*. *Paleoanthropology* (in press).

Zihlman, A. L., Mcfarland, R. K., & Underwood, C. E. (2011). Functional anatomy and adaptation of male gorillas (Gorilla gorilla gorilla) with comparison to male orangutans (Pongo pygmaeus). *The Anatomical Record*, *294*, 1842–1855.

Zipfel, B., & Berger, L. R. (2007). Shod versus unshod: The emergence of forefoot pathology in modern humans? *The Foot*, *17*, 205–213.

Zipfel, B., DeSilva, J. M., & Kidd, R. S. (2009). Earliest complete hominin fifth metatarsal—Implications for the evolution of the lateral column of the foot. *American Journal of Physical Anthropology*, *140*, 532–545.

Zipfel, B., DeSilva, J. M., Kidd, R. S., Carlson, K. J., Churchill, S. E., & Berger, L. R. (2011). The foot and ankle of *Australopithecus sediba*. *Science*, *333*, 1417–1420.

Zipfel, B., & Kidd, R. (2006). Hominin first metatarsals (SKX 5017 and SK 1813) from Swartkrans: A morphometric analysis. *Journal of Comparative Human Biology*, *57*, 117–131.

Zipfel, B., & Kidd, R. S. (2008). Size and shape of a human foot bone from Klasies River main site, South Africa. *Paleontological Africana*, *43*, 51–56.

Zipfel, B., Kidd, R.S., & Clarke, R.J. (2010). *The 'second australopithecine species hypothesis' in Sterkfontein member 4: The post-cranial evidence.* Proceedings of the 16th Conference of the Palaeontological Society of Southern Africa. Howick, 5–8 August, 2010, Interpak Books, Pietermaritzburg, pp. 124–125.

SUPPORTING INFORMATION

Additional supporting information may be found online in the Supporting Information section at the end of the article.

How to cite this article: DeSilva J, McNutt E, Benoit J, Zipfel B. One small step: A review of Plio-Pleistocene hominin foot evolution. *Am J Phys Anthropol*. 2018;1–78. https://doi.org/10.1002/ajpa.23750